The Use of Advanced Analytical Techniques to Enable Batch and Source Matching of Homemade Explosives

A thesis submitted for fulfilment of the degree of Doctor of Philosophy

Paul Matthew McCurry

Bachelor of Technology (Forensic and Analytical Chemistry)
Bachelor of Science (Honours)

Australian Government
Department of Defence
Defence Science and
Technology Organisation

Flinders
UNIVERSITY

Flinders University of South Australia
Faculty of Science and Engineering
School of Chemical and Physical Sciences

Centre of Expertise in Energetic Materials (CEEM)

February 2015

Contents

i

Figures

ix

Tables

Abbreviations

AAS	Atomic Absorption Spectroscopy
AC	Alternating Current
ADF	Australian Defence Force
AES	Atomic Emission Spectroscopy
AFP	Australian Federal Police
AN	Ammonium Nitrate
AN/Al	Ammonium Nitrate/Aluminium
Al	Aluminium
amu	Atomic Mass Unit
ANFO	Ammonium Nitrate – Fuel Oil
AN/S	Ammonium Nitrate / Sugar
AN/S/Al	Ammonium Nitrate / Sugar / Aluminium
AR	Analytical Reagent
ASIO	Australian Security Intelligence Organisation
ATR	Attenuated Total Reflectance
BAA	Broad Area Announcement
Bp	Boiling Point
BSE	Back Scattered Electron
BSIA	Bulk Stable Isotope Analysis
C-4	Plastic explosives consisting primarily of RDX
C-IRMS	Carbon Isotope Ratio Mass Spectrometry
CAM	Crassulacean Acid Metabolism
CAN	Calcium Ammonium Nitrate
CAN/Al	Calcium Ammonium Nitrate / Aluminium
CAN/Sugar	Calcium Ammonium Nitrate / Sugar
CAN/Sugar/Al	Calcium Ammonium Nitrate / Sugar / Aluminium
CEEM	Centre of Expertise in Energetic Materials
CF-IRMS	Continuous Flow Isotope Ratio Mass Spectrometry
CIED	Counter Improvised Explosive Device
CE	Capillary Electrophoresis
CNTH	Calcium Nitrate Tetrahydrate
COAG	Council of Australian Governments
C/V	Coefficient of Variation
DADP	Diacetone Diperoxide
DAP	Diammonium Phosphate
DC	Direct Current
DNA	Deoxyribonucleic Acid
DSC	Differential Scanning Calorimetry
DSTL	Defence Science and Technology Laboratory
DSTO	Defence Science and Technology Organisation
EA	Elemental Analyser
ELSD	Evaporative Light Scattering Detector
ETA	Euskadi Ta Askatasuna
ET-AAS	Electrothermal Atomic Absorption Spectroscopy
ETN	Erythritol Tetranitrate
F-AAS	Flame Atomic Absorption Spectroscopy
FEL	Forensic Explosives Laboratory
FIA	Flow Injection Analysis
FIRMS	International Forensic Isotope Ratio Mass Spectrometry Network
FOX	Fuel-Oxidiser Mixture

FT	Fourier Transform
FT-IR	Fourier Transform Infrared Spectroscopy
GC/ECD	Gas Chromatography with Electron Capture Detector
GC/FID	Gas Chromatography with Flame Ionization Detector
GC/IRMS	Gas Chromatography with Isotope Ratio Mass Spectrometry
GC/MS	Gas Chromatography with Mass Spectrometry Detector
GC/TEA	Gas Chromatography with Thermal Energy Analyser
GF-AAS	Graphite Furnace Atomic Absorption Spectroscopy
GSR	Gunshot Residue
HCA	Hierarchical Cluster Analysis
HME	Home Made Explosive
HMTD	Hexamethylene Triperoxide Diamine
HMX	Cyclotetramethylenetetranitramine
HPLC	High Performance Liquid Chromatography
HPLC/RI	High Performance Liquid Chromatography with Refractive Index Detector
HPLC/TEA	High Performance Liquid Chromatography with Thermal Energy Analyser
HPLC/UV	High Performance Liquid Chromatography with Ultraviolet Detector
IAEA	International Atomic Energy Agency
IC	Ion Chromatography
IED	Improvised Explosive Device
IMS	Ion Mobility Spectrometry
IP	Identification Particles
IR	Infrared Spectroscopy
IRMS	Isotope Ratio Mass Spectrometry
ISAF	International Security Assistance Force
IST	Ignition Susceptibility Test
ICP	Inductively Coupled Plasma
ICP-MS	Inductively Coupled Plasma Mass Spectrometry
ICP-OES	Inductively Coupled Plasma Optical Emission Spectrometry
KT	Kaltenbach-Thuring
LC/MS	Liquid Chromatography with Mass Spectrometry
LOD	Limit of Detection
LOQ	Limit of Quantification
MAP	Monoammonium Phosphate
MECC	Micellar Electrokinetic Capillary Chromatography
MEKP	Methyl Ethyl Ketone Peroxide
MDL	Method Detection Limit
mp	Melting Point
MQL	Method Quantification Limit
MU	Measurement Uncertainty
m/z	Mass to Charge Ratio
NATA	National Association of Testing Authorities
NG	Nitroglycerine
N-IRMS	Nitrogen Isotope Ratio Mass Spectrometry
NP-Acid	Nitrophosphoric acid
NPK	Nitrogen-Phosphorous-Potassium
PC	Potassium Chlorate
PCA	Principal Component Analysis
PIRA	Provisional Irish Republican Army
PE4	Plastic explosives consisting primarily of RDX
PET	Polyethylene Terephthalate

PETN	Pentaerythritol Tetranitrate
PIXE	Particle Induced X-ray Emission
PLM	Polarized Light Microscopy
ppb	Parts Per Billion (µg/L)
ppm	Parts Per Million (mg/L)
ppt	Parts Per Trillion (ng/L)
PVC	Poly(Vinyl Chloride)
Py-GC/MS	Pyrolysis Gas Chromatography with Mass Spectrometry Detector
R	Coefficient of Correlation
REE	Rare Earth Elements
RDX	Cyclotrimethylenetrinitramine
RSD	Relative Standard Deviation
SA	Stearic Acid
S.D.	Standard Deviation
SE	Secondary Electron
SEM/EDX	Scanning Electron Microscope with Energy Dispersive X-Ray Analysis
SEMTEX H	Plastic explosive containing RDX and PETN
SIP	Stable Isotope Profiling
SSAN	Security Sensitive Ammonium Nitrate
STA-IR	Simultaneous Thermal Analysis Coupled With Infrared Spectroscopy
TATB	Triaminotrinitrobenzene
TATP	Triacetone Triperoxide
TGA	Thermal Gravimetric Analysis
TLC	Thin Layer Chromatography
TNT	2,4,6-Trinitrotoluene
TMS	Trimethylsilyl
TTP	Tactics, Techniques and Procedures
UK	United Kingdom of Great Britain and Northern Ireland
UN	Urea Nitrate
US/USA	United States of America
USGS	United States Geological Survey
UV	Ultraviolet
VoD	Velocity of Detonation
WTI	Weapons Technical Intelligence
XRD	X-Ray Diffraction
XRF	X-Ray Fluorescence

µg	Microgram
kg	Kilogram
g	Gram
mg	Milligram
ng	Nanogram
pg	Pictogram
nm	Nanometer
mm	Millimetre
km	Kilometre
L	Litre
mL	Millilitre
µL	Microliter
°C	degrees Centigrade
K	degrees Kelvin
M	Moles
kPa	Kilopascals
atm	Atmosphere
δ	delta notation
‰	per-mil
%	Percent
ε	enrichment factor
α	fractionation factor

Summary

This thesis describes the application of advanced analytical techniques: namely isotope ratio mass spectrometry (IRMS) and inductively coupled plasma mass spectrometry (ICP-MS) to the analysis of a variety of ammonium nitrate (AN) based homemade explosives.

AN has been widely used in the preparation of homemade explosives (HME) due its relative stability and ease of acquisition. The aim of this research was to develop methods that enable the identification of batch-to-batch matches between samples and to determine the origin of source materials used in such mixtures.

The work described in Chapter 2 indicated that the IRMS technique has the potential to discriminate samples of AN-based explosives due to the variations in their isotopic composition, e.g. nitrogen and carbon. An investigation on the ICP-MS technique is also described, which allowed for the multi-elemental profiling of trace impurities present in AN and AN-based explosives. These trace impurities may be used to compare samples in order to identify samples that have a similar origin or manufacturing process.

Lab based samples (as analysed in Chapter 2) tend to be considerably simpler to analyse than real samples, so in order to test the validity of the methods developed, DSTO provided realistic HME samples for analysis. These samples were used as they have been prepared in a manner directly analogous to HME samples commonly encountered in a real world scenario. Analysis of these genuine samples is covered in Chapter 3. The analysis of genuine samples highlighted a number of problems with the interpretation of results obtained from a single measurement of the bulk HME sample. These included: contamination, sampling issues, storage issues, dual carbon sources and dual nitrogen sources. The process used to concentrate and purify AN from calcium ammonium nitrate (CAN) also proved to be an important factor for the analysis of AN-based HMEs The results obtained in Chapter 3 highlights the usefulness of IRMS and ICP-MS for batch-to-batch matching of HME, but indicated that analysis of bulk sample is not sufficient for determining sourcing information and has limited intelligence value.

In Chapter 4 a new technique is described which mitigates the problems determined in Chapter 3. This technique is based on the separation and analysis of the nitrogen sources in AN, namely nitrate ion and ammonium ion. The isotopic ratio of the nitrogen in the nitrate ion was shown to be unchanged regardless of the purification process used, thus is an important marker for determining sourcing relationships. This Chapter described the separation technique and uses IRMS to determine the provenance of AN and CAN based explosives to their source/precursor materials.

Chapter 5 discusses the problem associated with dual carbon sources commonly encountered in fuel-oxidiser-based HME. It details a new method for gaining forensic intelligence from the exploitation of HME comprising CAN/sugar compositions.

Chapter 6 details techniques and methodologies for the analysis of non-explosive components occasionally found in HME compositions. The non-explosive component

considered in this examination is glitter. Glitter is often found in paint grade aluminium flake to introduce various lustre effects, however, if this paint grade aluminium flake is used in the fabrication of HME, such as AN/aluminium, then those glitter particles become a useful marker. The different types of analysis are detailed in this Chapter and the usefulness of this extra layer of information for linking HME samples is demonstrated.

The chemical analysis of a number of organic-based HME is detailed in Chapter 7. A series of experiments illustrating that both IRMS and ICP-MS can be utilised to extract information from samples of organic-based HME. This information can be used for batch-to-batch matching of samples but also to determine the origin of source materials.

The conclusions and recommendations from this research task are detailed in Chapter 8 of this thesis. It describes two new analytical methodologies for the analysis of HME samples using IRMS. These methodologies improve the confidence of source matching, which is important for of the provision of chemical intelligence. These techniques highlight a need to change from the bulk analysis of CAN-based HME to the separate analysis of each individual component (carbonate/nitrate) by IRMS. This new methodology has shown potential to be implemented as a way to determine the origin of the CAN used in the preparation of CAN-based HME.

The research described in this thesis has sort to highlight the use of IRMS and ICP-MS for the provision of chemical intelligence in the analysis of HME. By understanding the limitations of bulk analysis and how various processes affect the isotope ratios, or the introduction of trace impurities, it is now possible to link like samples and identify their source materials. The use of the analytical techniques described in this thesis may now be used as an additional layer of information in the general intelligence picture, which when combined with other intelligence collection methods may allow for "attack the network" operations.

Declaration

'I certify that this thesis does not incorporate without acknowledgment any material previously submitted for a degree or a diploma in any university; and that to the best of my knowledge and belief it does not contain any material previously published or written by another person where due reference is made in the text.'

Paul Matthew McCurry

Acknowledgments

Publications

Defence Publications

Hall, B., Davies, P. and McCurry P. (2010) Isotope Ratio Mass Spectrometry: *Analysis of Ammonium Nitrate and Ammonium Nitrate/Aluminium Explosives (U)*, Technical Note DSTO-TN-0951, Defence Science and Technology Organisation. Restricted Report

Hall, B., Davies, P., Armitt, D., McCurry P and Walker, S. (2013) Ammonium Nitrate Based Explosives I: Production of Ammonium Nitrate and Calcium Ammonium Nitrate *(U)*, Technical Note DSTO-TN-1217 [FOUO], Defence Science and Technology Organisation.

Hall, B., Davies, P., Armitt, D., McCurry P and Walker, S. (2013) Ammonium Nitrate Based Explosives II: Separation and Isotopic Analysis of Ammonium Nitrate and Calcium Ammonium Nitrate *(U)*, Technical Report DSTO-TR-2899 [FOUO], Defence Science and Technology Organisation.

Hall, B., Davies, P., Armitt, D., McCurry P and Walker, S. (2013) Ammonium Nitrate Based Explosives III: Characterisation of Sugar in Explosive Mixtures *(U)*, Technical Note DSTO-TN-1218 [FOUO], Defence Science and Technology Organisation.

Hall, B., Davies, P., Armitt, D., McCurry P and Walker, S. (2013) Ammonium Nitrate Based Explosives IV: Characterisation of Glitter in Explosive Mixtures *(U)*, Technical Note DSTO-TN-1219 [FOUO], Defence Science and Technology Organisation.

Conference Proceedings

P.M. McCurry et al. *Characterisation of Ammonium Nitrate Based Explosives by IRMS and Other Techniques*. International Symposium on the Analysis and Detection of Explosives (ISADE), 2013. Oral Presentation.

P.M. McCurry et al. *Characterisation of Energetic Materials and Explosive Ingredients by IRMS and Other Techniques*. Australian Energetic Materials Symposium (AEMS), 2012. Invited Speaker. Oral Presentation.

P.M. McCurry et al. *Characterisation of Energetic Materials and Explosive Ingredients by IRMS and Other Techniques*. The 21st International Symposium on the Forensic Sciences, 2012. Keynote Speaker. Oral Presentation.

P.M. McCurry et al. *Combining Nitrogen and Carbon Isotope Ratios for Discrimination of Ammonium Nitrate and Ammonium Nitrate Based Explosives*. The Australian and New Zealand Society for Mass Spectrometry Conference (ANZSMS23), 2011. Oral Presentation.

P.M. McCurry et al. *Combining Nitrogen and Carbon Isotope Ratios for Discrimination of Ammonium Nitrate and Ammonium Nitrate Based Explosives*. Australian Energetic Materials Symposium (AEMS), 2010. Oral Presentation.

P.M. McCurry et al. *Combining Nitrogen and Carbon Isotope Ratios for Discrimination of Ammonium Nitrate and Ammonium Nitrate Based Explosives*. International Symposium on the Analysis and Detection of Explosives (ISADE), 2010. Oral Presentation.

P.M. McCurry et al. *Combining Isotopes and Trace Metal Analysis for Characterisation of Energetic Materials – IRMS and SEM/EDX*. International Symposium on the Analysis and Detection of Explosives (ISADE), 2010. Poster Presentation.

P.M. McCurry et al. *Combining Isotopes and Trace Metal Analysis for Characterisation of Energetic Materials – IRMS and SEM/EDX*. The 20th International Symposium on the Forensic Sciences, 2010. Poster Presentation.

1. Introduction

In western societies, the use of improvised explosive devices (IEDs) are usually characterised as a unique criminal or terrorist event, resulting in a one-off investigation by police or national security agencies. The investigations performed are largely limited to associative evidence (i.e. linking a person to the crime) and physio/chemical evidence.

However in wartime conflicts, such as recent operations in Iraq and Afghanistan, the large-scale use of IEDs has provided opportunities for analysts to research potential analytical techniques that can links samples and determine the origin of source materials in order to identify insurgent groups.

The widespread use of IED in Afghanistan, prompted the Afghan government on the 22nd of January 2010, to completely ban the use of ammonium nitrate (AN) fertiliser, leaving farmers dependent on either a diammonium phosphate (DAP), super phosphate or urea based fertiliser [1, 2]. Despite the ban, large stockpiles of AN remain in the country and smuggling operations from adjacent countries have done little to reduce the widespread use of AN-based explosives [3, 4].

Calcium ammonium nitrate (CAN) was developed by fertiliser manufacturers and was claimed to be a non-detonable alternative to pure AN, due to the composition containing 25% calcium carbonate. This fertiliser was approved for legitimate use in Afghanistan, however, insurgent bomb makers developed purification techniques that enabled the separation of AN from the carbonate impurity, producing AN that could still be used for the preparation of IEDs. Bombmakers routinely use two approaches to reprocess CAN before combining it with a fuel. In one method, the very soluble AN is separated from insoluble carbonate by dissolving it in hot water and decanting the concentrated AN solution. Excess water is evaporated and the ammonium nitrate is dried and crushed. Another processing method is to utilise commercial grinders to grind the CAN prills into a fine powder without extracting the inert material. The production of viable explosives is achieved through mixing with "paint grade" aluminium flake, powdered sugar or a combination of both which act as the fuel [3-9].

A study conducted by Zygmunt and Buczkowski focussed on the utilisation of agricultural AN as a basic ingredient in massive explosive charges [10]. They found that aluminium powder exhibits strong sensitising properties with CAN-based fertilisers (containing 22% carbonate). It was also noted that to eliminate the detonation of an explosive charge prepared from ground CAN and powdered aluminium, the AN content in the source fertiliser would need to be reduced to approximately 50%. The authors stated that even this method does not completely prevent the use of CAN type fertilisers (with a large amount of inert content) in the production of explosive charges [10].

As insurgent forces in Iraq and Afghanistan are not able to fight directly against coalition forces, this has seen an escalation in IED use. The success achieved by insurgents with their low tech IED approach has caused a re-evaluation of how to best counter IEDs. This response has led to the formation of organisations directly tasked with the defeat of IEDs. Their goal is to conduct research to develop tactics, techniques and procedures to predict, prevent, detect, neutralise and exploit IEDs in order to reduce the effectiveness of IEDs when used against deployed forces. One such example of this is the Joint Improvised

Explosive Device Defeat Organisation (JIEDDO), which focuses on three lines of operation: attacking the network, defeating the device and training the force.

JIEDDO has determined that ground truth studies are needed so that forensic information can be gathered from recovered Home Made Explosive (HME) samples. From a recent broad agency announcement (BAA) they have stated that there is a need for:

"Studies that determine the chemical, electrical, magnetic and physical signatures and observables of HME to aid in forensic capabilities are of interest. For example, more information is needed to determine what chemical or other markers would be appropriate to determine a material or mixtures history. In addition, studies that develop methods that will yield information on the sources of HME precursors, or their processing and handling are of interest" [9].

1.1 Intelligence

Intelligence is the product resulting from the collection, processing, integration, evaluation, analysis, and interpretation of available information concerning foreign nations, hostile or potentially hostile forces or elements, or areas of actual or potential operations. Intelligence can be gathered using many methods and listed below are some of the common collection disciplines [11-16].

- Human intelligence (HUMINT);
- Signals intelligence (SIGINT);
- Geospatial intelligence (GEOINT);
- Measurement and signatures intelligence (MASINT);
- Open-source intelligence (OSINT); and
- Technical intelligence (TECHINT).

Intelligence can also be defined based on the context and level in which it is applied. Three types of intelligence have been identified in the field of policing [17, 18]. These also have relevance to counter terrorism and counter insurgency operations:

Tactical - Supports front-line enforcement officers in taking case-specific action and as a consequence is relevant to specific investigations. The criminal environment of interest is local. The use of this intelligence is case-by-case and lacks a greater understanding of long term or wider geographical problems [17, 18].

Operational - Assists in planning crime reduction activities. It supports decision makers that are responsible for geographical areas or who command teams. It allows for the identification of main priorities and is thus relevant to a part of a crime series [17, 18].

Strategic - Provides an understanding of patterns and functioning of criminal behaviour (terrorist/bomb maker behaviour) and environments. It is future-orientated and proactive. It explores long-term solutions and accommodates delays more easily than in an operational perspective. It is used by top-level managers and will influence not only policing activities but also non-law enforcement agencies [17, 18].

There are no defined boundaries between these three types of intelligence. For example, collating tactical or operational intelligence on different cases will contribute to an overall strategic goal, while strategic intelligence can guide efforts towards specific events [17].

Weapons technical intelligence (WTI) is a key component of IED exploitation where recovered devices, explosives or other materials are characterised in order to achieve intelligence outcomes. The primary goals of such investigations are to determine what the device is, who made it and with what materials. The aim of any exploitation is to provide a rich picture of the device to inform the CIED domains, namely prediction, prevention, detection, neutralisation and mitigation.

The improvised nature of these explosive devices often means that the components used in their manufacture may be characteristic of a bomb maker, region and commonly available materials they have access to. An IED has several components that may be investigated to compile information and will typically contain the following components:

- An outer casing – The physical size and shape of the IED;
- An explosive main charge – Determines the role and effectiveness of the device;
- Detonator – The initial part of the explosive train, needed to initiate the main charge;
- Electronic components – Enables both passive and active remote triggering or targeting a specific vehicle or person; and
- Power source – Powers electronic devices or electric detonators.

The focus of this research is to identify batch-to-batch matches of like explosives. This has the potential to identify a bomb maker, their area of operation, and identifying batch-to-source, which can be used to determine where the bomb-makers are sourcing their materials.

This objective may be achieved through the use of advanced chemical analytical techniques such as isotope ratio mass spectrometry (IRMS) and inductively coupled plasma mass spectrometry (ICP-MS). This thesis explores a number of analytical techniques, which may be useful in the investigation of multiple IED events and focuses on determining what information can be exploited to provide further confidence in linking HME samples. These analytical techniques will be applicable to a wide range of explosives related investigations.

1.2 Explosives

Explosives are substances or mixtures, which undergo a rapid chemical change without an external supply of oxygen. This change causes the liberation of large quantities of energy and is generally accompanied by the evolution of hot gases or vapours [19].

Explosives are normally divided into two categories, namely primary or secondary.

1.2.1   Primary Explosives

Primary explosives are very sensitive to stimuli such as heat, friction, impact and electrostatic discharge and will detonate or burn rapidly in very small quantities. Primary explosives are used in the manufacture of detonators and are normally composed of molecular explosives (compounds which require no additives to detonate) [20]. Examples of these explosives are lead azide ($Pb(N_3)_2$), mercury fulminate ($C_2N_2O_2Hg$) and lead styphnate ($C_6HN_3O_8Pb$). Triacetone triperoxide (TATP) is also a primary explosive encountered in improvised detonators/initiators [21].

1.2.2   Secondary Explosives

Military and commercial explosive systems usually employ multiple explosives in an explosives train. Examples of secondary explosives include compositions of 2, 4, 6-trinitrotoluene (TNT), cyclotrimethylenetrinitramine (RDX), pentaerythritol tetranitrate (PETN) and mixtures such as ammonium nitrate-fuel oil (ANFO). These types of explosives are used in military and commercial applications where safety and explosive reliability is of great importance.

1.3 Types and Uses of Explosives

1.3.1   Military

Explosives which are utilised in military applications need to meet stringent criteria for performance, safety, storage and transport [22]. An increasing area of interest has been the development and implementation of insensitive munitions. Examples of military explosives currently used are shown in Table 1-1.

Type	Application	Example
Melt cast explosives	Main charge	TNT Comp B (RDX/TNT/Wax) ARX-4024
Cast cured/ polymer bonded explosives	Blast Fragmentation	PBXN-109 (RDX/Al/binder)
Pressed polymer bonded explosives	Boosters Main charge	TR-1 (RDX/Wax)
Fuel-oxidiser mixtures	Propellants	Ammonium Perchlorate/Al

Table 1-1: Selected examples of military explosive types

1.3.2   Commercial

Commercial explosives are usually encountered in mining or construction industries. Dynamite is no longer a commonly used explosive in North America, Western Europe or Australia. For most commercial applications, dynamites have now been replaced by AN-based formulations, which offer a better combination of performance, safety and cost [22]. Modern commercial explosives are typically mixtures of AN and fuel. These mixtures tend to not have the high detonation velocities exhibited by military explosives and are usually selected for a specific effect, such as shattering and heaving sections of earth, without widespread dispersal in open cut mining operations.

The key to their performance is the intimate mixing of an oxidiser and a fuel, such as in the formulation ANFO, where fuel oil is allowed to soak into porous AN prills, leading to a fuel content of 6% which is near a zero oxygen balance. AN formulations are sold as AN prill or solution, ANFO premixed, AN water-gel, AN emulsions and also heavy ANFO (which is ANFO folded into an AN emulsion). AN formulations usually require the use of a high explosive booster (such as detcord which contains PETN), however, cap-sensitive formulations are also commercially available [22].

1.3.3 Homemade Explosives

Home Made Explosives (HMEs) are explosive materials that can be prepared from commonly available, low cost materials and are an area of growing concern for law enforcement and national security agencies. Recipes and techniques for their manufacture are widely available in the open literature and on the internet.

HMEs have no legitimate use and often incorporate mixtures or compounds that do not meet the safety/performance requirements for either industry or military application. These types of explosives are normally based on inorganic salts and/or peroxides.

Many HMEs are comprised of simple oxidiser/fuel mixtures. Historically, the most common oxidisers encountered in HMEs is AN and potassium chlorate. Common fuel sources incorporated with these oxidisers are diesel fuel oil, sugar and metals such as aluminium and magnesium. Table 1-2 [23-25] details the optimum fuel percentage for a variety of common AN/fuel explosive mixtures.

Oxidiser	Fuel	Optimum Percentage of Fuel	
ANFO	AN	Fuel oil	5.5
AN/Al	AN	Aluminium powder	18.4
AN/S	AN	Sugar	16

Table 1-2: Optimum fuel percentages for AN/fuel mixtures

Some HMEs are based on organic peroxides, these are easily synthesised using readily available precursors. Triacetone triperoxide (TATP) is produced from acetone, hydrogen peroxide and acid.

Homemade versions of the previously described military and commercial explosives can also be prepared. This includes PETN, RDX, nitrogylcerin and TNT.

Some examples of HMEs that have been used in various incidents are detailed in the following sections.

1.3.3.1 Fuel-Oxidiser Mixtures

Examples of cases where AN-based explosives were utilised will be discussed in Section 1.4.2. Chlorates, particularly potassium chlorate, are commonly found in improvised explosive mixtures. Some of the devices used in the Bali bombings of 2002 were found to be mixtures containing potassium chlorate, sulphur and aluminium [26, 27].

Black powders are usually comprised of 75% potassium nitrate, 15% charcoal and 10% sulphur. These types of mixtures have been used for years as a propellant, but have been superseded commercially by smokeless powders based on nitrocellulose. Commercially available smokeless powders and black powders could potentially be incorporated into homemade devices and be used for illegitimate purposes [27-29].

1.3.3.2 Unitary Explosives

An example of a homemade unitary explosive is urea nitrate (UN), which can be prepared by the addition of nitric acid to a solution of urea. UN was the main explosive utilised in the 1993 bombing of the World Trade Centre in New York City [22, 30-32].

1.3.3.3 Peroxides

Peroxide-based explosives are notoriously sensitive to initiation by accidental stimuli, such as impact and friction. TATP, hexamethylene triperoxide diamine (HMTD), diacetone diperoxide (DADP) and methyl ethyl ketone peroxide (MEKP) are all examples of peroxide-based explosives. The shoe bomber Richard Reid used TATP in his failed attempt in bombing a US airliner in 2001 [22, 33]. Umar Farouk Abdulmutallab, a 23-year-old Nigerian, attempted to detonate a device containing PETN and TATP sewn into his underwear on a trans-Atlantic flight on Christmas Day, 2009 [34].

It is also possible to produce a detonable mixture by combining a fuel with a high concentration of hydrogen peroxide, this technique has been used extensively for propellant applications. This explosive mixture was allegedly used in the failed bomb attacks in London on 21 July 2005. In this attack, the main explosive charge was thought to be a mixture of concentrated hydrogen peroxide and chapatti flour [22, 35].

1.3.3.4 Organic-based

PETN and erythritol tetranitrate (ETN) are examples of nitrate esters which can be synthesised from readily available materials. PETN was recently discovered in parcel destined to board airplanes in England recently [36]. The use of ETN is also increasing due the ease of access of its precursor (erythritol is a natural sweetener). TNT and RDX are examples of military explosives which can be easily synthesised and employed in IEDs.

1.4 Ammonium Nitrate

AN is a relatively stable compound that is classified as an oxidiser (Dangerous goods class 5.1) that is used worldwide as a nitrogen rich, water soluble fertiliser and for the manufacture of explosives. Explosive materials may be prepared using AN as long as it is intimately mixed with suitable fuel source and appropriate initiation conditions are met (heat/shock/confinement). ANFO is the most widely used commercial explosive in the world, predominantly used by the mining industry.

1.4.1   Industrial Accidents

The main focus of AN use in this thesis is its application within criminal activities. It is worth noting that under some circumstances AN can be detonated without the presence of a fuel. These instances are most often observed during industrial accidents. There have been several major accidents worldwide involving AN, details of recent incidents is shown in Table 1-3 [37].

Year	Location	Details
2001	France	Fertiliser Factory
2004	North Korea	Train Wagon
2004	Romania	Truck containing AN
2007	Mexico City	Truck carrying 25 tonnes of AN (explosion which killed 28 people and injured 154)

Table 1-3: Recent accidental explosions involving AN

The most recent industrial accident occurred in West, Texas, USA on the 17th of April 2013 which saw the deaths of 15 people and the destruction of the plant and surrounding area. The factory contained a variety of agricultural chemicals and produced AN and ammonia.

The last audit of the site indicated that it held 300 tons of AN and 50 tons of anhydrous ammonia [38].

1.4.2 Terrorism and Insurgency

Governments around the world have recognised the security risks posed by the use of AN in the preparation of HME. AN remains an attractive material to terrorist organisations as it is readily availability, inexpensive and the explosive produced is easily handled.

Examples of common fuels that can be used with AN include oil, paraffin, sugar, sulphur, charcoal, ground coal and flour. To date, various groups have utilised fuel oil, icing sugar (little associated odour), or aluminium (enhanced thermal effects) [22].

Irish terrorist groups conducted numerous bombings during the period between 1969 and 2000 [22]. These have used commercial explosives or HME based on AN, chlorates or nitrobenzene. In 1972, the UK and Irish governments introduced stringent controls on the sale of sodium chlorate, nitrobenzene and AN throughout Ireland [20, 22, 39]. AN fertiliser was replaced by an agriculturally acceptable material, CAN, which is AN adulterated with either calcium carbonate or dolomite (a naturally occurring mix of calcium carbonate and magnesium carbonate). Nevertheless, large fertiliser-based devices continued to be used throughout the 1990s in attacks in Northern Ireland and various other sites including London, Manchester and Birmingham [22, 40, 41].

During the same time period, the Basque nationalist and separatist organisation, Euskadi Ta Askatasuna (ETA) employed a HME explosive comprised of a mixture of AN and aluminium powder [22, 42].

In July 2011, Anders Behring Breivik detonated a vehicle borne improvised explosive device (VBIED) in the city of Oslo, Norway which killed eight people. This device contained a HME based on fertiliser grade CAN, which was purchased from an online store in Poland [43]. CAN fertilisers have also been successfully used to produce HMEs in Iraq, Afghanistan and Syria [44].

In other countries, AN has been used less frequently in bombings, however a notable exception was the bombing of the Murrah Federal building in Oklahoma City (April 1995) [22, 39, 40]. This event generated concern in the US regarding the explosive nature of AN. This highlighted the fact that AN explosives can be prepared easily and the devastating effect of such explosives. This resulted in the development of a number of research projects to desensitise commercially available AN [22, 39]. Sales restrictions were also considered.

1.4.3 Regulation of Ammonium Nitrate

1.4.3.1 Australia

In late 2002, in response to concerns about AN being used for illegal purposes, the Council of Australian Governments (COAG) commenced a review of the security risks associated with the use of hazardous materials and how such risks could be mitigated. The aim of the review was to enhance national security by limiting opportunities for, and enhancing detection of, the illegal and unauthorised use of hazardous materials by improving regulations and other controls [37].

On June 25th 2004, COAG agreed to:

"… A national approach to ban access to AN for other than specifically authorised users. The agreement will result in the establishment in each jurisdiction of a licensing regime for the use, manufacture, storage, transport, supply, import and export of AN [37]."

To achieve this outcome, COAG endorsed a set of agreed principles that set out the policy aims, as well as the minimum requirements for the licensing and permit system. As a result, a new classification called security sensitive ammonium nitrate (SSAN) was defined. Under the agreed principles, SSAN is defined as:

"... AN, AN emulsions and AN mixtures containing greater than 45% AN, excluding solutions [37]."

The agreed principles require that an authorisation be obtained at each stage of the supply chain (the use, storage, manufacture, supply, transport, import, export or disposal of SSAN). To obtain an authority, an entity (person or company) must demonstrate a legitimate need for the SSAN product and prove their probity through police and Australian Security Intelligence Organisation (ASIO) background checks [37].

1.4.3.2 Internationally
A range of regulatory approaches have been adopted to mitigate the security risks posed by AN. Some countries such as the United Kingdom have taken an alternative approach, emphasising education, training and information sharing rather than legislative controls. In contrast, other countries such as Indonesia, South Africa, Peru and Colombia have banned the use of all AN fertilisers. Differences in the reliance on AN fertilisers and in the capacity of regulators to administer more complex regulatory regimes may account for some of the divergence in approaches [37].

Research on methods to limit the criminal use of agricultural grade AN is continuing, recent work conducted at Sandia National Laboratories suggests that the inclusion of iron sulfate to AN may produce a non-detonable fertiliser that is not easily separated by simple purification techniques [45].

1.5 Ammonium Nitrate Manufacturing Process

The main focus of this thesis is the chemical analysis of fuel-oxidiser explosives incorporating AN by IRMS and ICP-MS. Using these techniques, it is important to understand the processes used during the manufacture of AN and CAN, as the various manufacturing processes has an effect on the isotopic and elemental composition of the AN / CAN produced.

These potential variations in isotopic and elemental compositions may prove to be very useful from a forensic standpoint, as they lead to differentiation of source materials, which in turn are reflected in the HMEs produced.

A brief overview of the relevance of each stage in the manufacturing processes of AN/CAN is shown in Table 1-4.

Processing Stage		Forensic Significance	Comment
Starting Materials	Ammonia Synthesis	Isotopic Ratio (N)	Isotopic fractionation during ammonia synthesis
	Nitric Acid Synthesis	Isotopic Ratio (N)	Isotopic fractionation during nitric acid synthesis
	Phosphate Rocks	Trace Elements (Isotopic Ratio (C))	Trace elements in source phosphate rocks
AN/CAN Synthesis	AN Synthesis	Isotopic Ratio (N)	Isotopic fractionation during AN synthesis
	CAN Synthesis	Isotopic Ratio (N & C)	Nitrogen Isotopic fractionation during CAN synthesis
			Carbon Isotope of calcium carbonate
		Trace Elements	Trace elements may be indicative of source of phosphate rocks
Finishing Process	Prilling / Granulation	Particle Sizing/ Isotopic Ratio (N)	Heating and cooling may cause isotopic fractionation (N)
	Additives / Anti-Caking	Trace Elements	Presence of carbon due to anticaking agents

Table 1-4: Brief overview of the relevance of each stage in the production of AN and CAN

1.5.1   Overview

AN is manufactured on an industrial scale by a number of techniques, such as the TOPAN (a process developed by Orica for the production of Nitropril), Kaltenbach-Thuring (KT Process) and Stengel process [46-48].

Differences between manufacturers are based on the process used, additives, neutralisation processes, operating pressures of the equipment and cooling methods employed [49]. The precursors, additives and neutralisation processes may be critically important for the introduction of variations that can be used for batch matching and sourcing materials.

Prilling involves the formation of discrete granules by the solidification of droplets (as it falls down a prilling tower). Granulation generally involves the use of agglomeration or crushing to form the end product [49-51].

Most large scale AN manufacturing plants produce the key reagents (nitric acid and ammonia) on site. The purity of industrial grade AN is very high (≈ 99.9%) and samples are routinely tested by manufacturers to ensure consistent process control and quality of the final product [49]. From a forensic stand point, this level of control may allow for the reliable determination of origin as the degree of variation from batch to batch may be minimal (however this would need to be proven through long term analysis projects via engagement with AN manufacturers).

1.5.1.1 Ammonia Synthesis

Ammonia is produced using the Haber process, and is formed by the reaction of nitrogen with hydrogen at high pressure, as shown in Equation 1-1. The nitrogen used in this reaction is sourced by extraction from the atmosphere, while the hydrogen is obtained from natural gas.

$$N_{2(g)} + 3H_{2(g)} \rightarrow 2NH_{3(g)} \hspace{3cm} \text{(Equation 1-1)}$$

The production of ammonia is the key ingredient for the production of fertilisers. The flow diagram shown in Figure 1-2 provides an overview of the industrial synthesis of ammonia [48, 49].

The steps involved in the formation of ammonia are as follows:

1) Natural gas (methane) is fed into the plant at high pressure. The natural gas provides the hydrogen component of ammonia. The gas contains a small amount of sulfur, which is removed prior to reaction. The natural gas is then reformed, first with steam in heated catalyst tubes in the primary reformer and then with air in the secondary reformer.

2) Nitrogen is extracted from the atmosphere.

3) The natural gas is then heated to high temperature (800-940 °C) and reacted with water to convert it into hydrogen, carbon monoxide and carbon dioxide, as shown below. The reaction is exothermic and the residual heat is recycled to generate steam in a boiler.

$$CH_{4(g)} + H_2O_{(g)} \rightarrow CO_{(g)} + 3H_{2(g)} \hspace{2cm} \text{(Equation 1-2)}$$
$$CH_{4(g)} + 2H_2O_{(g)} \rightarrow CO_{2(g)} + 4H_{2(g)} \hspace{2cm} \text{(Equation 1-3)}$$
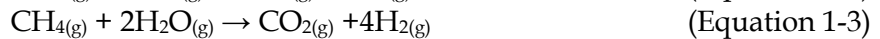
4) Unwanted carbon oxides are removed by catalytic conversion of carbon monoxide to carbon dioxide in the shift converter, which is then removed by a recirculating activated solution in an absorber.

5) Final elimination of carbon oxides is by conversion of the remaining traces back to methane over a catalyst in the methanator.

6) A 3:1 mix of hydrogen and nitrogen, compressed to 14000 kPa, is passed to the recirculating ammonia synthesis loop.

7) The nitrogen and hydrogen gas mixture is passed over an iron or ruthenium-based catalyst at 450-500 °C. The reaction product is then cooled to condense liquid ammonia (-25°C).
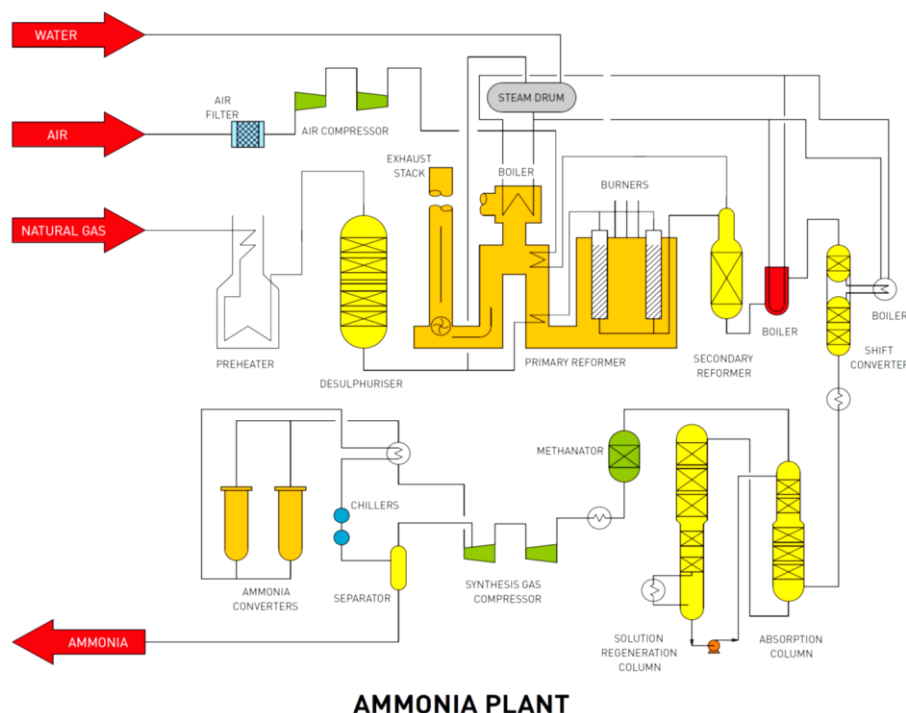
Figure 1-2: Flow diagram of ammonia synthesis

1.5.1.2 Nitric Acid Synthesis

Nitric acid is the other key raw material used in the production of AN. The flow diagram shown in Figure 1-3 provides an overview of the industrial synthesis of nitric acid [48, 49].

Nitric acid is a strong mineral acid and is the primary reagent used for nitration of explosive precursors. Commercial production of nitric acid is performed using the Ostwald process.

In the Ostwald process, ammonia is converted into nitric acid in a two-step reaction. In the first stage, ammonia is oxidised at ~ 800 °C in the presence of a platinum/rhodium catalyst to form nitric oxide and water, as shown in Equation 1-4.

$$4NH_{3(g)} + 5O_{2(g)} \rightarrow 4NO_{(g)} + 6H_2O_{(g)} \qquad \text{(Equation 1-4)}$$
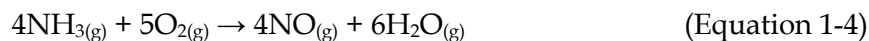
The second stage, involves further oxidisation of the nitric oxide to produce nitrogen dioxide. The nitrogen dioxide produced is then reacted with water in the presence of oxygen to produce nitric acid, the condensate is collected to yield dilute nitric acid, as shown in Equations 1-5, 1-6 and 1-7.

$$2NO_{(g)} + O_{2(g)} \rightarrow 2NO_{2(g)} \qquad \text{(Equation 1-5)}$$
$$3NO_{2(g)} + H_2O_{(l)} \rightarrow 2HNO_{3(aq)} + NO_{(g)} \qquad \text{(Equation 1-6)}$$
$$4NO_{2(g)} + O_{2(g)} + H_2O_{(l)} \rightarrow 4HNO_{3(aq)} \qquad \text{(Equation 1-7)}$$
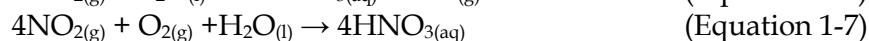
The nitric acid is further purified by distillation, which produces the concentrated product.
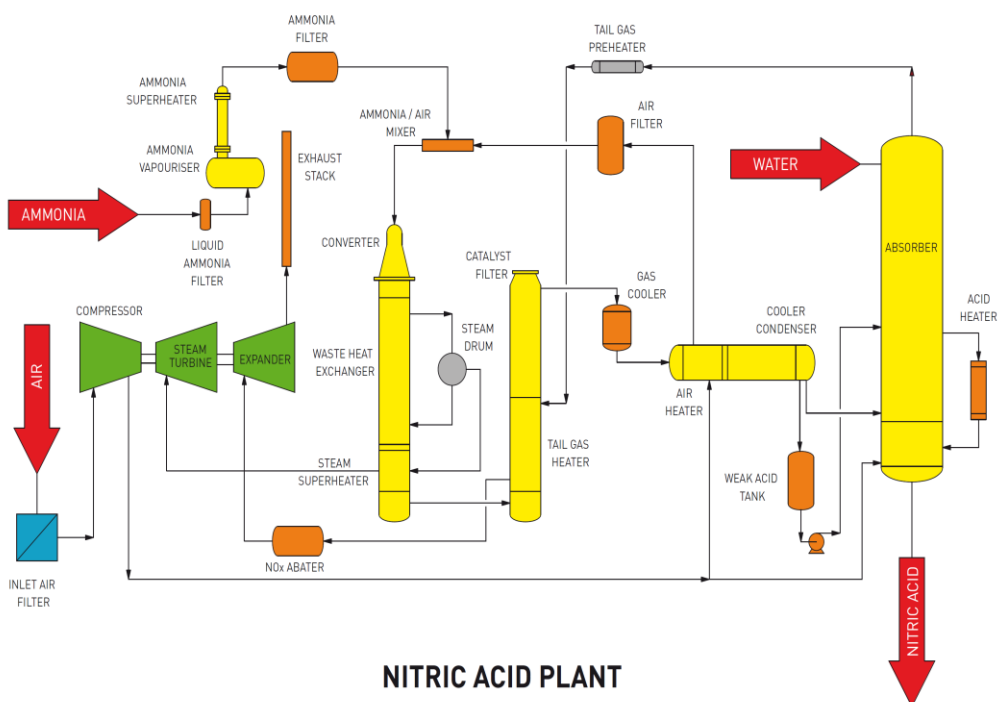
NITRIC ACID PLANT

Figure 1-3: Flow diagram of nitric acid synthesis

1.5.1.3 Ammonium Nitrate Synthesis

A flow diagram of the TOPAN process used for the manufacture of AN is shown in Figure 1-4. Different plants may employ variations of these procedures (i.e. KT process [47]); however, the basic methods used for the industrial production of AN are the same. The overview below gives a detailed description into the processes involved in an ammonium nitrate plant [48, 49].

1) Nitric acid and gaseous ammonia are combined, in a violent exothermic reaction as shown in Equation 1-8. The AN produced at this stage has a concentration of about 83%.

$$HNO_{3(aq)} + NH_{3(g)} \rightarrow NH_4NO_{3(aq)} \qquad \text{(Equation 1-8)}$$
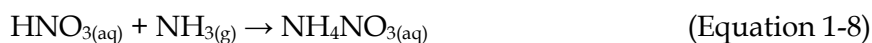
2) The AN solution is concentrated further by passing the solution through an evaporator to remove the majority of water. This process further concentrates the AN solution to 95-99%.

3) In the TOPAN process, the molten AN is formed into prills by dropping the solution down a cooling tower, during the descent, the droplets cool to form spherical granules of 1-3 mm diameter. The prills are dried with hot air then cooled in rotating drums.

4) The final product is then passed through a sorter to remove over and undersized particles, those which meet the size criteria are coated with an anticaking agent to improve storage and handling properties.

5) The final product is stored in bulk in a climate controlled facility.
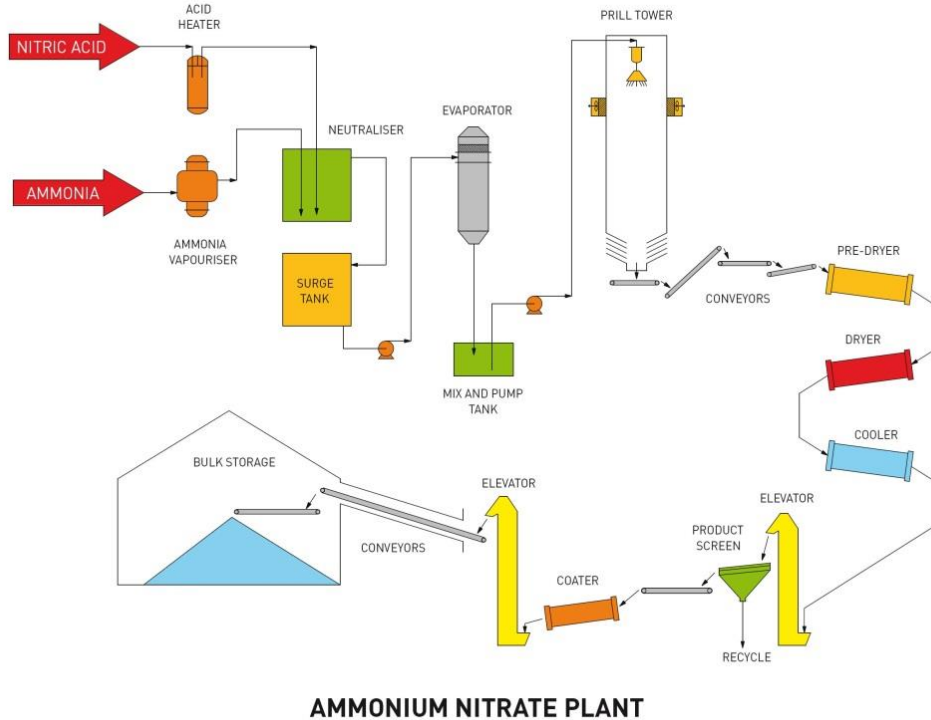
Figure 1-4: Flow diagram of AN synthesis and prilling (TOPAN process)

1.6 Calcium Ammonium Nitrate Manufacturing Process

1.6.1 Production of Calcium Ammonium Nitrate

CAN is one of the products of the Odda process, which can also be used for the co-manufacture of nitrophosphates [50, 52-56].

Rock phosphate is acidified with nitric acid to produce calcium nitrate and phosphoric acid. From these materials, several different fertilisers can then be manufactured:

- The calcium nitrate can be reacted with ammonia in the presence of phosphoric acid to produce AN;
- If the calcium nitrate is combined with a potassium salt, typically potassium chloride or potassium sulphate, then a Nitrogen-Phosphorus-Potassium (NPK) fertiliser is produced; and
- CAN is produced if the calcium nitrate is reacted with ammonia in the presence of carbon dioxide.

A block diagram of the manufacturing processes to achieve the production of each of these fertilisers is shown in Figure 1- 5 [52].
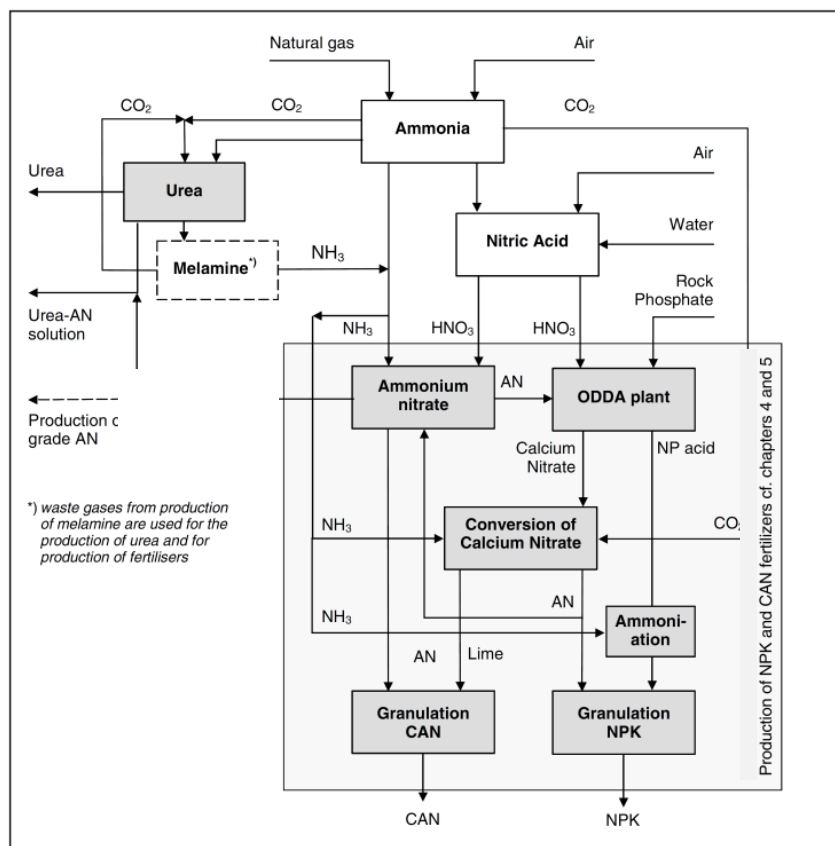
Figure 1-5: Block diagram of the production of fertilisers and of substances used for the production of fertilisers at Agrolinz Melamin GmbH

1.6.2 Source Materials for CAN Fertiliser Production

1.6.2.1 Ammonia
Ammonia is produced by the Haber process as described in Section 1.5.1.1.

1.6.2.2 Nitric Acid
Nitric acid is produced by the Ostwald process as detailed in section 1.5.1.2.

1.6.2.3 Rock Phosphate
The global production of phosphate rock amounted to 182.1 million tons in 2010 [57] principally mined in Morocco, the United States and Jordan [52, 58]. The composition of phosphate rock depends on where the material is mined but is generally found as a calcium phosphate apatite, namely hydroxylapatite ($Ca_5(PO_4)_3OH$), fluorapatite ($Ca_5(PO_4)_3F$) or chlorapatite ($Ca_5(PO_4)_3Cl$). Rock phosphate can be broadly divided into two classes which is dependent on how they were formed – sedimentary phosphate rocks and igneous phosphate rocks [52].

1.6.2.4 Carbon Dioxide
Carbon dioxide is required for the production of CAN fertilisers. The carbon dioxide is produced as a by-product of hydrogen formation by the reaction of natural gas with steam prior to the Haber process, as shown in Equation 1-9 [52, 54].

$$CH_{4(g)} + 2H_2O_{(g)} \rightarrow CO_{2(g)} + 4H_{2(g)} \qquad \text{(Equation 1-9)}$$

14
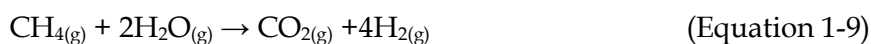
1.6.2.5 Other Raw Materials

Apart from the materials specified above, important compounds such as: potash salts, phosphoric acid, ammonium sulphate, ammonium phosphates (mono-ammonium phosphate and di-ammonium phosphate), magnesium salts, dolomite, boron compounds, zinc sulphate, talcum powder and coating agents may be used for fertiliser production. The use of anti-foaming agents may be necessary for the phosphate rock digestion with nitric acid [52].

1.6.3   The Odda Process

The main steps of the Odda process are [52, 55]:

- Digestion of phosphate rock with nitric acid;
- Crystallisation and separation of calcium nitrate tetrahydrate (CNTH) from the nitrophosphoric acid (NP-acid); and
- Conversion of CNTH into ammonium nitrate and lime (for production of CAN fertilisers).

A schematic diagram of the steps involved in the Odda process is shown in Figure 1-6 [52].
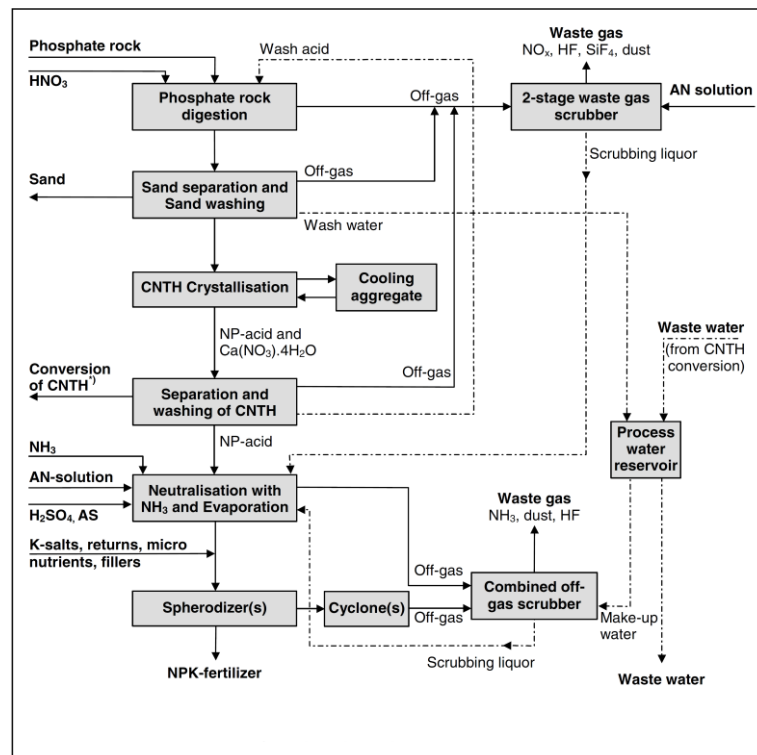
Figure 1-6: Industrial production of NPK fertiliser

1.6.3.1 Digestion of Phosphate Rock

Rock phosphate, typically fluorapatite ($Ca_5(PO_4)_3F$), is dissolved in an excess of dilute nitric acid (<60% HNO_3) using a cascade reactor. The reaction takes place at a temperature of about 70 °C, the exothermic nature of this reaction maintains the heat of reaction [52]. The formation of calcium nitrate ($Ca(NO_3)_2$) is expressed in Equation 1-10:

$$Ca_5(PO_4)_3F_{(s)} + 10HNO_{3(aq)} \rightarrow 5Ca(NO_3)_{2(aq)} + 3H_3PO_{4(aq)} + HF_{(g)} \qquad \text{(Equation 1-10)}$$
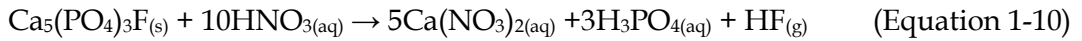
1.6.3.2 Crystallisation and Filtration of Calcium Nitrate Tetrahydrate

The calcium nitrate ($Ca(NO_3)_2$), is purified by cooling the liquid to 0 °C. At this temperature, the calcium nitrate precipitates out of the mother liquor as CNTH ($Ca(NO_3)_2.4H_2O$). The CNTH crystals are separated and washed prior to further reaction [52].

1.6.3.3 Production of Calcium Ammonium Nitrate

The block diagram in Figure 1-7 shows the stepwise manufacture of CAN by conversion of CNTH [52].

Ammonia and carbon dioxide are initially dissolved into an AN solution which is circulating in a carbonising column. The ammonia reacts with the carbon dioxide to form ammonium carbonate as shown in Equation 1-11 [52].

$$2NH_{3(g)} + CO_{2(g)} + H_2O_{(l)} \rightarrow (NH_4)_2CO_{3(aq)} \qquad \text{(Equation 1-11)}$$
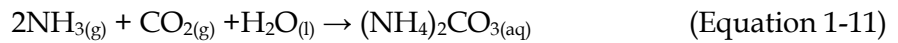
Separately, the CNTH is also dissolved in an AN solution. The ammonium carbonate formed in the previous reaction is then combined with the dissolved CNTH, to form AN and calcium carbonate, as shown in Equation 1-12.

$$Ca(NO_3)_{2(aq)} + (NH_4)_2CO_{3(aq)} \rightarrow 2NH_4NO_{3(aq)} + CaCO_{3(s)} \qquad \text{(Equation 1-12)}$$
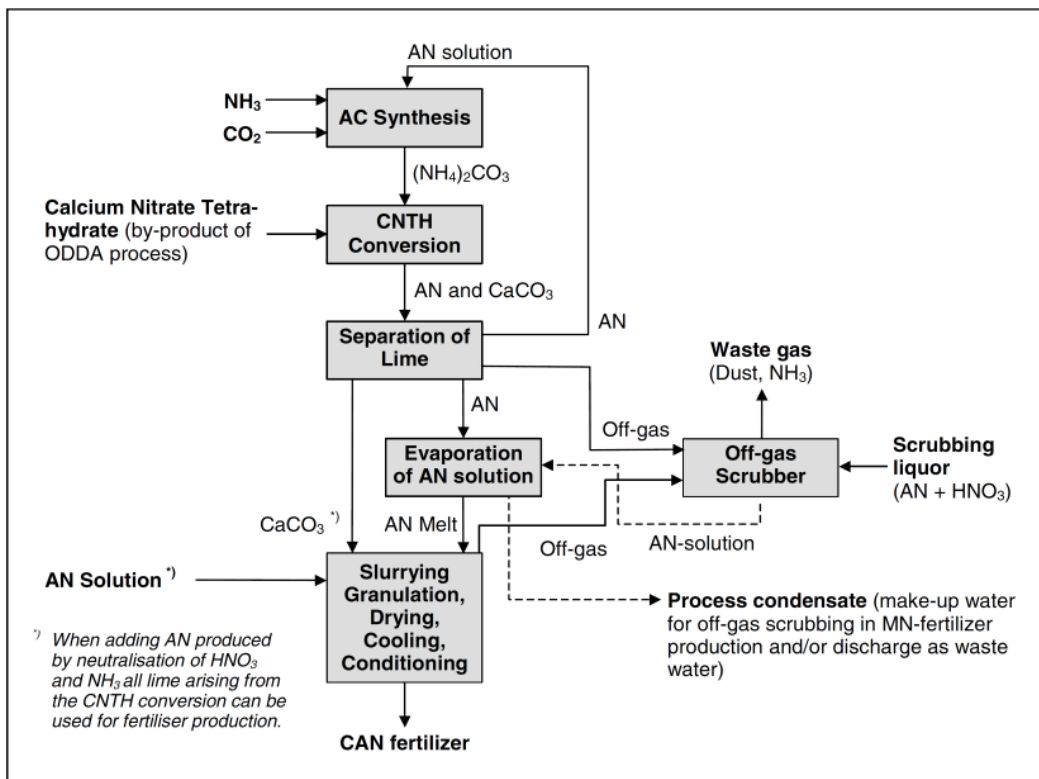
Figure 1-7: Block diagram of the production of CAN fertilisers by the conversion of CNTH

When producing AN in an additional AN synthesis (for example using the TOPAN or KT processes), all lime arising from the CNTH conversion can be used for fertiliser production. An additional AN synthesis also maintains continuity of AN availability during the Odda section shutdown or during non-availability of carbon dioxide from the ammonia plant [52].

1.7 Prilling and Granulation

The greatest variation (in relation to the physical form of the final AN product) between manufacturers in the production of AN occurs during the finishing process.

In the finishing process, the fertiliser is converted into a form that improves storage and ease of transport. There are two main ways this is achieved:

- Formation of a spherical prill by gravity assisted cooling of molten AN solution; and
- Granulation by evaporation of an AN solution in a heated rotating drum.

1.7.1 Prilling

The prilling starts with a molten solution that contains ~ 0.5% water. This solution is piped to the top of a prilling tower and discharged as a fine spray, which aggregates to form discrete droplets. As the droplets fall down the tower, cold air is drawn up the tower, which causes the droplets to cool and solidify as spherical prills [52]. A flow diagram of the prilling process is shown in Figure 1-8 [52].
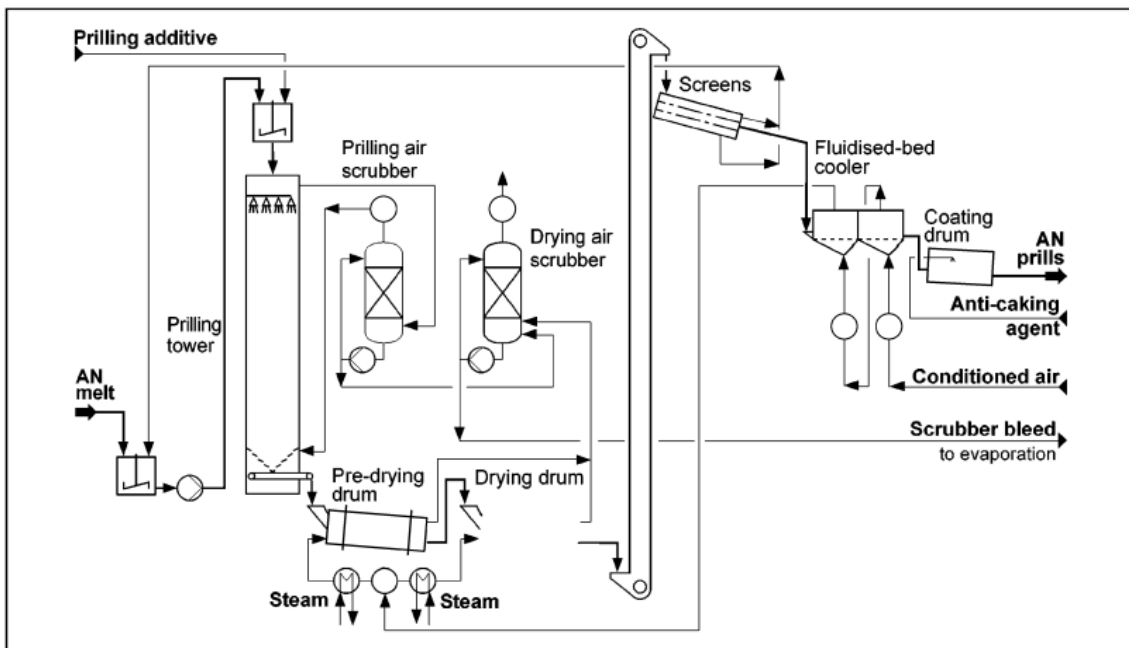
Figure 1-8: Schematic diagram of the production of technical grade AN

The prills are then passed through screens to filter for size; incorrectly sized prills are remelted and are recycled back into the system. The correctly sized prills are coated with anti-caking agents and are packed for transport or long term storage.

1.7.2 Granulation by Rotating Drum

Granulation is achieved by an inclined rotary drum consisting of two zones: the granulation zone and the drying zone.

In the granulation zone, recycled material consisting of undersize and rushed oversize particles (granulation loop) are added to the slurry (containing 10-20% water) and rotated.

In the drying zone, preheated air is directed into the chamber which evaporates the water from the slurry whilst the barrel is rotated. Over time, the drying of the slurry slowly builds up granules, with a final water content <1.5% [52].

Common AN/CAN granulation processes can be divided into high solid recycle processes [59, 60]:
- Pugmill;
- Spherodizer; and
- Drum.

And low solid recycle processes:
- Fluidised bed;
- Pan; and
- Fluidised drum.

Recycle in this case is defined as the amount of solid material going back to the granulator in relation to the amount of product being produced. These differences result in different AN concentrations or amount of liquid phase required by the granulation process. A high solid recycle granulation process usually requires a lower AN concentration (94-96.5%) than a lower solid recycle process (98-99.5%). This correspondingly means that the amount of water to be removed from the product by drying is higher for the higher recycle process. Some low recycle processes operate with such a low water content that a dryer is not required [59, 60].

In a high solid recycle process the filler can be introduced into the granulator without any heating. Due to the lower AN concentration (high water content) in the melt, this is even possible for grades with low N contents which require large amounts of filler (up to 15-20% of production). Low solid recycle processes producing low CAN grades with low N content are difficult as the filler must be mixed with the AN solution before it enters the granulator. This requires a heated and agitated mixing vessel [59, 60].

Low solid recycle processes have the advantage of being able to add magnesium nitrate to produce granular AN. This is a very effective method of stabilising AN as it changes the phase change temperature. It also reduces caking and dust formation during storage and transport due to thermal cycling. The main disadvantage of this is the considerable increase in moisture pick-up of the product. This is a reason why magnesium nitrate cannot be easily used in a high recycle process due to the higher liquid phase in the granulator. For CAN production the addition of magnesium nitrate is only of minor importance [59, 60].

1.7.3 Modern Pugmill Granulation Process

The modern pugmill granulation process has been highlighted as a method for granulating AN/CAN which has certain advantages over the "old" prilling processes highlighted in Sections 1.6.1 and 1.6.2. A modern pugmill granulation plant consists of the following units [56, 59]:

- Granulation loop;
- Product treatment;
- Process air treatment;
- Process water treatment; and
- Wash water treatment system.

A schematic diagram of the pugmill granulation system can be observed in Figure 1-9 [59].

The granulation loop forms the actual product from AN melt, the required additives and the filler to adjust the nitrogen content. The main equipment of the loop comprises a granulator and a dryer, screens, crushers and necessary transport equipment.
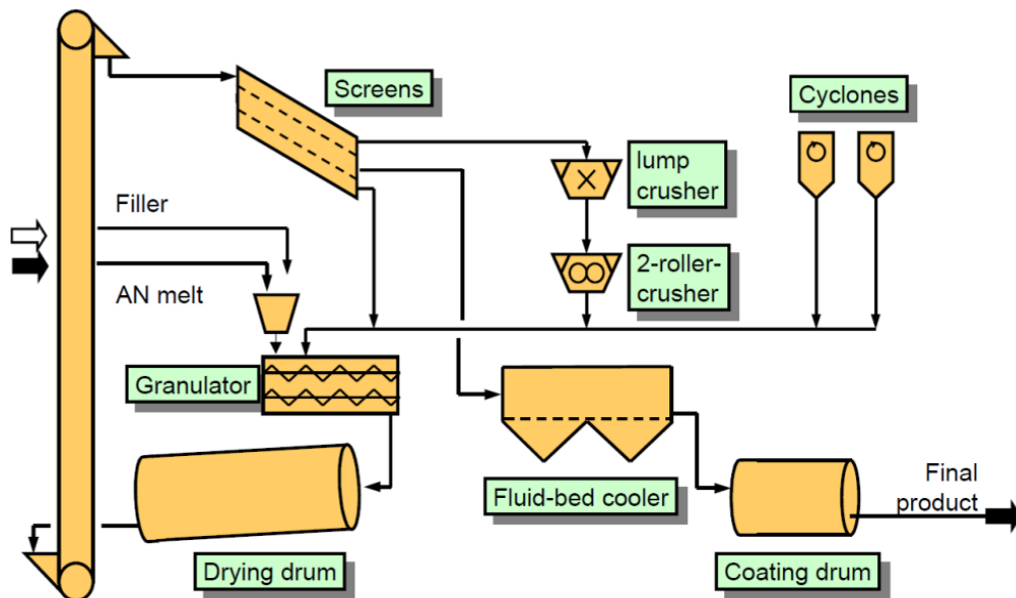
Figure 1-9: Pugmill granulation and recycle system

Characteristics of the pugmill process are as follows [56, 59]:

- A single pugmill plant is capable of producing the whole range of N contents from 22-33.5 %N. The switching from AN to CAN is done quickly;
- The pugmill process is very tolerant regarding the filler materials and additives. Most natural dolomites and limestone can be used. It can also process synthetic limestone from nitrophosphate plants;
- The addition of additives is relatively straight forward. These do not have to be added to solutions, but can be fed directly into the granulator; and
- The pugmill plant is able to produce most CAN grades autothermally (no external heating required).

1.8 Alternative CAN Manufacturing

The industrial production of CAN or AN fertilisers usually includes the addition of a filler material, such as dolomite or limestone, to reduce the rate of AN decomposition. This improves the safety of the production process and the stability of the fertilisers during storage and transport. It also serves as a pH buffer in the soil after application of the fertiliser [59, 60].

Dolomite is a naturally occurring mixture of calcium carbonate and magnesium carbonate. Limestone can be from natural sources or synthetic calcium carbonate from a nitrophosphate plant.

The chemical reactions that occur during the granulation process are shown in Equations 1-13 and 1-14 [59, 60]. The occurrence of these reactions would be minimal due to the small chance of reaction between the AN and the carbonate based filler without the presence of water. The small amount of ammonia which is produced from this interaction between the AN and the carbonate filler (without water) is indicative of limited reactions occurring.

$$2NH_4NO_{3(s)} + CaCO_{3(s)} \rightarrow Ca(NO_3)_{2(s)} + 2NH_{3(g)} + H_2O_{(g)} + CO_{2(g)} \quad \text{(Equation 1-13)}$$
$$2NH_4NO_{3(s)} + MgCO_{3(s)} \rightarrow Mg(NO_3)_{2(s)} + 2NH_{3(g)} + H_2O_{(g)} + CO_{2(g)} \quad \text{(Equation 1-14)}$$
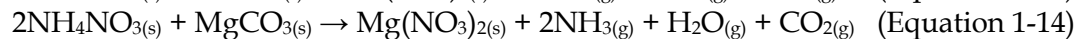
All reactions can only occur if water is present, e.g. dissolution of AN as shown in Equation 1-15.

$$NH_4^+ + NO_3^- + H_2O \rightleftharpoons H_3O^+ + NO_3^- + NH_3 \quad \text{(Equation 1-15)}$$
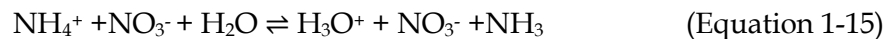
The reactivity of the filler is a measure of the extent of the reaction between AN and the carbonate compounds of the filler. It is expressed as the total weight percent of nitrate in the form of calcium nitrate and magnesium nitrate in the granules or in a lab test. A high reactivity means that more calcium nitrate and magnesium nitrate is formed [59, 60]. In general, the reactivity of a filler decreases with the calcium oxide content of the filler - with pure calcium carbonate at the highest, followed by limestone, dolomite and finally magnesite (magnesium carbonate) [59, 60].

While a certain low amount of calcium nitrate and magnesium nitrate improves granulation conditions by helping to form well-bound and round granules, a high content leads to products with a low critical humidity and a tendency to cake in storage.

Additionally, if the reactivity of the filler is too high then the rate of reaction must be limited. This can be achieved by changing the pH, the residence time (the time period between initial mixing and crystallisation in the granulator) or by blending fillers with high and low reactivity, such as ammonium sulphate which suppresses the conversion reaction. In most pugmill plants the AN melt and the filler are directly added to the granulator. This gives plants which use a pugmill system a relatively short and fixed residence time when producing AN [59, 60].

1.9 Additives and Anti-Caking Agents

AN and CAN are prone to a process that is called 'caking'. Caking is the formation of a solid mass due to the finely divided solids (whether powdered, granulate or prilled) losing their

fluidity and forming hard blocks or lumps. Caking is mainly due to the highly hygroscopic nature of AN.

Hygroscopicity is the ability of a substance to attract and hold water molecules from the surrounding environment. In the case of AN, water molecules are absorbed from the air causing some of the AN to dissolve. Upon evaporation the dissolved AN particles become fused to form a solid lump. Caking usually appears during storage, handling or transportation [61]. To prevent caking, additives are introduced during manufacture. These may be added to the prill internally, or applied as a coating [40, 49-51]. The purpose of anti-caking additives is to maintain fluidity of the material during storage and handling. Additives can be classified into two main categories, according to their method of application [61].

1.9.1   Inert Additives and Dusts

Inert additives are materials that are added (sub 1% quantity) to alter the physical properties of AN and CAN compositions, but are chemically inert and do not significantly alter the composition of the material. The additives used are normally low cost fine powders (sub-micron size) of low density with high adherence properties. Inert additives prevent the caking of AN and CAN by the following mechanisms [61]:

- Diffusion of the crystallising phase over the granule surface;
- Nucleation of small, finer crystals during a solution/recrystallisation process;
- Removal of moisture by absorption;
- Reduction in the formation of visible contact area; and
- Reduction of the tensile strength of the bond across the visible contact area.

However despite their simple application and advantageous properties, inert additives also have a number of disadvantages [61]:

- They have limited effect on formulations that have a high tendency to cake;
- It is often necessary to add a high concentration of these inert materials to minimise the hygroscopic nature of AN; and
- Inert dusts can build up an electrical charge due to static while in storage, which increases the handling difficulty.

Some of the common inert additives used to prevent caking in AN and CAN are shown in Table 1-5 [59, 60]:

Compound	Common Name	Formula	Additional Actions
Iron sulphate	-	$FeSO_4$	Granulation aid and micronutrients
Aluminium sulphate	Alum	$Al_2(SO_4)_3$	Granulation aid and stabiliser
Calcium sulphate	Gypsum	$CaSO_4$	Sulphur Fertiliser
Ammonium sulphate	-	$NH_4(SO_4)_2$	Sulphur Fertiliser
Magnesium sulphate heptahydrate	Epson Salt	$MgSO_4.7H_2O$	Micronutrients
Magnesium sulphate monohydrate	Kieserite	$MgSO_4.H_2O$	Micronutrients
Magnesium nitrate	-	$Mg(NO_3)_2$	Stabiliser

Table 1-5: Common inert additives used in AN and CAN

1.9.2   Organic Surfactants and Other Surface Active Agents

Surfactants are chemicals that alter the surface tension of a liquid by modifying the interfacial tension between two liquids or between a liquid and a solid. By reducing the surface tension between the liquid phase (protective substance) and the solid phase (AN or CAN prill) better surface adherence and internal penetration of the AN or CAN prill is achieved [61].

A surfactant molecule generally consists of hydrophilic and hydrophobic moieties; their classification is dependent on their polar head group.

A surfactant that carries no charge is termed non-ionic, while a polar head unit that carries a charge is termed ionic. The ionic classification can be further broken down into three groups [61]:
    1) Positively charged species are called cationic;
    2) Negatively charged species are called anionic; and
    3) Molecules that have both positive and negative charges are called zwitterionic.

1.9.2.1 Non-ionic surfactant
The largest class of non-ionic surfactants are the polyoxyethylene condensates, but these have only a moderate effect and are not widely used. Silicon fluids may be regarded as non-ionic surfactants, though their high cost limits their use on fertilisers.

Other non-ionic surfactants include fatty acid esters, substituted ureas, aldehydes and ketones with low molecular weight [61].

1.9.2.2 Cationic surfactants
Cationic surfactants are dominated by the fatty amines, especially those with long carbon chain lengths, such as octadecyclamine [61]. Caking is prevented by three different mechanisms:
    1) By the formation of a hydrophobic coating on the surface of the particles;
    2) By reducing capillary adhesion between particles; and
    3) By inhibiting nucleation or modifying crystal growth and reducing the number of contact points.

1.9.2.3 Anionic surfactants
Anionic surfactants are mainly alkyl and aryl sulphonates (e.g. sodium dodecyl sulphonate). Their hydrophobic nature increases the contact angle of fertiliser solution and reduces the tensile strength of caking bond [61]. Commonly used organic surfactants to prevent caking in AN and CAN are detailed in the Table 1-6 [61].

Name of Anticaking	Agents Physical State	Name of Suppliers
Lilamine	Semi-solid	Uhde Germany
Boroflow	Semi-viscous	Bombay Oil Ltd.
Filcon-108	Semi-solid	Transmetal India
Canpol-16	Semi-solid	Transmetal India
Lubrash AA-B	Semi-solid	Tashkent Oil (P). Ltd.
ZadeL-20	Liquid	Transmetal India
Lubrash-LL	Liquid	Tashkent Oil (P). Ltd.

Table 1-6: Commonly used organic surfactants to prevent caking in AN and CAN

1.10 Homemade Ammonium Nitrate

1.10.1 Precursors

The restrictions put in place by COAG have limited the availability of explosively viable AN. It should be noted that other nitrates such as potassium nitrate and sodium nitrate are also listed as chemicals of security concern by the Australian government but this approach of limiting access to these chemicals has not been adopted globally. Homemade AN can be produced from readily available materials purchased from agricultural, hardware and chemical suppliers (Table 1-7). Precursors that are typically used to manufacture homemade AN include potassium nitrate, calcium nitrate and ammonium sulphate [62].

Name	Formula	Available Form
Ammonium Hydroxide	NH_4OH	Liquid
Ammonia	NH_3	Liquid/Gas
Ammonium Chloride	NH_4Cl	Solid
Ammonium Sulphate	$(NH_4)_2SO_4$	Solid
Ammonium Bicarbonate	NH_4HCO_3	Solid
Nitric acid	HNO_3	Liquid
Potassium Nitrate	KNO_3	Solid
Sodium Nitrate	$NaNO_3$	Solid
Barium Nitrate	$Ba(NO_3)_2$	Solid
Calcium Nitrate	$Ca(NO_3)_2$	Solid
Sulphuric Acid	H_2SO_4	Liquid
Sodium hydroxide	$NaOH$	Solid/Liquid
Ozone	O_3	Gas

Table 1-7: Precursors for the homemade preparation of AN

1.10.2 Synthesis

Methods describing the production of homemade AN is readily available from online science and anarchist discussion boards, such as "Science Madness", and instructional videos are also available on YouTube [62]. Using the precursor materials identified in Table 1-7, a number of synthetic methods can be used to produce homemade AN, as shown in Table 1-8. As these reactions tend to be simple anion/cation exchanges, these reactions do not require any formal chemical training or dedicated laboratory equipment. The main limitation of these manufacturing techniques is that they produce relatively small amounts of material (kg scale), so it is generally not feasible to produce a large (ton scale) explosive devices using these methods.

Method	Chemical Equations
Cation/anion exchange with ammonium chloride	$MNO_3 + NH_4Cl \rightarrow NH_4NO_3 + MCl$ (M = metal (e.g. K or Na))
Cation/anion exchange with ammonium sulphate	$2MNO_3 + (NH_4)_2SO_4 \rightarrow 2NH_4NO_3 + M_2SO_4$ (M = metal (e.g. K or Na))
Ammonium hydroxide and nitric acid	$NH_4OH + HNO_3 \rightarrow NH_4NO_3 + H_2O$
React ammonia gas with ozone	$2NH_3 + 4O_3 \rightarrow NH_4NO_3 + 4O_2 + H_2O$
Acidification of ammonium bicarbonate, then reaction with potassium nitrate (2 steps)	$2NH_4HCO_3 + H_2SO_4 \rightarrow (NH_4)_2SO_4 + 2H_2O + 2CO_2$ $2KNO_3 + (NH_4)_2SO_4 \rightarrow K_2SO_4 + 2NH_4NO_3$
Formation of nitric acid, ammonia formation and subsequent reaction (3 steps)	$KNO_3 + H_2SO_4 \rightarrow HNO_3 + KHSO_4$ $NH_4HCO_3 + NaOH \rightarrow NH_3 + NaHCO_3 + H_2O$ $HNO_3 + NH_3 \rightarrow NH_4NO_3$

Table 1-8: Potential methods for the preparation of AN

1.10.3 Purification of Commercial Ammonium Nitrate

Another way of obtaining pure AN is by purifying commercially sourced CAN fertiliser. These purification methods remove additives that were included to reduce its explosive potential, such as calcium carbonate and anti-caking agents. Purification is achieved by dissolving the CAN prills in water then subsequent filtering or decanting of the liquid to separate out the insoluble calcium carbonate. Pure AN crystallises out when the water evaporates or the solution cools. A summary of possible purification methods is shown in Table 1-9 [62].

Published Methodologies For The Evaporation and Purification of Ammonium Nitrate	
Purification Method for AN	Dissolve AN in warm-hot water Filter solution to remove any particulates Air dry AN solution (or place in a desiccator) Dissolve AN in methanol. Filter solution and put in freezer (AN should drop out of solution).
Purification Method for CAN	Dissolve CAN in minimum warm-hot water Calcium carbonate forms an insoluble sludge at bottom of container Siphon off solution and evaporate water. The recrystallised AN will fall out of solution ready to be filtered.

Table 1-9: Published methods for the evaporation/purification of AN and CAN.

Similarly, relatively pure AN can be obtained from instant cold packs, marketed for relief of strain or sprain injuries (Figure 1-10). A video describing the purification of AN obtained from an instant cold pack has been uploaded to YouTube [63].

The method used is summarised below:
1) Mix water and AN (60:40), making sure all the AN is dissolved,
2) Remove the insoluble anti-caking agent by filtering through paper,
3) Evaporate the water from the AN solution to produce a fine white powder, then
4) Leave to air dry or dry in an oven.

Figure 1-10: Images of Instant cold pack which contains loose AN prills and a water capsule (A&B) and prills of AN obtained (C).

1.11 AN-Based Homemade Explosives

One of the main HMEs under investigation in this thesis, is an AN/fuel composition containing aluminium, namely AN/Al. Aluminium powder is added to AN-based explosives as a fuel source, which results in a considerable increase in the heat of explosion. This is largely due to the high heat of formation of alumina (Al_2O_3), which leads to a higher temperature [64]. Any aluminium which has not reacted in the detonation may be oxidized by atmospheric oxygen and induce 'post-heating' in the blast zone and may lead to an increase in the air blast [64].

Aluminium powder has a number of important characteristics, namely small particle size and shape. The small particle size of the aluminium powder allows for intimate contact with the AN and ensures an even distributed throughout the mixture, maximising the effectiveness of the fuel.

The aluminium powder is often coated with stearic acid, oleic acid or Teflon to protect the powder from oxidation, thus maintaining the viability of the fuel. The protective coating used may also be a useful identifier in the characterisation of explosive mixtures containing aluminium flakes and the identification of the source.

The heat of explosion (Q) can also be increased by adding to the explosive composition fuels which have a high heat of combustion (ΔH_c). Such fuels can be found with the lighter elements of the periodic table as shown in Table 1-10 [65].

Element	Relative Atomic Mass	ΔH_c(kJ mol^{-1})	ΔH_c (kJ g^{-1})
Beryllium	9.0	-602.1	-66.9
Boron	10.8	-635.0	-58.8
Lithium	6.9	-293.9	-42.6
Aluminium	27.0	-834.3	-30.9
Magnesium	24.3	-602.6	-24.8
Sulphur	32.1	-295.3	-9.2
Zinc	65.4	-353.2	-5.4

Table 1-10: Heats of combustion of some light elements.

Beryllium has the highest heat of combustion of the solid elements, followed by boron, lithium and aluminium. However, aluminium is utilised in explosive compositions as it is a relatively cheap and effective fuel. Aluminium is used in some commercial blasting explosives, particularly in water-based slurry explosives which contain a high percentage of ammonium nitrate.

1.11.1 Addition of Aluminium

The oxidation of aluminium is highly exothermic producing -1590 kJ as shown in reaction Equation 1-16.

$$2Al_{(s)} + \tfrac{1}{2}O_{2(g)} \rightarrow Al_2O_{3(s)} \quad \Delta H_c = \text{-1590 kJ} \qquad \text{(Equation 1-16)}$$
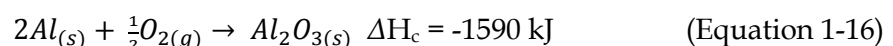
In an explosive composition, the aluminium reacts with the gaseous products particularly in oxygen-deficient compositions (where no free oxygen exists) as shown in Equations 1-17, 1-18 and 1-19 [65].

$$3CO_{2(g)} + 2Al_{(s)} \rightarrow 3CO_{(g)} + Al_2O_{3(s)} \quad \Delta H_c = -741 \text{ kJ} \qquad \text{(Equation 1-17)}$$
$$3H_2O_{(g)} + 2Al_{(s)} \rightarrow 3H_{2(g)} + Al_2O_{3(s)} \quad \Delta H_c = -866 \text{ kJ} \qquad \text{(Equation 1-18)}$$
$$3CO_{(g)} + 2Al_{(s)} \rightarrow 3C_{(s)} + Al_2O_{3(s)} \quad \Delta H_c = -1251 \text{ kJ} \qquad \text{(Equation 1-19)}$$
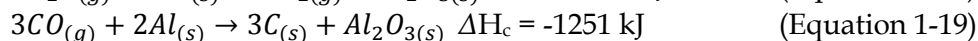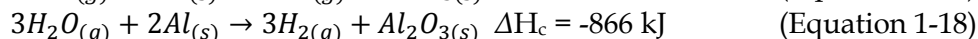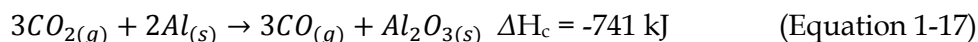
The volume of gas does not change in the first two reactions (i.e. 3 moles → 3 moles). Consequently, the increase in the output of heat from the oxidation of aluminium prolongs the presence of high pressures. This effect is utilised in explosive compositions for airblasts, lifting and heaving, or producing large underwater bubbles. However there is a limit to the amount of aluminium that can be added to produce an effective explosive composition as shown in Table 1-11 [65].

Aluminium % weight	Q (kJ kg^{-1})	V(dm^3 kg^{-1})	Q x V (10^4) (kJ dm^3 kg^{-2})
0	4226	750	317
9	5188	693	360
18	6485	586	380
25	7280	474	345
32	7657	375	287
40	8452	261	221

Table 1-11: Effect of the addition of aluminium in the heat of explosion and volume of gaseous products for TNT/Al

It can be noted that the heat of explosion increases with an increase in the quantity of aluminium. This increase in aluminium quantity however decreases the gas volume which results in the power (QxV) reaching a maximum value of 380 x 10^4 kJ (dm^3 kg^{-2}) at 18% wt. aluminium. The same effect can be observed for other explosive compositions containing aluminium, where a maximum value for the power can be achieved by adding 18-25% aluminium. In the case of pure AN/aluminium mixtures, 18.4% aluminium powder provides the optimum fuel/oxidiser mixture. It should be stated that other aluminium percentages (e.g. 10%) have proven to be effective.

1.12   Current Analysis Methods

A wide number of methods have been used for the identification of explosives and of post-blast residues. These include a simple hammer test to gauge the sensitivity, infrared (IR) and Raman spectroscopy to determine the functional groups, Ion Mobility Spectroscopy (IMS) to match drift times against an explosives database and wet chemistry kits which are based on colorimetric reactions [26, 66-69]. The Technical Working Group for Fire and Explosives (TWGFEX) Laboratory Explosion Group has also released guidelines for the forensic identification of post-blast residues [70].

These types of tests can be used to determine whether the explosive is a primary or secondary explosive and to which explosive class the sample belongs to. For a more definitive characterisation further examination using other techniques is required. The analysis steps for identification of pre- and post-blast explosives follow the general schematic shown in Figure 1-11 [20].

Debris Exhibit

Vapour Examination
Visual Examination
Microscopic Examination

Particles or Intact Explosives

Microscopic
Burning (IST)
SEM/EDX
IR
XRD

No Particles Found

Organic Extract
TLC
HPLC/TEA
GC/TEA
GC/MS
GC/FID
IR
Spot Tests

Water Extract
Spot Tests
IR
PLM
IC
EDX
XRD
TLC
HPLC
CE

Organic Extract
TLC
HPLC/TEA
GC/TEA
GC/MS
GC/FID
IR
Spot Tests
PLM
XRD

Water Extract
Spot Tests
PLM
IR
IC
XRD
TLC
CE

Figure 1-11: Flow chart for the examination of explosives and residues

The main techniques utilised by laboratories in the analysis of organic explosive residues are high performance liquid chromatography (HPLC) and gas chromatography coupled with a mass spectrometer (GC/MS). Chromatography separates the individual components of the explosive depending on their retention time in a column, while mass spectrometry of these fractions provides additional information. Ion chromatography (IC) is a technique which can be utilised in the analysis of inorganic ions and sugars. There is also a variety of other techniques utilised in the analysis of explosives and are detailed in Table 1-12 [26]. These analysis techniques are selective, sensitive and quite reliable. However these techniques generally take considerable time and normally require expert operators. Another limitation with these techniques is that the equipment can be expensive to purchase and operate.

Analytical Method	Target Explosives	Detection Limit	Advantages	Limitations
TLC	Organic	μg to sub-μg	Simple Inexpensive Rapid	Low resolution, susceptible to contamination
GC-ECD	Nitrogen-containing	pg	Rapid Selective Highly sensitive	Requires volatile analytes. Insensitive to hydrocarbons
GC-TEA	Nitro-containing	pg	Sensitive Selective	Requires volatile analytes. Expensive Limited to nitro compounds
HPLC-UV	Organic	ng	Sensitive	Low selectivity
IR	Organic and inorganic	μg	Characteristic spectra	Residues require separation prior to analysis
MS	Organic and inorganic	pg to ng	Selective Sensitive Reliable	
GC-MS	Organic (low bp) Plasticisers Stabilisers	pg to ng	Selective Sensitive Reliable	Limited to volatiles
LC-MS	Organic	pg to ng	Analysis of non-volatiles	Requires interface between HPLC and MS
SEM/EDX	Inorganic		Organic samples Inorganic samples	Expensive Requires expert operators

Table 1-12: Analytical methods for explosive residue analysis.

To establish the identity of a sample it is seen that the results have to be confirmed by two independent techniques in a process called "orthogonal" testing [26]. An example of this would be seen in an identification based on infrared spectrum and a chromatogram where retention times have been shown to be accurate and reproducible.

These techniques are able to identify the chemicals present in the explosive, however they do not readily provide sourcing intelligence and cannot link one sample to another, e.g. whether two samples came from the same batch, manufacturer or source materials. Two techniques that show the potential to be able to distinguish between samples and sources of explosives are IRMS and ICP-MS.

1.12.1 The Application of Intelligence to Forensic Investigations

The use of forensic science to assist with resolving intelligence gaps has previously been applied to issues such as the manufacturing and distribution of illicit substances. An example of this is drug profiling which is the extraction of a drug sample's chemical and/or physical profile, which can be used in the application of policies against the illegal use of drugs [71].

The profile of a drug is defined as a subset of the sample's characteristics specifically chosen with respect to the purpose of the process [71]. Class is defined as a group of samples which have similar profiles [71]. Profile and class can be chemical, physical or both, depending on the nature of characteristics considered.

In the analysis of various drugs, the scientist needs to be able to select target compounds specific for each drug type, while also identifying various cutting agents (which may be specific to manufacturer or dealer) [72].

Similar approaches could be applied to the origin of explosives, especially when homemade as these are more likely to contain components characteristic of the individual bomb maker.

The application of intelligence to drug investigations has been applied to heroin, which is a semi synthetic product derived from morphine (obtained from *Papaver somniferum*).

Differences in the agricultural and manufacturing procedures can alter the presence and concentration of opium alkaloids and the derivatives after acetylation. The appearance of diluents and adulterants can provide extra information about the origin and the trafficking of illicit heroin samples. All these parameters constitute a profile which can be used in comparative analysis [73].

Comparative analysis deals with the comprehensive examination of the chemical and physical characteristics of a drug exhibit. This consists of two steps: characterisation of the sample and interpretation of the data.

For the characterisation, a variety of analytical techniques (mainly chromatographic) can be applied. Often a combination of more than one technique will be used to obtain a significant number of data for an overall characteristic profile. The results of such multi-component analysis of complex drug mixtures are called chemical fingerprints or impurity profiles.

The overall purpose of comparative analysis is the derivation of strategic and tactical intelligence for developing or enhancing enforcement initiatives. An example of the utilisation of the comparative analysis of drugs (in this case heroin) for forensic intelligence purposes is highlighted below [73]:

Analytical techniques
- Visual inspection of colour;
- Thin layer chromatography (TLC);
- GC/MS (also headspace GC/MS);
- IRMS;
- Micellar electrokinetic capillary chromatography (MECC);
- Atomic absorption spectroscopy (AAS); and
- ICP-MS.

Interpretation of data
- Principal component analysis (PCA); and
- Hierarchical clustering analysis (HCA).

Conventional chemical profiling methods are based on determining and quantifying the illicit substance and identifying the organic impurities present, which has been detailed previously. Conventional physical and chemical profiling of illicit drugs aims to establish links among seizures in order to [74]:

- Identify dealer-user networks;

- Determine geographical origin of the seizure;
- Monitor the time a clandestine lab has been in operation;
- Gather sufficient information to create national and international drug databases; and
- Monitor the extent of international drug trafficking.

Similar data/information and observations would be useful in countering the proliferation of HME across given regions.

Various studies incorporating multiple analytical techniques and statistical analysis have been completed and have been instrumental in the development of forensic intelligence for combating the illicit drug trade [17, 71-84]. Over the past few decades, IRMS and ICP-MS have been applied to both licit and illicit drugs for the purpose of determining geographic origin and/or discriminating between batches or manufacturer [74, 80, 85-105]. The stable isotopes of carbon, nitrogen, hydrogen and oxygen have been investigated for these chemical profiling purposes.

Conventional chemical profiling of methamphetamine has been used for many years to determine the synthetic route employed and, where possible, to identify the precursor materials. In a recent study IRMS was investigated as a means of determining the origin of methamphetamine precursors (ephedrine and pseudoephedrine). Ephedrine and pseudoephedrine may be prepared industrially by many routes. They were able to determine that utilising the carbon, hydrogen and nitrogen stable isotopes in high purity methamphetamine samples allowed the origin of the ephedrine or pseudoephedrine precursor (being natural, semi-synthetic or fully synthetic) to be determined [93].

A similar study was also undertaken, however, focused on the isotopic fractionation during the precipitation of methamphetamine hydrochloride. The authors were able to determine that if the entire sample did not completely precipitate, it resulted in isotopic fractionation of the sample (in the case of nitrogen and hydrogen isotope ratios). They determined that homogenising several precipitates of the same samples may eliminate this fractionation. However in a clandestine situation this fractionation could lead to a greater than expected $\delta^{15}N$ and δ^2H variability between illicit samples of methamphetamine hydrochloride that have been synthesised from the same source of ephedrine [97].

Carbon and nitrogen isotope ratios have also been used to describe the growth conditions of marijuana. The authors of this paper were able to obtain a large number of samples from the USA, Mexico and Columbia. They were able to determine whether the marijuana was grown in an indoor or outdoor environment, and whether fertiliser was used. This kind of information would be of great use for intelligence purposes (especially determining geographical origin) [100].

IRMS analysis of illicit drugs has been shown to be useful in combination with the conventional analytical techniques. It is thought that the same approach could be undertaken with explosive samples to increase the amount of information available for forensic investigations.

The contribution of forensic science to crime analysis, investigations and forensic intelligence continues to be examined and as such, debates continue to occur as to how best integrate forensic science into intelligence led policing [17, 71, 106-110].

1.13   Isotope Ratio Mass Spectrometry

It has been suggested that it may be possible to discriminate between explosives by the natural variation between manufacturers, sources or batches by the analysis of their elemental profiles, elemental ratios or isotopic ratios [40, 44, 86].

IRMS is a technique that allows the comparison of two chemically identical compounds by comparing the ratio of stable isotopes which differ in the number of neutrons present in their nuclei, such as $^{13}C/^{12}C$ for carbon.

Each element has a major isotope (carbon (^{12}C), nitrogen (^{14}N) and oxygen (^{16}O)) and one or two minor isotopes (carbon (^{13}C), nitrogen (^{15}N) and oxygen (^{17}O and ^{18}O)). Table 1-13 details relative abundances of naturally occurring isotopes of elements that are analysed by IRMS [86].

Element	Isotope	Relative Abundance (%)
Hydrogen (H)	^{1}H	99.984
	^{2}H	0.0156
Carbon (C)	^{12}C	98.892
	^{13}C	1.108
Nitrogen (N)	^{14}N	99.635
	^{15}N	0.365
Oxygen (O)	^{16}O	99.759
	^{17}O	0.037
	^{18}O	0.204
Sulfur (S)	^{32}S	95.02
	^{33}S	0.76
	^{34}S	4.22
	^{36}S	0.014

Table 1-13: The relative abundance of the isotopes analysed using IRMS.

Delta notation (δ) is used to represent the ratio of the heavier isotope compared to the lighter isotope in the sample relative to a standard. Delta values can be calculated using Equations 1-20 and 1-21 and can be expressed in units of per mil (‰) [86, 105, 111-113].

$$ratio\ (R) = \frac{abundance\ of\ the\ heavy\ isotope}{abundance\ of\ the\ light\ isotope}$$
(Equation 1-20)

$$\delta = \left(\frac{R_{Samp}}{R_{Std}} - 1 \right)$$
(Equation 1-21)

Where: R_{Samp} = ratio of the heavy to the light isotope measured for the sample
R_{Std} = ratio of the international standard (defined by the International Atomic Energy Agency (IAEA)).
δ-values are commonly multiplied by 1000 so that they are reported in units of per mil.

Variations in the isotope ratios of materials are commonly expressed in ‰ difference from the following international agreed zero points:

- Hydrogen ($^{2}H/^{1}H$) – VSMOW (Vienna Standard Mean Ocean Water);
- Carbon ($^{13}C/^{12}C$) – VPDB (Vienna Peedee Belemnite);
- Nitrogen ($^{15}N/^{14}N$) – Atmospheric nitrogen (Air-N$_2$); and

- Oxygen ($^{18}O/^{16}O$) – VSMOW (Vienna Standard Mean Ocean Water).

As IRMS is used to determine the relative variations of isotopic ratios it is not necessary to know the absolute isotopic composition of materials used for calibration and quality control. These materials have defined or agreed δ values, for one or more elements which enable laboratories to obtain results that are both internally consistent and directly comparable with other laboratories [112, 114, 115].

A negative δ value indicates that the sample is light (or depleted) in the heavy isotope relative to the agreed zero point. Whereas a positive δ value indicates that the sample is isotopically heavy (or enriched) in the heavy isotope relative to the agreed zero point [86].

Natural variations occur in the isotopic composition and are due to fractionation effects, resulting in isotope ratio values that are characteristic of the origin, purity and manufacturing processes of the products and constituents. Isotopic fractionation can occur during chemical, physical and biological processes [86]. Figure 1-12 shows the potential variations in the carbon and nitrogen isotopic composition of a range of different materials [111].

IRMS can potentially be used to determine whether two chemically identical substances are in fact different (i.e. not from the same origin or source) through stable isotope fingerprinting. It has been suggested that the use of multidimensional isotopic analysis of a given material could provide the same discriminating power as seen in DNA analysis [105, 116].
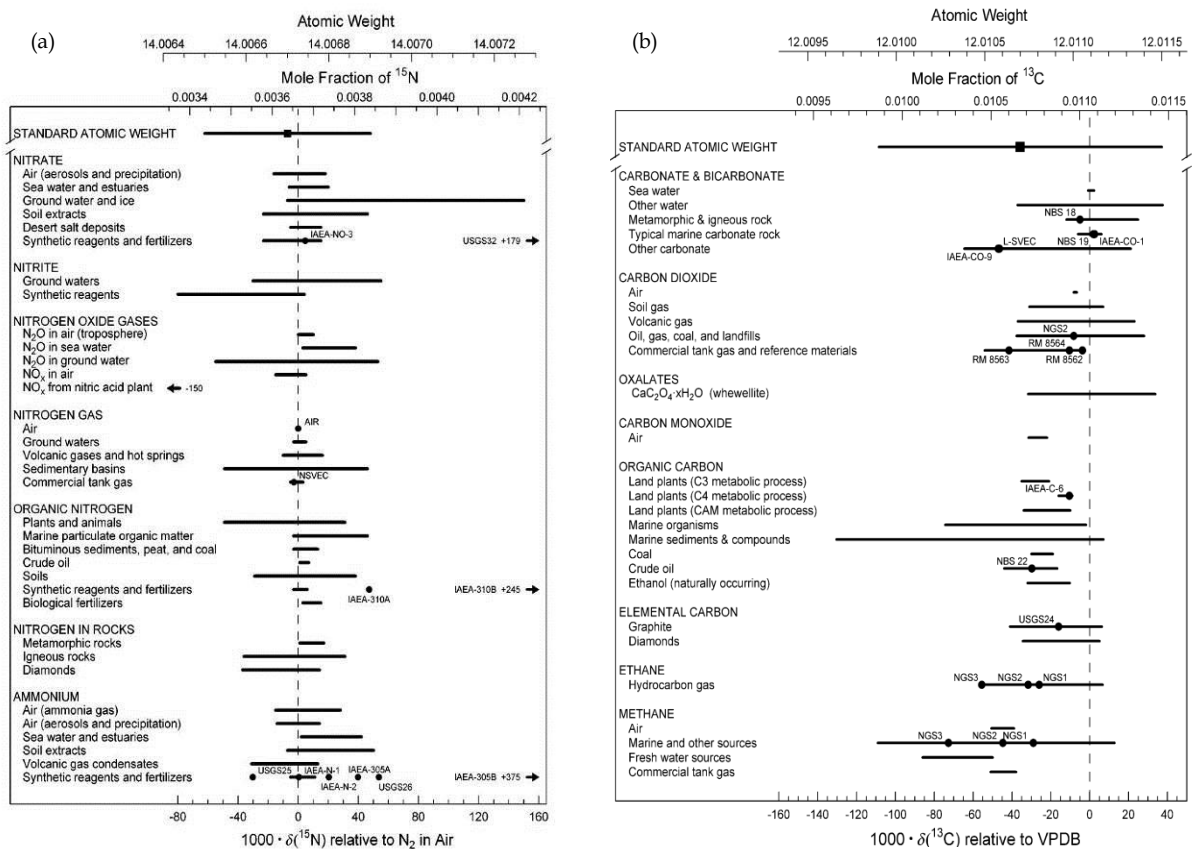
Figure 1-12: Potential variations in the nitrogen (a) and carbon (b) isotopic composition of a range of different materials

32

1.13.1 Instrumentation

IRMS instruments are specifically designed to measure precisely small differences in the abundances of isotopes such as $^2H/^1H$, $^{13}C/^{12}C$, $^{15}N/^{14}N$ and $^{18}O/^{16}O$ [112]. The instrument is different from a conventional mass spectrometer in the fact that they do not scan a mass range for characteristic fragment ions to provide structural information about the sample being analysed [86, 105].

An IRMS instrument comprises of three main sections: an ion source, a mass analyser and a multiple ion collection assembly. A schematic diagram of an IRMS is shown in Figure 1-13 [116], using carbon isotope ratio analysis as an example. In the analysis of carbon isotope ratios, the mass spectrometer monitors ions with mass m/z of 44, 45 and 46 which corresponds to the ions produced from CO_2 molecules containing ^{12}C, ^{13}C, ^{16}O, ^{17}O and ^{18}O in various combinations [112].

When gaseous samples enter the ionisation chamber of the mass spectrometer, the sample interacts with a focused electron beam, which is located in a high vacuum.

This interaction causes the loss of electrons from the molecules, and produces positive ions. These ions are then accelerated out of the chamber and through a flight tube between the poles of an electromagnet, where they are separated based on their mass to charge ratio *(m/z)*. The ions are collected by a collector array consisting of three Faraday cup collectors [86].

The Faraday cups are positioned so that the major ion currents simultaneously strike the middle of the entrance slit of their respective cup. Each ion contributes one charge and no stray ions or electrons can enter the cup. The accumulated charge is integrated typically every 0.1 seconds, by discharge through a high ohmic resistor, then amplified and digitised using a voltage-to-frequency converter, and then transferred to a computer. The computer integrates the peak area for each isotopomer and calculates the corresponding ratios [105].
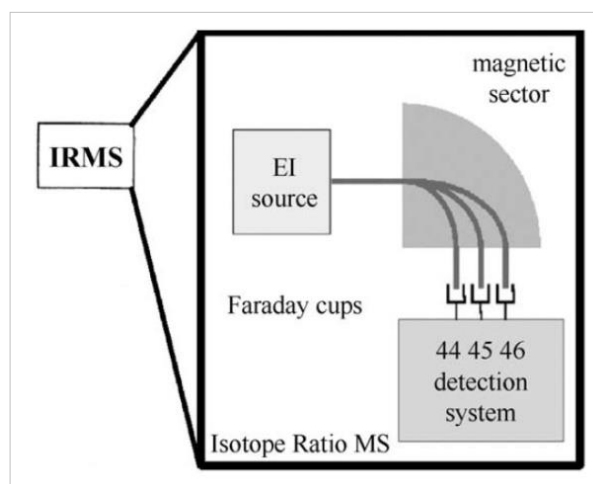
Figure 1-13: Schematic of an IRMS showing the configuration for $^{13}C/^{12}C$ isotope ratio measurements

The sample preparation technique utilised for the work described in this thesis was bulk stable isotope analysis (BSIA). It is based on the use of an elemental analyser, which is an automated sample preparation instrument for the conversion of the sample of interest into

simple gases for IRMS analysis. The isotopic values obtained from these analyses represent the isotopic composition of the mixture as a whole.

There are two common techniques for the preparation of samples for BSIA. These are quantitative conversion and quantitative combustion which are conducted at high temperatures.

1.13.1.1   Quantitative High Temperature Conversion

Quantitative conversion through the use of a high temperature elemental analyser is used for the analysis of hydrogen and oxygen isotope ratios of bulk samples. The sample is released into the reaction tube where the high temperature conversion takes place via a reduction reaction where organic oxygen is converted to CO by the Unterzaucher procedure [117].

1.13.1.2   Quantitative High Temperature Combustion

The solid sample is weighed into a tin capsule and loaded into the autosampler. The sample is dropped into the combustion reactor, which is held at 1050 °C. The sample and capsule melts in an atmosphere temporarily enriched with oxygen, where the tin promotes flash combustion. The combustion products are carried through an oxidation catalyst of chromium oxide by a constant flow of helium. The oxidation products are then passed through a reduction reactor at 650 °C containing copper granules, where oxides of nitrogen (NO, N_2O and N_2O_2) are reduced to gaseous nitrogen and the excess oxygen is removed.

The resulting gas species (CO_2, N_2, SO_2 and H_2O) are then passed through a magnesium perchlorate filter to remove water. The remaining CO_2, N_2 (if nitrogen was present in the sample) and sulfur dioxide (if sulfur was present in the sample) then pass through a short chromatographic column where they are time separated. They then pass through a thermal conductivity detector, and out of the vent on the top of the instrument. In the specific instrument used for this work, this vent is connected via one open split to the inlet of the mass spectrometer where carbon, nitrogen or sulfur isotope ratios can be measured against a pulse of working gas of known composition. Nitrogen and carbon isotopes can be analysed sequentially or separately. Sulfur is analysed separately. Figure 1-14 describes the various components of a combustion elemental analyser, used for nitrogen and carbon analysis [118].
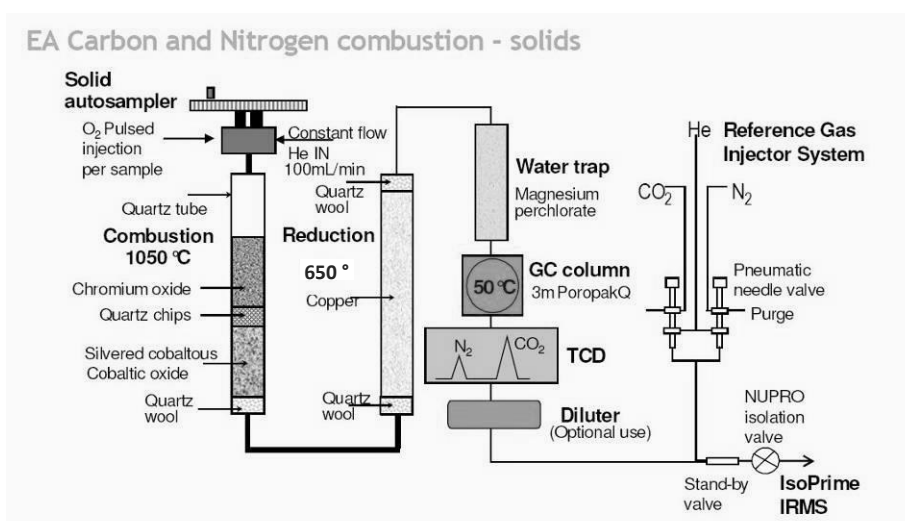
Figure 1-14: The various components of a combustion elemental analyser, used for nitrogen and carbon analysis

1.13.2 Common Forensic Uses of IRMS

1.13.2.1 *Drug Analysis*

Isotope analysis can be utilised as part of an analytical scheme for the analysis of licit and illicit drugs, for the purpose of determining geographic origin and/or discriminating between batches or manufacturer [49, 85, 86, 105]. A number of different illicit drugs have previously been analysed and these include marijuana, steroids, methylamphetamine, amphetamine, 3,4-methylenedioxy-*N*-methylamphetamine (MDMA), gamma-butyrolactone (GBL), cocaine and mephedrone [85, 93-100, 102-104, 119].

1.13.2.2 *Poisons*

Castor Oil *(Ricinus communis)* seeds contain the toxic plant protein Ricin, which is declared by the Chemical Weapons Convention as a schedule 1 agent, and has the highest priority on the list for terrorism agents by the United States Centre for Disease Control. Metabolomic and isotope analysis has been conducted on samples of interest to determine their origin [120, 121].

1.13.2.3 *Food Authenticity*

Isotope analysis has been incorporated within food research, and this analysis allows for quality control monitoring and proof of authenticity of various food products. Samples of interest to these studies have included sugars, sweeteners, tea, coffee, beef, juices and honey [86, 101, 105, 122-129].

1.13.2.4 *Other Materials of Forensic Interest*

Materials of interest (masking tape, cling film, duct tape, PVC tape, safety matches and plastic grip bags) can all be encountered at a crime scene, either as methods of packaging contraband or as materials utilised as part of arson. Therefore a requirement of forensic case work will be to compare seized materials found at different locations. IRMS has been applied as part of a greater analytical scheme which allows the comparison and discrimination of like materials [103, 104, 130-133]. Another example of the utilisation of such techniques was an investigation into whether post-blast plastic debris from IEDs could be analysed using IRMS. It was determined that in some cases a combination of δ^2H and $\delta^{13}C$ values could be utilised to determine an association between pre- and post-blast samples of an IED device (plastic radio) [134].

1.13.2.5 *Explosives*

One of the first papers published involving the use of stable isotope ratios as a tool for discrimination of explosives was written by Nissenbaum [135]. The carbon isotopic compositions of TNT from different countries were determined and the results indicated that the carbon isotopic ratio can be used to correlate or discriminate between samples. The author also identified possible sources of variation between samples, which were suggested to be due to different source materials and different manufacturing processes.

A significant amount of research conducted on explosives is performed by or in collaboration with the International Forensic Isotope Ratio Mass Spectrometry (FIRMS) network [102, 103] and by government agencies such as the United Kingdom's (UK's) Defence Science and Technology Laboratory (DSTL) [136], and as such a vast amount of results' are not available in the public domain.

In 1999, the Forensic Explosives Laboratory (FEL) which is part of DSTL commenced a three-year UK Home Office funded project. The aim of the project was to see whether it was possible to establish meaningful isotopic ratio measurements for different explosives samples; and to see whether these measurements would enable similarities and distinctions to be identified between explosive samples from different sources [137-139]. AN samples were analysed for their ^{15}N, ^{13}C and [18]O isotopic ratios. The authors determined that a combination of the isotopic measurements gives a better classification of the samples than the individual isotopic measurements. This combination of measurements suggested that not only can manufacturers be differentiated, but also the different grades of purity from the same manufacturer [139].

Research has also been conducted into the use of IRMS to determine whether there is an isotopic linkage between precursor and product in the synthesis of a high explosive [140, 141]. It was determined that by carbon and nitrogen isotope analysis of hexamine (precursor for the synthesis of RDX and HMTD) and RDX products, that a reproducible relationship between the reactant and the precursor is seen [140]. The synthesis of HMTD (using hexamine as a starting material) also yielded an isotopic relationship which may be utilised in the forensic investigations of homemade explosives [141].

An evaluation of isotopic analysis (^{13}C and ^{15}N) to link various Semtex samples was conducted, and the authors were able to determine that samples of Semtex could be differentiated using isotope analysis; however they also stated that to apply statistical analysis to such data, international collaboration is necessary [142].

Belanger discussed the analysis of the isotopic composition of various explosives (including AN) and the work confirmed that there was a range of carbon and nitrogen isotope values in the samples [143]. Lott *et al.* reported on the successful differentiation between sources of PETN, RDX, HMX and AN [144]. The effect of using different raw materials and different manufacturing processes in the isotopic composition of the product was evaluated [144].

Vitoria *et al.* described the detailed isotopic composition ($\delta^{15}N_{Bulk}$, $\delta^{15}N_{Nitrate}$, $\delta^{18}O_{Nitrate}$, $\delta^{34}S_{Sulfate}$, $\delta^{18}O_{Sulfate}$ and $\delta^{13}C_{Bulk}$) of 27 commercial fertilisers used in Spain. The AN-based samples which were analysed as part of this study were able to be discriminated based on the variables detailed previously. The authors stated that the multi-isotopic analyses allow us to see beyond the fractionation effects to the fertiliser stable isotope signatures and a better distinction from other anthropogenic contaminants [145].

The Australian Federal Police (AFP) conducted a series of evaluations to determine whether IRMS could supplement investigations by providing a level of discrimination not achievable by traditional forensic techniques [40, 49, 86]. This research developed an AN classification scheme based on nitrogen isotope ratios of Australian manufactured AN samples, however they also highlight the dangers of discriminating samples just on the $\delta^{15}N_{Bulk}$ values alone. In an effort to minimise these dangers, the authors investigated the use of isotopic ratios of other elements (e.g. $\delta^{18}O$ and $\delta^{2}H$) in conjunction with $\delta^{15}N$ values. A study was also conducted of Australian and overseas AN samples, the results indicate that it is feasible to discriminate samples from within a region, i.e. Australian AN samples, but the differentiation becomes less obvious when multiple regions are simultaneously compared. Pre- and post- blast $\delta^{15}N$ isotope analysis was also conducted on AN prills and recovered blast residues, the results indicated that the $\delta^{15}N_{Bulk}$ value was different as a result of the blast. This ultimately limits the technique to pre-blast energetic materials [40, 49].

Benson *et al.* investigated the potential of IRMS to differentiate between samples of TATP (prepared using different starting materials and methods). Samples of PETN were also subjected to isotope analysis to determine the usefulness of the technique. This research was able to demonstrate the successful application of IRMS to the analysis of explosives, which assists in discriminating samples from different sources [33].

In 2009, Widory *et al.* presented a multi-stable isotope (δ^{15}N, δ^{18}O, δ^{2}H and δ^{13}C) approach for evaluating the possibility of discriminating explosives. The results from 30 distinct PETN, TNT and ANFO samples show that different families of explosives are clearly differentiated by both their specific isotope signatures and their combination with corresponding elemental concentrations. They determined that coupling two or more of the studied isotopes yields an even more precise differentiation on the basis of their raw material origin and/or manufacturing process [146].

In 2009, McCurry *et al.* investigated the discrimination of AN, with the aim of distinguishing batches and sources, through the use of carbon and nitrogen isotopic ratios. While carbon is not directly a component of AN, a carbon source is often introduced as a coating to the AN prill, coating on the aluminium flake or as a calcium carbonate additive. Results indicate that IRMS had the potential to discriminate between batches, manufacturers and the source of samples based on variations in their intrinsic isotopic composition. Discrimination between batches and sources of AN and AN/fuel sources based on carbon and nitrogen isotope values was also demonstrated. It was also determined that AN/Al explosive mixtures could be linked to the original AN source used to prepare the mixtures. This technique thus has the ability to provide valuable forensic information to aid investigations and provide actionable intelligence [147].

Gentile *et al.* detailed a preliminary study which involved illustrating the potential of isotopic analysis and also the limitations of current isotopic knowledge when facing forensic problems [148]. This study focussed on the analysis of black powder, looking at intra-variability within a 1 kg sample, a batch and between batches of sample. The study also looked at the effect of storage conditions on the isotopic composition of the black powder. The results emphasise the need for a comprehensive knowledge of the intra- and inter-variability for samples, as well as factors which may affect the isotopic ratio. The information will allow an assessment of the value of the isotopic evidence in source discrimination studies [148].

UN is an improvised explosive that can be made from readily available materials. The carbon and nitrogen isotope composition of UN and its component ions (uronium and nitrate) could be utilised in forensic investigations. A recent study on UN was conducted and they were able to successfully separate UN into its component ions [30]. It was also indicated that the synthesis of UN under various conditions did not appear to affect the carbon and nitrogen isotope composition of the product UN and its component ions. The authors also found that carbon and nitrogen isotope ratios differ significantly between two field collected UN samples, as well as their own laboratory synthesised UN. These observed variations indicate that this type of approach is useful for discriminating between materials that are otherwise chemically identical [30].

Brust *et al.* detailed a study in which ICP-MS and IRMS were utilised for the chemical profiling of ammonium nitrate [149]. The study found that it was possible to discriminate between ammonium nitrate samples from different sources by using a combination of ^{15}N

and [18]O isotope ratios and trace element composition. Elements analysed as part of this study included magnesium, calcium, iron and strontium [149].

1.14   Inductively Coupled Plasma – Mass Spectroscopy

ICP-MS was developed as a commercial analytical technique in the early 1980s for the determination of trace elements. Strengths of this technique include [150]:

- Wide elemental coverage – most of the elements in the periodic table can be measured by ICP-MS;
- Performance – high sensitivity and low background signals combine to give very low detection limits;
- Fast analysis times – the simultaneous measurement of a large number of elements can take only about 4 minutes per sample; and
- Isotopic information – the isotopic composition of a sample can be determined for certain elements.

The elements that can be analysed by ICP-MS with detection limits at or below the parts per trillion (ppt) range is shown in colour in Figure 1-15. Elements that are in white are either not measurable by ICP-MS or do not have naturally occurring isotopes. The lines shown for each element depict the number and relative abundance of the natural isotopes for that element [151].

ICP-MS is seen as the premier technique for trace metal analysis. It provides greater sensitivity than inductively couple plasma optical emission spectroscopy (ICP-OES) and higher sample throughput than the sensitive but slow graphite furnace atomic absorption spectroscopy (GF-AAS) [150]. It is routinely used in medicine, quality control of pharmaceutical manufacturing, environmental monitoring and minerals exploration. The main drawback of ICP-MS is that it has limited tolerance to high sample concentrations due to the creation of blockages and decreased ion transmission from the deposition of sample residues.
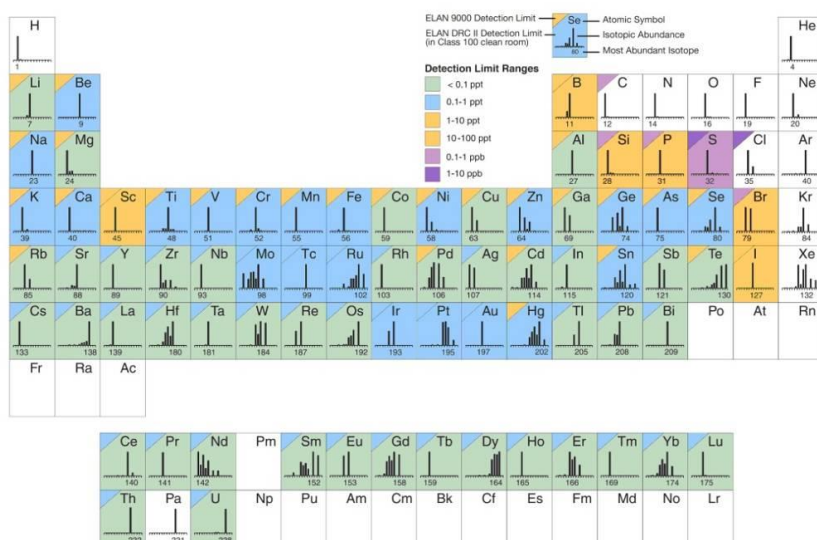
Figure 1-15: Elements determined by ICP-MS and approximate detection capability

An ICP-MS instrument consists of several distinct parts, with the processes that occur in the different parts depicted in Figure 1-16 [150].
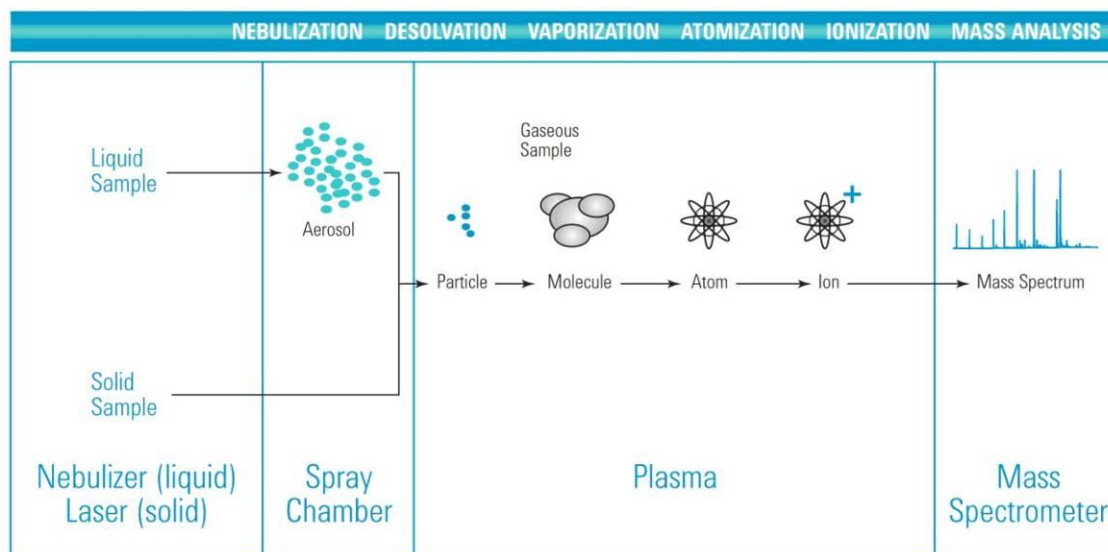
Figure 1-16: Schematic representation of processes in ICP-MS from sample introduction to mass analysis

The sample is usually introduced into the ICP as an aerosol, produced by passing a liquid sample through a simple concentric nebuliser. Alternatively, a relatively high-powered laser can be used to ablate material from the surface of solid to create a plume which is introduced into the plasma.

The sample aerosol is passed into the plasma, which is generated in a stream of argon contained in a quartz tube or "torch". The torch is located in the centre of a cooled copper coil, through which a high power, high frequency electric current is passed. The intense magnetic field created by the electric current causes collisions between free electrons and argon atoms, producing ions and more electrons until a stable, high temperature plasma is formed. The very high temperature of the plasma (up to 10,000 K maximum and around 7500 K in the central channel) means that the aerosol droplets are rapidly dried, decomposed, vaporised, atomised and then ionised.

The formation of ions from the sample atoms is achieved by the removal of a single electron. This occurs with varying ease and efficiency for different elements. This variation is usually quoted as the "ionisation efficiency" for each element, which is a function of the first ionisation potential of the element (the energy required to remove one electron from a neutral atom), together with estimated values for plasma electron temperature and density [150].

The positively charged ions that are produced in the plasma are extracted into the vacuum system, via a pair of interface cones. Electrostatic lenses keep the ions focused in a compact ion beam as they pass through the vacuum system to the final chamber, where the mass spectrometer and the detector are housed. The ion lenses perform a second, essential, function of separating the ions from the photons and residual neutral material.

There are three types of mass analyser that have been used with ICP-MS; these are quadrupole, magnetic sector and time of flight analysers. The most common analyser is the

quadrupole. The quadrupole uses a combination of direct current and alternating current electric fields to separate ions based on their mass to charge ratio.

Since the plasma produces almost exclusively singly-charged ions, the *m/z* is equal to the mass of the ion, making the spectrum simple to interpret. An electron multiplier detects each ion as it exits the quadrupole. The detector electronics count and store the total signal for each *m/z*, creating a mass spectrum. The spectrum that is produced provides a simple and quantitative representation of the sample. The magnitude of each peak is directly proportional to the concentration of an element in a sample; quantitative results are produced by comparing signal intensities to those generated by calibration standards.

1.14.1 Limitations of Inductively Coupled Plasma – Mass Spectroscopy for Analysis

ICP-MS is an immensely powerful multi-element analytical technique, but it does suffer from some well documented interferences, which can be especially problematic when complex and variable samples are analysed. In most cases the correct choice of operating conditions or element isotope mass minimises the impact of interferences.

Most interferences occur due to an overlap from a molecular (or polyatomic) ion at the same nominal mass as the analyte of interest. Commonly reported interferences can be broadly divided into:

- Those derived from the plasma and aqueous solution (plasma based), such as $^{40}Ar^{16}O$ overlap with ^{56}Fe. Often these are oxides in the form of MO^+. Plasma-based polyatomic ions are both predictable and reasonably constant, regardless of the sample matrix;
- Those derived from sample matrix components (matrix based), such as $^{35}Cl^{16}O$ and $^{32}S^{34}S$. Matrix based polyatomic ions are less predictable and vary with sample matrix components and their relative concentrations [152];
- Direct overlap from a different element with an isotope at the same nominal mass (isobars) – known as an isobaric interference (e.g. ^{114}Sn overall on ^{114}Cd); and
- Doubly charged species resulting from ions created by the loss of two electrons instead of just one. Because the quadrupole separates ions based on *m/z*, a doubly-charged ion (M^{2+}) will appear at mass *M/2*. An example of a doubly charged interference would be the $^{136}Ba^{2+}$ overlap on $^{68}Zn^+$.

It has been demonstrated that the MO^+ level is directly proportional to other matrix based interferences such as those derived from chloride and sulfate matrices. Thus a low level of MO^+ (typically CeO/Ce is measured since the CeO bond is very strong and CeO is stable in the plasma) is a highly desirable property in an ICP-MS instrument. The CeO/Ce ratio is often referred to as a measure of plasma robustness in ICP-MS. The most efficient ICP-MS plasma systems (those which create and maintain the highest effective plasma temperature) can decompose the sample matrix more effectively and so MO^+ levels are significantly lower than other systems. Generally if a high plasma temperature is maintained, most polyatomic interferences will be reduced, often to levels where in practice they become negligible. A more robust plasma (lower CeO/Ce) reduces the reliance on mathematical interference

correction equations, and also makes interference removal techniques (such as collision/reaction cells) more efficient [150].

Collision/reaction cells are also used to minimise spectra interferences from polyatomic ions. The cell is filled with a gas which removes the unwanted ions, either by chemical reaction or by reducing the kinetic energy of the larger polyatomic species below a certain threshold through collisions; ions with low kinetic energy are then prevented from reaching the detector by the application of electric fields. Helium is often used as the collision gas as it is inert (and therefore does not produce new interferences) and non-specific (removes plasma and matrix based interferences) [152].

Sample carry-over or memory interferences can occur which result from sample deposition on the skimmer and sample cones and also from build-up of material within the plasma torch and the spray chamber. The site where these effects occur is dependent on the element and can be minimised by a suitable rinse program.

1.14.2 Elemental Analysis as a Forensic Tool

Elemental analysis techniques have been used or postulated in a forensic context previously, including for energetic materials. In the majority of cases, the aim was to compare measured elemental profiles against a known database of authentic reference materials to determine or confirm the likely source of an unknown sample. Some examples taken from the recent literature are discussed in the following sections.

1.14.2.1 *Explosives and Gunshot Residue*

Trace elements in explosive compositions can originate from multiple sources, but will have little or no influence on its explosive effect. They can be included as impurities in the precursor materials used to prepare the explosives, or can be introduced during manufacturing through contamination by processing equipment. Incorporation into explosives can also occur after manufacturing by packaging, storage and handling. Trace elements can therefore by considered to give a convoluted record of both the original materials used in the manufacturer of the explosive and its history [153].

Identification particles (IPs) (which are commonly known as "tags") are added to some industrial explosives for the purpose of post-blast identification in the event of their misuse. They have a coding system based on the combination of metal oxides and their various concentrations which provides information on the place and date of manufacture.

A suitable analytical method has to be used for an accurate characterisation of these metal components in the particles in order to find the required information (place/year of production). One study focussed on developing a microwave digestion and flame atomic absorption spectroscopy (F-AAS) method for an accurate determination of certain metals in a few novel types of IP and applied to their characterisation. A total of 71 samples were analysed and classified by multivariate methods to verify the suitability of this procedure for the purpose of the identification of explosives [154].

Particle induced X-ray emission (PIXE) was investigated as a technique for the forensic analysis of high explosives by establishing whether trace elements can be used as 'fingerprints' for the year of manufacture of the explosives and their residues [153]. The authors concluded that PIXE has great potential for the analysis of trace elements in plastic

explosives. In particular, the results showed that PIXE has the potential to determine if a batch of PE-4 explosive was manufactured after 1985 and possibly even link it to a year of manufacture. Ashing of the sample pre-analysis has shown to improve the sensitivity of the technique to the trace elements, while retaining a correlation with their original concentration [153].

An investigation into a case involving the death of an individual due to injuries sustained from the explosion of a letter bomb was complimented by the utilisation of ICP-OES, sometimes called atomic emission spectroscopy (AES) analysis of trace metal residues. This was completed to provide information to identify the explosive material used in the device [155].

The elemental analysis of gunshot residue (GSR) is used as one of the tools in the interpretation of a criminal event. Some answers to the question of "accepted uniqueness" of GSR particles can be given by the quantitative determination of specific elements [156]. This is routinely completed using a scanning electron microscope combined with an energy dispersive X-ray detector (SEM/EDX), but ICP-MS and ICP-OES have gained popularity as methods that could be utilised for the analysis and classification of GSR [156-160].

1.14.2.2   *Determining Food Origin*

The globalisation of food markets and the relative ease with which food commodities are transported between countries has resulted in an increasing concern about the origins of food [128]. A vast number of research articles have been published detailing the use of natural abundance isotope variation and elemental concentrations as geographic "tracers" to determine the provenance of food [128]. This has spawned the term "food forensics" to describe this area of research. Examples of food types analysed using ICP-MS for food forensics studies include wine, tea, beef and cane/beet sugars [122, 123, 127, 128, 161]. The latter is particularly of interest, as sugars are often used as fuels in explosive mixtures.

1.14.2.3   *Illicit Drugs*

One area where the use of a chemical "fingerprint" to classify and compare unknown samples is relatively mature is in illicit drug analysis. Elemental profiling of illicit drug samples, in combination with other analytical methods and specific chemometric data processing techniques, has provided the possibility of gaining robust intelligence for criminal investigations. Elemental analysis techniques used include F-AAS, ICP-OES, ICP-MS and electrothermal atomic absorption spectroscopy (ET-AAS) [160-166].

For uncut (pure) samples, the trace elements are useful parameters for sample-to-sample comparison at the production level and to some extent determining the source of the drug. However to increase the bulk of the sample, the drug is commonly "cut" with adulterants (caffeine, paracetamol, phenobarbitone, quinine and sucrose are examples of adulterants) [162, 163]. The trace metals found in the sample are therefore unintentionally added as contaminants from the water, solvents and utensils used during the cutting process. As a result, these trace metals are the sum of impurities that are only useful for sample-to-sample comparison at the distribution/street level [164]. The presence or absence of elements in the final synthesised products could also be linked to the synthetic route, salting out method and potentially the solvents used in the precursor extraction process [165].

1.14.2.4   *Elemental Analysis of Homemade Explosive Precursor Materials*

HME use by politically disaffected and criminal organisations is prevalent as the precursor materials are often easily accessible in large quantities, cheap and require little technical

expertise to incorporate into improvised explosive devices. A large proportion of HMEs are mixtures containing AN, as discussed earlier.

Phosphate rocks are one of the main starting materials used in the production of CAN fertilisers via the Odda (or Nitrophosphate) Process [166]. The composition of phosphate rock largely depends on its type and origin. Sedimentary rocks contain a high concentration of heavy elements (uranium, thorium and rare earth elements), along with environmentally polluting elements (cadmium, arsenic, antimony, vanadium, chromium, zinc, copper and nickel). The amounts of these hazardous elements vary widely, not only among various phosphate rock sources, but also within the same deposit. There is currently no commercial means of completely removing these pollutants during the fertiliser manufacturing process [167]. There have been increasing concerns regarding the chemical impact of agricultural activities on the environment, so efforts have been made to identify any contaminants and their sources. For this reason a number of studies into the elemental composition of fertilisers have been conducted using F-AAS [167], ICP-MS [168-170], ICP-OES [168-171] and X-ray fluorescence (XRF) analysis [172]. Results have shown that elemental profiles for each fertiliser can be utilised to trace the source of phosphate rock used in the preparation of the fertiliser (the ability to distinguish between phosphorite and carbonatite derived fertilisers). Fertilisers prepared from carbonatites have higher concentrations of rare earth elements, whereas fertilisers derived from phosphorites have higher concentrations of metals of environmental concern.

To date the application of elemental analysis to aluminium samples has been limited to quality control of bulk alloys and has not been applied in a forensic context. Techniques used include F-AAS [173], XRF [174], spark-OES [174], laser-induced breakdown spectrometry (LIBS) [175, 176] and glow discharge mass spectrometry [177]. Trace metal impurities in the alloys alter the properties, possibly making them unfit for their purpose.

This previous research indicates that there is the potential to utilise ICP-MS as a technique for the analysis and characterisation of HME precursor and ingredient samples. The trace element profiles for each sample may provide an insight into the original source of the material and also information into the production methods used in the manufacturing of the material.

Intentionally Blank

2. Initial Investigation into the Forensic Profiling of Ammonium Nitrate and Calcium Ammonium Nitrate

2.1 Isotope Ratio Mass Spectrometry

The objective of this research was to develop a method for the measurement of bulk nitrogen ($^{15}N_{Bulk}$) and bulk carbon ($^{13}C_{Bulk}$) isotope ratios of AN-based materials, in order to determine whether IRMS could be used to discriminate or link samples of AN/CAN. Bulk analysis refers to an IRMS measurement performed on the sample as received without any further purification.

Caveat – Due to the nature of the samples analysed and limitations with the analytical instrumentation used, the isotopic data presented in this research is fit for the purpose of a comparative exercise (proof of concept) but should not be compared to data from other laboratories. All of the δ values displayed within this research have an associated error range (error bars) of ± 1 standard deviation.

2.1.1 Instrumentation

An IsoPrime (GV Instruments) Stable Isotope Ratio Mass Spectrometer (IRMS) was coupled to a EuroEA3000 Series (EuroVector) Elemental Analyser. The system utilised GV Instruments Micromass MassLynx mass spectrometry software [178]. The sampling technique utilised was continuous flow (CF-IRMS), which consisted of a helium carrier gas to carry the analyte gas into the IRMS ion source.

2.1.2 Nitrogen Isotope Analysis

For nitrogen IRMS analysis, approximately 80 µg of nitrogen is needs to be present in the sample. The calibrated laboratory standard for nitrogen analysis is urea (99.9% EuroVector, product code. E11003): $\delta^{15}N_{AIR}$ = -1‰. Samples were weighed into a tin capsule (5 x 9 mm Sercon) using a microbalance and then sealed for subsequent IRMS analysis. Each sample of AN/CAN was analysed in quadruplicate for nitrogen IRMS analysis.

Sample sizes needed for nitrogen-IRMS analysis of AN and CAN samples are detailed in Table 2-1

Sample	Description	% Nitrogen	Sample Mass (µg)
Ammonium Nitrate	-	34.99	229
CAN	80% AN + 20% $CaCO_3$	28	286
Urea	-	46.64	172
AN/Al	90% AN + 10% Al	31.49	254
CAN/Al	90% CAN + 10% Al	25.2	318

Table 2-1: Sample sizes needed for nitrogen IRMS

2.1.3 Carbon Isotope Analysis

For carbon IRMS analysis, approximately 20-30 µg of carbon is needs to be present in the sample. The calibrated laboratory standard for carbon analysis is sucrose (99.9% EuroVector, product code. E11017): $\delta^{13}C_{VPDB}$ = -11‰. Samples were weighed into a tin capsule (5 x 9 mm

Sercon) using a microbalance and then sealed for subsequent IRMS analysis. Each sample of AN/CAN was analysed in triplicate for C-IRMS analysis.

Sample sizes needed for carbon IRMS analysis of AN and CAN samples are detailed in Table 2-2.

Sample	Description	% Carbon	Sample Mass (µg)
Ammonium Nitrate	-	~ 0.1 %	15000
CAN	80% AN + 20% CaCO$_3$	2.4	1250
Sucrose	-	42.11	72
Calcium Carbonate	-	12	250
AN/Al	90% AN + 10% Al	~ 0.1 %	15000
CAN/Al	90% CAN + 10% Al	2.17	1382

Table 2-2: Sample sizes needed for carbon IRMS

2.1.4 Samples of Interest

The samples analysed by IRMS are shown in Tables 2-3 to 2-5.

AN and CAN samples were sourced from Australia and from locations around the world, these manufacturers use different manufacturing techniques and source materials, which may give rise to a distribution of isotopic ratios.

Code	Sample Details	Origin	Batch Number	Date
DSTO-AN-1	ORICA Nitropril	Australia	LOT 008/DFN/7/01	13/03/2009
FU-AN-1	Porous Prill (KT Process)	Australia	-	6/02/2009
FU-AN-2	Porous Prill (TOPAN Process)	Australia	-	6/02/2009
FU-AN-3	PPAN	Australia	-	6/02/2009
FU-AN-4	-	-	A826089	1/01/1997
FU-AN-5	-	-	36947	-
FU-AN-6	-	-	200089	1/12/1999
FU-AN-7	-	-	210714	1/01/2002
FU-AN-8	-	-	AF505117	-
FU-AN-9	-	-	AF503238	-
FU-AN-10	-	-	AF505117	-
FU-AN-11	-	-	102155	-
FU-AN-12	-	-	(10) 230305	1/08/2001
FU-AN-13	-	-	(10) 230305	1/08/2001
FU-AN-14	-	-	(10) 226544	1/08/2001
FU-AN-15	Porous AN (ANFO Explosive Grade) (Detoprill)	Australia	-	2005
FU-AN-16	Fertiliser AN (Nitram)	Australia	-	2005
FU-AN-17	Porous AN (ANFO Explosive Grade) (Detoprill)	Australia	-	2005
FU-AN-18	Porous AN (ANFO Explosive Grade) (Blue Ribbon)	China	-	2005
FU-AN-19	Porous AN (ANFO Explosive Grade) (Blue Ribbon)	China	-	2005
FU-AN-20	High Density for Emulsion (HDE grade AN)	France	-	2005
FU-AN-21	High Density for Emulsion (HDE grade AN)	France	-	2005
FU-AN-22	High Density for Emulsion (HDE grade AN)	France	-	2005
FU-AN-23	PPAN (KT Process)	Iran	-	6/02/2009
FU-AN-24	Porous Prill (KT Process)	Korea	-	6/02/2009
FU-AN-25	Chemically Pure High-Density AN	Korea	-	6/02/2009
FU-AN-26	General AN	Lithuania	-	2005
FU-AN-27	Unknown Process – Low Density AN	Mexico	-	6/02/2009
FU-AN-28	AR grade AN	Mexico	Lot SHBC5882V	-
FU-CAN-1	Fertiliser AN (Analysis: CAN)	Romania	-	2005
FU-CAN-2	Fertiliser AN (Analysis: CAN)	Romania	-	2005

Table 2-3: Sample descriptions of AN and CAN samples analysed

46

Code	Sample Details	Origin	Batch Number	Date
FU-AN-29	Low-Density AN	Russia	-	6/02/2009
FU-AN-30	High Density AN	Russia	-	6/02/2009
FU-AN-31	High Density AN	Russia	-	6/02/2009
DSTO-CAN-1	Incitec Pivot CAL-AM	Possible Ukraine	-	-
DSTO-CAN-2	Incitec Pivot CAL-AM	Possible Ukraine	-	-
FU-AN-32	Granulated AN	South Africa	-	6/02/2009
FU-AN-33	Porous Prill (KT Process)	Turkey	-	6/02/2009
FU-AN-34	Porous Prill (KT Process) (Sample from different batch)	Turkey	-	6/02/2009
FU-AN-35	General AN (Explosive Grade)	Ukraine	-	2005
FU-AN-36	General AN (Explosive Grade)	Ukraine	-	2005
FU-AN-37	Porous Prilled AN (PPAN)	USA	-	6/02/2009
FU-AN-38	PPAN	USA	-	6/02/2009
FU-AN-39	Ammonium Nitrate	-	-	2006
FU-AN-40	-	-	-	2007
FU-AN-41	-	-	-	2007
FU-AN-42	-	-	-	2007
FU-AN-43	-	-	-	2007
FU-AN-44	-	-	-	2007
FU-AN-45	-	-	-	2008
FU-AN-46	-	-	-	2008
FU-CAN-3	Analysis: CAN	-	-	2008
FU-AN-47	-	-	-	2008
FU-AN-48	-	-	-	2008
FU-AN-49	-	-	-	2008
FU-AN-50	-	-	-	2008
FU-AN-51	-	-	-	2009
FU-AN-52	-	Possible South African	-	2009
FU-AN-53	-	-	-	2011
FU-AN-54	-	-	-	2011
FU-AN-55	-	-	-	2011

Table 2-4: Sample descriptions of AN and CAN samples analysed

In addition to the AN and CAN samples listed above, an initial analysis of several HME formulations was attempted. These samples of HME were supplied as blind samples and were prepared by DSTO. In this initial analysis, care was taken to ensure that the fuel component of the HME did not contain any additional sources of nitrogen. These samples were analysed to determine if the HME production process induced any isotopic fractionation and also verify if IRMS was a potential technique to link or discriminate between samples of HME. A more in-depth analysis of HME formulations of AN/CAN-based explosives is discussed in Chapter 3.

Code	Description
DSTO-HME-1	10% Silveral 16 aluminium flake and 90% AN (DSTO-AN-1)
DSTO-HME-2	10% Silveral 16N aluminium flake and 90% AN (DSTO-AN-1)
DSTO-HME-3	10% Silberline DF1667 and 90% AN (DSTO-AN-1)
DSTO-HME-4	10% CAP45A aluminium powder and 90% AN (DSTO-AN-1)
DSTO-CAN-3 and 4	CAN (Odda Process)
DSTO-HME-5 and 6	CAN/Al reference material
DSTO-AN-2 and 3	Orica Nitropril (used in preparation of DSTO-HME-5 and 6)
DSTO-CC-1 and 2	$CaCO_3$ (used in preparation of DSTO-HME-5 and 6)

Table 2-5: Sample descriptions of AN and CAN based HME samples analysed

2.1.5 Detectable Variations in Ammonium Nitrate

At the precision of the instruments used in this research, samples will always contain some unique trace material or component that may be used to differentiate one material from another. These variations can be introduced at any stage of the manufacturing process or are present in the source materials.

2.1.5.1 Manufacturing Process

A close examination of the method previously described for the manufacture AN and CAN reveals several points in the manufacturing process that involve chemical reactions and physical processes where variation in samples may occur due to isotopic fractionation. Isotopic fractionation is any process, which alters the ratio of heavy and light isotopes of atoms within a material.

Isotopic fractionation is important as it is a mechanism by which variation is induced. By determining the ratio of heavy and light isotopes, an isotopic fingerprint for a particular material can be determined. This information may be used to identify where a particular sample may have been produced (i.e. source matching), or link samples that have the same isotopic fingerprint (batch matching).

The potential for fractionation (which will affect nitrogen, oxygen and hydrogen isotopes) exists at multiple stages during the synthesis on AN and CAN, for example:

- Isotopic exchange during the vaporisation of ammonia (liquid and vapour phase);
- Isotopic exchange between nitrogen oxide with oxygen in air and process water during synthesis of nitric acid;
- Isotopic exchange between the AN solution during concentration in the evaporation process;
- Isotopic exchange due to interactions of air with AN during the prilling process;
- Isotopic fractionation due to the high temperatures involved;
- Isotopic fractionation due to the loss of ammonia and AN in the air stream during prilling;
- Isotopic fractionation due to the drying process; and
- Isotopic fractionation due to exchange with air during storage.

Variations may also be imparted due to the differences in machinery and processing equipment used at each plant. Additionally, some of the materials used in the manufacturing process are recycled, such as water, air, steam and other chemicals [49].

2.1.5.2 Source Materials

The source of the starting materials used in the manufacture of AN and CAN are reflected in the isotopic composition of the final product [49].

Some sources of variation are outlined below:

- The hydrogen used in the synthesis of ammonia is derived from a local gas source;
- The hydrogen component of nitric acid is derived from process water, which is comprised of approximately 60% recycled reaction water, with the remaining 40% originating from a local water source; and
- The oxygen component of nitric acid is extracted from the air.

Due to the natural variations in the isotopic ratios of water, the isotopic values for this starting material utilised in the production of AN may also be varied. This variation may be

prevalent in the final AN produced, such that each fertiliser factory may be producing isotopically unique materials which can be differentiated.

The isotopic composition of atmospheric nitrogen has been adopted as the zero point for all nitrogen isotope ratio analyses as it does not vary measurably around the world or over time [112, 114]. Due to the fact that the isotopic composition of atmospheric air (with the exception of trace gases) has been demonstrated as homogeneous to the precision of the IRMS, the air utilised as a precursor material for the production of ammonia and nitric acid should not impart variability on the isotopic composition of the final product.

2.1.6   Nitrogen Isotope Analysis Results for All AN and CAN Samples

The $\delta^{15}N_{Bulk}$ values obtained for 71 AN and CAN samples analysed is shown in Figure 2-1. The range of $\delta^{15}N_{Bulk}$ values obtained for AN samples was ($\delta^{15}N$ = +8.930 to -2.36‰) and the range of $\delta^{15}N_{Bulk}$ values obtained for the CAN samples was ($\delta^{15}N$ = +3.35 to -0.9‰). A proportion (88.7%) of the $\delta^{15}N_{Bulk}$ values obtained in this research project corresponds to the range of $\delta^{15}N_{Bulk}$ values obtained in the previous research task undertaken by Benson *et al* [40, 49].

Samples FU-AN-33 and FU-AN-34 are porous AN prills that were produced in different batches from the same manufacturer. The samples were made using the KT process by a manufacturer based in Turkey. Isotopically these two samples are indistinguishable, the $\delta^{15}N_{Bulk}$ values obtained were +1.54 and +1.61‰ respectively. The results obtained in this study indicate that that the isotopic fractionation is consistent across different batches of AN produced by the same manufacturer, which would be due to the use of the same precursor material and manufacturing process. However this finding would need to be qualified via a long term study analysing multiple samples from AN manufactures.

Two samples of analytical reagent (AR) grade AN, labelled FU-AN-8 and FU-AN-10, have quite different values for their $\delta^{15}N_{Bulk}$ analyses when compared against the other 69 samples. The $\delta^{15}N_{Bulk}$ values obtained for both these samples were approximately +8.9‰, which indicates that these samples are isotopically enriched in ^{15}N. This highly positive $\delta^{15}N$ value may indicate that the AN was prepared from different sources of ammonia and nitric acid i.e. not prepared on-site using the same nitrogen source, as mentioned in Chapter 1.

The samples identified as DSTO-HME (1 to 4) are of interest as these HME samples were prepared using the same source AN, DSTO-AN-1. The only variation between these samples is the aluminium fuel source used. The $\delta^{15}N_{Bulk}$ values obtained for the four DSTO-HME samples ($\delta^{15}N$ ≈ +0.66‰) are isotopically indistinguishable from the source AN, DSTO-AN-1 ($\delta^{15}N$ ≈ +0.69‰). This result shows how it may be possible to link like samples and identify the source materials. However care should be taken with this assessment as the aluminium fuel sources used in these samples do not contain any source of nitrogen and the processes used in their manufacture would not lead to isotopic fractionation.
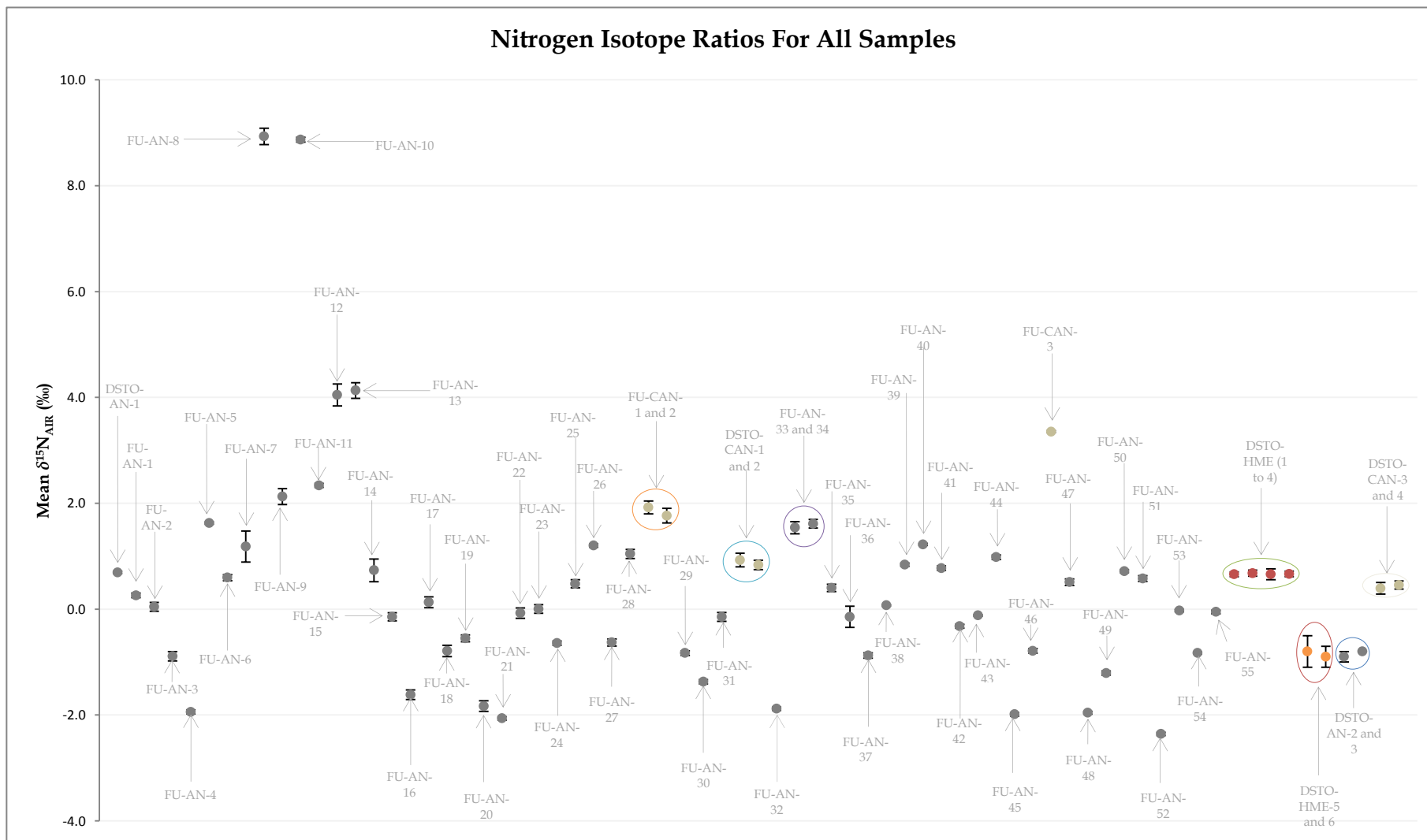
Figure 2-1: Bulk nitrogen IRMS results for AN and CAN samples

2.1.7   Carbon Isotope Analysis Results for All AN and CAN Samples

The bulk carbon isotope analysis of AN has previously been mentioned as a potential variable which could be utilised for the discrimination of samples of AN [49, 139].

In the case of AN, carbon is generally present as a coating agent on prills (as discussed in Chapter 1). AN prills may have a carbon content as high as 0.29% [179]. For example the TOPAN process utilises lilamine in paraffin oil as a coating agent and this amount of carbon is sufficient for carbon isotope analysis. It should be noted that not all types of AN samples tested have coating agents added, this is especially true of the AR grade ANs tested. Despite this, the presence or omission of a coating agents (and subsequently carbon) can also be used as a parameter for the discrimination of AN samples.

For CAN samples, the main source of carbon is calcium carbonate. CAN samples can contain up to 25% calcium carbonate, which is sufficient for carbon isotope analysis. Therefore the bulk carbon isotope value obtained from CAN samples is directly attributable to the carbonate source, and can be used for the discrimination of CAN samples.

The $\delta^{13}C$ values obtained for the AN and CAN analysed is shown in Figure 2-2, due the lack of carbon present in some samples only 43 of the 71 samples analysed gave a $^{13}C_{Bulk}$ value. The range of $\delta^{13}C_{Bulk}$ values obtained for AN samples ranged between -37.26 to -23.11‰ and the range of $\delta^{13}C_{Bulk}$ values obtained for the CAN samples was -37.58 to -3.00‰. The large error bars indicate that there is a higher degree of variability in the $\delta^{13}C_{Bulk}$ values obtained, this is due to the small amount of carbon being analysed. This limitation needs to be understood when attempting to use $\delta^{13}C$ values for differentiating samples of AN and CAN.
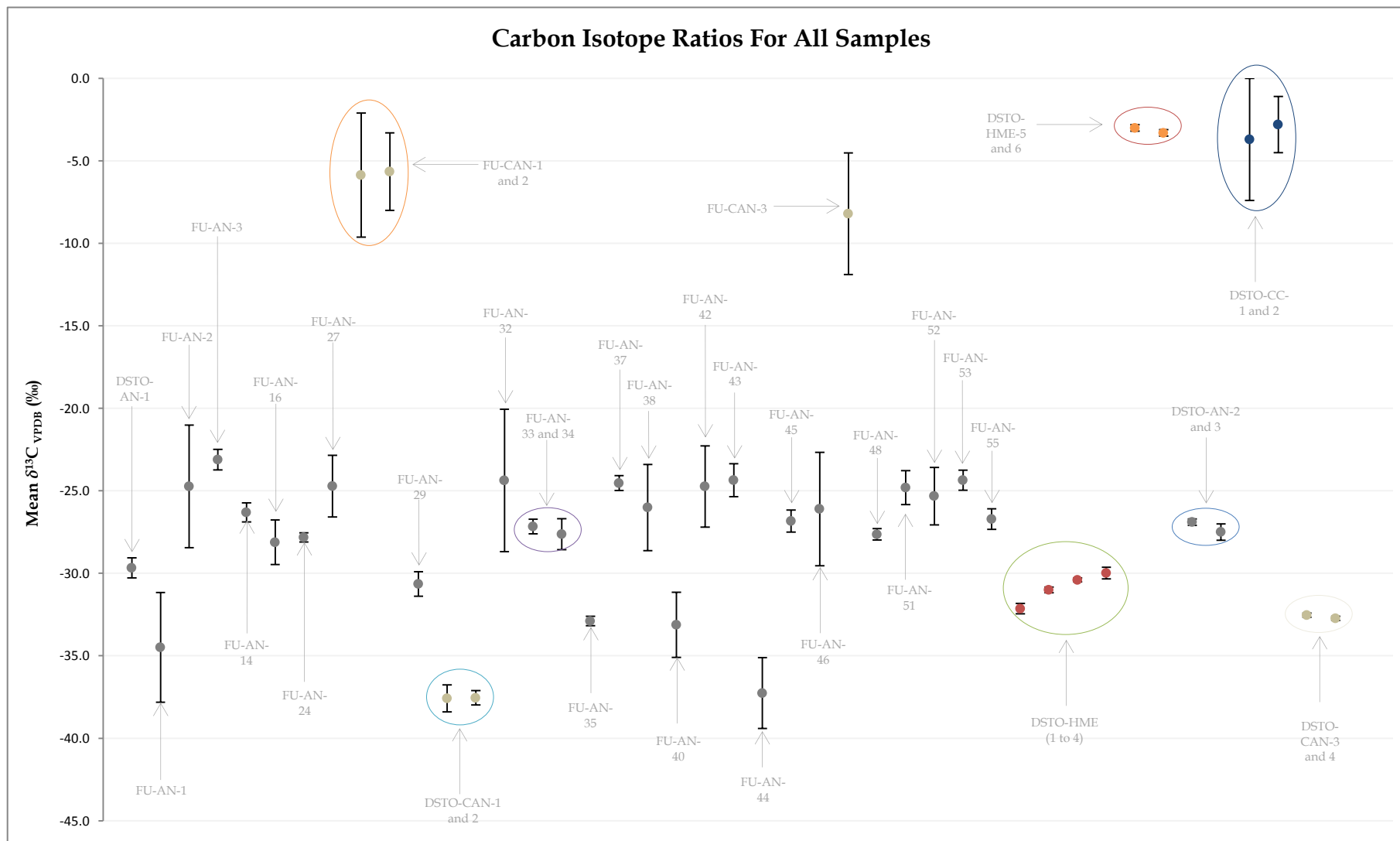
Figure 2-2: Bulk carbon IRMS results for AN and CAN samples

The samples identified as DSTO-AN-1 and DSTO-HME (1 to 4), which were previously identified in the $^{15}N_{Bulk}$ analysis (Section 2.1.5) are highlighted in Figure 2-2. The $^{13}C_{Bulk}$ values obtained for these samples show a slight variation, as shown in Table 2.6. This difference is due to the presence of carbon based protective coatings used on aluminium powders and flakes to protect the material from oxidation. The HME samples were prepared from different sources of aluminium powder which utilised different coating agents, namely stearic acid, oleic acid or Teflon$^{®}$. The inclusion of coating agents to aluminium powders will generally add about 0.1% carbon to the HME; however even at this level, the results obtained indicate the $\delta^{13}C_{Bulk}$ value will be altered, and should be taken into account when using the bulk value for comparing samples.

Sample	$\delta^{13}C_{VPDB}$ (‰)
DSTO-AN-1	-29.67 ± 0.61
DSTO-HME-1	-32.14 ± 0.32
DSTO-HME-2	-31.01 ± 0.17
DSTO-HME-3	-30.40 ± 0.12
DSTO-HME-4	-29.99 ± 0.35

Table 2-6: $\delta^{13}C$ values for DSTO-AN-1 and DSTO-HME (1 to 4) samples.

Based on the result obtained from this study, the determined $\delta^{13}C_{Bulk}$ values are still a useful variable for differentiating AN-based HME, however a thorough understanding of the materials present and their effect of the bulk isotope value obtained is needed.

2.1.8 Carbon and Nitrogen Isotope Results for Selected CAN Samples

Thus far, we have only compared each sample on the basis of a single element. Analysis of multiple elements, such as the nitrogen and carbon isotopic value, may enhance the ability to discriminate CAN samples to enable the easy visualisation of samples originating from different sources. In order to test this, the $^{15}N_{Bulk}$ and $^{13}C_{Bulk}$ values for nine CAN samples were analysed, and plotted on the same graph, as shown in Figure 2-3.

The combination of nitrogen and carbon isotope results showed linkages and grouped the following samples:

- FU-CAN-1 and FU-CAN-2
    - Two samples of CAN sourced from Romania
- DSTO-CAN-1 and DSTO-CAN-2
    - Two samples of CAN sourced from Ukraine
- DSTO-CAN-3 and DSTO-CAN-4
    - Two samples of CAN sourced from a fertiliser plant which uses the Odda process
- DSTO-HME-5 and DSTO-HME-6
    - Two samples of CAN/Al prepared in-house at DSTO.

These results demonstrate that for samples in which no isotopic fractionation has occurred, the combination of carbon and nitrogen analysis produces distinct clusters, which enable the easy identification of samples that are of similar origin.
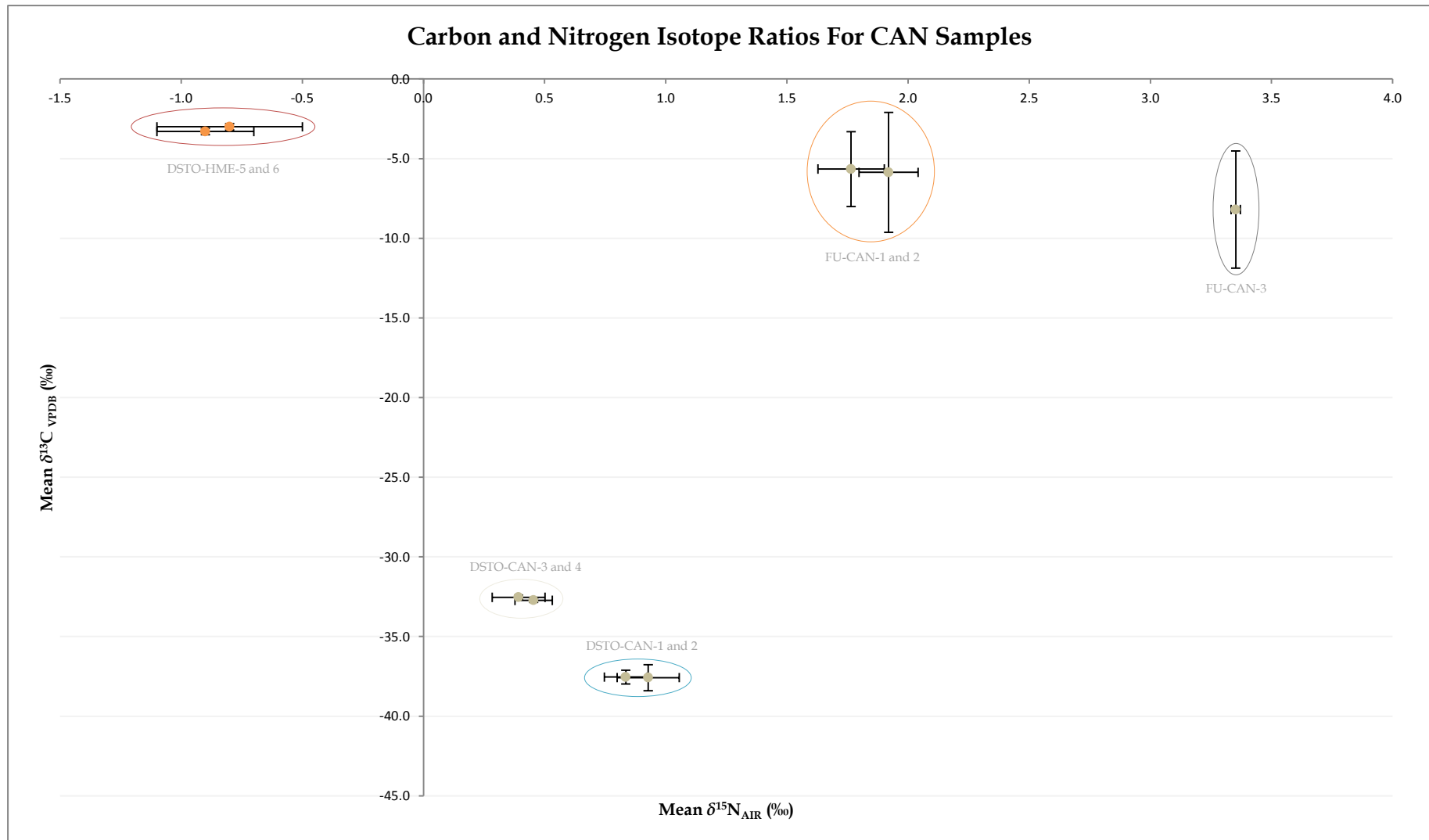
Figure 2-3: Bulk nitrogen and carbon IRMS results for selected CAN samples

2.1.9   Carbon and Nitrogen Isotope Results for AN Samples

Having demonstrated the benefit of combining both nitrogen and carbon isotope analysis, which leads to the formation of distinctive clusters, as similar approach was attempted to show cluster linkages of AN samples. The results obtained are shown in Figure 2-4, which depicts the clustering of thirty-two different AN samples that have been analysed.

The combination of nitrogen and carbon isotope results saw the formation of some clustering amongst the samples analysed. Most notable was the previously identified samples, DSTO-AN-1 and DSTO-HME (1 to 4), which were prepared from the same source AN (Orica Nitropril). Similarly, FU-AN-33 and FU-AN-34, the two samples of Turkish AN Prill formed a tight cluster.

The research conducted on the analysis of the bulk isotopic value for nitrogen and carbon demonstrates the potential use of IRMS to discriminate or link samples of AN/CAN and AN/CAN-based HME.

The analysis of other elements, such as oxygen, was also considered. However due to the hygroscopic nature of the samples, oxygen measurements would be challenging to interpret. Oxygen isotope analysis was not undertaken as the results obtained may be indicative of the storage and handling of the sample prior to analysis rather than its synthesis.

This initial study has highlighted the potential in utilising IRMS for the discrimination of precursor materials (and thus identification of AN source). However more rigorous examination of HME samples with different fuel types will need to be undertaken to determine the full potential of IRMS as a technique for linking HME sample to their precursor materials.
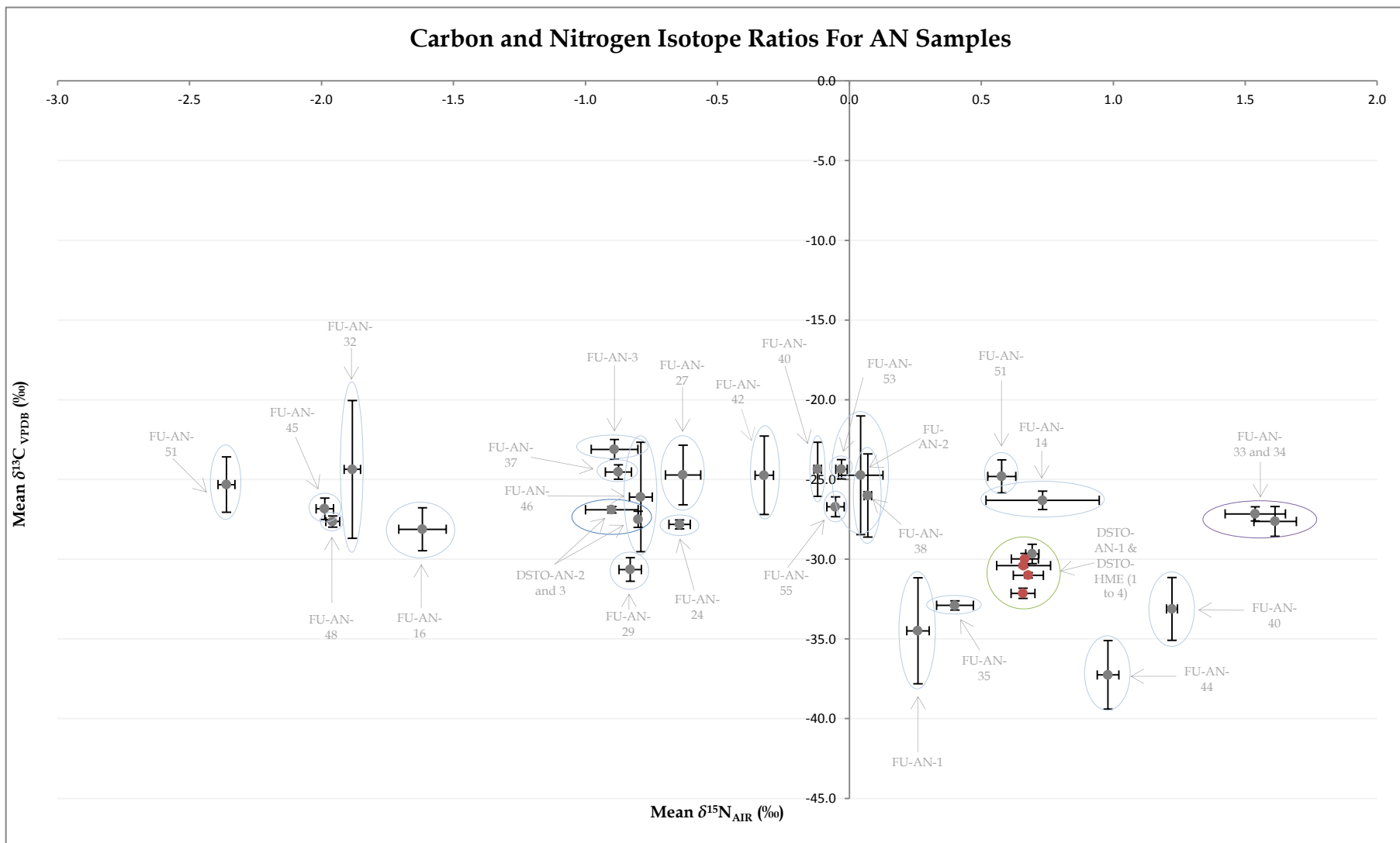
Figure 2-4: Nitrogen and Carbon IRMS results for AN samples

2.2 Inductively Coupled Plasma – Mass Spectrometry of AN and CAN

An investigation into the suitability of ICP-MS as a technique for the forensic analysis of precursor materials and the corresponding explosive sample was undertaken. The aim of this work was to establish whether trace elements can be used to develop a chemical "fingerprint" of a sample, which can be used to link and discriminate between samples. In order to achieve this aim, a robust analytical method was developed and validated for an Agilent 7500cx ICP-MS instrument.

2.2.1 Experimental

2.2.1.1 Instrumentation

The instrument used to develop these methods was an Agilent 7500cx, which is a quadrupole inductively coupled plasma mass spectrometer, a schematic of the internal componentry is shown in Figure 2-5 [150].
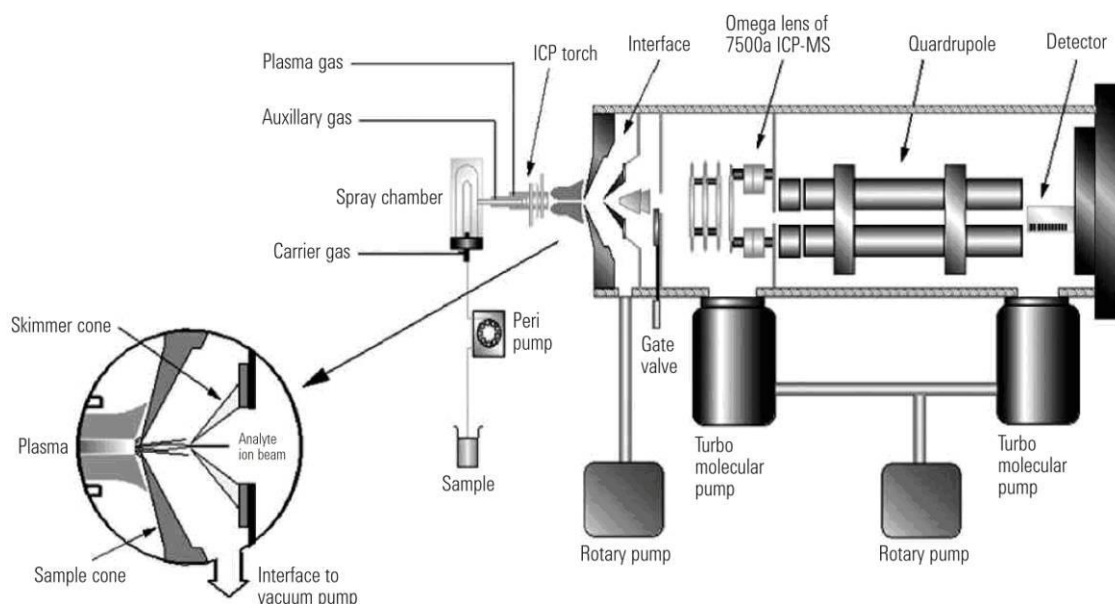
Figure 2-5: Schematic diagram of Agilent 7500 series ICP-MS instrument

Before each analysis, the ICP-MS was tuned using a multi-element standard solution containing 1 µg/L each of Li, Y, Co, Ce and Tl. This is performed to optimise sensitivity across the mass range of interest (^{7}Li, ^{80}Y and ^{205}Tl) and minimise doubly charged (M^{2+}) and oxide species levels (MO^+) [180]. Tables 2-7 and 2-8 show the specific conditions and programs used for the development of this ICP-MS method.

ICP-MS Specifications	
Instrument	Agilent 7500cx
Plasma forward power	1.5 kW
Carrier gas	0.9 L/min
Makeup gas flow	0.12 L/min
Nebuliser pump	0.1 rps
Spray chamber temperature	2°C
Sampling depth	9.5 mm
Nebuliser	Glass concentric
Spray chamber	Scott double pass
Sample cone	Nickel
Skimmer cone	Nickel
Octopole Collision Cell System	
Helium gas flow	4.5 mL/min
Data Acquisition	
Detector mode	Dual Mode (Pulse Counting and Analogue)
Replicate integrations	3
Mass range	2–260 *amu*
Integration time	Element dependent

Table 2-7: Operating conditions for the ICP-MS instrument

Typically utilised ion counting detectors are ideal for measuring low count rates, however they are not suitable for very high ion count rates as the detector becomes "saturated" and fails to register some of the ions, leading to a non-linear response. To overcome this problem, ICP-MS detectors are able to operate in "extended dynamic range" or "dual" mode, to allow the measurement of higher count rates. These dual mode detectors use pulse counting at lower count rates (up to a few million counts per second) and then, at high count rates, switch to analogue mode, in which the current generated by the electron stream is measured, rather than the pulse that derives from each individual ion impact [150].

Peristaltic Pump Program			
Before Acquisition			
Uptake speed	0.30 rps		
Uptake time	45 sec		
Stabilisation time	60 sec		
After Acquisition (Rinse Port)			
Rinse speed	0.30 rps		
Rinse time (Sample)	45 sec		
Rinse time (STD)	60 sec		
After Acquisition (Rinse Vial)			
	Step 1	**Step 2**	**Step 3**
Rinse vial	1 (10% HNO$_3$)	2 (10% HNO$_3$)	3 (10% HNO$_3$)
Rinse speed (rps)	0.30	0.30	0.30
Rinse time (sec)	30	30	30

Table 2-8: Peristaltic pump program parameters

2.2.1.2 Sampling and Contamination

Consideration must be given to the sample preparation process in order to efficiently deliver the analytes of interest to the plasma for ionisation. Generally samples must be dissolved so they can be introduced as an aerosol in a process known as digestion. The most common method is to use strong acids and heating to effect the digestion, however the most appropriate choice of acid depends on the analyte. For example, hydrochloric acid should be avoided where the analysis of silver is required due to the formation of insoluble silver

chloride. Similarly sulfuric acid should be avoided where calcium, lead or barium are important analytes due to the formation of insoluble precipitates. Nitric acid is commonly used, as most nitrate salts are soluble, but care should be taken with samples containing tin, as insoluble tin oxides may be formed by oxidation.

Two commonly used techniques to digest samples include open vessel digestion and microwave digestion. However in the case of open vessel digestion, care must be taken to avoid contamination from airborne particulates or cross contamination from adjacent samples if multiple samples are being prepared. A further consideration is the potential for loss of volatile analytes from open acid digestions, particularly if the sample is allowed to go dry during the digestion.

The digestion acids and reagents used are a significant potential source of trace metal contamination. ICP-MS is capable of extremely low detection limits for most elements, but the requirement for high purity reagents is determined by the required reporting limits of any given application, rather than the measurement capability of the instrument.

Generally for trace level work, water with an 18 MΩ.cm^{-1} resistivity and very low levels of trace metal ions is needed. Acids used in dilution or digestion must be sufficiently low in target trace metals as to not adversely affect the assays, this requirement generally necessitates the use of high purity, trace metals grade acids.

Contaminated glassware and plastic ware is another common source of trace impurities. These impurities are introduced during sample collection, storage, transport and sample preparation. Impurities may also come into direct contact with the sample on labware and equipment such as pipettes, pipette tips, gloves, beakers and spatulas.

Personal contamination is contamination introduced to the sample by exposure to the analyst. It can be in the form of fingerprints and flakes of dead skin, hair, lint from clothing, and aerosols generated from coughs and sneezes which naturally contain high levels of many metals. This can be exacerbated by the use of various lotions and cosmetics. Many shampoos contain zinc, selenium or lead. Skins creams contain aluminium, titanium, zinc, magnesium and many trace components [181-184]. Jewellery can also contribute to trace (µg/L or ppb) metal background. For these reasons, it is always advisable to wear a clean, lint-free laboratory coat and metal free gloves when handling samples. Shoe covers, bonnets, facemasks and full body suits may be necessary for ultra-trace (ng/L or ppt) analysis.

2.2.1.3 Reagents and Labware
For the preparation of standards and samples all types of glassware and metal were avoided to prevent possible contamination. One plastic bottle was acquired for making solutions up to volume. This was washed once with 69% HNO_3 and twice with 10% HNO_3, then immediately before use the bottle was washed with water.

For digestion of the samples 15 mL and 50 mL polypropylene digestion vials (Environmental Express) were purchased from DKSH (Hallam, Victoria, Australia) and used after rinsing with HNO_3 and water as above).

The acid used for digestions, dilutions and washings was nitric acid, 69%, for trace analysis (Scharlau Chemie), obtained from Chem-Supply (Gillman, South Australia, Australia). The

water used for this analysis was MilliQ water (18.2 MΩ.cm @ 25°C) obtained from a Merck Synergy UV Millipore System (Kilsyth, Victoria, Australia).

Elemental standards (Australian Chemical Reagents, Moorooka, Queensland, Australia) were purchased from Chem-Supply (Gillman, South Australia, Australia). Table 2-9 details the elements in the multi-element standard. Table 2-10 shows the details for 10 individual element standards.

Element	Concentration (mg/L)	Matrix	Supplier	Cat No.	Lot No.
Be	10 α /10 β	2% HNO_3 with trace HF	ACR Chemical Reagents	4902	JB1505
Na	1000 α /1000 β	2% HNO_3 with trace HF	ACR Chemical Reagents	4902	JB1505
Mg	1000 α /1000 β	2% HNO_3 with trace HF	ACR Chemical Reagents	4902	JB1505
Al	10 α /10 β	2% HNO_3 with trace HF	ACR Chemical Reagents	4902	JB1505
K	1000 α /1000 β	2% HNO_3 with trace HF	ACR Chemical Reagents	4902	JB1505
Ca	1000 α /1000 β	2% HNO_3 with trace HF	ACR Chemical Reagents	4902	JB1505
V	10 α /10 β	2% HNO_3 with trace HF	ACR Chemical Reagents	4902	JB1505
Cr	10 α /10 β	2% HNO_3 with trace HF	ACR Chemical Reagents	4902	JB1505
Mn	10 α /10 β	2% HNO_3 with trace HF	ACR Chemical Reagents	4902	JB1505
Fe	1000 α /1000 β	2% HNO_3 with trace HF	ACR Chemical Reagents	4902	JB1505
Co	10 α /10 β	2% HNO_3 with trace HF	ACR Chemical Reagents	4902	JB1505
Ni	10 α /10 β	2% HNO_3 with trace HF	ACR Chemical Reagents	4902	JB1505
Cu	10 α /10 β	2% HNO_3 with trace HF	ACR Chemical Reagents	4902	JB1505
Zn	10 α /10 β	2% HNO_3 with trace HF	ACR Chemical Reagents	4902	JB1505
As	10 α /10 β	2% HNO_3 with trace HF	ACR Chemical Reagents	4902	JB1505
Se	10 α /10 β	2% HNO_3 with trace HF	ACR Chemical Reagents	4902	JB1505
Mo	10 α /10 β	2% HNO_3 with trace HF	ACR Chemical Reagents	4902	JB1505
Ag	10 α /10 β	2% HNO_3 with trace HF	ACR Chemical Reagents	4902	JB1505
Cd	10 α /10 β	2% HNO_3 with trace HF	ACR Chemical Reagents	4902	JB1505
Sb	10 α /10 β	2% HNO_3 with trace HF	ACR Chemical Reagents	4902	JB1505
Ba	10 α /10 β	2% HNO_3 with trace HF	ACR Chemical Reagents	4902	JB1505
Tl	10 α /10 β	2% HNO_3 with trace HF	ACR Chemical Reagents	4902	JB1505
Pb	10 α /10 β	2% HNO_3 with trace HF	ACR Chemical Reagents	4902	JB1505

Table 2-9: Multi-element standard (α = Nominal concentration and β = Certificate of analysis concentration)

Element	Concentration (mg/L)	Matrix	Supplier	Cat No.	Lot No.
Li	1000 α /999 β	2% HNO_3	ACR Chemical Reagents	0707	GE2289K
B	1000 α /1001 β	H_2O	ACR Chemical Reagents	0665	HD2259G
P	1000 α /1002 β	H_2O	ACR Chemical Reagents	0727	IB1256B
Cl	1000 α /1000 β	H_2O	ACR Chemical Reagents	2617	JD1789
Sc	1000 α /998 β	2% HNO_3	ACR Chemical Reagents	0741	JD1779
Sr	1000 α /1000 β	2% HNO_3	ACR Chemical Reagents	0751	JB1613
Y	1000 α /1000 β	2% HNO_3	ACR Chemical Reagents	0775	HK1920E
Zr	1000 α /999 β	2% HCl	ACR Chemical Reagents	0779	JD1782
U	1000 α /1000 β	2% HNO_3	ACR Chemical Reagents	0769	IE1823C
In	1000 α /999 β	2% HNO_3	ACR Chemical Reagents	0699	JD1776

Table 2-10: Ten individual element standards (α = Nominal concentration and β = Certificate of analysis concentration)

2.2.2   Results and Discussion

2.2.2.1 Method Development and Validation

The procedure used to develop and validate the ICP-MS method for the analysis of AN-based HME samples is outlined below:

1) Prepare calibration standards covering estimated concentration ranges of elements in real samples, based on literature values from fertiliser studies.
2) Determine optimum integration times for each element using triplicate analyses of each calibration standard. Construct calibration plots using linear regression analysis. This was repeated more than five times with fresh standards to confirm.
3) Determine limits of detection for each element using blank (2% HNO_3) and calibration standard samples.
4) Estimate limits of quantification from data collected at step 2.
5) Analyse a number of test samples. Determine method detection limits, working ranges, measurement uncertainties, spike recoveries, and sample masses and dilutions required to generate suitable analyte concentrations empirically.
6) Adjust calibration standards and repeat steps 1–6 as required.
7) Commence authentic sample analysis with quality control checks (reference samples, spike samples, standards). Monitor measurement uncertainties, recoveries and response factors. Adjust method as required.

It was unknown at the outset which elements would prove to be the most useful for AN-based HME sample classification and discrimination, and thus a relatively large number of elements were chosen for monitoring. After reviewing the results from a reasonable number of "real" samples, it may be possible to reduce the number of significant elements and therefore the complexity of the analysis.

2.2.2.2 Preparation of Calibration Standards
Calibration standards for each of the elements of interest were prepared following a general procedure that is illustrated in this section using the final optimised concentrations.

The initial step in the production of the calibration standards was to prepare each of the elemental standards, so that they can be made into two stock solutions. Nominal concentration values were used in the preparation of the stock calibration solutions. Table 2-11 shows the dilutions needed to prepare each of the elemental standards.

Element Standard	Initial Concentration (mg/L)	Volume of Standard (µL)	Volume of 69% HNO₃ (µL)	Volume of Water (µL)	Final Concentration (mg/L)
23 Element Mix	Major – 1000 Minor – 10	-	-	-	Major – 1000 Minor – 10
Li	1000	5	100	4895	1
B	1000	50	100	4850	10
Sc	1000	50	100	4850	10
Sr	1000	50	100	4850	10
Y	1000	50	100	4850	10
Zr	1000	50	100	4850	10
P	1000	-	-	-	1000
Cl	1000	-	-	-	1000
U	1000	50	100	4850	10

Table 2-11: Details for preparation of dilute elemental standard solutions

Two stock solutions [A (lower concentration) and B (higher concentration)] are needed to prepare the necessary number of calibration standards needed for this method. Table 2-12 shows the formulations for the preparation of the two stock solutions.

32 Element Stock Solution A (50 mL) (4% HNO₃)		
Solution	Volume (µL)	Final Concentration (µg/L)
Water	47590	-
69% HNO₃	2000	-
23 Element Standard	50	Major – 1000; Minor – 10
Dilute Li Standard	50	1
Dilute B Standard	50	10
Dilute Sc Standard	50	10
Dilute Sr Standard	50	10
Dilute Y Standard	50	10
Dilute Zr Standard	50	10
Dilute P Standard	25	500
Dilute Cl Standard	25	500
Dilute U Standard	10	2
32 Element Stock Solution B (50 mL) (4% HNO₃)		
Solution	Volume (µL)	Final Concentration (µg/L)
Water	28500	-
69% HNO₃	2000	-
Dilute 23 Element Standard	2500	Major – 50000; Minor – 500
Dilute Li Standard	2500	50
Dilute B Standard	2500	500
Dilute Sc Standard	2500	500
Dilute Sr Standard	2500	500
Dilute Y Standard	2500	500
Dilute Zr Standard	2500	500
Dilute P Standard	750	15000
Dilute Cl Standard	750	15000
Dilute U Standard	500	100

Table 2-12: Composition of the 32 element high and low stock solutions.

The final step in the preparation of the calibration standards is to make up each standard. For this method 16 calibration standards were needed. Table 2-13 shows the method to prepare each standard. All of the standards are in a matrix of 2% HNO₃.

32 Element Calibration Standard	32 Element Stock Solution	Volume of Stock Solution (µL)	Volume of 69% HNO$_3$ (µL)	Volume of Water (µL)	Final Concentration (Minor Elements) (ng/L)
0	-	0	100	4900	Blank
1	A	2.5	100	4897.5	5
2	A	5	100	4895	10
3	A	25	100	4875	50
4	A	50	100	4850	100
5	A	100	100	4800	200
6	A	250	100	4650	500
7	A	350	100	4550	700
8	A	500	100	4400	1000
9	A	1000	100	3900	2000
10	A	1500	100	3400	3000
11	A	2500	100	2400	5000
12	B	100	100	4800	10,000
13	B	200	100	4700	20,000
14	B	500	100	4400	50,000
15	B	1000	100	3900	100,000

Table 2-13: Composition of the final calibration standards

2.2.2.3 Internal Standard

Indium was chosen as an internal standard for this method, as it will not interfere with the analysis of elements of interest. The recovery percentage for the internal standard is measured for each sample analysed, and this is performed to monitor for any potential matrix effects which may interfere with and nullify the analytical results.

The indium standard was prepared by spiking 50 mL of 2% HNO$_3$ with 5 µL of indium standard (1000 mg/L). This solution was simultaneously injected (through a second/independent channel) into the nebuliser with the sample solution. The flow rate for the internal standard to the nebuliser is 15 µL per minute, while the flow rate for the sample is 335 µL per minute.

The Agilent 7500cx ICP-MS output signal is expressed as a response factor, i.e. a ratio of detector response (ion counts/current) due to each element compared to detector response due to the internal standard.

2.2.2.4 Optimisation of Integration Times

Each data point for either calibration standards or samples was an average of 3 replicate readings for each element. To increase the robustness of the ICP-MS method, the acceptable precision for the measurements was set at no more than 5% relative standard deviation (RSD) for the three replicates for every element. This provided an acceptable level of confidence in the stability of the response factor over the data acquisition period.

To meet the requisite 5% RSD precision, integration times were optimised by analysing the 16 calibration standards in triplicate, adjusting the integration time if necessary and repeating until all elements met the criterion. Results of the optimisation process are shown in Table 2-14.

Integration Time (Seconds)				
Element	**Isotope**	**per Point**	**per Mass**	**Detector Mode**
Li	7	1.0	3.0	Auto
Be	9	1.0	3.0	Auto
B	11	1.0	3.0	Auto
Na	23	0.010	0.030	Auto
Mg	25	0.010	0.030	Auto
Al	27	1.0	3.0	Auto
P	31	1.0	3.0	Auto
Cl	35 and 37	1.0	3.0	Auto
K	39	0.010	0.030	Auto
Ca	44	0.010	0.030	Auto
Sc	45	0.10	0.30	Auto
V	51	1.0	3.0	Auto
Cr	52	1.0	3.0	Auto
Mn	55	0.10	0.30	Auto
Fe	56 and 57	0.010	0.030	Auto
Co	59	0.10	0.30	Auto
Ni	60	1.0	3.0	Auto
Cu	63	0.10	0.30	Auto
Zn	66	0.10	0.30	Auto
As	75	1.0	3.0	Auto
Se	82	1.0	3.0	Auto
Sr	88	0.10	0.30	Auto
Y	89	0.10	0.30	Auto
Zr	60	1.0	3.0	Auto
Mo	95	1.0	3.0	Auto
Ag	107	1.0	3.0	Auto
Cd	111	0.10	0.30	Auto
In	115	0.10	0.30	Auto
Sb	121	1.0	3.0	Auto
Ba	138	0.10	0.30	Auto
Tl	205	1.0	3.0	Auto
Pb	208	0.10	0.30	Auto
U	238	1.0	3.0	Auto

Table 2-14: Optimised integration times for each element

Auto detector mode indicates that both dual and pulse modes are available, and if the signal intensity is too high, the detector can switch from pulse to analogue mode. However for optimal calibrations, the entire calibration range for each element should be within one of the detection modes (i.e. pulse or analogue). If this was not possible, the "switch over" was calibrated monthly with pulse/analogue factor tuning as part of an auto tune.

2.2.2.5 Construction of Calibration Plots

Calibration plots were constructed with fresh calibration standards for each batch for analysis. The Agilent software performs linear regression analysis using the average response factors of three replicate analyses of all 16 calibration standards and need to fulfil a coefficient of correlation (R) value of 0.98 for each element to be accepted.

Element	Mass	Equation of the Line	Coefficient of Correlation (R)
Li	7	y = 0.002611174x + 5.43731E-06	0.999977257
Be	9	y = 0.00212826x + 1.09078E-05	0.999944026
B	11	y = 0.001052729x + 0.000694172	0.999975999
Na	23	y = 0.01522309x + 0.191864126	0.999989169
Mg	25	y = 0.001070358x + 0.000271826	0.999937891
Al	27	y = 0.003776776x + 0.002506907	0.999948105
P	31	y = 0.000298621x + 0.003663939	0.999931721
Cl	35	y = 3.28257E-05x + 0.017876066	0.999263344
Cl	37	y = 3.12644E-05x + 0.620982851	0.976009232
K	39	y = 0.006567256x + 0.196182687	0.999933554
Ca	44	y = 0.000375012x + 0.004796678	0.999922425
Sc	45	y = 0.025914706x + 0.000390985	0.999947635
V	51	y = 0.062498873x + 0.00011884	0.999857613
Cr	52	y = 0.072837925x + 0.003812366	0.999923983
Mn	55	y = 0.049577945x + 0.000391447	0.999626872
Fe	56	y = 0.065538788x + 0.022272409	0.999943339
Fe	57	y = 0.0016427x + 0.000375808	0.999929016
Co	59	y = 0.114475764x + 0.000166875	0.999947791
Ni	60	y = 0.029829131x + 0.000177315	0.999973048
Cu	63	y = 0.080372638x + 0.003814647	0.999830557
Zn	66	y = 0.013712979x + 0.003397135	0.999888149
As	75	y = 0.012723663x + 2.21343E-05	0.999927921
Se	82	y = 0.000744735x + 0.001998475	0.999948456
Sr	88	y = 0.059733998x + 0.000346823	0.999683232
Y	89	y = 0.114689182x + 1.027E-05	0.999946169
Zr	90	y = 0.082168585x + 6.12969E-05	0.999873451
Mo	95	y = 0.034698532x + 0.000741065	0.999701767
Ag	107	y = 0.108041508x + 0.000103344	0.999655514
Cd	111	y = 0.018146046x + 4.78058E-05	0.999961042
Sb	121	y = 0.050633376x + 5.90937E-05	0.999731744
Ba	138	y = 0.117358026x + 0.009967572	0.999919237
Tl	205	y = 0.234076698x + 0.000182786	0.999900423
Pb	208	y = 0.165542056x + 0.001451574	0.999938039
U	238	y = 0.386354381x + 5.50799E-05	0.999926458

Table 2-15: Examples of analytical data obtained as part of a calibration procedure

Table 2-15 details representative equations of lines of best fit and the R values for each element of interest. Values of the y-intercepts of lines of best fit are indicative of the concentrations of elements present in blank samples. Representative calibration plots for ^{27}Al and ^{31}P are shown in Figure 2-6, which also illustrates that the output on the y-axis is a response factor of the element compared to the internal standard. It should be noted that these calibrations plots were only a partial snapshot of the full calibration as standards of a higher concentration were also analysed. As per NATA recommendations [185] the residuals were plotted by Flinders Analytical through the method development process to confirm linearity and check for outliers.
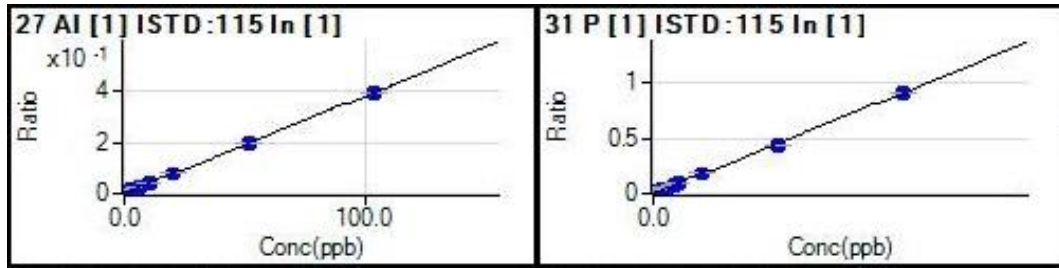
Figure 2-6: Examples of calibration plots for aluminium and phosphorus.

2.2.2.6 Estimation of Limits of Detection and Quantification for Elements of Interest

The limit of detection (LOD) is defined as the lowest quantity or concentration of a substance that can be distinguished from the absence of that substance by a measurement within a confidence limit. A common way to estimate the LOD, also known as the instrument detection limit, is based on measurements of the background signal produced by ten replicate blank samples. The LOD is then derived the by adding three standard deviations (indicative of confidence limit) to the mean of those measurements [186-189]. The drawback of this method is that no evidence has been collected to prove that a low concentration sample does provide a signal distinguishable from the blank.

Equation 2-1 was utilised to calculate an estimate of LOD for each element. This methodology for LOD estimation is often used for ICP-MS [190], as it takes into account the background equivalent concentrations of blank samples. Raw ion count data is used for the calculations of mean signal and standard deviations, because ICP-MS software often converts the low count data obtained from blank samples into negative concentrations, or adjusts the reported result as zero or less than a certain threshold, making the common LOD estimation meaningless. The concentration of the standard used for LOD calculations was element dependent and was either 1 µg/L or 10 µg/L.

$$LOD = \frac{3 \times s_b \times C_s}{\mu_s - \mu_b}$$

(Equation 2-1)

Where: s_b = standard deviation of signal from blank (ten replicates) in ion counts

C_s = concentration of a standard in µg/L

μ_s = mean signal from the standard (seven replicates) in ion counts

μ_b = mean signal for the blank (ten replicates) in ion counts

The limit of quantification (LOQ) is the lowest concentration, where the relative uncertainty on a single measurement is reproducible within ± 20% [191, 192]. Similar to the LOD, the LOQ is often estimated based only on the results of blank sample replicates by adding ten standard deviations to the mean of the signal output, with the same drawback. Thus the LOQ was estimated using Equation 2-2, again using raw ion count data.

$$LOQ = \frac{10 \times s_b \times C_s}{\mu_s - \mu_b}$$

(Equation 2-2)

Where: s_b = standard deviation of signal from blank (ten replicates) in ion counts

66

C_s = concentration of a standard in μg/L

μ_s = mean signal from the standard (seven replicates) in ion counts

μ_b = mean signal for the blank (ten replicates) in ion counts

LOD and LOQ estimates for the elements of interest are given in Table 2-16 in Section 2.2.2.8.

2.2.2.7 Preparation of Test Samples

A number of representative test samples were then prepared, digested and analysed for method validation purposes. These included:

- Ground AN (unspiked and spiked with calibration standards);
- Ground calcium carbonate;
- Aluminium powder;
- Icing sugar;
- Blend of ground AN and ground calcium carbonate (to represent CAN); and
- Blend of ground AN, ground calcium carbonate and aluminium powder (to represent CAN/Al).

A number of replicate samples of each type were accurately weighed and digested through reaction with nitric acid, then diluted with MilliQ water to 15 mL volumes. Further dilutions were then carried out to bring the analyte concentrations within the linear response region of the calibration plots where necessary. The data collected from the analysis of the diluted solutions was used to:

- Determine the method detection limits of analytes;
- Determine the working range of analyte concentrations;
- Determine analyte recoveries;
- Estimate measurement uncertainties of the method;
- Inform adjustments to calibration standard concentrations; and
- Inform appropriate sample masses and dilutions for analysis.

2.2.2.8 Method Detection Limit (MDL) and Working Ranges of Elements of Interest

A method detection limit (MDL), which takes into account the effects on and uncertainties in the output signal introduced by the sample matrix and preparation processes, was established for all analytes. To determine MDL values, seven AN samples (ground Orica Nitropril) which had been spiked with a calibration standard containing approximately two to five times the estimated LOD were processed through the entire analytical method [186]. The calculation for the MDL is shown in Equation 2-3.

$$MDL = t \times s_s \qquad \text{(Equation 2-3)}$$

Where: t = Students t value for a 95% confidence level and n-1 degrees of freedom (t = 2.447 for seven replicates)

s_s = standard deviation of signal from spiked samples (seven replicates) in μg/L

The working range is defined as "the region between limits within which a quantity is measured, received or transmitted, expressed by stating the lower and upper range values" [193].

The determination of the working range was based on the analysis of all test samples throughout this initial method development, which allowed a determination of which elements were to be analysed quantitatively. From this data, a suitable linear calibration range was designed and implemented.

It should be noted that this method requires a large number of elements to be analysed (32) and as such there are limits applied to protect and extend the life of the detector. This is set at a maximum of 20 mg/L of each element in solution, where the total concentration of elements in solution should not exceed 200 mg/L. This is an important factor to take into account for a typical AN-based sample, as the range of concentrations of elements covers several orders of magnitude. Table 2-16 details the LOD, LOQ, MDL and working ranges for each element in this method.

Element	LOD (µg/L)	MDL (µg/L)	LOQ (µg/L)	Working Range (µg/L)
Li	0.078	0.020	0.259	0.3 to 3
Be	0.038	0.110	0.126	0.1 to 3
B	1.274	0.200	4.246	5 to 50
Na	1.979	2.990	6.597	5 to 2000
Mg	1.048	1.200	3.494	5 to 2000
Al	0.607	0.015	2.024	5 to 500
P	4.832	35.000	16.110	35 to 600
Cl	12.870	4.800	42.910	42 to 600
K	3.499	3.600	11.660	10 to 10000
Ca	18.230	29.000	60.990	50 to 10000
Sc	0.006	0.014	0.021	0.05 to 3
V	0.007	0.070	0.024	0.5 to 20
Cr	0.019	0.287	0.063	0.5 to 20
Mn	0.100	0.245	0.333	0.5 to 100
Fe	0.723	7.250	2.409	5 to 2000
Co	0.008	0.006	0.026	0.05 to 3
Ni	0.009	0.010	0.028	0.3 to 20
Cu	0.024	0.070	0.079	0.05 to 5
Zn	0.042	0.300	0.141	0.5 to 20
As	0.043	0.005	0.144	0.05 to 2
Se	0.154	0.400	0.514	0.5 to 5
Sr	0.017	0.040	0.055	0.2 to 100
Y	0.007	0.070	0.024	0.1 to 20
Zr	0.006	0.050	0.019	0.05 to 2
Mo	0.031	0.013	0.104	0.1 to 20
Ag	0.043	0.004	0.142	0.15 to 2
Cd	0.020	0.014	0.067	0.1 to 20
Sb	0.023	0.006	0.077	0.08 to 2
Ba	0.014	0.050	0.045	0.1 to 100
Tl	0.019	0.003	0.062	0.06 to 5
Pb	0.030	0.003	0.100	0.05 to 2
U	0.001	0.002	0.003	0.01 to 4

Table 2-16: LOD, LOQ, MDL and working range for each element analysed in this method

2.2.2.9 Spike Recovery

A recovery study was undertaken for all the elements to determine the effectiveness of the ICP-MS method, and to reveal potential bias in the results obtained. As there are no certified reference materials for the samples of interest, these were performed on single AN samples at two different spike levels (low and high).

Recoveries in the range of 80–120% of the spike values indicate that the sample preparation (including digestion) procedures do not have an appreciable effect on the quantification and no bias correction factors are needed when reporting the results. The results for typical spike recovery tests at low and high levels are shown in Table 2-17. It can be observed that the obtained recoveries for both the high and low spike confirm that there are no significant element losses during the sample preparation procedure, and the results are not biased towards high or low apparent readings for individual elements.

As previously detailed, "ionisation efficiency" is an important factor in the utilisation of ICP-MS as a method to measure elements within a sample. Chlorine was an element of interest for this research task. When chlorine is ionised, it is not efficient in forming cations (Cl^+), it much prefers to ionise to Cl^-. This poor ionisation efficiency results in higher detection limits, as the ICP-MS does not have negative ion detection capability. Bromine (Br) and iodine (I) also suffer from the same ionisation problems, but these elements were deemed to be of little importance for the analysis of AN-based explosive samples. As part of this research task, the limitations with analysing chlorine have been identified, and as such we are only interested in qualitative chlorine results (i.e., the presence of Cl) rather than the quantitative determination of chlorine amounts. It should be stated that the chloride content of each of the HME samples of interest were determined by IC as part of DSTO's routine analysis protocols.

	Low Spike				High Spike			
Element	**Initial Conc. (µg/L)**	**Spike Conc. (µg/L)**	**Final Conc. (µg/L)**	**Spike Recovery**	**Initial Conc. (µg/L)**	**Spike Conc. (µg/L)**	**Final Conc. (µg/L)**	**Spike Recovery**
Li	0.004	0.099	0.113	111%	0.004	2.000	2.009	100%
Be	0.000	0.045	0.051	88%	0.000	5.029	5.008	100%
B	0.690	1.019	1.658	95%	0.690	51	51.584	100%
Na	30.983	20.292	51.197	100%	30.983	2064.1	2110.097	101%
Mg	1.595	5.093	7.355	113%	1.595	5155.8	5265.603	102%
Al	13.074	5.01	17.717	93%	0.803	400	409.121	102%
P	1.067	49.821	50.530	96%	1.067	605.9	585.110	96%
Cl	*Due to poor ionisation efficiency analysis of ^{35}Cl is limited*							
K	6.962	20.292	25.060	89%	6.962	5155.8	5222.254	101%
Ca	6.424	101.957	107.933	100%	6.424	5155.8	5134.161	99%
Sc	0.00033	0.052	0.045	86%	0.00033	5.091	5.016	99%
V	0.015	0.203	0.217	100%	0.015	10.3	10.177	99%
Cr	0.223	0.203	0.428	101%	0.223	10.3	10.389	99%
Mn	0.143	0.203	0.350	102%	0.143	102.71	103.103	100%
Fe	12.744	5.093	17.979	103%	12.744	2064.1	2079.049	100%
Co	0.019	0.203	0.229	103%	0.019	10.3	10.256	99%
Ni	0.230	0.203	0.445	106%	0.230	20.6	20.848	100%
Cu	0.302	0.501	0.794	98%	1.899	5.029	5.295	105%
Zn	0.210	0.502	0.787	115%	1.148	20.6	22.743	105%
As	0.005	0.203	0.203	97%	0.005	5.1	4.937	97%
Se	0.017	1.020	0.934	90%	0.017	5.1	4.838	95%
Sr	0.030	0.052	0.086	108%	0.030	52.3	52.295	100%
Y	0.001	0.052	0.051	96%	0.001	10.4	10.198	98%
Zr	0.010	0.209	0.192	87%	0.010	5.175	5.955	115%
Mo	0.033	0.051	0.090	112%	0.033	5.029	4.999	99%
Ag	0.002	0.051	0.053	99%	0.002	5.029	4.978	99%
Cd	0.006	0.051	0.055	95%	0.006	5.029	5.05	100%
Sb	0.015	0.051	0.064	97%	0.015	5.029	5.057	101%
Ba	0.553	0.203	0.204	100%	0.553	102.8	101.396	99%
Tl	0.000	0.051	0.049	96%	0.000	5.029	5.127	102%
Pb	0.399	0.203	0.616	107%	0.399	5.029	5.129	102%
U	0.0003	0.044	0.043	98%	0.0003	4.2	4.186	100%

Table 2-17: Recovery percentage for spike tests

2.2.2.10 Measurement Uncertainty Calculations

Determination of estimates of measurement uncertainty (MU) for a method is a key component of any validation process. MU has been defined as 'a parameter associated with the result of a measurement that characterises the dispersion of values that could reasonably be attributed to the measure and (the sample or standard being measured)' [194]. MU allows end users to ensure that the reported results are fit for purpose and traceable to international or national standards [49, 195-198].

Every test or calibration result is subject to some level of error. Estimates of MU provide information about how large this error might be. As such, MU is an important part of a reported result and it may be argued that a result is incomplete unless accompanied by an estimate of MU [194].

Two ways of representing the estimate of the MU for the measurement of trace elements in AN-based HME samples are used in this report; these are standard uncertainty and coefficient of variation. The former is recommended by the National Association of Testing

Authorities (NATA) for reporting estimates of the MU [194], while the latter is often used to allow comparisons of MU for data that have markedly different magnitudes.

The standard uncertainty, u(ỹ), is an accepted measure of uncertainty that is dependent on the actual signal value, and is calculated using Equation 2-4 below. This is an absolute value and has the same units as the measurement it relates to, in this case µg/L. The standard uncertainty (also known as the standard error of the mean) is used to provide an estimate of MU for a small number of measurements based on the results from a larger number of previous identical measurements.

$$u(\tilde{y}) = \frac{s}{\sqrt{n}}$$ (Equation 2-4)

Where: s = standard deviation of observed (measured) results
n = number of measurements

A coverage factor (k) is a numerical factor that is used as a multiplier of the standard uncertainty in order to obtain the desired confidence level in a MU [196, 199, 200]. If u(ỹ) is based on sufficient data, a coverage factor of k = 2 gives an approximate level of confidence of 95% [196, 199, 200]. This estimation of absolute MU [2u(ỹ)] has been used throughout for reporting the results of element concentration (e.g., C = µ ± 2u(ỹ) where µ is the mean of three replicate measurements and 2u(ỹ) is the MU estimated from many measurements).

The coefficient of variation (CV) is the relative standard deviation of a measurement expressed as a percentage, and is calculated as shown in Equation 2-5 [201, 202].

$$CV = \frac{s \times 100}{\mu}\%$$ (Equation 2-5)

Where: s = standard deviation of observed (measured) results
µ = mean value of observed (measured) results

Table 2-18 details the estimated MU for each of the elements of interest to this task. This statistical analysis was performed on the seven samples of AN (Orica Nitropril) that were used for the MDL calculations. This set of samples was analysed as a proof of concept for the method, as all elements were present which allows for a full evaluation. The absolute MUs [2u(ỹ)] do not indicate a large amount of variability for most of the elements of interest. The CVs were quite reasonable and the only elements with a high CV were samples which contained element levels which were towards the lower end of the calibration range (e.g., Fe, K and Ba). The lower signals seen for these elements resulted in a higher level of variability and therefore a higher CV value. The data indicates that this analysis technique is fit for purpose.

Spiked AN Sample (7 replicates)			
Element	Mean Value (µg/L)	2u(ȳ) (µg/L)	CV
Li	0.09	0.005	6.8%
Be	0.05	0.004	9.3%
B	2.20	0.060	3.6%
Na	11.89	0.924	10.3%
Mg	4.35	0.375	11.4%
Al	0.10	0.005	6.0%
P	105.86	11.00	13.7%
Cl	69.58	1.48	2.8%
K	3.85	1.11	38.3%
Ca	76.12	4.85	7.8%
Sc	0.05	0.004	12.0%
V	0.51	0.022	5.6%
Cr	0.68	0.089	17.3%
Mn	0.60	0.076	16.7%
Fe	14.54	2.24	20.4%
Co	0.04	0.002	6.7%
Ni	0.06	0.003	6.5%
Cu	4.06	0.002	0.1%
Zn	1.06	0.097	12.0%
As	0.03	0.002	6.3%
Se	2.28	0.120	6.9%
Sr	0.26	0.014	7.0%
Y	0.04	0.002	6.9%
Zr	0.04	0.001	2.5%
Mo	0.10	0.004	5.6%
Ag	0.04	0.001	3.5%
Cd	0.04	0.004	13.4%
Sb	0.05	0.002	5.1%
Ba	0.08	0.014	23.1%
Tl	0.04	0.001	3.0%
Pb	0.01	0.0003	2.9%
U	0.01	0.0003	5.1%

Table 2-18: Uncertainties for each element analysed from seven replicate spiked AN samples

2.2.2.11 Sample Preparation

The results from analysis of the test samples led to the development of a general sample preparation procedure.

Materials submitted for analysis (typically 50–300 mg) were generally sub-sampled from a larger amount. It should be noted that there were issues with this sub sampling process due to the unknown nature of the samples. This if further discussed in section 2.2.3.4.

These were homogenised at DSTO Edinburgh and were left in a desiccator over silica gel overnight before sample preparation to ensure that there was minimal moisture within the sample, thereby minimising its influence on comparative results between samples.

Approximately 50 mg of the sample (AN-based HME) was weighed (accurately and with the weight recorded) into a 15 mL polypropylene digestion vial. Table 2-19 details the masses needed for the digestion of other various types of sample of interest, optimised after analysis of the test samples.

Sample Type	Mass Needed (mg)
AN	50
Calcium Carbonate	15
CAN	50
Aluminium Powder	5
AN-based HME	50

Table 2-19: Masses needed for the digestion of various samples.

The samples were digested by adding 100 µL of water followed by 300 µL of nitric acid to the vial. Samples were then heated in a water bath for 3 hours at 60°C and then subsequently shaken for 24 hours.

After 24 hours the samples were made up to volume (15 mL) using MilliQ water. Due to matrix effects and the high concentrations of certain elements, this solution is then used to prepare the three dilutions that are currently being used for this method. Table 2-20 details these dilutions and also the possible elements which may be analysed at each dilution. This is however sample dependent and not all dilutions are needed for all samples. Sample volumes for the triplicate ICP-MS analysis is 5 mL and has a matrix of 2% HNO_3.

Dilution	Elements Analysed	Vol. of Digest Solution (µL)	Vol. of H_2O (µL)	Vol. of 69% HNO_3 (µL)
1 in 2	Be, Na, Mg, K, V, Cr, Mn, Co, Ni, Cu, As, Se, Mo, Ag, Cd, Sb, Tl, Pb, Li, B, Cl, Sc, Sr, Y, Zr and U	2500	2400	100
1 in 10	Ca, P, Ba, Fe and Zn	500	4400	100
1 in 800	Al	6.25	4893.75	100

Table 2-20: Sample preparation dilutions.

2.2.3 Authentic Sample Analysis and Quality Control

To date a significant number of authentic AN-based HMEs and ingredients (provided by DSTO) have been analysed using this method in several batches, with the results reported in Chapter 3. A number of quality control checks were put in place and key parameters are continuously monitored to ensure the method remains fit-for-purpose.

2.2.3.1 Calibration
Fresh calibration standards were prepared and calibration plots were calculated for each batch as instrument response is dependent on tuning, plasma conditions and environmental conditions. Acceptance of the calibration was conditional on meeting the conditions of ≤ 5% CV for responses with each calibration standard (triplicate analysis) and R ≥ 0.98 for the calculated linear plot.

2.2.3.2 Quality Controls
Within every batch of samples that is analysed using this method, a number of quality control measures are undertaken. These include:
- Results of the triplicate analyses are discarded if the CV is greater than 5% for any element and the response was above the LOQ, indicating instrument instability.
- Internal standard ion counts were monitored for each analysis. In the occurrence that this data was not within 80–120% of the ion count reading for the blank calibration,

73

the standards were discarded and the results for the entire batch may be rejected (Figure 2-7).

- A check sample containing all elements of interest was prepared with the minor elements being at a concentration of 1 µg/L. This check sample was analysed every ten samples to assess response drift over time. Results obtained following the last acceptable check sample were discarded if responses for any element fall outside the range of 80–120% of the nominal value.

- Spike recovery samples were also run every ten samples within a batch to monitor elemental recoveries. These were prepared by adding 50 µL of either a 500 µg/L (for minor elements) or a 50 mg/L (for major elements) standard solution to 2.45 mL of 2% HNO_3 and 2.50 mL of a random sample solution (5 or 500 µg/L spike). Results from the entire batch were discarded if responses for any element fall outside the range of 80–120% of the spike value.

Duplicate samples were prepared randomly from a single acid digest solution and analysed every ten samples. Results from that sample were discarded if the response for any element fell outside the range of 80–120% of the first analysis and the response was above the LOQ.

Results for element concentrations were discarded if the responses exceeded the upper limit of the working range. Sample solutions were then further diluted and retested.
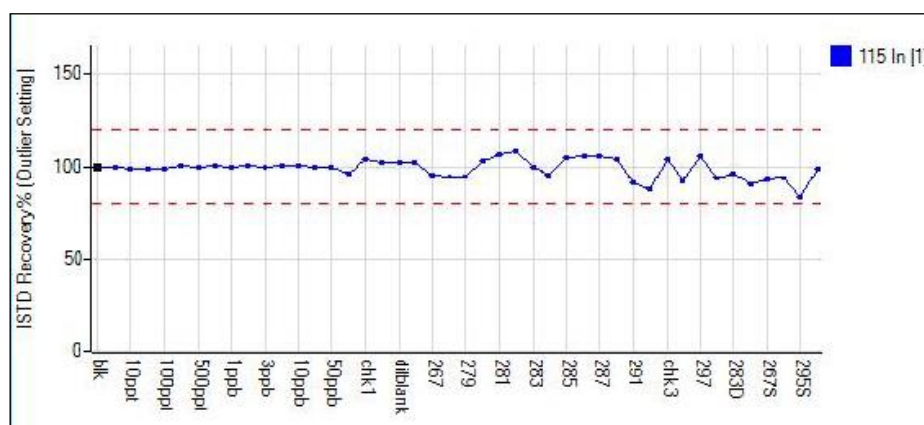
Figure 2-7: Internal standard recovery percentages from a typical batch

2.2.3.3 Reference Material

There are currently no certified reference materials that we could utilise as a check of sample preparation methods.

As such, a large batch of CAN/Al was prepared from known ingredients at DSTO to be used as an in-house reference material. This reference material was homogenised within its anti-static container on a regular basis utilising a tumbler mixer. This was used as a longer-term check of the consistency of the ICP-MS procedure. Smaller samples of this CAN/Al mixture were delivered with each batch and a total of 34 reference samples were analysed at different times over a 10 month period. Table 2-21 details the results obtained for each of the elements of interest using data accrued for 34 samples of CAN/Al.

CAN/Al reference material (analysed 34 times)			
Element	Mean Value (µg/L)	u(ȳ) (µg/L)	CV
Li	Below LOD	Below LOD	Below LOD
Be	Below LOD	Below LOD	Below LOD
B	Below LOD	Below LOD	Below LOD
Na	49.20	2.18	12.7%
Mg	498.40	11.64	6.8%
Al	87.24	2.40	7.9%
P	Below LOD	Below LOD	Below LOD
Cl	Below LOD	Below LOD	Below LOD
K	10.73	0.58	15.2%
Ca	50.45	0.78	4.2%
Sc	52.78	2.81	10.3%
V	7.74	0.25	9.1%
Cr	3.86	0.17	12.3%
Mn	37.94	0.94	6.9%
Fe	627.66	22.51	10.1%
Co	0.39	0.02	15.0%
Ni	4.24	0.16	10.9%
Cu	2.10	0.28	35.6%
Zn	2.15	0.17	22.5%
As	104.23	13.19	34.1%
Se	1.54	0.41	75.7%
Sr	35.15	1.56	12.0%
Y	0.22	0.004	4.8%
Zr	Below LOD	Below LOD	Below LOD
Mo	0.42	0.02	12.2%
Ag	Below LOD	Below LOD	Below LOD
Cd	Below LOD	Below LOD	Below LOD
Sb	Below LOD	Below LOD	Below LOD
Ba	139.35	11.79	23.2%
Tl	Below LOD	Below LOD	Below LOD
Pb	0.77	0.05	18.1%
U	0.092	0.005	14.4%

Table 2-21: Uncertainties for each element analysed for 34 replicate CAN/Al samples

It can be noted that not all of the elements of interest are present in this sample. The variability in the elemental profile of the CAN/Al control samples taken from the bulk mixture over a period allows for a greater understanding of the MU inherent in the overall sub-sampling and analysis procedure for AN-based explosives.

The $2u(\bar{y})$ values for the elements which are present in these control samples are all acceptable. The obtained CV values were quite high for some elements in this sample set and in this case the CV values were used as a measure of sampling and contamination issues.

Potential issues with heterogeneity, sub-sampling and settling out within the batch of CAN/Al reference material have been highlighted. Some unusual variability was observed in Cu and Zn.

This could be due to some statistical variability in the aluminium powder particulates (i.e. changing aluminium powder content in each subsample). In general, the levels of Cu and Zn were quite low. As, Se and Ba variability was due to changing calcium carbonate content. This gives an indication of the potential variability in samples of unknown origin.

It was also found that boron results were unreliable, due to contamination from some of the glass vials in which the samples were transported (the vials differed throughout the analysis period). This has resulted in the elimination of boron from the final ICP-MS results.

Throughout the duration of the task a record of calibrations was kept. It was identified that some elements had issues throughout the calibration process (i.e. poor calibrations due to poor stability of certain elements at lower concentration levels). Due to these calibration issues, the qualitative selenium results will be of greater significance in comparison to the quantitative data (the presence of Se is more important than how much of it is present). This qualitative assessment has also been applied to chlorine (Cl) and phosphorus (P) due to the low ionisation efficiencies of these elements.

2.2.3.4 Influence of Sample Collection and Preparation

It should be noted that the digestion of some authentic AN-based HMEs was not complete. Unfortunately due to safety considerations, the samples could not be subjected to any harsher digestion conditions and as such not all materials (i.e. plant material, plastic particulates, soil/sand and fibres which were present in some HME samples) were completely digested. The amount of undigested material after the sample preparation was typically less than 2% of the sample mass, and as such has not been identified as a major problem. This factor has been taken into account when reporting MU for any ICP-MS results, and as all of the HME samples were "digested" in the same way, it is possible to compare the samples to each other.

Sampling issues have been flagged as an issue with the analysis of AN-based HME using ICP-MS, as noted in the previous section. Better control of this sub-sampling would reduce the uncertainty of results.

One solution would be to homogenise the entire sample; it is however, a challenge to safely homogenise several grams of energetic material. A way to get around this would be to increase the mass of material which is being digested. An example of this would be to digest 100 mg of HME in 30 mL instead of using the current method of 50 mg of HME in 15 mL. However, this approach is dependent on the availability of sufficient quantities of material for destructive testing, and must be balanced with requirements and priorities for other analytical tests.

An initial attempt to strike this balance was made using approximately 1 g test batches of CAN/Al reference material that had been subjected to selective extraction with MilliQ water and trace metal analysis grade acetic acid. This procedure was used to separate components of CAN/Al for compositional analysis and generated samples that were amenable for further analytical testing. However it was found that the labware used (despite multiple washings with nitric acid and MilliQ water) and the extensive manipulation of the sample in this process introduced too many opportunities for contamination and increased the MU of the results to unacceptable levels.

For operational reasons genuine HME samples provided by DSTO generally are collected and sampled under uncontrolled conditions and as such potential contaminations may be present in the samples. Unfortunately these contaminations are unable to be regulated and as such have been taken into consideration when reporting the analytical data.

2.2.3.5 Interpretation and Presentation of ICP-MS Data

The raw data produced by the ICP-MS gives the elemental concentrations of the solutions analysed in µg/L (parts-per-billion, ppb), which firstly need to be converted into mass fractions of the original sample, expressed as µg/kg. This is accomplished using Equation 2-6.

$$m_e = \frac{C_e \times V_s \times df}{m_s}$$
(Equation 2-6)

Where: m_e = mass fraction of element in sample in µg/kg
               C_e = measured concentration of element in solution analysed in µg/L
               V_s = volume of digest solution in L (0.015 L)
               df = dilution factor for solution analysed by ICP-MS (2, 10 or 800)
               m_s = mass of sample digested in kg

Method quantification limits (MQLs) for each element were calculated as mass fractions using Equation 2-6 and substituting the concentration of the lowest calibration standard in the working range for C_e. As the mass fraction calculation is dependent on the mass of the sample, two MQLs are reported; one for samples of 50–70 mg (AN, CAN and AN-based HME) and one for samples of 5–15 mg [Al and calcium carbonate ($CaCO_3$)]. These MQLs are reported in Table 2-22, along with values of CV derived from the average CV for that element found from the spiked AN tests and reference material analyses.

Element	MQL (AN/CAN/HME)	MQL (Al/CaCO₃)	CV
Li	180 µg/kg	900 µg/kg	6%
Be	60 µg/kg	300 µg/kg	8%
Na	3 mg/kg	15 mg/kg	6%
Mg	3 mg/kg	15 mg/kg	6%
Al	0.003 g/kg	0.015 g/kg	4%
P	21 mg/kg	105 mg/kg	10%
Cl	25.2 mg/kg	126 mg/kg	2%
K	7.2 mg/kg	36 mg/kg	17%
Ca	0.03 g/kg	0.15 g/kg	4%
Sc	30 µg/kg	150 µg/kg	7%
V	0.3 mg/kg	1.5 mg/kg	4%
Cr	0.3 mg/kg	1.5 mg/kg	9%
Mn	0.3 mg/kg	1.5 mg/kg	8%
Fe	6 mg/kg	30 mg/kg	10%
Co	0.03 mg/kg	0.15 mg/kg	5%
Ni	0.18 mg/kg	0.9 mg/kg	5%
Cu	0.06 mg/kg	0.3 mg/kg	7%
Zn	0.3 mg/kg	1.5 mg/kg	9%
As	84 µg/kg	420 µg/kg	10%
Se	0.3 mg/kg	1.5 mg/kg	16%
Sr	0.12 mg/kg	0.6 mg/kg	5%
Y	0.06 mg/kg	0.3 mg/kg	4%
Zr	30 µg/kg	150 µg/kg	3%
Mo	0.06 mg/kg	0.3 mg/kg	5%
Ag	90 µg/kg	450 µg/kg	3%
Cd	0.06 mg/kg	0.18 mg/kg	10%
Sb	0.048 mg/kg	0.24 mg/kg	4%
Ba	0.06 mg/kg	0.3 mg/kg	13%
Tl	36 µg/kg	180 µg/kg	3%
Pb	0.06 mg/kg	0.3 mg/kg	5%
U	0.006 mg/kg	0.03 mg/kg	5%

Table 2-22: MQL and CV values applied to ICP-MS data converted to mass fractions

To present the ICP-MS results for reports and presentations it was decided that a logarithmic radar plot fits the requirements. Initially tables and bar plots were investigated as ways of presenting the data, but were eventually disregarded due to the nature of the data (31 variables made visual comparisons impossible using these two techniques).

Radar plots, otherwise known as star or spider plots, are useful in presenting multivariate data from a single measurement and can be used to decide which measurements are most similar [203].

The plots give a visual representation of the ICP-MS data (31 variables) and these can be seen as "chemical fingerprints" for each sample. These fingerprints, however, do not include the measure of uncertainty as shown in Table 21. The plots make it quite simple to observe differences and similarities between samples (based on shape) and as a crude method of comparison, samples can be overlapped on each other to show similarities/differences. Automated sample matching or discrimination algorithms would still make use of the tabulated data and take into account the MU quoted.

2.2.4   ICP-MS of AN

Figure 2-8 shows three examples of the radar plots, which were obtained for samples of AN using ICP-MS. As a whole the AN samples analysed did not contain a large amount of trace metals. This is due to the fact that the samples were mainly explosive (DSTO-AN-1) or AR grade and they are stringently monitored for trace metal contaminations. The samples which were fertiliser grade (i.e. FU-AN-16) did contain a larger variety of trace elements. This has highlighted the potential to utilise trace element data to discriminate between different types of AN.

It can be observed in Figure 2-8 that the three samples have very different chemical fingerprints, and this factor can be utilised for comparing and linking samples of AN together. The trace element profiles obtained highlighted and potentially linked some of the samples of AN which were thought to be related to each other (i.e. same manufacturer or similar visual properties).
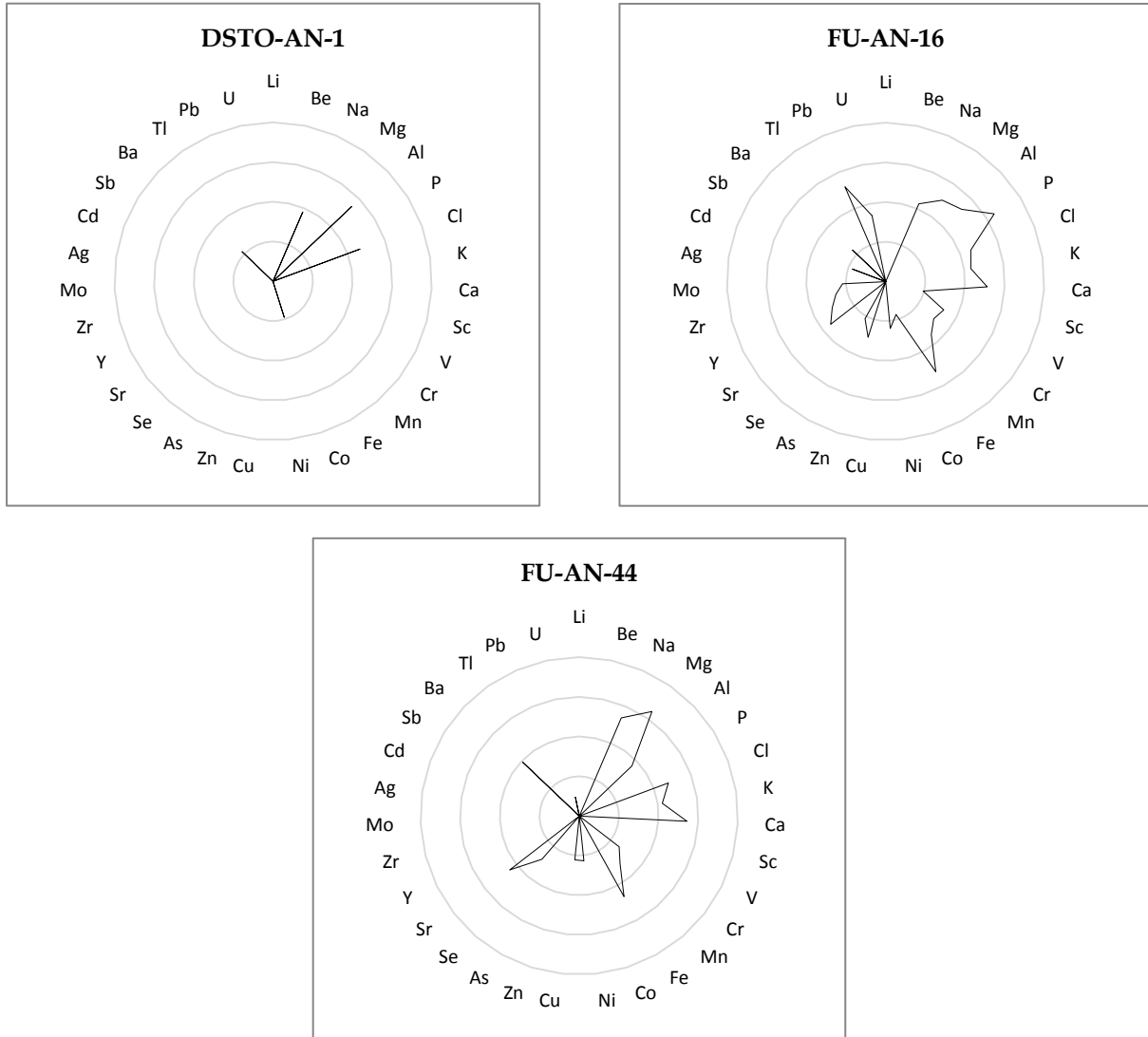
Figure 2-8: Log radar plots for three samples of AN

The prevalence of trace elements in samples of AN is due to the use of coating agents as previously detailed in Chapter 1. O'Connor et al. [204] detailed the prevalence of various coating agents used on AN prills through synchrotron radiation diffraction (SRD). These coating agents included aluminium sulphate ($Al_2(SO_4)_3$), sodium nitrate ($NaNO_3$), magnesium oxide (MgO), magnesium nitrate ($Mg(NO_3)_2$), calcium nitrate ($Ca(NO_3)_2$) and ammonium sulphate (($NH_4)_2SO_4$). A series of trace elements were also identified as being prevalent in the same AN samples using ICP-OES. The elements of interest identified in this study which could be utilised to compare samples of AN were: Al, Ca, Fe, K, Mg, Mn, Na, S and Si [204].

Different manufacturers may utilise different coating agents when producing their AN prills, this will ultimately alter the chemical fingerprint for each AN sample. This factor could be exploited as the chemical fingerprint obtained from a sample of AN may be indicative of its origin.

79

2.2.5   ICP-MS of CAN

Figure 2-9 shows three examples of the radar plots, which were obtained for samples of CAN using ICP-MS analysis.
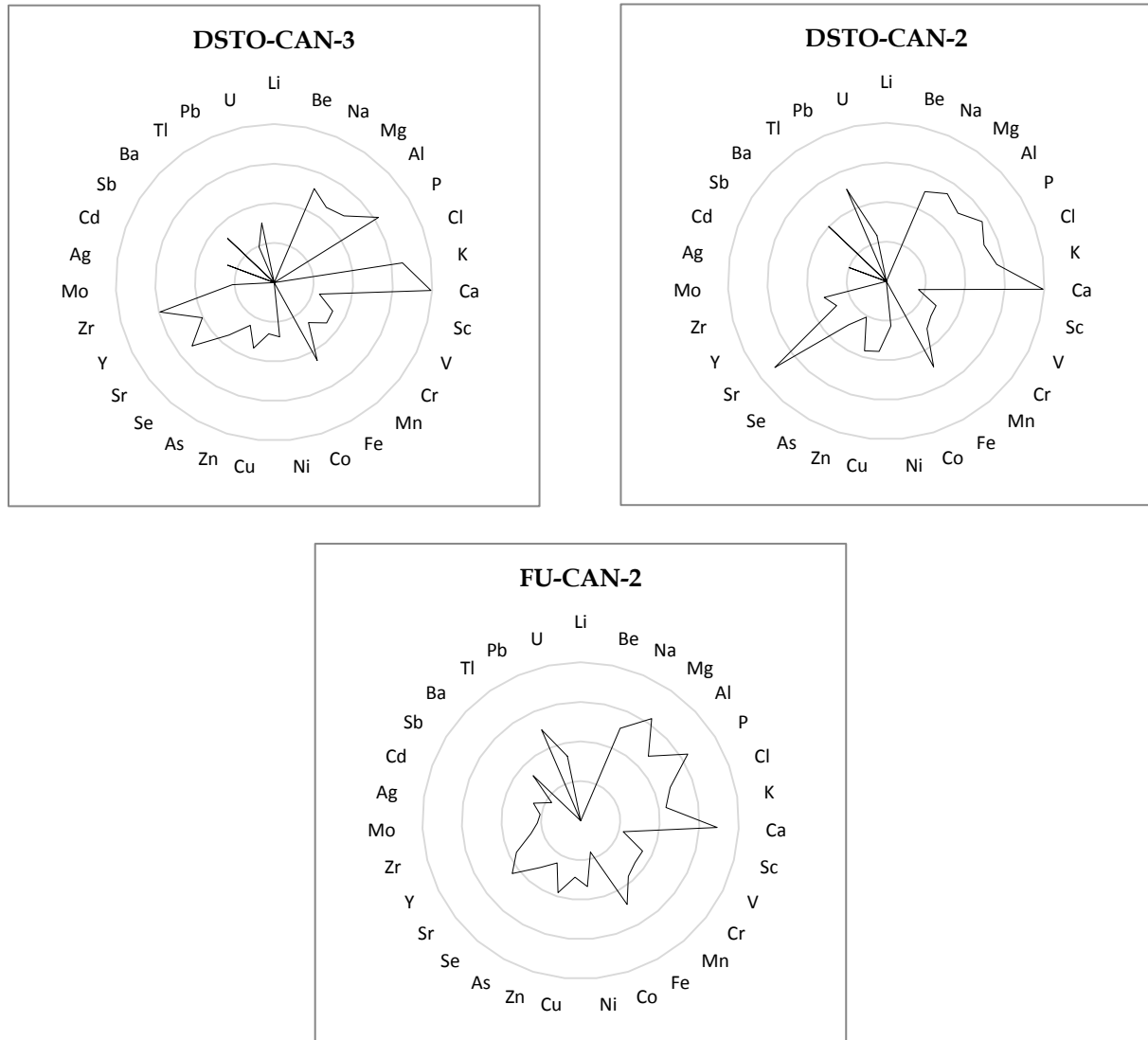
Figure 2-9: Log Radar Plots for three samples of CAN

It can be observed in Figure 2-9 that the three samples have very different chemical fingerprints, and this factor can be utilised for comparing and linking samples of CAN together. As a whole the CAN samples analysed contained a larger amount of trace metals than any of the AN samples. Samples which were thought to be related to each other (FU-CAN-1 and FU-CAN-2) had very similar trace element profiles. This highlighted the potential to link samples together using trace metal profiles.

The prevalence of trace elements in samples of CAN is due to the presence of calcium carbonate in the samples as previously detailed in Chapter 1. Potassium sulphate (K_2SO_4) may also be added to CAN fertiliser, and this addition ensures an efficient supply of potassium to crops.

A number of elements which may be prevalent in CAN samples were collated from a number of product data sheets. Elements which may be observed in samples of CAN include Ca, Cd, K, Mg, S, Cu, Pb and Hg [205, 206].

The source of the calcium carbonate will determine the nature of the trace elements present in a sample of CAN. Samples which contain limestone will have a higher proportion of calcium in a sample than a CAN which was prepared using dolomite which will naturally have a larger concentration of magnesium.

Samples of CAN which contain calcium carbonate as a by-product of the Odda process will contain a number of trace elements specific to the phosphate rocks used. This can include elements such as phosphorus, selenium, cadmium, uranium and arsenic. The prevalence of various elements in phosphate rocks was highlighted in Chapter 1.

The ability to determine the source of the calcium carbonate based on the presence of various elements in a sample will be of great use to determine the origin of the sample. This factor can be exploited as the chemical fingerprint obtained from a sample of CAN could be indicative of its origin.

2.3 Conclusions

This preliminary investigation has demonstrated the potential use of IRMS (nitrogen and carbon) as a method not only to discriminate but also show linkages between samples of AN, CAN, AN-based HME and CAN-based HME.

An ICP-MS method was developed to determine the suitability of this technique for the profiling of trace metals found in samples of explosive precursors (AN, CAN, $CaCO_3$ and Al) and HMEs (AN/Al, CAN/Al). The method was validated using spiked AN samples to determine that MUs were within acceptable bounds and that matrix effects did not adversely affect detection and quantification limits.

Quality control measures were put in place to ensure the continued validity of the data generated, and were found to be acceptable except in the case of boron, which was subsequently removed from the list of analytes. Ongoing monitoring of the quality control checks may result in slight modifications to the list of elements capable of being reliably quantified, working ranges and MUs applied to each element, as the method is utilised for the analysis of working samples.

A suitable visual representation of a chemical "fingerprint" has been created for each sample of interest by presenting the results obtained as a radar plot on a logarithmic scale, and furthermore demonstrated its ability to discriminate and/or show linkages between samples.

Intentionally Blank

3. Bulk IRMS and ICP-MS Analysis of CAN-based HME

3.1 Introduction

The primary focus for this research is to develop techniques that can be used for intelligence purposes based on the results obtained from the chemical analysis of explosive samples. For the war fighter, being able to identify batch-to-batch matches of like explosives enable the linking of explosive samples to a common source. This is a desirable outcome from an intelligence point of view, as this information can be used to identify explosives produced by the same bomb-maker, the distribution network associated with the materiel or identify an insurgents groups area of operation. Additionally, batch-to-source information can be used to determine where the bomb-makers are sourcing their materials.

Laboratory-made HME samples that were included in the initial analyses performed in Chapter 2 were simple mixtures that had been specifically formulated to demonstrate the utility of IRMS, however real world samples, in which these tight controls do not exist, may prove more difficult to analyse in this way. In order to test the robustness of the IRMS technique, a range of HME samples that are representative of real HME samples were produced by DSTO, these formulations were based on HME samples used by insurgents in recent operations in the Middle East. The HME samples obtained have both subtle and significant differences in their formulation, and will be used to test the validity of analytical techniques employed herein. These samples are used for illustrative purposes to show the complexity of analytical outcomes that must be overcome when using analytical techniques. The component ratios used in the HME samples prepared are detailed in Table 3-1.

Component	Levels in HME samples (%)
AN	57 - 98
Calcium carbonate	2 to 19
Aluminium powder	0 – 25
Sugar	0 – 13
Wood/Plastics	< 2

Table 3-1: Approximate compositions of HME samples

Caveat – All samples of CAN based HME were analysed in-house by DSTO to compare the physical and chemical compositions of the samples via a number of analytical techniques as highlighted in section 1.12. Subsequently a selected number of HME samples where then chosen to be analysed by IRMS and ICP-MS.

3.2 Isotope Ratio Mass Spectrometry of CAN-based Explosives

3.2.1 Objective

The initial analysis performed on AN/CAN based HME described in Chapter 2, indicated that it may be possible to link HME produced from the same batch, and possibly link the sample to the source material. This initial investigation was performed on a relatively simple HME blend, in which the sampling and storage was well controlled. The next step in on the development of the IRMS analysis methodology was to determine whether the technique was sufficiently robust for samples in which those controls were not so strong, in order to

reflect how "real world" samples may be utilised. This research was intended to determine the limitations of the IRMS technique and whether the analysis of samples by IRMS can assist in discriminating and/or linking samples of CAN-based HME.

3.2.2   Instrumentation

An IsoPrime (GV Instruments) IRMS was coupled to a EuroEA3000 Series (EuroVector) elemental analyser. The system utilised GV Instruments Micromass MassLynx mass spectrometry software [178]. The sampling technique utilised was continuous flow (CF-IRMS), which consisted of a helium carrier gas to carry the analyte gas into the IRMS ion source.

Caveat – Due to the nature of the samples analysed and limitations with the analytical instrumentation used, the isotopic data presented in this research is fit for the purpose of a comparative exercise (proof of concept) but should not be compared to data from other laboratories. All of the δ values displayed within this research have an associated error range (error bars) of ± 1 standard deviation.

3.2.3   Nitrogen Isotope Analysis

The nitrogen IRMS analysis was performed in triplicate for each sample of CAN-based HME. Sample sizes needed for nitrogen IRMS analysis is detailed in Table 3-2.

Nitrogen IRMS Analysis			
Sample	**Description**	**% Nitrogen**	**Sample Mass (µg)**
CAN	80% AN + 20% $CaCO_3$	28.00	286
CAN/Al	90% CAN and 10% Al	25.20	318
CAN/Sugar	85% CAN and 15% Sugar	23.80	337
CAN/Sugar/Al	85% CAN, 10% Sugar and 5% Al	23.80	337
Urea/Al	90% Urea and 10% Al	41.98	191

Table 3-2: Sample sizes needed for nitrogen IRMS

3.2.4   Carbon Isotope Analysis

Each sample of CAN-based HME was analysed in triplicate for carbon IRMS analysis. Sample sizes needed for carbon IRMS analysis is detailed in Table 3-3.

Carbon IRMS Analysis			
Sample	**Description**	**% Carbon**	**Sample Mass (µg)**
CAN	80% AN + 20% $CaCO_3$	2.40	1250
CAN/Al	90% CAN and 10% Al	2.17	1383
CAN/Sugar	85% CAN and 15% Sugar	8.36	360
CAN/Sugar/Al	85% CAN, 10% Sugar and 5% Al	6.26	480
Urea/Al	90% Urea and 10% Al	18.01	167

Table 3-3: Sample sizes needed for carbon IRMS

3.2.5   Carbon and Nitrogen Isotope Analysis Results for CAN-based HME Samples

The bulk nitrogen and carbon isotopic values for 155 CAN-based HME samples supplied by DSTO were determined by IRMS, the result obtained are shown in Figure 3-1. The samples are colour coded representing the general category of each HME blend. The samples

analysed were blends of CAN, sugar and aluminium in various ratios, also included were samples of urea/Al and CAN/Al/Fuel oil.
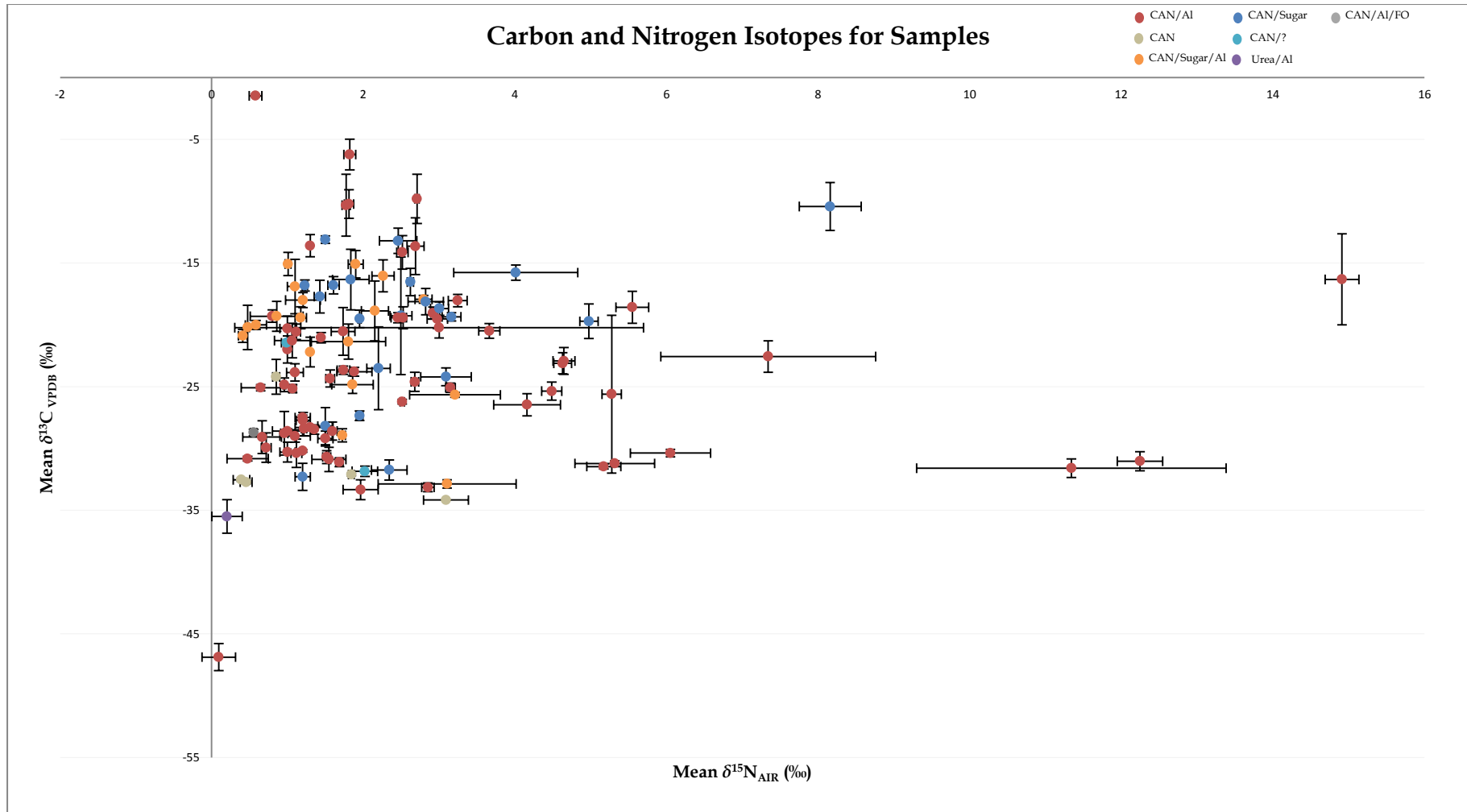
Figure 3-1: Bulk carbon and nitrogen IRMS results for CAN-based HME samples.

A general observation of the graph indicates that all of the $\delta^{15}N_{Bulk}$ values for the HME samples are positive, meaning that they are enriched in ^{15}N relative to atmospheric nitrogen. The $\delta^{13}C_{Bulk}$ values are negative, indicating that the samples are depleted in ^{13}C relative to VPDB.

The analysis of CAN-based HME samples by IRMS showed a wide distribution of samples and for large sample sizes, it becomes quite apparent that it is difficult to identify the formation of distinct clustering. It should be stated that X-Y scatter plots provide a convenient means to examine the patterns and trends that exist within a dataset (Figure 3-1) but are quite simplistic and more sophisticated tools such as Kernel density estimation may be more appropriate for data analysis, as recently reported by Carter *et al* [207]. Chacón *et al* stated that multivariate kernel density estimation is an important technique in exploratory data analysis [208]. Its utility relies on its ease of interpretation, especially by graphical means [208]. This type of data analysis is recommended as part of the future research in this area.

Despite the difficulty in identifying clusters, there seems to be a concentration of 15 HME samples around $\delta^{15}N_{Bulk} \sim$ +1‰ and $\delta^{13}C_{Bulk} \sim$ -28‰. Another possible cluster ($\delta^{15}N_{Bulk} \sim$ +0.4‰ and $\delta^{13}C_{Bulk} \sim$ -20‰) of three samples was identified as a blend of CAN/Sugar/Al. Wet chemistry breakdown of these samples also showed that the composition ratio was also the same. As these samples have the same composition and composition ratios, whilst also having similar isotopic ratios, this cluster may indicate that these samples are from the same batch.

The observed ranges in both the $\delta^{15}N_{Bulk}$ (+0.09‰ to +14.91‰) and $\delta^{13}C_{Bulk}$ (-1.5‰ to -46.9‰) values are quite large, which on initial inspection, may suggest multiple precursor source materials have been employed for the production of these HMEs. However, what bulk analysis fails to take into account is that these samples of HME may contain different proportions of the precursor materials (CAN/aluminium powder/sugar) which may alter the isotopic value significantly. The analysis of the bulk material also fails to take into account any isotopic fractionation that may have occurred to the sample after manufacture due to poor storage and handling.

What Figure 3-1 highlights is the difficulties posed for analysts when a large number of real world samples are investigated by IRMS where analysis is performed sampling the bulk material. The boundaries between potential clusters becomes blurred which makes batch-to-batch matching difficult. This also means that identifying source materials is nearly impossible. A factor to also consider is that the samples of HME analysed were only subsamples of bulk material and therefore the analysed samples may not be representative of the whole HME charge. It has been identified that the addition of a second carbon source (i.e. sugar as a fuel source) can have a vast effect on the carbon isotope value obtained for a HME sample. Any additional nitrogen sources (i.e. TNT within an amatol mixture (amatol is a mixture of 60% AN and 40% TNT)) would also vastly affect the bulk nitrogen isotope value obtained. The purification of the CAN (through wet processing) could also potentially affect the nitrogen and carbon isotope values for the samples.

The bulk IRMS analysis of CAN-based HME samples may be useful for identifying possible batch-to-batch linkages between samples, provided it is supported by other observations (physical arrangement of the IED, visual profile and other physical markers). In the absence of this, bulk sample IRMS analysis of CAN-based HME does not provide a high level of

87

confidence in being able to discriminate samples and identify the source of precursor materials used.

3.3 ICP-MS Analysis of CAN-based HME

Similarly, an investigation into the suitability of ICP-MS as a technique for the forensic analysis of explosive precursor materials and HME was conducted. The aim of this work was to determine whether trace elements present in the sample can be used to identify a chemical "fingerprint" which can be used to link or discriminate between samples and precursors.

ICP-MS analysis was performed on 115 AN/CAN-based HME samples using the methodology detailed previously in Chapter 2. As mentioned in Chapter 1, there are various methods to commercially produce AN and CAN and ICP-MS is a technique which may be useful for differentiating between these methods.

However, it should be noted that the digestion of the real world CAN-based HME samples are more complicated due to the inclusion of various particulates, such as plastics, wood, soil and sand. These particulates may not be completely digested using the acid digestion methodology detailed in Chapter 2. However, the amount of undigested material was estimated to be less than 2% of the sample mass and may not contribute significantly to the total "fingerprint" of a sample. This identified problem will be taken into account when comparing the ICP-MS results. Alternatively, it may be possible to select specific elements for use in comparison of ICP-MS results that reduce the impact of components that are not easily digestible.

Through an evaluation of open source data relating to CAN based fertilisers (previously reported within this thesis) a number of elements were identified as significant markers for the comparison of CAN-based explosives, these elements were selected as they are likely to be present in the source materials (rock phosphate) used in fertiliser production, these elements and their approximate composition within each sample are:

- Calcium (≈ 85 g/kg)
- Strontium (≈ 100 mg/kg)
- Barium (≈ 2 mg/kg)
- Magnesium (≈ 40 mg/kg) (marker for the presence of dolomite)
- Phosphorus (≈ 1000 mg/kg)
- Uranium (≈ 1 mg/kg)
- Selenium (≈ 3 mg/kg)
- Potassium (≈ 3500 mg/kg)
- Zirconium (≈ 900 µg/kg)

Prior analysis of the samples indicated that all but one sample was CAN based, this sample was a mixture of urea and aluminium. ICP-MS analysis was performed on the samples and the values obtained for elements listed above were recorded. Comparing the results indicated that there was more than one source of CAN used to prepared the HME samples, this was evident by comparing the amounts of phosphorous, uranium and selenium. The results obtained through ICP-MS analysis correlates with the data obtained from the IRMS which indicated that there may have been more than one source of CAN used in the

preparation of these HME samples. The ICP-MS results also identified that some of the extreme values present in the IRMS results shown in Figure 3-1 have used a very different source material, containing elements such as beryllium and silver at high levels.

The results obtained by ICP-MS analysis indicate that it is possible to categorise samples based on their trace element profiles, in doing so, it became clear that there is more than one source of CAN used for the production of the CAN-based HMEs analysed.

Care does need to be taken when using the results obtained from the ICP-MS analysis of the HME samples, as there are a number of factors that are intrinsic of the sample that cannot be ignored, namely:

1) Samples of CAN-based HME contain varying amounts of calcium carbonate depending on the success of the purification process;
2) The aluminium powders used as a fuel may contain impurities similar to those found in CAN;
3) The history of the sample is unknown, so it is not possible to determine whether the sample provided is representative of the material; and
4) The homogeneity of HME material may not be consistent, leading to sampling errors.

Using the display methodology described previously in Section 2.9, radar plots of selected CAN-based HMEs are shown in Figures 3-2 and 3-3. A visual comparison of the radar plots shown in Figure 3-2 is becomes rapidly apparent that the three materials presented are different. This was later confirmed through physical separation and identification. The sample DSTO-HME-17 was identified as a CAN/Sugar mixture, whilst samples DSTO-HME-70 and DSTO-HME-131 were identified as CAN/Al mixtures.
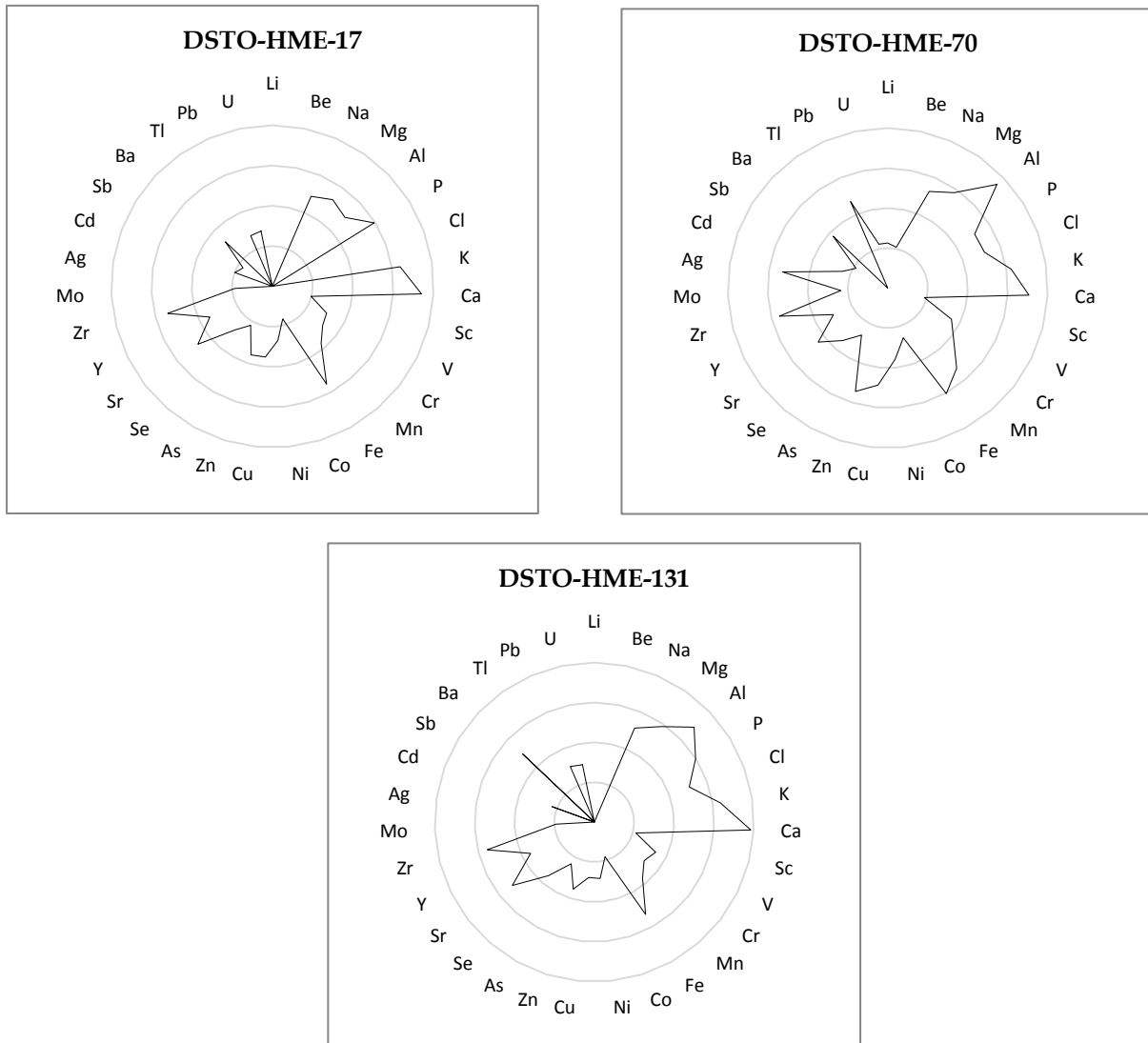
Figure 3-2: Trace element fingerprints for three CAN-based HME samples of interest (DSTO-HME-17, DSTO-HME-70 and DSTO-HME-131)

The radar plots produced for the three HME samples shown in Figure 3-2 have an obviously different shape, however with the exception of a few elements, share a number of similar features. These similarities may be due to the HME mixtures using the same source of CAN, with the differences introduced with the inclusion of the fuel component. The presence of fuels and other materials influence the overall elemental content and subsequently effects the radar plots produced This contribution to the overall elemental content means that it is not possible to use ICP-MS for analysis of a complex bulk mixture and link it to a source, however, the ICP-MS technique is suited for the matching of samples originating from the same batch.

In the previous Chapter, $\delta^{15}N_{Bulk}$ and $\delta^{13}C_{Bulk}$ IRMS analysis of three HME samples identified as CAN/Sugar/Al formulations showed the formation of a cluster. ICP-MS was performed on these samples and their elemental compositions were compared, the radar plot produced is shown in Figure 3-3.
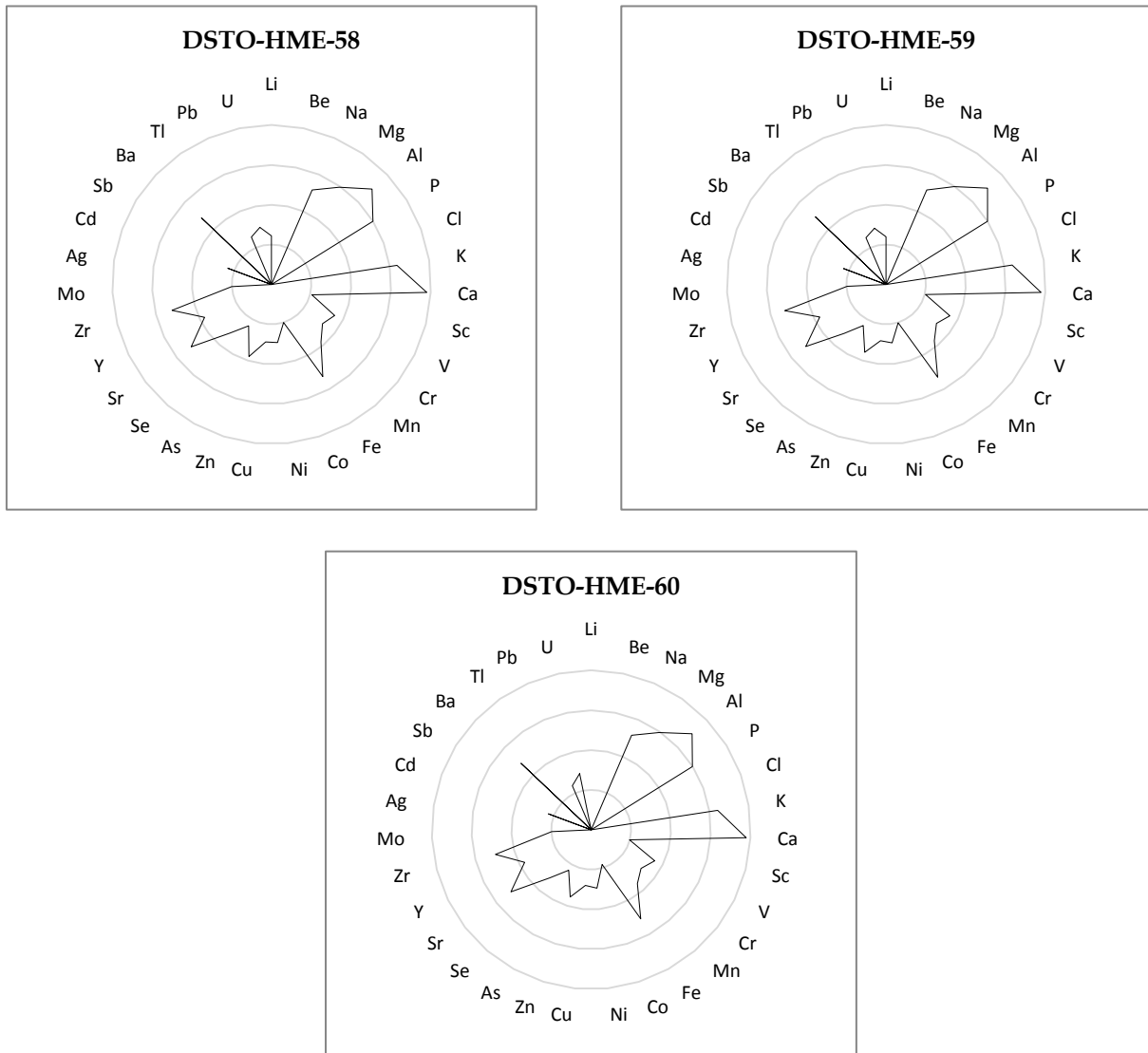
Figure 3-3: Trace element fingerprints for three CAN/Sugar/Al samples

The radar plots for these previously IRMS linked CAN/Sugar/Al HME samples are also very similar, which adds further weight to the fact that these materials may have a similar origin. Closer inspection of the radar plots show some slight differences, however, this can be explained due to sampling or contamination errors. What this data demonstrates though, is that the combination of IRMS and ICP-MS is sufficient to provide a high level of confidence for establishing batch-to-batch links between HME samples.

Overall, the chemical fingerprints obtained using ICP-MS can be utilised to compare (highlight differences) samples of CAN-based HME. It can also be used to highlight similarities between samples and this capability results in the fact that chemical fingerprints can be utilised for batch-to-batch matching of CAN-based HME.

3.4 The Purification of CAN-based Fertilisers

In order for CAN to be used for the construction of HMEs, it must undergo a purification process in order to reduce the amount of calcium carbonate present. In the analyses performed so far, we have not considered the isotopic fractionation that may occur during

the purification process, as this would lead to a change in the isotopic ratio of the CAN material, potentially meaning that it may be impossible to link a HME back to the source CAN.

As previously mentioned, insurgent bomb makers utilise two different approaches to reprocess CAN before mixing it with a fuel in order to produce a HME. This is done either by grinding the CAN prills to a fine powder, or through a wet processing technique colloquially termed "cooking" [5].

In order to understand the effect that the wet processing purification process has on the final isotopic and elemental profile of the purified CAN a series of experiments were conducted to replicate these known cooking processes on several CAN fertilisers. The final materials obtained were then analysed to determine their final isotopic and elemental profiles.

3.4.1   Materials

3.4.1.1 Experiments involving the small-scale "cooks" utilised the following materials
- CAN (a prepared mixture of 75% AN (DSTO-AN-4) & 25% $CaCO_3$ (AR Grade)) (3 batches of this CAN mixture were prepared)
- Water

3.4.1.2 Experiments involving the large-scale "cooks" utilised the following materials
- CAN (Incitec Pivot - 75% AN & 25% $CaCO_3$)
- Water
- 1% wt. salt water solution which was utilised to represent a sample of bore water.

3.4.2   Experimental

3.4.2.1 Small-scale (Triplicate "cook" for each time period)

20 g CAN + 2 mL H_2O (within a beaker)

↓

Placed into oil bath (163-170 °C)

↓

Heated & mixed for a set period of time (15, 30, 45 or 60 minutes)

Note: It took 20-30 Seconds for AN to dissolve and mixture become fluid

↓

Final slurry removed, cooled and desiccated until constant dry weight

↓

IRMS analysis (δ^{13}C and δ^{15}N)
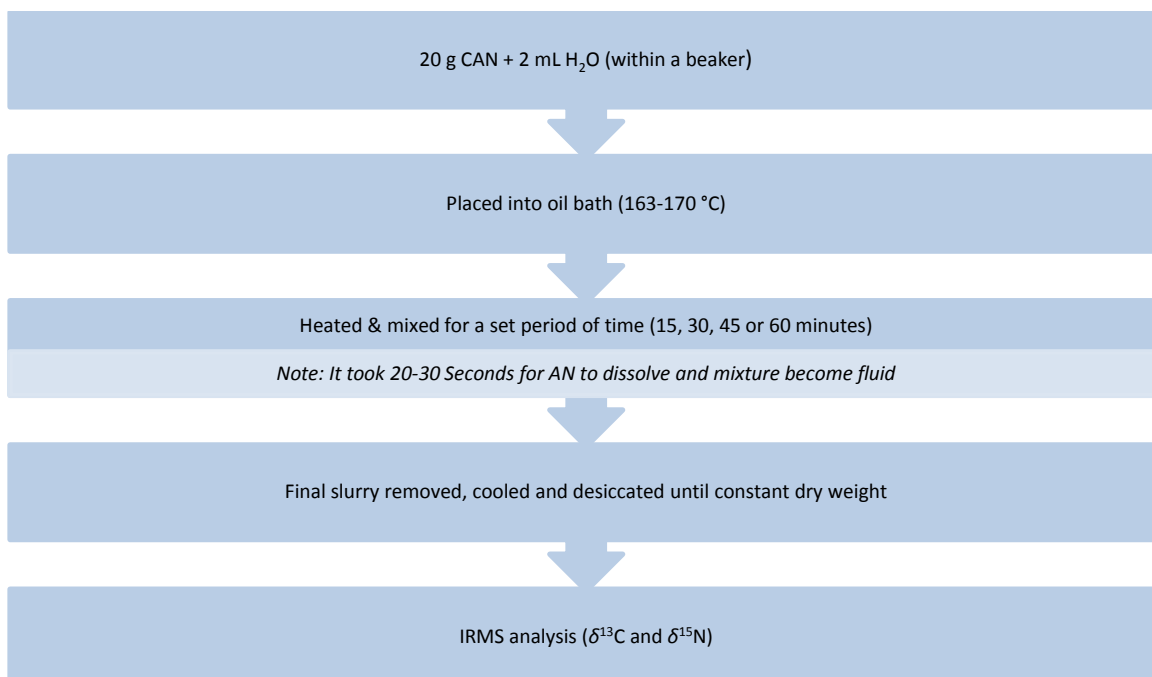
Photographs of the experimental setup and procedure used for the small-scale wet processing of CAN are detailed in Figure 3-4.

Note: After 1-3 minutes (over ~ 110 °C), ammonia odour is evident (accompanied by boiling)
Note: After 20-30 minutes the colour began to darken to a tan colour (which increased in intensity to completion) (less effervescence was seen over this darkening period)

Release of ammonia after 1-2 minutes (over ≈ 110°C)	Effervescence	Darkening to tan colour	Darkening to tan colour
Darkening to tan colour/reduced effervescence	Darkening to tan colour	Continued release of ammonia after 50 minutes	Drying is an exothermic process and results in release of ammonia
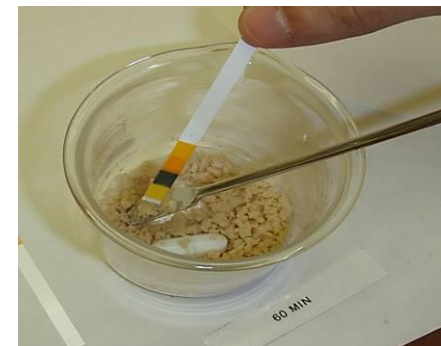
Final Product

Figure 3-4: Images and observations for a 60 minute "cook"

94

3.4.2.2 Large-scale (Two "cooks" completed)
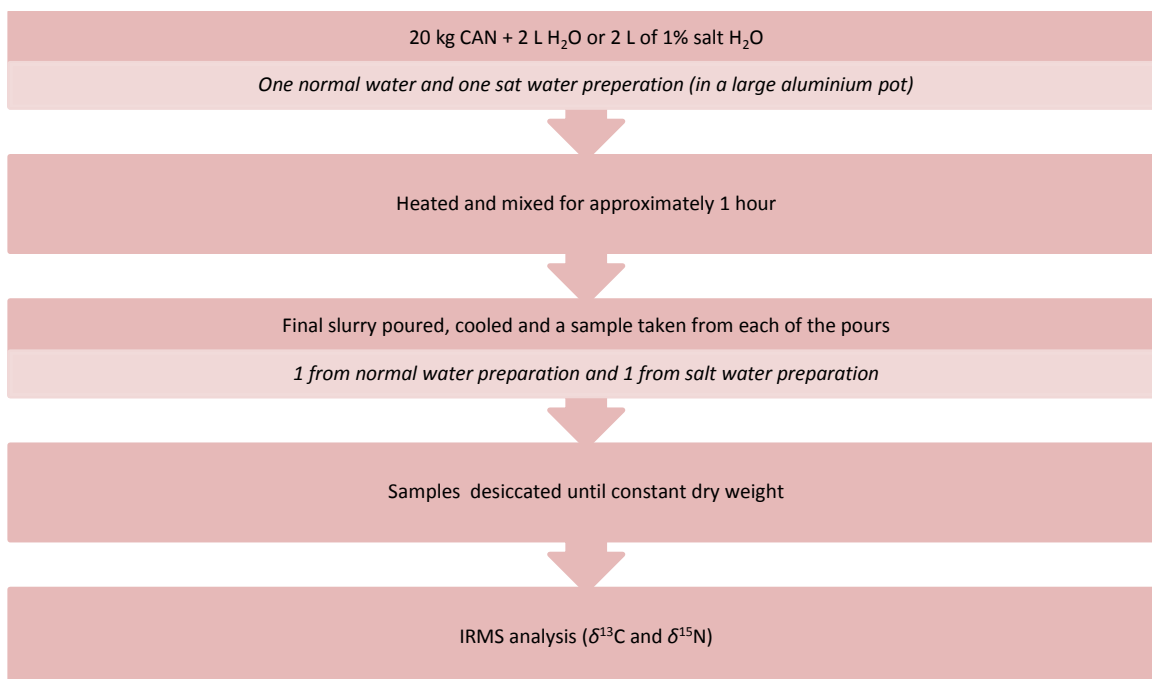
The method used for the large-scale purification of CAN is shown pictorially in Figure 3-5.

Step 1: CAN added to large container.

Step 2: Water added to the CAN.

Step 3: Solution heated till CAN is dissolved.

Step 4: Aqueous material decanted onto a tarpaulin, leaving insoluble calcium carbonate in the container.

Step 5: Purified AN left to crystallise, followed by air drying.

Step 6: Purified AN worked into a fine powder.
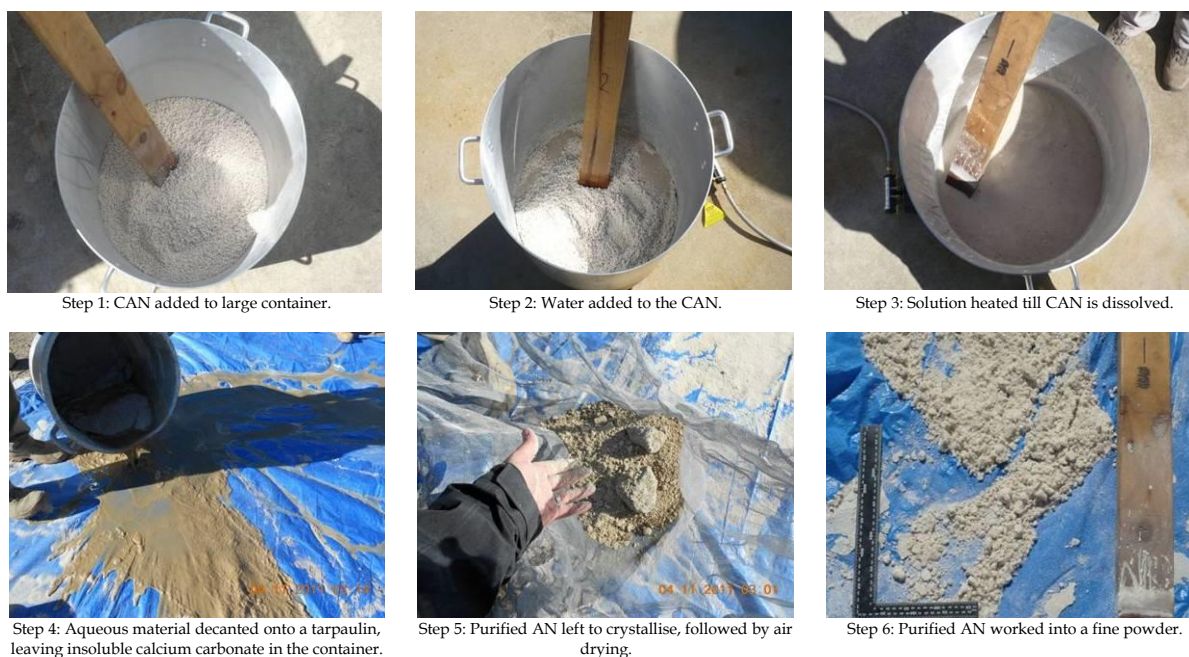
Figure 3-5: Large-scale wet processing of CAN

The observations noted during the large-scale wet processing are similar to that of the small scale procedure. The main difference between these two procedures is the final collection of the AN product. In the large scale preparation, the hot liquid containing dissolved AN is decanted onto a tarpaulin, leaving an insoluble white precipitate of calcium carbonate in the bottom of the cooking pot. The AN solution is left to cool on the tarpaulin, which leads to the formation of relatively pure AN crystals.

As the water used to dissolve the CAN is brought to boiling, there is an increase in the effervescence and the characteristic smell of ammonia is evolved from the cooking pot. This observation is important as the ammonia produced is due to the breakdown of the AN. The removal of ammonia during the cooking process may result in some level of isotopic fractionation and therefore a change in the isotopic composition of the final CAN product.

3.4.3   Analytical Methods

3.4.3.1 Isotope Ratio Mass Spectrometry
IRMS analysis was performed on a number of purified CAN samples using the methods detailed in Section 3.2 of this thesis.

3.4.3.2 Inductively Coupled Plasma Mass Spectrometry
ICP-MS analysis was performed on a number of purified CAN samples utilising the ICP-MS methods detailed in Section 2.2 of this thesis.

3.4.4   Small-scale Results

3.4.4.1 Isotope Ratio Mass Spectrometry
The average mass losses for each of the small-scale "cooks" were recorded and are detailed in Figure 3-6. It can be observed that as the cooking time increases, the mass loss also increases. The average temperatures for each of the small-scale cooks are represented in Figure 3-7.The small-scale cooks reached a maximum temperature of approximately 150°C during the cooking process, which was achieved after 15 minutes of heating, and maintained for the remainder of the purification process.
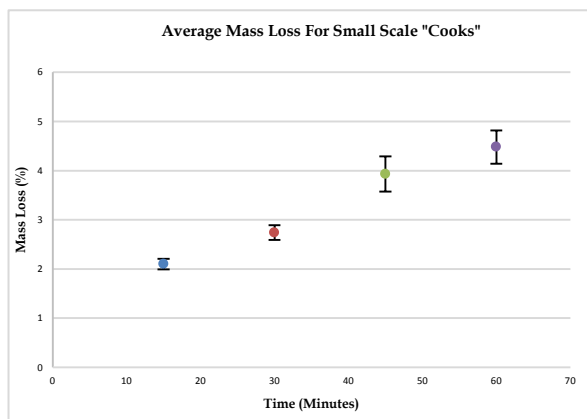
Figure 3-6: Average mass loss for small-scale "cooks"
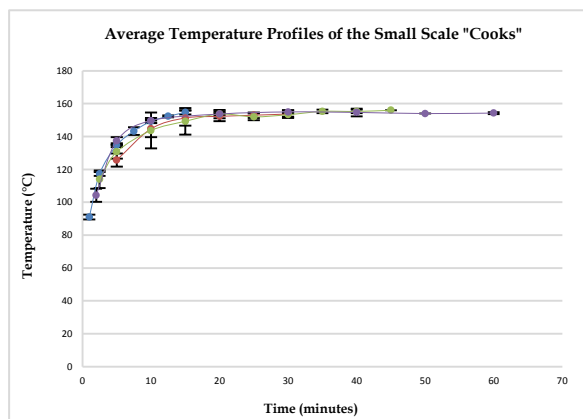
Figure 3-7: Average temperature profiles of the small-scale "cooks"

The carbon and nitrogen isotope results obtained for each of the CAN samples purified using the small-scale cooking process are shown in Table 3-4 and Figure 3-8. The IRMS results indicate that as the cooking time increases the $\delta^{15}N$ values shift to become more positive (enriched), while the $\delta^{13}C$ values shift to become slightly more negative (depleted). It should be stated that although the change in $\delta^{13}C$ is quite minimal it will be investigated further to develop an understanding of the CAN cooking process. These results suggest that as the mass loss increases with longer cooking time, the isotopic fractionation seen also increases. This result highlights that the purification process does lead to a change in the isotopic ratios of wet processed CAN, and that bulk analysis of HME by IRMS is unlikely to provide any useful information on linking a sample of HME to a source material.

Sample	Mean $\delta^{15}N$	S.D. $\delta^{15}N$	Mean $\delta^{13}C$	S.D $\delta^{13}C$
Initial	+0.20	0.02	+0.58	0.12
15 minutes	+0.70	0.07	+0.54	0.04
30 minutes	+0.96	0.09	+0.50	0.16
45 minutes	+1.16	0.06	+0.44	0.06
60 minutes	+1.32	0.06	+0.35	0.19

Table 3-4: IRMS results for small-scale "cooked" samples.
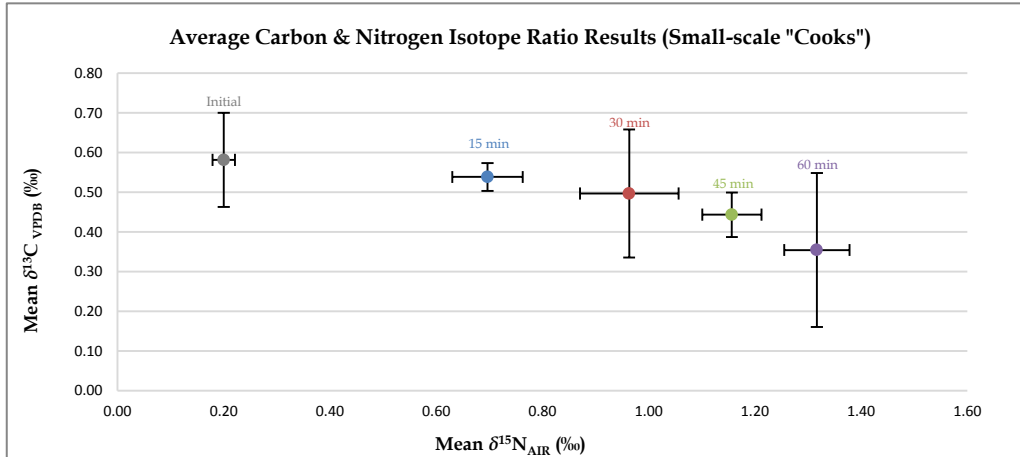
Figure 3-8: Average carbon and nitrogen IRMS results (small-scale "cooks")

The isotopic fractionation seen in the nitrogen values can be explained due to the loss of ammonia throughout the cooking process. The loss of ammonia was evident throughout the process due to the evolution of a strong ammonia odour and through testing the pH of the vapour being released from reaction.

The isotopic fractionations observed in the nitrogen isotopes are due to kinetic isotope effects. Kinetic isotope effects are a result of differences in bond strength (i.e. vibration energy levels of bonds) between heavier isotopes and lighter isotopes. When different isotopes of the same element are involved in a reaction/process, this difference in bond strength can result in different reaction rates for the bond. Kinetic isotope effects represent changes in bonding between the ground state and the transition state of a reaction. Statistical models predict that the lighter (lower atomic mass) of two isotopes of an element will form the weaker bond during kinetic isotope processes. The lighter isotope is more reactive, hence is concentrated in reaction products and reactants are enriched with the heavier isotope [86].

One of the first steps in the thermal decomposition of AN results in the formation of ammonia and nitric acid, as shown in Equation 3-1.

$$NH_4NO_3 \leftrightharpoons NH_3 + HNO_3 \qquad \text{(Equation 3-1)}$$

The evolved ammonia is isotopically depleted (enriched in ^{14}N) causing the remaining AN to be is isotopically enriched (concentrated in ^{15}N).

The amount of isotopic fractionation increases as the cooking time increases, as more ammonia is evolved. This is evident in Figure 3-7, where samples became more isotopically enriched the longer they were cooked.

The carbon isotopic ratios obtained for the "cooked" CAN samples are quite different to the experimental results obtained for the nitrogen isotopic ratios. This is because the final product was isotopically depleted (enriched in ^{12}C) due to the thermal decomposition of the calcium carbonate, which results in the formation of carbon dioxide and calcium oxide (shown in Equation 3-2).

$$CaCO_3 \leftrightharpoons CaO + CO_2 \qquad \text{(Equation 3-2)}$$

If this process was undergoing a kinetic isotope effect, it would be expected that the isotopic ratio of the final product would be isotopically enriched (concentrated in ^{13}C), and this would be due to the loss of CO_2 which would be isotopically depleted (enriched in ^{12}C). The results however do not suggest that a kinetic isotope effect has occurred in this case. It is postulated that the isotope fractionation of the carbon was limited due to surface area reactions between the calcium carbonate and the water. This potential mechanism of isotopic fractionation is discussed in Section 3.4.4.2.

3.4.4.2 Potential Mechanisms for Purification/Degradation of CAN

A result of the cooking procedure is to purify the CAN to AN by removing the insoluble carbonate salt. Depending on the composition of the CAN fertiliser (i.e. if it contains calcium or magnesium carbonate) the decomposition mechanisms will also differ.

The following equations give insight into the decomposition mechanisms for three different types of CAN fertiliser [59, 60, 209]:

$$2NH_4NO_{3(l)} + CaCO_{3(s)} \rightarrow Ca(NO_3)_{2(aq)} + 2NH_{3(g)} + CO_{2(g)} + H_2O_{(g)} \qquad \text{(Equation 3-3)}$$
$$2NH_4NO_{3(l)} + MgCO_{3(s)} \rightarrow Mg(NO_3)_{2(aq)} + 2NH_{3(g)} + CO_{2(g)} + H_2O_{(g)} \qquad \text{(Equation 3-4)}$$
$$4NH_4NO_{3(l)} + CaCO_3MgCO_{3(s)} \rightarrow Ca(NO_3)_{2(aq)} + Mg(NO_3)_{2(aq)} + 4NH_{3(g)} + 2CO_{2(g)} + 2H_2O_{(g)} \qquad \text{(Equation 3-5)}$$
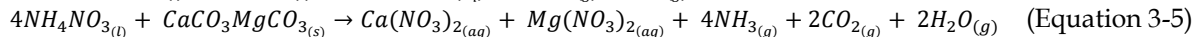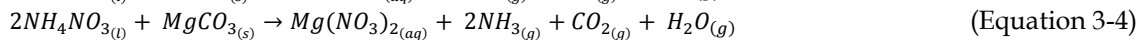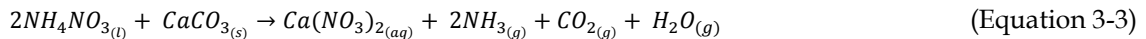
These proposed methods for the decomposition of CAN results in a loss of ammonia and carbon dioxide, and therefore predicts the isotopic fractionation as seen in the small-scale samples.

However, it should be noted that only a small proportion of AN would be converted into calcium nitrate as shown in Equation 3-3. This is due to the limited amount of calcium carbonate, which is relatively insoluble in water. Ultimately, the final collected product (in the case of Equation 3-3) would be a mixture of AN (high %), calcium carbonate (med %) and calcium nitrate (low %).

It is proposed that the isotopic fractionation seen in the δ^{13}C values is due to a loss of ^{13}C because of surface area reactions throughout the cooking process.

It is thought that the ^{12}C would react faster during formation of the $CaCO_3$. This would result in the accumulation of ^{12}C within the inner part of the $CaCO_3$ crystal. This would result in the outer layers of the $CaCO_3$ crystal being enriched in ^{13}C.

As the cooking process is taking place, it is proposed that because only the outer layer of the calcium carbonate is in contact with water, only this surface layer of calcium carbonate can react to form carbon dioxide. As the surface layer is more likely to contain ^{13}C, as it reacts it is lost as carbon dioxide, leaving an isotopically depleted $CaCO_3$.

The gradual loss of the isotopically heavier outer layers of calcium carbonate (leaving an isotopically depleted final product) is shown in Figure 3-9.
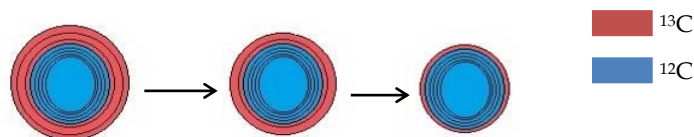
Figure 3-9: Schematic process of removal of isotopically labelled CaCO₃ layers during purification.

It should also be noted that there may be other reasons for the observed depletion in the final isotopic ratio of the calcium carbonate after the cooking process occurs. In the case where a sample of calcium carbonate is obtained from a natural source and therefore may contain organic carbon (e.g. coral) it may be possible that through the cooking process the inorganic carbon is lost (via the reaction between nitric acid and carbonate). This would leave the product enriched in organic carbon which is more likely to be isotopically depleted.

3.4.5 Thermal Analysis of the CAN/Water Cooking Process

3.4.5.1 Decomposition of Ammonium Nitrate
AN melts at 169°C and begins to decompose as soon as it melts, the first step being dissociation into ammonia and nitric acid (Equation 3-6). Previous studies have shown that the decomposition of AN operates by an ionic mechanism in the temperature range 200-300°C and formation of the nitronium ion is rate determining [210]. Acidic species (such as the ammonium ion, hydronium ion or nitric acid) increase the rate of AN decomposition dramatically (Equation 3-7), whereas basic species (such as ammonia or water) retard decomposition. Above 290°C a free radical decomposition mechanism dominates and homolysis of nitric acid is the rate controlling step [39, 211].

$$NH_4NO_3 \rightleftharpoons NH_3 + HNO_3 \qquad \text{(Equation 3-6)}$$

$$HNO_3 + HA \rightleftharpoons H_2ONO_2{}^+ \rightarrow NO_2{}^+ + H_2O \qquad \text{(Equation 3-7)}$$

Where HA = $NH_4{}^+$, H_3O^+ or HNO_3

$$NO_2{}^+ + NH_3 \xrightarrow{slow} [NH_3NO_2{}^+] \rightarrow N_2O + H_3O^+ \qquad \text{(Equation 3-8)}$$

$$NH_4NO_3 \rightleftharpoons N_2O + 2H_2O \qquad \text{(Equation 3-9)}$$
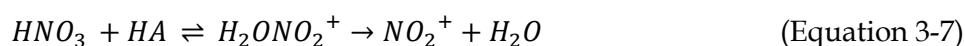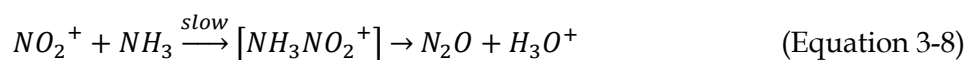
Differential scanning calorimetry (DSC) results (neat AN scanned at 20°C per minute from 50 to 450 °C) from previous analyses exhibited two endotherms and one exotherm followed by a final endotherm [39]. The first endotherm (~125°C) is the result of the II to I phase change and the second at about 169°C is the melting point of AN. The endotherm following the exotherm is due to the vaporisation of water formed during the AN decomposition. The observed exotherm from this study was about 100°C wide and had an exothermic maximum at 326°C [39]. The crystalline forms of AN are shown in Table 3-5 [212].

Designation	Temperature Range (°C)	Crystal Form
α	< - 18	Tetragonal
β	-18 to 32.1	β-Rhombic
γ	32.1 to 84.2	α-Rhombic
δ	84.2 to 125.2	Tetragonal
ε	125.2 to 169.6	Cubic

Table 3-5: Crystalline forms of AN.

Decomposition gases of AN mixed with 20 mol% calcium carbonate were determined to be nitrogen, nitrous oxide and carbon dioxide [210]. The authors have suggested that there is a trend that the more stabilising the additive (i.e. $CaCO_3$) the lower the N_2O/N_2 ratio and the higher the production of CO_2 [39]. Carbonates react with the acid proton of nitric acid (or of ammonium ion) to form carbonic acid and subsequently carbon dioxide and water. Ultimately, this results in the retardation of AN decomposition [39].

3.4.5.2 Simultaneous Thermal Analysis – Infrared Spectroscopy

To gain some insight into the decomposition processes occurring in the "cooking" of CAN and ultimately an explanation into the IRMS results obtained experiments were undertaken to simulate a CAN cook and monitor the reaction using thermal analysis techniques. This monitoring of a CAN cook was also undertaken to determine whether any ammonia or carbon dioxide could be detected as the reaction progressed (i.e. as the sample was heated).

A slurry of CAN (Initial mixture from "small cook" studies) (10 g) and water (1 mL) was prepared. Subsequently 17 mg of this mixture was transferred to the crucible (Al) of a PerkinElmer® simultaneous thermal analyser (STA) 6000, coupled to a PerkinElmer Spectrum™ 400 infrared spectrometer by the TL 8000 transfer line with a 10 cm gas cell. The transfer line and gas cell were heated to 350°C to avoid any risk of condensation of heavier compounds. The purge gas through the STA was nitrogen at a flow rate of 20 mL/min and the flow rate from the STA to the FT-IR was kept at 18 mL/min. The temperature was increased from 30 to 300°C at a constant rate of 20°C/min, then held for 5 minutes at 300°C. Infrared spectra were collected every five seconds.

Figure 3-10 shows the obtained thermal gravimetric analysis (TGA) and DSC trace for the simulated cook of a CAN/water sample.
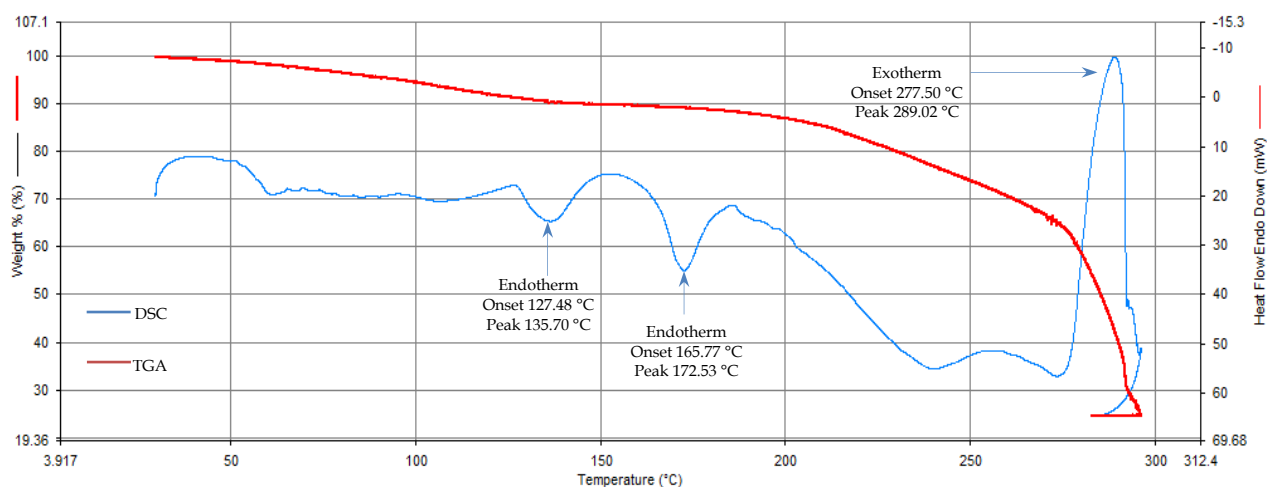
Figure 3-10: TGA and DSC trace of simulated CAN/water cook

The TGA of the CAN/water mixture shows a gradual mass loss up until approximately 200°C where the rate of decomposition of the AN mixture increases. The DSC trace is typical of prior thermal analysis of AN which has been previously detailed in this document. The temperatures at which the endotherms and exotherm occur are slightly different from literature but this may be due to the fact that this analysis was performed on a CAN/water mixture and also to different experimental conditions (i.e. different heating rate and different heating pans).

As previously stated, this study was interested in identifying the presence of ammonia and carbon dioxide throughout the cooking process. Figures 3-11, 3-12 and 3-13 illustrate the gaseous products released. Ammonia production is detected at approximately 9.14 minutes into the run (which occurs at a temperature in the region of 182°C). The presence of carbon dioxide was also confirmed by this technique. It can also be observed in Figure 3-12 that the formation of N_2O and NO has occurred and this indicates that AN has begun to undergo decomposition. This experiment adds further validity (by the observed loss of ammonia and carbon dioxide) to the previously seen isotopic changes (nitrogen and carbon) in the samples which underwent wet purification (cooking).
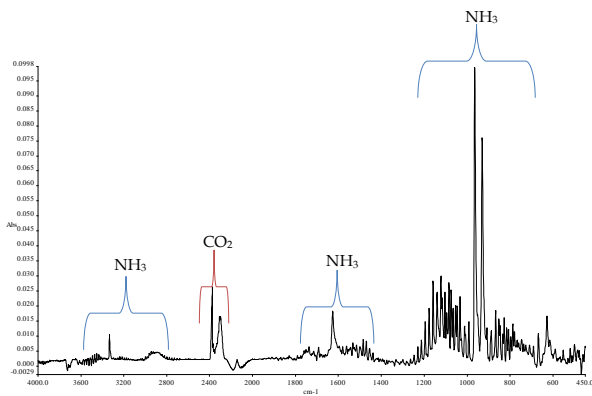
Figure 3-11: Snapshot of IR spectra from STA-IR analysis of CAN cook at 11.76 minutes
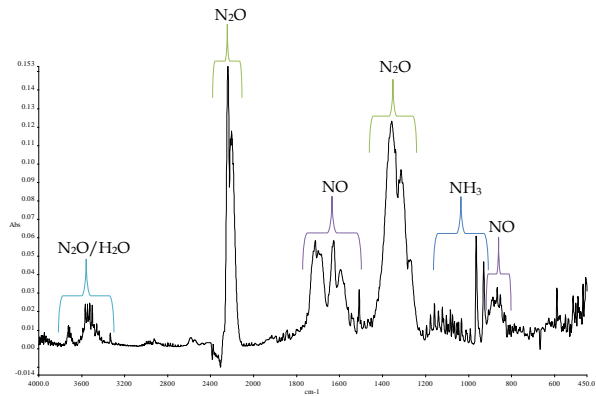
Figure 3-12: Snapshot of IR spectra from STA-IR analysis of CAN cook at 13.54 minutes
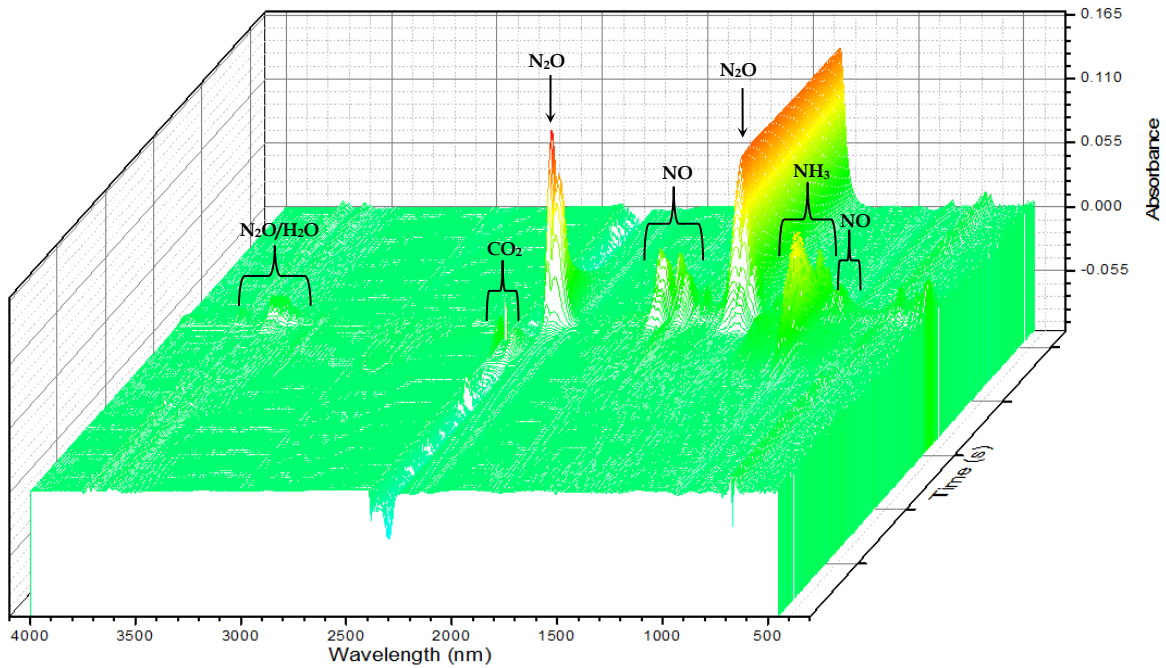
Figure 3-13: STA-IR thermogram representing absorbance with respect to time (s) and wavenumber (nm) for a CAN cook (at heating rate of 20°C/min, 30°C to 300°C)

3.4.6 Large-scale Results

3.4.6.1 Isotope Ratio Mass Spectrometry

The carbon and nitrogen isotope results for each of the large-scale "cooks" are shown in Table 3-6 and Figure 3-14. The IRMS results obtained from the wet processed CAN for the $\delta^{15}N_{Bulk}$ and $\delta^{13}C_{Bulk}$ values shift to become more negative. This is an unexpected result for nitrogen.

Sample	Mean $\delta^{15}N$	S.D. $\delta^{15}N$	Mean $\delta^{13}C$	S.D. $\delta^{13}C$
Bag 1	+0.93	0.13	-37.58	0.82
Bag 2	+0.84	0.09	-37.55	0.43
Cook 2	+0.57	0.03	-37.87	0.46
Cook 1	+0.54	0.04	-38.11	0.27

Table 3-6: IRMS results for large-scale "cooked" samples
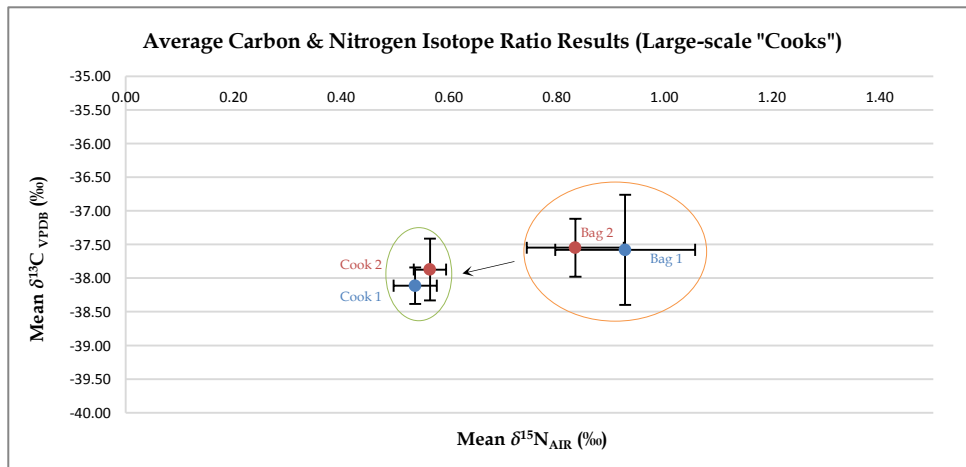
Figure 3-14: Average carbon and nitrogen IRMS results (large-scale "cooks")

102

The isotopic fractionation seen in the nitrogen values is due to the loss of ammonia throughout the cooking process. The loss of ammonia was evident throughout the process due to the evolution of a strong ammonia odour. However, unlike the small-scale cooks which became isotopically enriched in ^{15}N due to the purification process, these samples of commercial CAN became isotopically depleted (increase in ^{14}N content). It is thought that these samples may contain other carbonate salts ($MgCO_3$ and $CaMg(CO_3)_2$) or potentially other sources of nitrogen (i.e. other ammonium or nitrate salts). It is thought that this secondary source of nitrogen is the cause of the isotopic depletion as after the purification process it now makes up a larger proportion of the formulation.

The isotopic fractionation (i.e. depletion in ^{13}C) observed in these large-scale cooks follow a similar pattern to the results previously observed in the small-scale "cooks" and the reasoning for this isotopic fractionation was discussed in section 3.4.4.2.

	Carbon		Nitrogen	
	α	ε	α	ε
Cook 2	0.9997	-0.3377	0.9997	-0.2698
Cook 1	0.9994	-0.5533	0.9996	-0.3896

Table 3-7: Fractionation and Enrichment Factors for large-scale "cooks"

Table 3-7 details the fractionation and enrichment factors for the large-scale CAN "cooks". It can be seen that in both samples isotopic depletion was observed for both nitrogen and carbon. These enrichment values compliment the information presented in Table 3-6 and Figure 3-14. The enrichment and fractionation factors were calculated using equations 3-10 and 3-11(Rayleigh equations for enrichment and fractionation factors) [113, 140, 213]:

$$\alpha = \frac{(1000 + \delta_{product})}{(1000 + \delta_{reactant})}$$
(Equation 3-10)

$$\varepsilon = (\alpha - 1) \times 1000$$
(Equation 3-11)

3.4.6.2 Inductively Couple Plasma – Mass Spectrometry

Trace metals analysis was completed on samples of unpurified CAN and then samples of purified CAN, which were obtained after the large scale "cooks". This task was completed to determine what effect of the purification process has on the elemental composition of the purified material. This will ascertain whether samples that have undergone purification retain the elemental composition of their source material, and what elemental markers may be introduced into a sample that has undergone a "wet purification" process.

Figure 3-15 depicts both samples of CAN prior to the purification process; these samples have a similar overall chemical fingerprint. Both samples, labelled Bag 1 and Bag 2, were received from the same supplier and therefore are potentially produced from the same manufacturer. These samples were selected as there should be a degree of 'natural' variation in trace element levels.

Slight differences in the elemental composition was observed between the two samples, these are detailed below:
- Bag 1 has a higher content of Mo and As (these elements are quite close to the LOQ)
- Bag 2 has slightly higher levels of Na, Mg, Al, P, Cl, Sc, V, Cr, Mn, Fe, Cu, As, Se, Sr, Y, Zr, Cd, Ba and Pb.
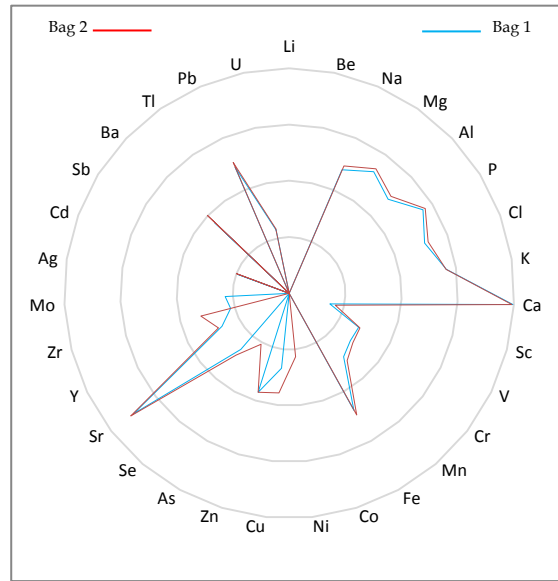
Figure 3-15: Trace element fingerprints for Bag 1 and Bag 2.

Figure 3-16 shows the two elemental fingerprints for the two independently purified samples (Cook 1 and Cook 2). It can be observed that the two purified samples have similar overall chemical fingerprints. There are some slight differences between the two samples and these are detailed below:

- Cook 1 (Bag 1) has a higher level of Na, Cl. Cook 1 consisted of wet processing using a 1% salt (NaCl) solution, and this increase in the sodium and chlorine content are due to elements present in the water used.
- Cook 2 (Bag 2) has slightly higher levels of P, K, Ca, Sc, V, Cr, Mn, Fe, Zn, Sr, Y, Zr, Ba, Pb and U.
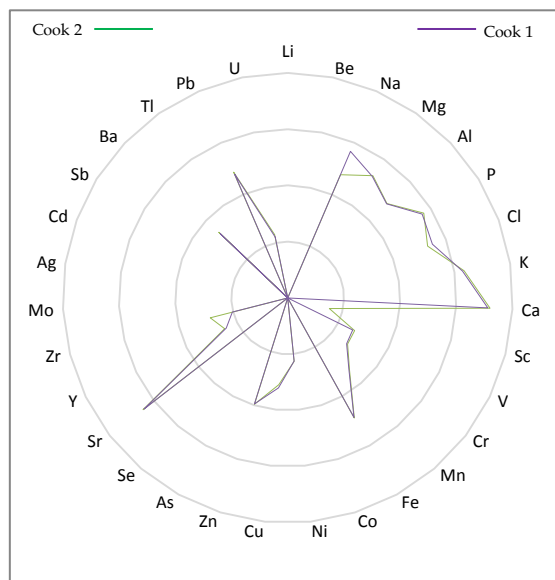
Figure 3-16: Trace element fingerprints for Cook 1 and Cook 2

A comparison between an unprocessed CAN (Bag 2) and a purified CAN (Cook 2) can be observed in Figure 3-17. There are a few distinct changes in the chemical fingerprints pre and post purification. However overall the trace element fingerprints are quite similar.

- The purified sample (Cook 2) shows an increase in the K, Zn and Mn content.
- The purified sample (Cook 2) shows a decrease in the amount of Na, Mg, Al, Ca, Sc, V, Cr, Mn, Fe, Cu, Se, Sr, Y, Zr, Cd, Ba, Pb and U present (As, Se, Cd close to LOQ in Bag 2).
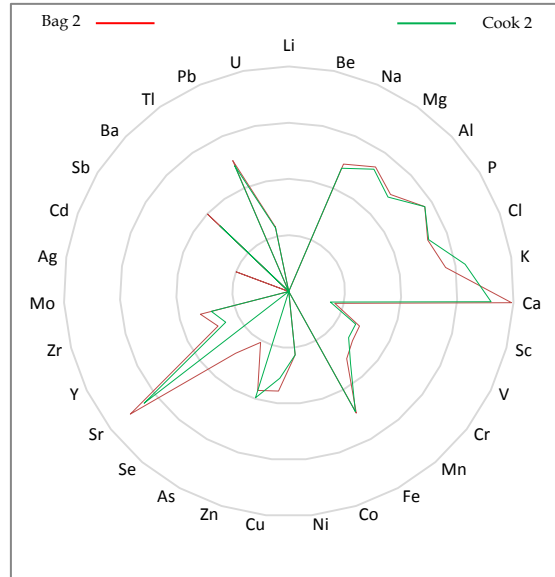
Figure 3-17: Trace element fingerprints for Bag 2 and Cook 2

Figure 3-18 highlights the differences between another unprocessed CAN (Bag 1) and a purified CAN (Cook 1). Once again, there are a few distinct changes in the chemical fingerprints pre and post purification. However overall the trace element fingerprints are quite similar.

- The purified sample (Cook 1) shows an increase in Na, Cl, K, Mn, Fe, Ni, Cu and Zn content. As previously mentioned, the increase in Na and Cl content is due to the 1% salt solution used in the purification process.
- The purified sample (Cook 1) shows a decrease in the amount of Ca, Sc, V, Cr, As, Se, Sr, Y, Zr, Mo, Cd, Ba, Pb and U present (Sc, Cd, Se, Mo were close to LOQ in Bag 1).

The decrease in trace elements for both purifications were slightly lower than expected in comparison to how much of the calcium carbonate was removed as an insoluble sludge. This indicates that a lot of the elements may have been present in the CAN as water soluble salts and as such passed through the wet purification process. This is of interest as this kind of information can be utilised for the purposes of linking samples back to a manufacture or manufacturing method.
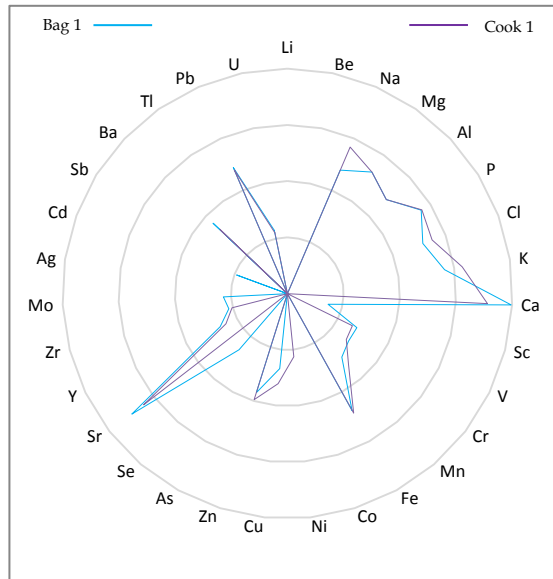
Figure 3-18: Trace element fingerprints for Bag 1 and Cook 1.

The potential to use trace element fingerprints for the comparison of CAN samples pre and post purification has been demonstrated. It has also been shown that elemental fingerprints can also be utilised to show linkages between pre and post purification samples. There are a few factors, which need to be taken into account when interpreting and utilising these trace element fingerprints:

It can be observed that in both of the purified samples (Cook 1 and Cook 2) there was a decrease in the content of quite a few elements (compared to the original elemental concentrations of Bag 1 and Bag 2). This decrease in trace element composition was a direct consequence of the cooking and purification process.

The purification process is completed to remove the calcium carbonate from the CAN mixture. A majority of the elements present in these samples are due to the presence of calcium carbonate (i.e. Ca, As, Se, Sr, Y, Cd, Ba and U) derived from mineral sources (limestone/dolomite or rock phosphate). As the calcium carbonate is removed from the sample, a number of elements associated with the calcium carbonate are also removed. Final elemental composition will be dependent on the efficiency of the cooking and purification processes (i.e. decanting the final AN liquor from the $CaCO_3$ insoluble precipitate).

The trace element fingerprint for Cook 1 indicates that the salt water processing has led to an increase in sodium and chlorine levels in the final CAN product. This finding leads us to the conclusion that the CAN may take on any trace elements, which are within the water, used to process it. Therefore, as there may be a carry through of elements from the water used to process the CAN, these impurities may be used as markers for wet processing.

The higher levels of trace elements in the purified CAN products (K, Fe, Ni, Cu and Zn) form readily soluble salts, whereas those that are depleted in the cooked CANs generally have a poorly soluble salt. Contamination from the use of stirring and cooking implements may also be a factor as wooden sticks were utilised for stirring of the CAN mixtures while the purification procedure was undertaken in aluminium cooking pots. These factors and

106

sources of contamination need to be taken into consideration when looking at the trace element fingerprints for the comparison of samples.

An evaluation was undertaken to determine the extent of calcium carbonate removal by the wet processing of CAN in order to assess its impact on the trace metal content of samples. This evaluation was calculated from the output of the thermal conductivity detector of the elemental analyser (EA) (nitrogen and carbon content) and ICP-MS (calcium content) results obtained from the large-scale cooks. The results are shown in Tables 3-8 and 3-9 and are displayed in Figure 3-19.

EA (Based on Nitrogen and Carbon content)				
Sample	Initial CaCO$_3$ %	Final CaCO$_3$ %	Initial AN%	Final AN %
Cook 1	26	9	74	91
Cook 2	28	8	72	92

Table 3-8: Estimated purification results based on carbon and nitrogen content values (EA)

ICP-MS (Based on Calcium content)				
Sample	Initial CaCO$_3$ %	Final CaCO$_3$ %	Initial AN %	Final AN %
Cook 1	22	4	78	96
Cook 2	24	3	76	97

Table 3-9: Estimated purification results based on calcium content (ICP-MS)

The compositions of the raw and wet processed CAN samples were calculated based on EA results (Table 3-8) by using both the raw carbon and raw nitrogen content values. This method takes into account all carbon sources (carbonate) and all nitrogen sources (ammonium and nitrate). If there were two different sources of carbonate (i.e. magnesium and calcium), this would have no bearing on the carbon content. The EA results indicate that purification process reduced the calcium carbonate content from 27% to 8.5%.

The extent of CAN purification was also estimated based on the ICP-MS results (Table 3-9) which measured the concentration of calcium (in μg/kg) in the samples. Unfortunately this only takes into account any calcium salts, and it is suspected that there may have been some magnesium carbonate or calcium magnesium carbonate in the samples. This was determined using the ICP-MS results, which were previously discussed (high Mg content). Due to this the calcium carbonate content may be underestimated and therefore the ICP-MS purification results may be indicating that the purification was more efficient than it actually was (calcium carbonate content reduced from 23% to 3.5%).
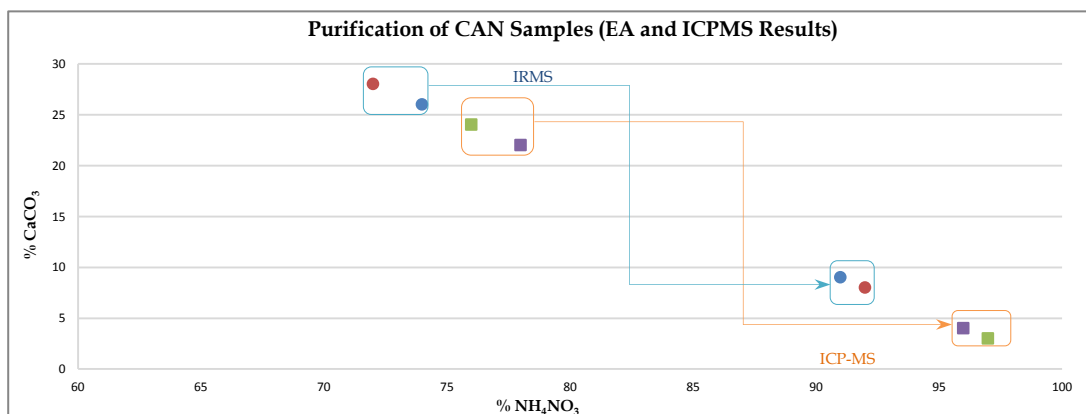
Figure 3-19: Graphical display of estimated purification results

These examples show that the reported purification methods being utilised do in fact purify the CAN to AN quite well. On average (utilising both the EA and ICP-MS results) the amount of calcium carbonate is reduced from 25% to 6% by this purification technique.

3.5 Problems Associated with Bulk Analysis of CAN-based HME

Due to the variability observed in genuine HME samples, it appears that neither technique (IRMS or ICP-MS) is globally applicable. The specific issues are identified below.

3.5.1 IRMS

A number of potential problems have been highlighted throughout the research task, which may affect the bulk isotopic analysis ($\delta^{15}N_{Bulk}$ and $\delta^{13}C_{Bulk}$) of CAN-based HME samples:

1) Dual nitrogen sources (i.e. amatol mixtures as detailed in Section 3.2.5);
2) Dual carbon sources (i.e. CAN/Sugar mixtures as detailed in Section 3.2.5); and
3) Purification of CAN.

3.5.2 ICP-MS

The following potential problems with the analysis of HME samples by ICP-MS have been highlighted, which may affect the chemical fingerprints obtained through the analysis of CAN-based HME samples using ICP-MS:

- Contamination of samples (major issue in genuine samples);
- Sampling issues (inhomogeneity); and
- Purification of CAN.

An attempt to balance these issues was made using approximately 1 g test batches of CAN/Al reference material. The material was subjected to selective extraction with MilliQ water and trace metal grade acetic acid. This procedure is used to separate components of CAN/Al for compositional analysis.

It was found that the labware used (despite multiple washings with trace nitric acid and MilliQ water) and the extensive manipulation of the sample in this process introduced too many opportunities for contamination and samples crossover. Therefore, we were unable to separate the HME into its individual components for ICP-MS analysis (for the purpose of determining the origin of source materials).

3.6 Investigation into Identified Problems

The work described in this thesis thus far has highlighted some of the problems associated with the use of IRMS and ICP-MS for the analysis of CAN-based HME samples for the development of intelligence, through the identification of batch-to-batch and batch-to-source matches. The remainder of this thesis describes research conducted to solve these problems.

3.6.1 Identified Weaknesses and Potential Problems with Bulk Nitrogen Isotope Analysis of Ammonium Nitrate

The $\delta^{15}N_{Bulk}$ values obtained for samples of AN may be isotopically enriched with ^{15}N due to isotopic fractionation. This isotopic fractionation is due to the loss of ammonia (e.g. through

purification processes/poor storage) which leads to a change in $\delta^{15}N_{Bulk}$. This was observed in the sample of AN which was heated/melted (Prep 1), where the $\delta^{15}N_{Bulk}$ after this process had an enrichment factor of 1.89. This was determined to have occurred due to the loss of ammonia, and the isotopic enrichment of the final product AN is because of kinetic isotope effects.

Kinetic isotope effects can be described as a ratio of rate constants of compounds containing light versus heavy isotopes at the reactive site, depicted by the formula: $^{light}k/^{heavy}k$. If the ratio is more than one (i.e. light isotopes react faster, heavy isotopes become enriched in the substrate), the isotope effect is referred to normal. If the ratio is less than one (i.e. light isotopes become enriched in the substrate), the effect is referred to as inverse [86].

Due to the difference in mass between isotopes of the same element, the reaction and processes occur at different rates. Fractionations as a result of chemical reactions and physical processes (such as evaporation and condensation) produce products that are isotopically lighter than their starting materials. These isotopic fractionations are more evident in lighter elements (e.g. ^1H and ^2H) because their isotopes show proportionally larger differences in mass than heavier elements (e.g. ^{12}C and ^{13}C) [86].

Ammonia is the major intermediate phase in the pathway of nitrogen transfer from the fixed N phases (e.g. crustal material) to free nitrogen (e.g. natural gas reservoirs). However the gaseous nitrogen isotopic behaviour during these nitrogen-cycling processes remains relatively unknown. Li et al, carried out a study to investigate the nitrogen isotopic effect associated with the thermal decomposition of ammonia ($2NH_3 \rightarrow N_2 + 3H_2$). Pure ammonia ($\delta^{15}N \sim +2\ ‰$) was sealed and thermally decomposed at different temperatures over various periods of time. With the progress of the reaction, the $\delta^{15}N$ of the remaining ammonia increased from -2 to +35 ‰ (isotopically enriched) [214].

Ammonia may be lost throughout the synthesis of AN; the following two statements are examples of when and how these losses may occur.

- During the synthesis of AN, a solution of AN (83-90%) is passed through evaporators to remove the majority of water and concentrate the solution to 95-99% for conversion into solid AN. During evaporation, some ammonia is lost from the solution, but this in normally replace before solidification.

- In the TOPAN process, molten AN is prilled down a tower to form 1-3 mm diameter roughly spherical granules. Some ammonia and AN may be lost to the air stream and some ammonium nitrate vapour is lost from the surface of the prill during this process. This loss is negligible in terms of mass; however it may be significant with respect to isotopic composition.

These potential losses may mean that it is unlikely that the $\delta^{15}N$ for ammonium could be utilised to provenance the ammonia used in the manufacturing of AN. Other potential variable which may contribute to the loss of ammonia from AN have been identified as part of this research program. These and previously identified problems with fertiliser (ammonia volatilisation) are detailed below.

The synthesis and purification methods obtained from the internet (YouTube and forums) provide conditions which allow for the loss of ammonia and therefore cause isotopic fractionation which affects the final AN product, namely:

109

- Evaporation - the longer a solution is left for the water to evaporate off, could result in a large fractionation seen in the recovered AN (due to extensive loss of ammonia).

- Heating – high temperatures used to drive water off (leaving AN crystals) will cause isotopic fractionation due to the loss of ammonia. The melting point of AN is 169 °C and it begins to decompose as soon as it melts, this could also be a cause of isotopic fractionation [39].

- Poor storage conditions could also contribute to the decomposition of AN which may lead to the release of ammonia. Some examples of storage conditions which may cause ammonia loss (and therefore isotopic fractionation) are:
  - Moisture;
  - Temperature;
  - pH (alkaline pH increases the volatilisation of NH_3);
  - Location (indoors/outdoors); and
  - Sealed/unsealed packaging.

The sampling of AN/CAN samples may also be an important variable, especially in the case of poorly stored samples. The loss of ammonia may not be uniform (i.e. in the case of a pile of AN prills, ammonia loss may only take place at the top of the pile). Therefore the bulk isotopic composition of AN sampled from the top of the pile may be different to a sample of AN taken from the middle of the pile.

Ammonia volatilisation has also been identified as a potential problem:

- Any surface applied ammonia/ammonium-based nitrogen fertiliser (including manure) can lose nitrogen to the atmosphere via ammonia volatilisation. The potential is greatest with urea and fluids containing urea (such as urea/AN) [215]. CAN is less subject to volatilisation than fertilisers that contain all of their nitrogen in ammonium form, or form ammonium after application to the soil (e.g. urea). Volatilisation may occur when fertilisers are applied to a surface without incorporation [205].

- The gaseous loss of ammonia from nitrogen fertilisers is undesirable, because of the detrimental effect on crop performance, the loss of input and consequent economic loss. Urea, which is used as an organic nitrogen source, is subject to ammonia loss. Yerokun conducted a study assessing ammonia volatilisation from a variety of nitrogen fertilisers applied to alkaline soils. The range of ammonia loss from an ammonium nitrate fertiliser was 0-0.32 %. It was also found that at all rates of application; the losses of ammonia were negligible [216].

- Butler et al, also conducted a study were their objective was to quantify the amount of ammonia volatilisation from various nitrogen fertilisers, which were applied to soil surfaces. They found that both CAN and AN provided low levels of ammonia volatilisation, especially in comparison to urea [217].

3.6.2 Limitations to Trace Metal Analysis Due to Contamination

Trace element analysis can be utilised as a useful parameter for sample-to-sample comparison of relatively pure and uncontaminated samples. However, due to several

processes undertaken to convert the CAN to HME and the subsequent collection and sub-sampling of these HME when seized, the final sample available for analysis may be contaminated. The potential sources of contamination must be considered when attempting to extract actionable intelligence outcomes from the ICP-MS analysis results obtained from HMEs. Sources of these contaminants may be due to human or environmental factors and are detailed below.

3.6.2.1 Contamination Considerations: Human Factors

Preparation contamination is contamination introduced to the sample by exposure to the handler. The personal contamination issues discussed in Section 2.2.1.2 that an analyst tries to eliminate, such as contact of the sample with skin, jewellery and cosmetics, are almost never adequately controlled during the manufacture and handling of charges and devices. As both the "cooking" and preparation of HME are labour intensive processes, the contamination from the handler may be an important factor.

HME explosive factories are usually located outdoors and are typically found to be disorganised and sloppy [218]. This leads to a higher chance of introducing contamination.

The "Cooking" process usually incorporates the use of metal cooking pots/barrels to contain and "cook" the mixture, while wooden spoons/paddles/wood (e.g. 2 x 4) are used for stirring the mixture [6]. The metal pots and wooden stirring implements can be a source of trace elements. Water used in the cooking process can also contain trace metals. This factor is further detailed in the next section.

The "Drying" process usually consists of air drying the purified CAN on tarpaulin (plastic or cloth), the tarpaulin is also used to crush and strain the purified CAN. Fibres and surface contamination from the tarpaulin can also be a source of trace elements [6].
The "Grinding" process can incorporate the use of industrial or hand grinders to crush CAN prills into powder. Bombmakers can also implement the use of artillery shells, rocks and bricks as a way to crush the CAN prills into powder [6]. A sifter then can be utilised to separate any granules/prills from fine powder.

"Mixing and Packing" methods usually incorporates the packing and use of fragmentation within a charge – these can include materials such as loose ball bearings, nuts, bolts, bullets, shell casings, scrap metal, rock, glass etc. These are all source of trace metals [6, 218].

Table 3-10 details commonly encountered container type, and the container in which the HME is stored can lead to an increase in trace metal content [6].

Commonly Encountered HME Containers	
Ammunition cans	Barrels and drums (plastic and metal)
Bags (flour/sugar or fertiliser)	Buckets (plastic and metal)
Bowls (plastic bowls and tupperware)	Cooking Pots (pressure cookers)
Jerry Cans (plastic and metal)	Water coolers
Munitions casings	Jugs (yellow palm oil container)
Tanks and cylinders	Steel or metal pipes

Table 3-10: Commonly encountered HME containers

The above processes usually occur in open areas, which means that the samples of HME are susceptible to airborne contamination. This is the result of the exposure of samples to

unfiltered air during handling. Sources of airborne contamination can include dust, flaking paint, carpeting, insects, animals and dirt.

As detailed above, the contamination of a sample due to handler is an important factor to consider. The collection and sampling of seized samples for forensic analysis is itself a process, which is susceptible to contamination. The collection process is uncontrolled and without knowledge of the factors detailed below, samples may not be fit for trace element analysis:

- Gloves (clean and single use);
- Spatulas (non-metal) (clean and single use);
- Sample vials (cleaned ICP-MS grade); and
- Sub-sampling of seized materials (homogeneity and representative of the bulk).

Ultimately, the sampling of seized HME samples was uncontrolled and this factor has to be accounted for when utilising any ICP-MS data.

3.6.2.2 Contamination Considerations: Environmental Factors

A situation where background environmental profiling of a location would be of benefit when interpreting ICP-MS results obtained from samples of HME would occur in places where conflicts have or are occurring. An example of this is the recent conflict in Afghanistan where it is known that CAN-based HME are widely utilised. Two examples of environmental contamination which would be beneficial to have a grasp of include water and soil sources. These types of contamination can alter the trace element profile of a sample and this can subsequently hinder batch-to-batch matching and source identification. However knowing about these issues may also help with the interpretation of results and allow a scientist to focus their analysis of a smaller number of elements which are not affected by these issues.

Water Sources – Water is utilised in the purification process and as such may influence the final trace element profile of the CAN or CAN HME sample. Below is an overview of thermal and spring water types located within Afghanistan.

There are a diversity of thermal water types in Afghanistan, i.e. bicarbonate, chloride, sulphate and sodium chloride, all produced by complex geological structures and the development of various metamorphic and metasomatic processes in different geological environments. This has resulted in a variety of geochemical and hydrogeological conditions. Table 3-11 illustrates examples of some of the thermal springs encountered in Afghanistan [219].

Discharge (Lit/Sec)	Temp (°C)	Chemistry	Geochemical Environment	Location
0.3	29-33	HCO_3, Na, K, Ca, Si, Br, F	Metamorphic, CO_2-bearing (4g/L)	Saranmorkhana, Uruzgan
6	20-35	HCO_3, Ca, Mg, Na	Metamorphic, CO_2-bearing	Wardak
0.7	20-35	HCO_3, Ca, Mg	Metamorphic, CO_2-bearing	Wardak
2.5	20-35	HCO_3, Mg, Na	Metamorphic, CO_2-bearing	Wardak
2	22-24	HCO_3, Cl, Ca, Mg, Na, K, F, Br, Si	Metamorphic, CO_2-bearing	Bande Aindjir, Uruzgan
0.1	>35	Cl, Na, Li, Rb, Cs, B	Metamorphic, CO_2-bearing (2g/L)	Nmk Shordg, Helmand
4	20-35	HCO_3, Ca	Metamorphic, CO_2-bearing	Wardak
50	20-35	HCO_3, Ca, Mg	Reducing	Uruzgan
60	20-35	HCO_3, Ca, Mg	Reducing	Uruzgan
2.5	>35	HCO_3, Ca, Mg	Reducing	Uruzgan
4	>35	HCO_3, Ca, SO_4	Reducing	Uruzgan
7	42-45	Cl, HCO_3, SO_4, Na, K, Ca, Si, Ti, Cu, Sr	Reducing, N-bearing	Wakhad, Helmand
25	>35	HCO_3, Ca, SO_4	Reducing	Helmand
3	38-40	HCO_3, SO_4, Ca, Mg, Na, K, Si, Ti, Cu, Sr	Reducing, N-bearing	Garmab Kajaki, Helmand
3	22-24	HCO_3, Ca, Si, Mn, Sr, V, Zr, Cu, Ga, Ti, Li, Ba, Cr, F	Metamorphic, CO_2-bearing (2.4g/L)	Jare Masjid, Ghor

Table 3-11: List of surface geothermal indications in Afghanistan (surface temperatures > 20°C)

There are three types of mineralised spring in Afghanistan: carbonated springs, nitrous and sulphurous springs, and water springs. Only the carbonated springs are associated with high rare-metal concentrations. In central Afghanistan, occurrences of rare metals have been identified in sediments below several lakes and depressions where brines contain higher than average metal concentrations. Trial pits have indicated that salt deposits covered by clay and loam layers contain high concentrations of lithium, boron, lead and zinc [220].

Soil and dirt contamination – During the purification of CAN and the preparation of the HME, the mixture may be contaminated with dirt/soil from the location in which the preparation takes place. Contamination by soil/dirt may also occur during the recovery of unexploded IEDs or during the recovery of partially detonated samples. Below is an overview of mineral deposits and surface material mapping of Afghanistan.

Industrial mineral occurrences in Afghanistan include fluorspar (grade 46.7% CaF_2), apatite, asbestos, graphite, mica, phosphorate, high-purity quartz, salt, silica sand, sulphur and specialty clays [221].

The United States Geological Survey (USGS) undertook hyperspectral mapping of Afghanistan in 2007. Map 3-1 shows the distribution of selected iron-bearing minerals and other materials derived from analysis of HyMap imaging spectrometer data [222]. Table 3-12 details the material classes that were identified though this Hyperspectral mapping program [222]. These materials may cause trace element contamination in samples.

Map 3-2 shows the distribution of selected carbonates, phyllosilicates, sulfates, altered minerals and other materials derived from analysis of HyMap imaging spectrometer data [223]. Table 3-13 details the material classes that were identified though this Hyperspectral mapping program [223]. These materials may cause trace element contamination in samples.
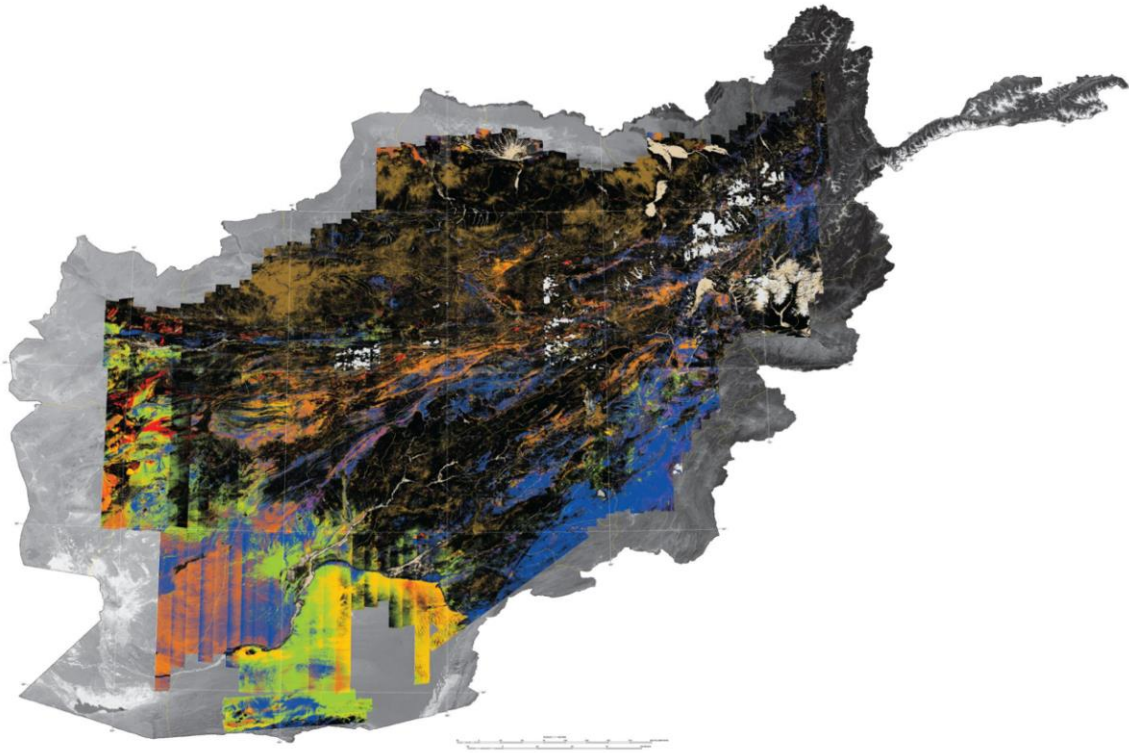
Map 3-1: Surface materials map of Afghanistan: Iron-bearing minerals and other materials

Map 3-1: Material Class
Hematite (Fe_2O_3)
Goethite $(FeO(OH))$
Epidote $(Ca_2Al_2(Fe^{3+};Al)(SiO_4)(Si_2O_7)O(OH))$
Ferrihydrite $(5Fe_2O_3 \cdot 9H_2O)$
Fe^{2+} and Fe^{3+}
Fe^{3+}
Iron hydroxide $(Fe(OH)_2$ or $Fe(OH)_3)$

Table 3-12: Identified material classes for map 3-1
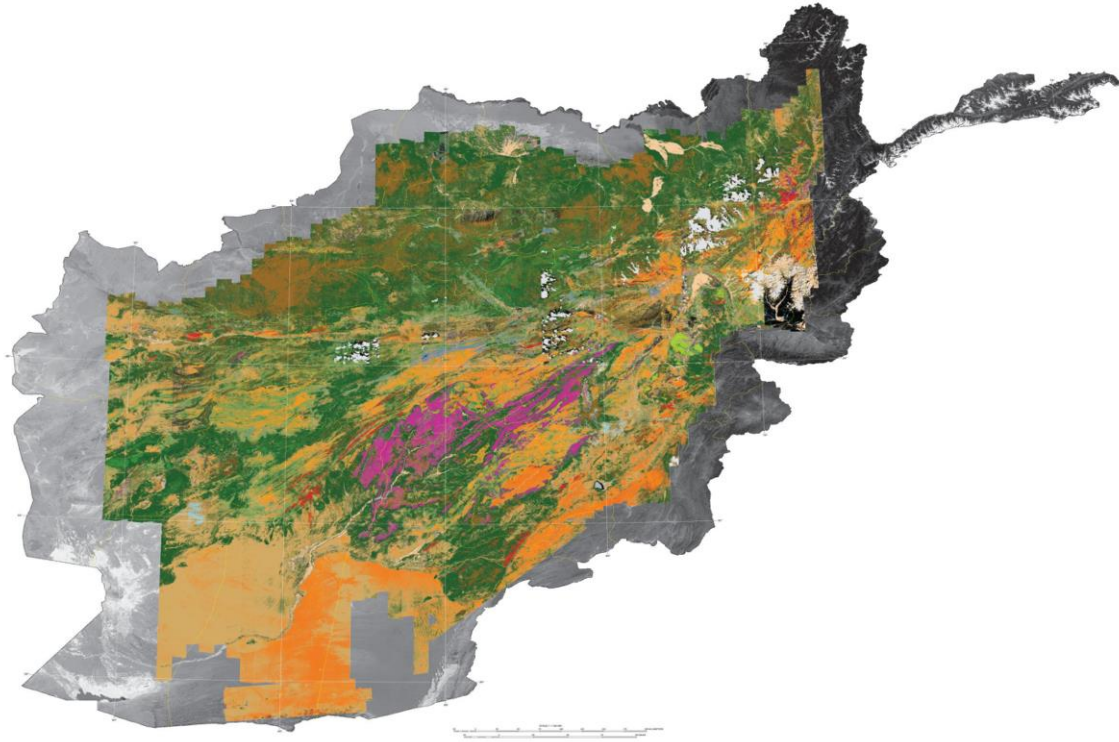
Map 3-2: Surface materials map of Afghanistan: Carbonates, phyllosilicates, sulfates, altered minerals and other materials

Map 3-2: Material Class
Dolomite $(CaMg(CO_3)_2)$
Muscovite $(KAl_2(AlSi_3O_{10})(F,OH)_2)$
Chlorite (ClO_2^-) or Epidote $(Ca_2Al_2(Fe^{3+};Al)(SiO_4)(Si_2O_7)O(OH))$
Kaolinite $(Al_2Si_2O_5(OH)_4)$
Calcite $(CaCO_3)$
Montmorillonite $((Na,Ca)_{0.33}(Al,Mg)_2(Si_4O_{10})(OH)_2\, nH_2O)$
Illite $((K,H_3O)(Al,Mg,Fe)_2(Si,Al)_4O_{10}[(OH)_2,(H_2O)])$
Calcite and muscovite/Illite

Table 3-13: Identified material classes for map 3-2

With a knowledge and understanding of the potential sources of sample contamination, the analytical data obtained using an ICP-MS is still quite valid for sample-to-sample comparisons. However, these sources of contamination and the overall manipulation/purification of samples may result in difficulties in linking samples back to manufacturer (i.e. fertiliser plant).

3.7 Conclusions

The research discussed in this Chapter has led to a better understanding of how the "wet processing" purification technique alters the isotopic and trace elemental profiles of CAN.

The act of wet processing results in isotopic fractionation (of both nitrogen and carbon isotopes) due to the evolution of ammonia during the cooking process, which means that isotopic composition of the purified material has no resemblance to the source material and cannot be linked through simple analysis of the bulk material.

The elemental composition is also shown to be affected by the wet processing procedure; however, they can still be utilised to show linkages/discriminate between samples produced in the same batch. Caution needs to be taken when using this data, as efficiency of the purification process can alter the final trace element composition. It was also noted that any impurities in the water used for the purification process are carried through to the final CAN product.

Trace element analysis does have a few limitations, especially when the history and sampling techniques of a material is unknown. A number of potential sources of contamination (human and environmental) have been identified in this report. This factor needs to be taken into account when using any trace element data.

The results obtained from this initial research indicate that there are significant limitations in the use of bulk isotope analysis ($\delta^{13}C_{Bulk}$ and $\delta^{15}N_{Bulk}$) for forensic intelligence purposes.

Intentionally Blank

4. Nitrogen Isotope Analysis of Nitrate Species Isolated From Ammonium Nitrate and Calcium Ammonium Nitrate

4.1 Potential Use for Separation of Ammonium Nitrate

Previous isotopic analysis of AN has highlighted potential areas of research which may help in the determination of the provenance of materials. This includes the potential for differentiating between sources of AN by separating the sources of nitrogen within the compound and measuring the nitrogen in the ammonium and/or nitrate ion independently [40]. This type of isotopic information may provide information into the materials (precursors) used to manufacture/prepare samples of AN. The objective of this task was to develop a suitable method for the $\delta^{15}N$ analysis of the nitrate species isolated from samples of AN and CAN.

A new labelling scheme for nitrogen and carbon isotope ratio results has been implemented from this section forward in the thesis. As a number of novel methodologies have been implemented for the isotopic analysis of CAN-based HME, they are specific to the different types of samples being analysed. They are listed below:

Nitrogen isotope ratio results:

- Analysis of the bulk HME material - $\delta^{15}N_{Bulk}$
- Analysis of the water soluble portion from bulk HME (AN) - $\delta^{15}N_{Water\ Soluble}$
- Analysis of the nitrate species isolated from AN - $\delta^{15}N_{Nitrate}$
- Calculated isotope value for ammonium species from AN - $\delta^{15}N_{Ammonium}$

Carbon isotope ratio results:

- Analysis of the bulk HME material - $\delta^{13}C_{Bulk}$
- Analysis of the water soluble portion bulk HME material (sugar) - $\delta^{13}C_{Water\ Soluble}$
- Analysis of the water insoluble portion from bulk HME (carbonate) - $\delta^{13}C_{Carbonate}$

4.2 Previous Work in the Separation of Ammonium Nitrate for Isotopic Analysis

4.2.1 Isotopic Analysis of Nitrates

4.2.1.1 Nitrate Fertilisers

Stable isotopes are useful as traces of agrochemical compounds in the environment. Several studies have been carried out using the $\delta^{15}N$ and $\delta^{18}O$ data of dissolved nitrates in order to discriminate between organic (human or animal waste) and inorganic (synthetic fertilisers) nitrogen contaminants in waters [224-229]. Nitrate isotopes have also been used to evaluate the fractionation processes in which nitrogen fertiliser compounds are involved ([145, 227]).

Figure 4-1 details common values of $\delta^{15}N$ and $\delta^{18}O$ of nitrate from synthetic nitrate fertilisers, ammonium fertilisers (including urea), soil, and sewage/animal waste. Figure modified from Silva *et al* [225].
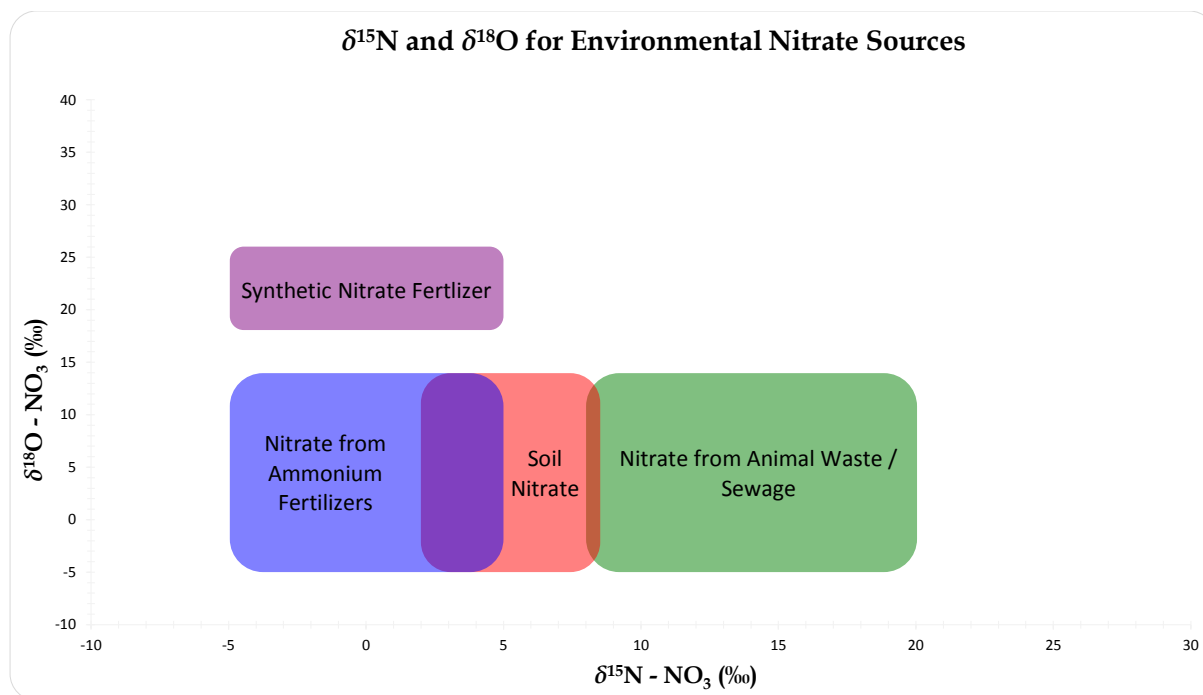
Figure 4-1: Common fields of $\delta^{15}N$ and $\delta^{18}O$ of nitrate from synthetic nitrate fertilisers, ammonium fertilisers, soil, and sewage/animal waste

Silva *et al.* describe a method for collecting and concentrating nitrate from fresh water for $\delta^{15}N$ and $\delta^{18}O$ analysis [230]. Nitrate is eluted from the anion exchange columns with dilute HCl. The nitrate-bearing acid eluent is neutralised with Ag_2O, filtered to remove AgCl precipitate, then freeze dried to obtain solid $AgNO_3$ which is then used for $\delta^{15}N$ analysis [230]. The authors have also detailed the fact that high concentrations of anions in solution can interfere with nitrate adsorption on the anion exchange resins, which may result in isotope fractionation of nitrogen and oxygen [230].

A European patent looked at a method of nitrate collection from different kinds of matrices. The method that was developed was suited for nitrate extraction in view of nitrogen and oxygen isotope ratio analyses. The matrices that were investigated were fresh water, sea water, urine, tomato juice, soil and plants. The general method developed is as followed [231]:

- Passing a nitrate-containing liquid sample to be analysed (preferably after a pre-treatment step) over an anion exchange material to retain the nitrates thereon.
- Eluting nitrates from the anion exchange material with an eluting agent comprising sulphuric acid, phosphoric acid or a mixture of these acids.
- Neutralising the nitrate-containing eluate with a neutralising agent selected from a group consisting of: lead oxide, calcium oxide, barium oxide, strontium oxide, corresponding hydroxides or mixtures of two or more of these compounds.
- Measuring the nitrate and/or oxygen isotope ratio in the nitrate-containing eluate.

The obtained nitrogen and oxygen isotopic ratios of nitrate may provide a powerful tool to investigate nitrate sources and recycling mechanisms.

Freyer and Aly published a paper with the objective of showing that the most commonly used ammonium (e.g. $(NH_4)_2SO_4$) and nitrate (e.g. KNO_3) fertilisers have different $\delta^{15}N$ values [232]. A series of NO_3^- fertilisers were reduced with Cr/HCl to ammonium ions according to Gehrke [233, 234]. The formed ammonium (and NH_4^+ fertilisers) were separated by steam distillation according to Bremner and Keeney and converted into nitrogen gas with alkaline lithium hypobromite solution by a modified technique of Ross and Martin [235, 236]. The nitrogen gas was purified from interfering gases by cycling through a heated, copper filled tube (to reduce any NO_x) and liquid nitrogen traps (to remove CO_2). The nitrogen gas was then isotopically analysed for their $\delta^{15}N$ values.

The nitrogen isotope values obtained for AN-based fertilisers and several precursors are shown in Table 4-1. The NH_4^+ nitrogen is generally isotopically depleted in comparison to atmospheric nitrogen (negative $\delta^{15}N$). This is due to the fact that the lighter ^{14}N isotope is kinetically favoured for incorporation into the molecule during the ammonia synthesis. On the other hand, the NO_3^- nitrogen is generally isotopically enriched in comparison to atmospheric nitrogen (positive $\delta^{15}N$). This is the consequence of isotopic exchange reactions occurring after oxidation of ammonia in the production of nitric acid [232]:

$$^{15}NO + H^{14}NO_3 \rightleftharpoons H^{15}NO_3 + {}^{14}NO \qquad \text{(Equation 4-1)}$$
$$^{15}NO_2 + H^{14}NO_3 \rightleftharpoons H^{15}NO_3 + {}^{14}NO_2 \qquad \text{(Equation 4-2)}$$
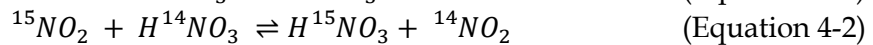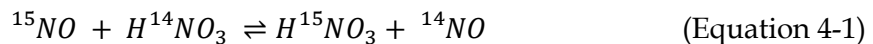
The depletion of $\delta^{15}N$ in the nitrogen oxides after isotopic exchange was demonstrated by the $\delta^{15}N$ value obtained for a sample of synthetic sodium nitrate ($\delta^{15}N$ = -22.7‰). This sample was produced by absorption of waste nitrogen oxides after the nitric acid process [232].

Sample	Nitrogen Compounds	$\delta^{15}N_{Ammonium}$	$\delta^{15}N_{Nitrate}$	Reference
Reagent	Nitric Acid	-	-0.4	[232]
Reagent	Nitric Acid	-	+1.4	[232]
Reagent	Nitric Acid	-	+1.8	[232]
Reagent	Nitric Acid	-	+3.0	[232]
Reagent	Nitric Acid	-	-1.8	[237]
Reagent	Nitric Acid	-	+2.4	[30]
Reagent	Nitric Acid	-	+4.0	[30]
Fertiliser	Ammonium Nitrate	-	+5.6	[145]
Fertiliser	Lime-ammonium nitrate (28% N)	-3.8	-2.2	[226]
Fertiliser	Lime-ammonium nitrate (28% N)	-4.0	-3.5	[226]
Fertiliser	Lime-ammonium nitrate (28% N)	+0.2	+1.8	[226]
Fertiliser	Lime-ammonium nitrate (69% NH_4NO_3)	+1.6	+5.7	[232]
Fertiliser	Lime-ammonium nitrate (75% NH_4NO_3)	-0.6	+1.3	[232]
Fertiliser	Lime-ammonium nitrate (75% NH_4NO_3)	-2.7	+2.0	[232]
Fertiliser	Ammonium Nitrate	-1.2	+2.1	[232]

Table 4-1: Compilation of published $\delta^{15}N$ values of nitric acids and ammonium nitrate fertilisers

The different $\delta^{15}N$ values found also depend on the temperature, concentration, and pressure in the production process, as the values for nitric acid of one production plant indicate (shown in Table 4-2) [232].

Nitric Acid		
Absorption Pressure *	Nitrogen Compound	$\delta^{15}N$
1.5 atm	45 % HNO_3	+ 1.8
3.0 atm	52.5 % HNO_3	+ 3.0
3.0 atm	56 % HNO_3	+ 1.4
3.9 atm	56 % HNO_3	- 0.4
*Absorption Pressure of the NO_x in the production plant		

Table 4-2: Mean $\delta^{15}N$ values for nitric acid produced by a German fertiliser company

The authors of this paper found that the mean difference of nitrogen isotopic ratio between fertiliser nitrate and fertiliser ammonium is:

$$\delta\ (^{15}N_{Nitrate}) - \delta\ (^{15}N_{Ammonium}) = +3.9 \pm 1.5.$$

Vitoria *et al.* described the detailed isotopic composition ($\delta^{15}N_{Bulk}$, $\delta^{15}N_{Nitrate}$, $\delta^{18}O_{Nitrate}$, $\delta^{34}S_{Sulfate}$, $\delta^{18}O_{Sulfate}$ and $\delta^{13}C_{Bulk}$) of 27 commercial fertilisers used in Spain [145]. The results could be used for two purposes:

- To identify the origin of the primary constituents and raw materials used in fertiliser manufacture and relate these to trace metal contents.
- To compare the fertiliser isotopic signatures with natural values and other anthropogenic pollutants and evaluate the usefulness of multi-isotopic analyses to trace fertiliser contaminations in future cases.

$\delta^{15}N_{Bulk}$ and $\delta^{34}S_{Bulk}$ have previously been used to trace fertiliser contaminations and it was shown that their utility can be improved by the coupled use of $\delta^{15}N_{Nitrate}$ and $\delta^{18}O_{Nitrate}$ to evaluate the fractionation processes that can affect contaminants. The dissolved nitrate from fertilisers were analysed using a modified method from Silva *et al.* [230].

4.2.1.2 Other Nitrate Sources

UN is an improvised explosive made from readily available materials. The carbon and nitrogen isotope composition of UN and its component ions, uronium and nitrate, could aid in a forensic investigation. Aranda et al [30] developed a method to separate UN into its component ions for subsequent $\delta^{15}N$ measurements; the methodology they employed is as follows [30]:

- Dissolve 2:1 molar ratio KOH to UN (recommended) in ~ 2-3 mL of water.
- Samples are then flash frozen in liquid N_2 and subsequently vacuum freeze dried overnight.
- The dried urea and KNO_3 are then washed four times with HPLC grade methanol to remove the liberated urea and any remaining KOH.
- The methanol supernatant, containing the urea and excess KOH, and residual KNO_3 solid were each dried under a stream of N_2 gas overnight.
- The separated urea + KOH, separated KNO_3 and bulk UN were each weighed and analysed for $\delta^{13}C$ and $\delta^{15}N$ values.

From this study it was identified that there was a preservation of isotopic composition of reactants in UN, along with a significant variability in isotopic composition of reactants. Nitrate isolated from UN has a nearly identical nitrogen isotope composition of the reactant nitric acid used to form the UN. The carbon isotope ratio of the bulk UN is identical to the reactant urea. The urea isolated from UN is slightly enriched in ^{15}N compared to the reactant urea [30].

These results indicate that isotope ratio analysis may be used to test if urea or nitric acid collected during an investigation is a possible reactant for a specific UN sample. This approach may be useful for discriminating between materials which are otherwise chemically identical [30].

4.2.2   Isotopic Analysis of Ammonium Ions

The results of a trial to determine whether the nitrogen isotopes from the ammonium ion versus the bulk AN could be used to potentially assist in the discrimination of sources of AN has been reported. In this trial, the ammonium ion was precipitated (using sodium tetraphenylborate) and subsequently filtered, dried and weighed. Six samples were prepared using this method and subsequently analysed for their $\delta^{15}N$ values. The results indicated that the isotopic signal of the ammonium ion was isotopically depleted compared to the bulk ammonium nitrate. These experiments highlighted the need for further research in this area of interest [40, 49].

4.3 Ion Exchange for the Separation of Ammonium and Nitrate

The isolation of the nitrate species from a variety of matrices has been successfully completed using ion exchange resins [230, 231]. Therefore it was hypothesised that a modified method utilising an ion exchange resin will allow the isolation of the nitrate species from AN.

Ion exchange resins are insoluble substances containing loosely held ions which are able to be exchanged with other ions in solutions. These exchanges take place without any physical alteration to the ion exchange material. Ion exchangers are insoluble acids or bases which have salts which are also insoluble, and this enables them to exchange either positively charged ions (cation exchangers) or negatively charged ions (anion exchangers) [238].

Ion exchange resins can be used either to remove unwanted ions from a solution passed through it or to accumulate a valuable mineral from the solution which can be subsequently removed from the resin. They can also be used to remove interfering ions during analysis or to accumulate trace quantities of ions from dilute solutions which can then be concentrated into a small volume by elution [238].

Ions are retained on the ion exchange sorbent due to electrostatic attraction between the ion and a charged group on the sorbents surface.

The order of affinity for some common cations is approximately [238]:

$Hg^{2+} < Li^+ < H^+ < Na^+ < K^+ \approx NH_4^+ < Cd^{2+} < Cs^+ < Ag^+ < Mn^{2+} < Mg^{2+} < Zn^{2+} < Cu^{2+} < Ni^{2+} < Co^{2+} < Ca^{2+} < Sr^{2+} < Pb^{2+} < Al^{3+} < Fe^{3+}$

The cation exchange resin utilised was:

Sigma Aldrich – DOWEX® 50WX8-400 ion exchange resin – Batch number 10715BD
Hydrogen form
200-400 Mesh
Exchange capacity – 1.7 meq/mL
Linear formula – $(C_{10}H_{12} \cdot [C_{10}H_{10}] \cdot C_8H_8)_x$.

This ion exchange material is comprised of a styrene-divinylbenzene matrix with sulfonic acid functional groups. The sulfonic acid group is strongly acidic (pKa <1), and attracts or exchanges cationic species in a contacting solution – thus the term strong cationic exchanger. An example of the structure of this type of resin is shown in Figure 4-2 [238]. The bonded functional group is charged over the whole pH range and therefore can be used to isolate strong cationic (very high pK_a, >14) or weak cationic (moderately high pK_a, <12) compounds as long as the pH of the solution is one at which the compound of interest is charged. For a cationic compound of interest, the pH of the matrix must be 2 pH units below its pK_a for it to be charged. In most cases, the compounds of interest are strong or weak bases. This kind of ion exchange resin should be used to isolate strong cations only when their recovery or elution is not desired [239].
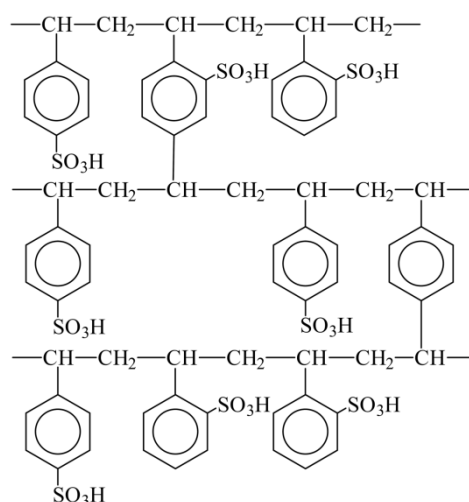
Figure 4-2: An example of a strongly acidic sulphonated polystyrene cation exchange resin

4.4 Experimental

4.4.1 Samples

For the preliminary studies the following chemicals were used:

- Potassium Nitrate – Ajax Chemicals
- Ammonium Chloride – Unknown source, obtained from Flinders University Undergraduate Laboratory;
- Aluminium nitrate (Ajax Chemicals)

Experiment 1: NH_4Cl (1 mg) and KNO_3 (1 mg) in water (200 µL) added to cation exchange resin (30 mg). Solution was mixed every 10 mins for 1 hour. 150 µL of eluent was then neutralised with 200 µL of sodium hydroxide (0.1 M) and sample dried.

Experiment 2: NH_4Cl (1 mg) and KNO_3 (1 mg) in water (200 µL) added to cation exchange resin (31.8 mg). Solution was mixed every 10 mins for 1 hour. Eluent was then removed and added to new cation exchange resin (33.0 mg) and mixed for an extra hour. 200 µL of eluent was then neutralised with 220 µL of sodium hydroxide (0.1 M) and sample dried.

Experiment 3: NH_4Cl (1 mg) and KNO_3 (1 mg) in water (300 µL) added to cation exchange resin (30 mg). Solution was mixed every 10 mins for 1 hour. Eluent was then removed and added to new cation exchange resin (29.8 mg) and mixed overnight. 200 µL of eluent was then neutralised with 200 µL of sodium hydroxide (0.1 M) and sample dried.

Experiment 4: KNO_3 (2.2 mg) in water (200 µL) added to cation exchange resin (33.4 mg). Solution was mixed every 10 mins for 1 hour. 150 µL of eluent was then neutralised with 200 µL of sodium hydroxide (0.1 M) and sample dried.

Experiment 5: KNO_3 (2 mg) in water (200 µL) added to cation exchange resin (31.8 mg). Solution was mixed every 10 mins for 1 hour. Eluent was then removed and added to new cation exchange resin (35.7 mg) and mixed overnight. 100 µL of eluent was then neutralised with 200 µL of sodium hydroxide (0.1 M) and sample dried.

Experiment 6: NH_4Cl (1.8 mg) in water (200 µL) added to cation exchange resin (32.7 mg). Solution was mixed every 10 mins for 1 hour. 150 µL of eluent was then neutralised with 300 µL of sodium hydroxide (0.1 M) and sample dried.

Experiment 7: NH_4Cl (1.9 mg) in water (200 µL) added to cation exchange resin (34.9 mg). Solution was mixed every 10 mins for 1 hour. Eluent was then removed and added to new cation exchange resin (31 mg) and mixed overnight. 100 µL of eluent was then neutralised with 250 µL of sodium hydroxide (0.1 M) and sample dried.

Experiment 8: NH_4Cl (2 mg) and KNO_3 (2 mg) in water (300 µL) added to cation exchange resin (30.9 mg). Solution was mixed every 10 mins for 1 hour. Eluent was then removed and added to new cation exchange resin (38.5 mg) and mixed overnight. 200 µL of eluent was then neutralised with 450 µL of sodium hydroxide (0.1 M) and sample dried.

Experiment 9: NH_4Cl (2.7 mg) and $Al(NO_3)_3$ (2.7 mg) in water (300 µL) added to cation exchange resin (32.2 mg). Solution was mixed every 10 mins for 1 hour. Extra cation exchange resin (37.8 mg) was added and the centrifuge tube mixed overnight. 200 µL of eluent was then neutralized with 500 µL of sodium hydroxide (0.1 M) and sample dried.

4.4.2   Synthesis of Homemade AN Samples

Preparation 1 – Potassium nitrate (10.106 g) and ammonium chloride (5.366 g) was dissolved in water (200 mL). The water was subsequently evaporated off at 60 °C over a period of 5 days. The recovered crystals were purified in methanol (100 mL) and any undissolved crystals were removed through filtering. The filtered methanol solution was evaporated off at 60 °C.

Preparation 2 – Calcium nitrate (2.742 g) and ammonium sulphate (1.460 g) was dissolved in water (40 mL). A white precipitate was formed ($CaSO_4$) and this precipitate was filtered off leaving a clear water solution. The water was subsequently evaporated off at room temperature in a desiccator.

Preparation 3 – Barium nitrate (3.265 g) and ammonium sulphate (1.651 g) was dissolved in water (40 mL). A white precipitate was formed ($BaSO_4$) and this precipitate was filtered off leaving a clear water solution. The water was subsequently evaporated off at room temperature in a desiccator.

4.4.3   Purification of AN from Cold Packs

AN recovered from an Instant Cold Pack (Surgical Basics – Instant Ice Pack (Imported from China by 3P PTY LTD) was purified utilising a method previously detailed in a YouTube purification process. The AN was dissolved in water and subsequently filtered to remove any insoluble components. The filter solution was then heated at 80°C for 60 min which subsequently allowed for a purified AN to be recovered.

This purification process did not affect the $\delta^{15}N_{Bulk}$, $\delta^{15}N_{Ammonium}$ or the $\delta^{15}N_{Nitrate}$ value. It can be noted that the heating process undertaken for this purification was not harsh enough to cause the loss of ammonia or isotopic fractionation.

4.4.4   Preparation of Representative AN-based HMEs

A series of representative samples of AN-based HMEs were prepared at DSTO. The following precursor materials were utilised:

- AN - Milled Orica Nitropril
- Sugar - CSR Pure Icing Sugar (< 45 µm)
- Aluminium 1 - Ecka Granules 25C (C0136712) (Uncoated Powder)
- Aluminium 2 - Ecka AC40X1-NS Al Flake
- Fuel Oil - Caltex Diesel
- Nitromethane - 100% Nitromethane (Hobby)
- Baby Formula - Nestle Lactogen
- Hexamine - M&B Hexamine 100%
- TNT - Thales TNT

These precursor materials were then hand blended in anti-static containers to produce the following AN-based HME compositions:

- HME 1 - 87% AN & 13% Aluminium 1
- HME 2 - 89% AN & 11% Aluminium 2
- HME 3 - 88% AN & 12% Sugar
- HME 4 - 77% AN, 13% Aluminium 2 & 10% Sugar
- HME 5 - 90% AN & 10% Fuel Oil
- HME 6 - 71% AN & 29% Nitromethane
- HME 7 - 87% AN & 13% Baby Formula
- HME 8 - 80% AN & 20% Hexamine

- HME 9 - 60% AN & 40% TNT
- HME 10 – 100% AN
- HME 11 - 75% AN, 15% $CaCO_3$ and 10% Aluminium 2

4.4.5   Isotope Ratio Mass Spectrometry (IRMS)

For isotopic analysis a mass of sample was weighed into a tin capsule (5 x 9 mm, EuroVector). The tin capsule is then sealed and subsequently placed in an autosampler ready for analysis. Table 4-3 details the approximate sample masses needed for nitrogen isotopic analysis.

Code	Molar Mass	Percentage N	Mass needed for IRMS (µg)
KNO_3	101.10	13.9	577.5
$Al(NO_3)_3$	375.13	11.2	711.1
NH_4Cl	53.49	26.2	305.5
NH_4NO_3	80.05	35.1	227.6
$Ba(NO_3)_2$	261.34	10.7	746.3
$Ca(NO_3)_2$	236.15	11.9	674.4
$(NH_4)_2SO_4$	132.14	21.2	377.4

Table 4-3: Sample sizes needed for IRMS analysis

Caveat – Due to the nature of the samples analysed and limitations with the analytical instrumentation used, the isotopic data presented in this research is fit for the purpose of a comparative exercise (proof of concept) but should not be compared to data from other laboratories. All of the δ values displayed within this research have an associated error range (error bars) of ± 1 standard deviation.

4.4.6   Fourier Transform Infrared Spectroscopy (FT-IR)

A Spectrum 400 FT-IR/FT-NIR Spectrometer (PerkinElmer) with a universal ATR sampling accessory was used to obtain IR spectra of various ammonium nitrate samples.

4.4.7   Flow Injection Analysis (FIA)

FIA is a continuous-flow technique for automated wet-chemical analysis. As a sample is drawn into the injection valve, reagents are simultaneously pumped through the system. The sample is then loaded into the sample loop of one or more injection valves. The injection valve is then switched to connect the sample loop in line with the carrier stream. This sweeps the sample out of the sample loop and onto the manifold. The sample and reagents then merge in the manifold (reaction module) [240, 241].

FIA was undertaken as a method to compare the ammonia content of a sample from each stage of the nitrate isolation process. The analysis method is based on the Berthelot reaction. Ammonia reacts in alkaline solution with hypochlorite to form monochloramine, which, in the presence of phenol, catalytic amounts of nitroprusside and excess hypochlorite gives indophenol blue. The amplitude of the absorption at 630 nm by indophenol blue is directly proportional to the original ammonia concentration in the sample [242].

A Lachat Instruments: QuikChem® 8500 Series 2 Flow Injection Analysis System was utilised for all FIA analysis undertaken in this thesis and the method used for Ammonia analysis was Lachat Instruments: QuikChem® Method 31-107-06-1-B. Examples of spectra obtained for the analysis of ammonia using the FIA system are shown in Figure 4-3.
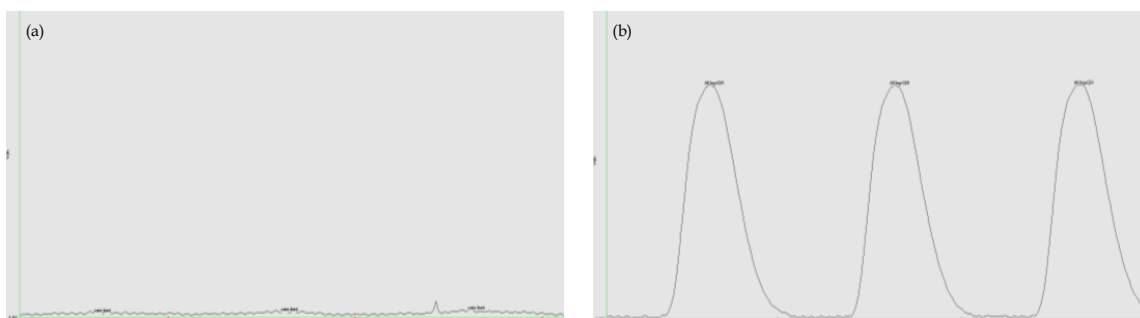
Figure 4-3: a) FIA spectra obtained for three blank samples (shows no ammonia peaks) and b) FIA spectra obtained for three separated samples (shows ammonia peaks)

4.5 Preliminary Studies

The purpose of this preliminary study was to determine whether or not utilising an ion exchange resin would be a suitable method for isolating a nitrate species from an ammonium/nitrate mixture. Section 4.4.1 details the separation procedures undertaken and the isotopic results from these procedures are detailed in Table 4-4. It should be noted that all nitrate samples analysed are in the form of sodium nitrate ($NaNO_3$) after the isolation process.

Experiment Number	$\delta^{15}N\ KNO_3$	NH_4Cl	$\delta^{15}N_{Nitrate}$	$\Delta\ \delta^{15}N$
1	-25.64	Y	-24.73	-0.91
2	-25.56	Y	-25.31	-0.24
3	-25.88	Y	-24.85	-1.03
4	-25.88	N	-25.74	-0.14
5	-25.88	N	-25.4	-0.48
6	Test for any residual NH_4Cl in Solution - Insufficient N for IRMS Analysis			
7	Test for any residual NH_4Cl in Solution - Insufficient N for IRMS Analysis			
8	-25.62	Y	-25.26	-0.35
9	-3.62	Y	-3.58	-0.05

Table 4-4: Results from experiments 1-8 (isolation of NO_3^- from KNO_3 and NH_4Cl mixtures)

From Experiment 1 a change in $\delta^{15}N$ was seen and may be due to incomplete separation of NH_4^+ and NO_3^-. This may be due to a competing reaction between the NH_4^+ and the K^+ to exchange with the cation exchange resin. As shown previously NH_4^+ and K^+ have similar affinities to exchange with a resin. A change was made and a second separation (addition of eluent from first separation to fresh resin) was added to the process. This extra resin takes into account any other cations which may be present in the sample. This change was implemented in Experiments 2 and 3 and had limited success as the $\delta^{15}N$ of the isolated nitrate was still different to the initial KNO_3.

Experiments 4 and 5 looked at only the interaction between KNO_3 and the resin. These two experiments differed by changing number of times the solution was exposed to fresh resin (1 or 2) and time of mixing with the resin. Once again the results showed slight differences in isotopic composition.

Experiments 6 and 7 looked only at the interaction between the NH_4Cl and the resin. The results from these experiments were positive as there was insufficient nitrogen for IRMS analysis in the final recovered solid. This indicates that the NH_4^+ completely exchanged for H^+.

Experiment 8 once again looked at a two-step separation where after the initial time period the eluent was taken and added to fresh resin. There was a difference in isotopic composition from final nitrate to the initial potassium nitrate and this may have been due to contamination from some NH_4Cl which may have not been completely exchanged.

From these experiments it was determined that some factors needed to be controlled for a sufficient separation to occur:

- Restrict the concentration of potassium in the mixture due to competing exchange problems. Sodium content should also be limited due to its affinity for exchanging.
- Time allows complete exchange between cations (NH_4^+/K^+) and resin. Time period of this exchange should be approximately 24 hrs.
- Eliminate touching/manipulation of sample during exchange as this may cause isotopic fractionation. Ultimately no removal of eluent until final neutralisation. This also means that as part of a two-step separation a second lot of cation exchange resin is added to the centrifuge tube (which already contains solution + resin).

Experiment 9 was undertaken implementing all of the conditions detailed above. After taking into account the potential flaws in the procedure the isolated nitrate from this adapted method had an isotopic value which was indistinguishable from the initial aluminium nitrate.

The results from this preliminary study allowed a suitable method to be developed to isolate nitrate from a mixture containing two nitrogen sources of opposite charge (ammonium and nitrate). This preliminary work also highlighted the need for excess cation exchange resin to be used in the procedure to account for any other cations with similar affinity to ammonium which may be present in the sample (K^+ or Na^+).

4.6 Final Separation Method Test and Validation

From the preliminary studies a final separation method was identified and this method is detailed in the flow diagram shown in Figure 4-4.
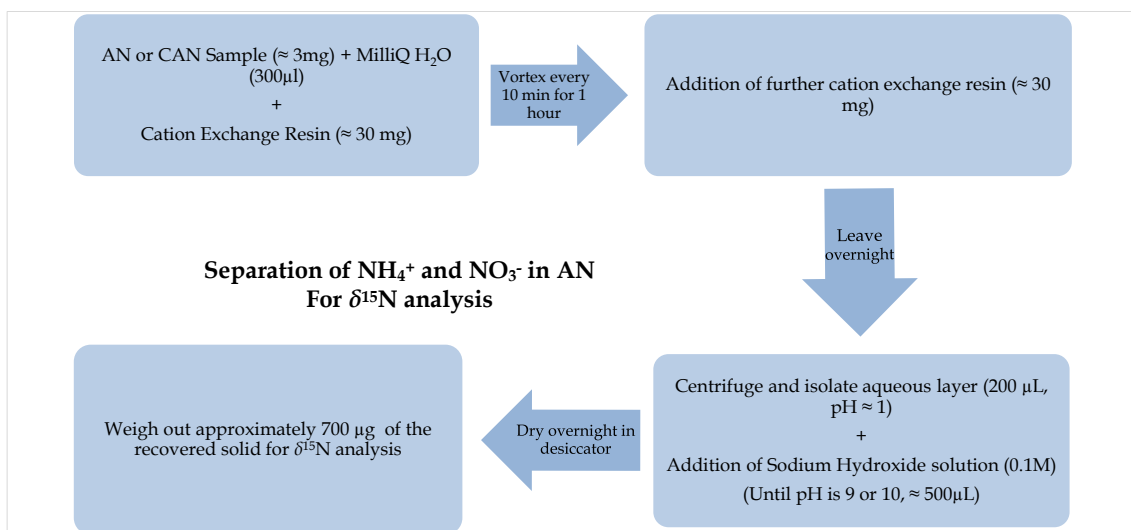
Figure 4-4: Final separation method for the isolation of NO_3^- from an AN sample for nitrogen IRMS

A set of three AN samples were subjected to a nitrate separation and isolation (10 replicates) for subsequent $\delta^{15}N$ analysis. This was completed to verify the process and also to determine the variability of $\delta^{15}N$ values obtained for NO_3^- using this method.

The three different AN samples were chosen as the isotopic values obtained for the nitrate species covered a range of values (a negative $\delta^{15}N$, a positive $\delta^{15}N$ and a $\delta^{15}N$ value close to zero).

The isotopic ratio for the ammonium ion is calculated using the bulk isotopic ratio and the isotopic ratio obtained for the nitrate species according to Equation 4-1 and the results are presented in Figure 4-5 and Table 4-5.

$$\delta^{15}N_{Ammonium}= (2(\delta^{15}N_{Bulk})) - \delta^{15}N_{Nitrate} \qquad \text{(Equation 4-1)}$$

Ammonium Nitrate Separation – Variability Study (10 separations per sample)									
Sample	$\delta^{15}N_{Bulk}$	**s.d**	**2u(ȳ)**	$\delta^{15}N_{Nitrate}$	**s.d**	**2u(ȳ)**	$\delta^{15}N_{Ammonium}$	**s.d**	**2u(ȳ)**
Cold Pack	-4.68	0.032	0.020	-4.28	0.078	0.050	-4.99	0.025	0.016
AN	+0.23	0.087	0.055	+1.39	0.111	0.070	-0.94	0.043	0.027
FU-AN-8	+8.96	0.133	0.084	+13.41	0.105	0.067	+4.51	0.099	0.062

Table 4-5: $\delta^{15}N$ results for AN samples analysed as part of the method variability study.
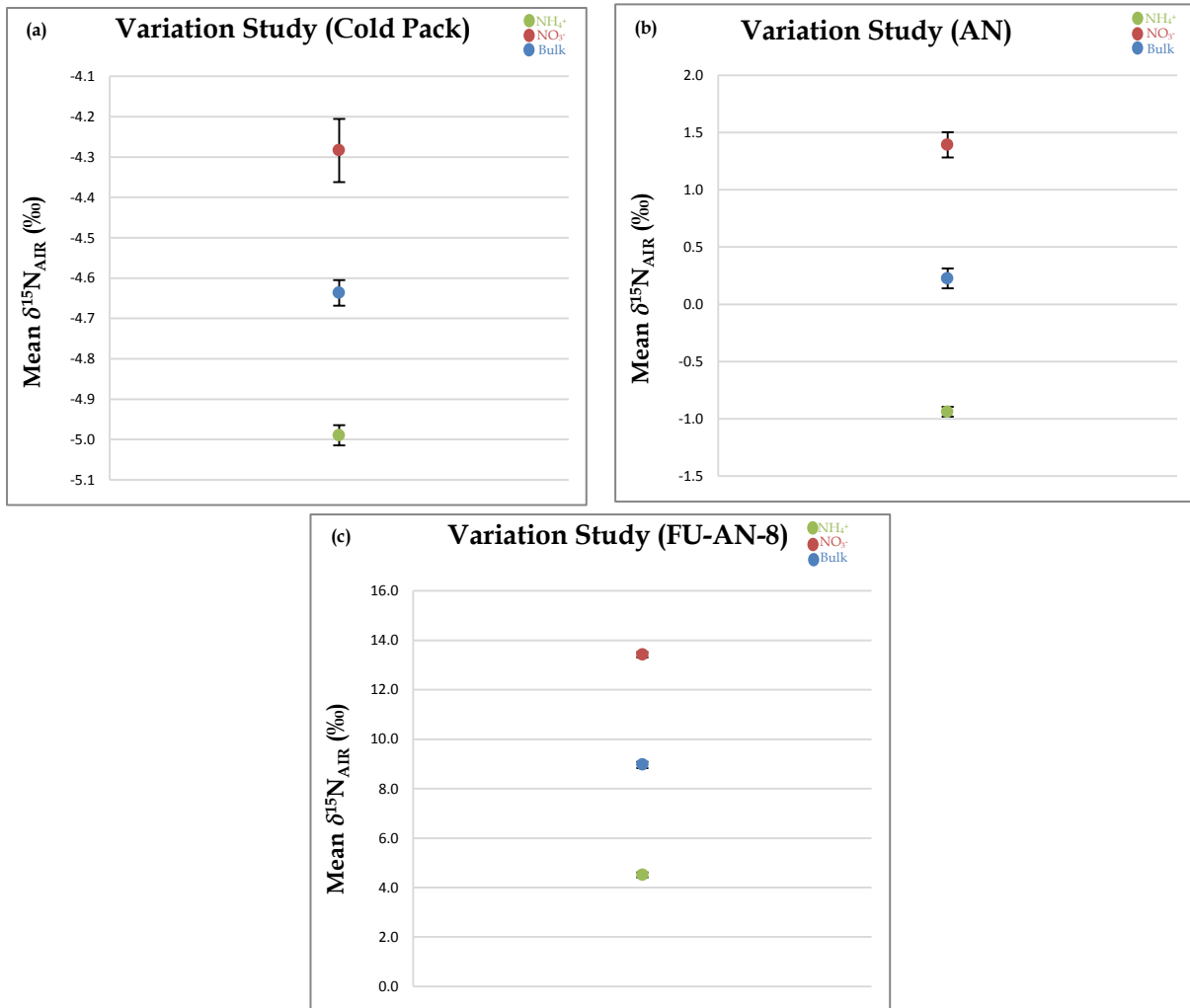
Figure 4-5: a) δ15N results for cold pack sample b) δ15N results for sample (AN) and c) δ15N results for sample (FU-AN-58) as part of the method variability study.

Standard uncertainties associated with the observed/measured results were determined by Equation 4-2 (a coverage factor of k=2 gives an approximate level of confidence of 95%, as discussed in Section 2.2.2.10).

$$u(\tilde{y}) = \frac{s}{\sqrt{n}} \quad \text{u}(\tilde{y}) = \left(\frac{\sigma}{\sqrt{n}}\right) \times 2 \qquad \text{(Equation 4-2)}$$

From Figure 4-5 and Table 4-5 it can be observed that there is minimal variability within the ten independent separations undertaken for each AN sample (for a total of 30 individual $\delta^{15}N_{Nitrate}$ analyses). The small amount of observed intra-variability for each sample indicated that $\delta^{15}N_{Nitrate}$ measurements could be used to discriminate between samples of AN.

FIA was undertaken as a method to compare the ammonia content of a sample from each stage of the nitrate isolation process (initial AN, exchanged aqueous solution and final solid

product). Figure 4-6 details the ammonium content at each stage of the separation process (for three samples of AN which underwent the final separation method).
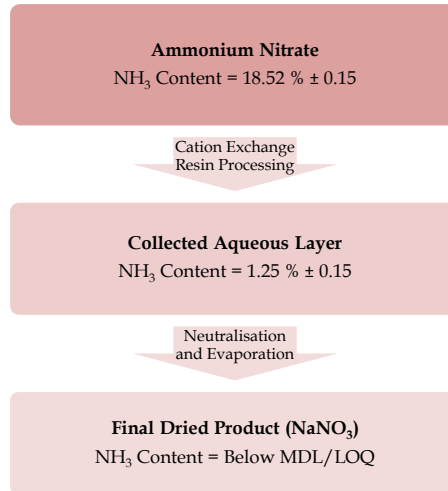
Figure 4-6: Ammonia content values at each stage of nitrate isolation process

The final solid product was also analysed using FT-IR, which confirmed the change from AN to sodium nitrate (Figure 4-7). The results obtained from this analysis have verified that the nitrate is isolated from the initial sample of AN, and the ammonium is lost either through cation exchange (with the resin) or through the loss as ammonia during the neutralisation/evaporation procedure.
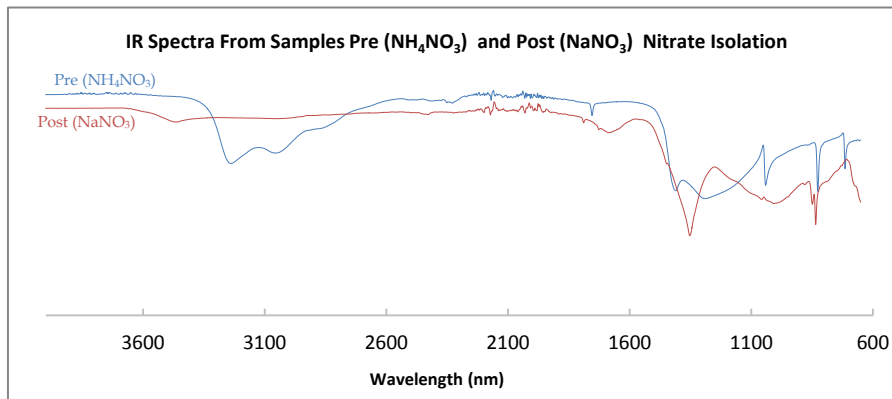
Figure 4-7: IR spectra of samples pre (NH_4NO_3) and post ($NaNO_3$) nitrate isolation

4.7 Application of Nitrate Separation to AN and CAN Samples

4.7.1 Samples

A random assortment of the previously analysed AN and CAN samples were selected to determine the usefulness of the nitrate separation process in linking AN and CAN samples. Table 4-6 shows details of each AN and CAN samples analysed.

Code	Description	Country of Origin	Source	Batch Number
DSTO-AN-4	BDH AR Grade AN	Unknown	DSTO	Unknown
DSTO-AN-1	Orica Nitropril	Australia	Orica	LOT 008/DFN/7/01
DSTO-AN-2	Orica Nitropril	Australia	Orica	Unknown
FU-AN-2	Porous Prill (TOPAN Process)	Australia	Orica	Unknown
FU-AN-8	Ajax Finechem	Unknown	Flinders University	AF505117
FU-AN-13	Chemsupply (Sold by Omega Scientific)	Unknown	Rostrevor College	(10) 230305
FU-AN-33	Porous Prill (KT Process)	Turkey	Orica	Unknown
FU-AN-34	Porous Prill (KT Process)	Turkey	Orica	Unknown
FU-AN-16	Fertiliser Grade AN (Nitram)	Australia	Quin Investments	Unknown
FU-AN-20	High Density for Emulsion (HDE grade AN)	France	Quin Investments	Unknown
FU-AN-21	High Density for Emulsion (HDE grade AN)	France	Quin Investments	Unknown
FU-AN-22	High Density for Emulsion (HDE grade AN)	France	Quin Investments	Unknown
FU-AN-52	Possible South African AN	Unknown	Orica	Unknown
DSTO-AN-4	BDH AR Grade AN	Unknown	DSTO	Unknown
Initial	75 % AN and 25 % CaCO$_3$	Unknown	DSTO	Unknown
60 Min	75 % AN and 25 % CaCO$_3$	Unknown	DSTO	Unknown
Bag 1	CAN (75 % AN and 25 % CaCO$_3$)	Russia	Incitec Pivot	Unknown
Bag 2	CAN (75 % AN and 25 % CaCO$_3$)	Russia	Incitec Pivot	Unknown
Cook 1	Bag 2	Russia	Incitec Pivot	Unknown
Cook 2	Bag 1	Russia	Incitec Pivot	Unknown
DSTO-CAN-3	CAN	-	-	-
FU-AN-56	Surgical Basics – Instant Ice Pack (Imported by 3P PTY LTD)	China	Pharmacy	20111230
P-FU-AN-56	Cold Pack – Purified using YouTube Method	China	Pharmacy	20111230

Table 4-6: Summary of AN samples

4.7.2 Ammonium Nitrate Samples

Figure 4-8 shows the measured $\delta^{15}N_{Bulk}$ and $\delta^{15}N_{Nitrate}$, and calculated $\delta^{15}N_{Ammonium}$ values obtained from the 13 selected AN samples. It can be observed that:

- $\delta^{15}N_{Nitrate}$ ranged between $\delta^{15}N$ = -2.34‰ and +13.25‰
- $\delta^{15}N_{Ammonium}$ ranged between $\delta^{15}N$ = -4.06‰ and +4.61‰
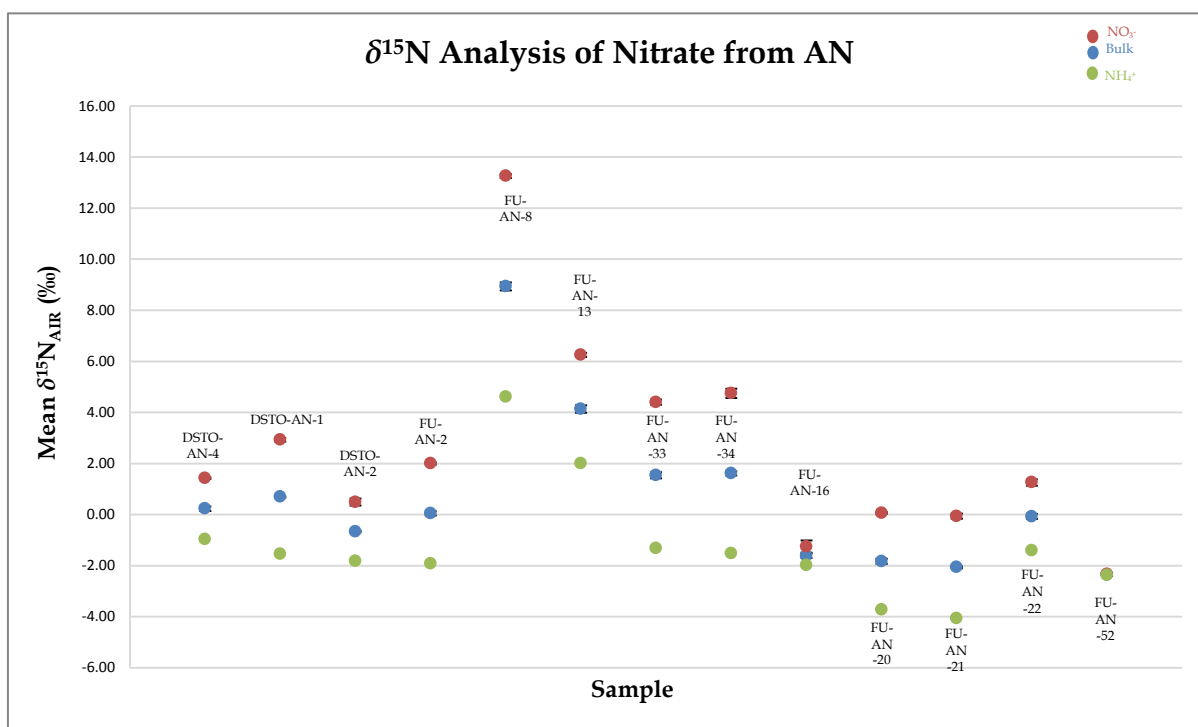
Figure 4-8: Overall δ15N results for AN samples of interest

As previously detailed in the introduction to this research, the ammonium nitrogen in general has a lower $\delta^{15}N$ value than atmospheric N_2 (negative $\delta^{15}N$ value). This is due to the lighter ^{14}N isotopes being kinetically favoured in the ammonia synthesis. The nitrate nitrogen however has a higher $\delta^{15}N$ value than atmospheric N_2 (positive $\delta^{15}N$ value). This is a consequence of isotopic exchange reactions occurring after oxidation of ammonia in the production of nitric acid [232], as discussed in Section 4.2.1.1.

In the samples analysed as part of this task it can be observed that most of the nitrate species are isotopically enriched compared to $\delta^{15}N_{AIR}$, which corresponds with the previously mentioned work. Most of the ammonium species (which are calculated after isotopic analysis) are observed to be isotopically depleted compared to $\delta^{15}N_{AIR}$ which also corresponds to the previously completed research [232]. One sample (FU-AN-52) is quite different to the other AN samples analysed due to the fact that the $\delta^{15}N_{Nitrate}$ and the $\delta^{15}N_{Ammonium}$ values are the same as the $\delta^{15}N_{Bulk.}$ The results obtained for this sample does not correlate with the previously mentioned research [232] and as such it is thought that in this case, the source of ammonia and nitric acid used to prepare the AN were different.

From the above results (Figure 4-8) the combination of three $\delta^{15}N$ values allows for greater discrimination between samples of AN. This in combination with carbon IRMS would be the preferred analytical methodology to employ in linking or discriminating AN samples.

4.7.3   Calcium Ammonium Nitrate and Processed Ammonium Nitrate Samples

Figure 4-9 shows the measured $\delta^{15}N_{Bulk}$ and $\delta^{15}N_{Nitrate}$, and calculated $\delta^{15}N_{Ammonium}$ values obtained from the 10 selected CAN and AN samples which have undergone wet processing or other purification. It can be observed that:

- $\delta^{15}N_{Nitrate}$ ranged between $\delta^{15}N$ = -4.28‰ and +1.53‰
- $\delta^{15}N_{Ammonium}$ ranged between $\delta^{15}N$ = -5.11‰ and +1.17‰.
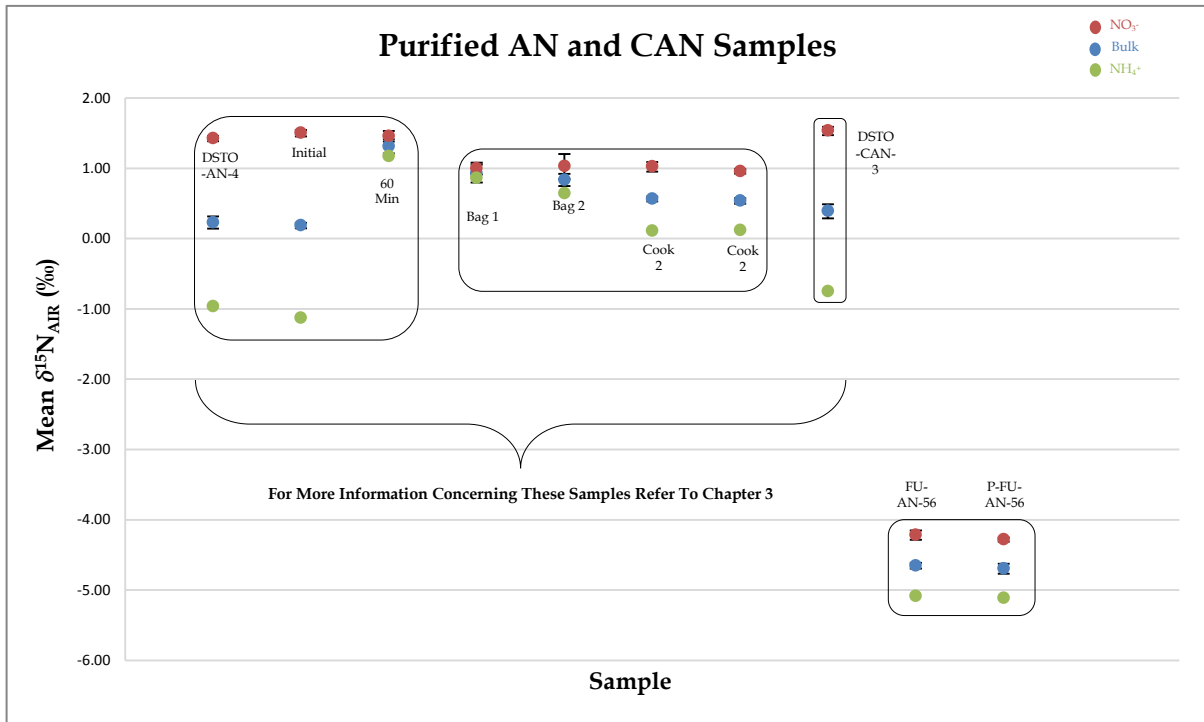
Figure 4-9: Overall $\delta^{15}N$ results for purified AN and CAN samples of interest

In the samples analysed as part of this task it can be observed that all of the nitrate species are isotopically enriched compared to $\delta^{15}N_{AIR}$, which corresponds with the previously mentioned work. All of the ammonium species (which are calculated after isotopic analysis) are observed to be isotopically depleted compared to $\delta^{15}N_{AIR}$ which also corresponds to the previously completed research [232].

Previous analysis in Section 3.6 indicated that $\delta^{15}N_{Bulk}$ values were affected by temperatures typically used for the wet processing of AN or CAN prills, which made the identification of the source material by IRMS extremely difficult. The drift of $\delta^{15}N_{Bulk}$ towards more positive values was ascribed to isotopic enrichment through a higher rate of loss of $^{14}NH_3$ from the samples. If this were true then it was expected that the $\delta^{15}N_{Nitrate}$ values of the processed samples would be relatively unchanged from that of the unprocessed prills. Hence some of the samples (small scale/large scale "cook") described in Section 3.6 were re-analysed using the ion separation technique to determine what information could attained.

From Figure 4-9 it can be observed that samples DSTO-AN-4 and Initial can be linked together based on all three variables ($\delta^{15}N_{Bulk}$, $\delta^{15}N_{Nitrate}$ and $\delta^{15}N_{Ammonium}$). Initial was the CAN sample which was used in the small scale cooks, and DSTO-AN-4 was a sample of AN used to prepare Initial. The sample named 60 minutes, was in fact the sample which underwent the "cooking" process for one hour. This sample was analysed in the same way as the Initial sample and encouragingly, both the $\delta^{15}N_{Bulk}$ and $\delta^{15}N_{Ammonium}$ changed (became isotopically enriched due to the loss of ammonia) while the $\delta^{15}N_{Nitrate}$ did not change (isotopically indistinguishable compared to the Initial $\delta^{15}N_{Nitrate}$ value).

This has allowed for a linkage between these two samples to be observed which may not otherwise have been made. This information may be quite valuable for determining the origin of precursor materials and forensic intelligence purposes.

It can also be seen in Figure 4-9 that samples coded Bag 1, Bag 2, Cook 1 and Cook 2 all had the same $\delta^{15}N_{Nitrate}$ values (isotopically indistinguishable). These samples (Cook 1 and Cook 2) underwent the large scale cooking, and by now utilising the $\delta^{15}N_{Nitrate}$ value, these purified samples can be isotopically linked back to their original precursor CAN.

DSTO-CAN-3 is a representative sample of CAN manufactured using the Odda process. This and the previous examples demonstrated that the nitrate separation process is amenable to CAN samples as well as relatively pure AN.

4.7.4 $\delta^{15}N$ Analysis of Homemade Ammonium Nitrate Samples

Due to the previously mentioned restrictions regarding obtaining AN (Chapter 1), a series of samples were also prepared through methods currently employed by "backyard chemists". This was attempted to identify any possible uses of $\delta^{15}N_{Nitrate}$ analysis in linking samples of AN together.

Preparation 1 - Potassium nitrate and ammonium chloride:
$$KNO_{3\ (s)} + NH_4Cl_{\ (s)} + H_2O_{\ (l)} \rightarrow NH_4NO_{3\ (aq)} + KCl_{\ (aq)}$$
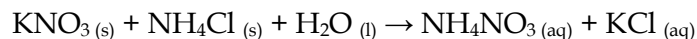
Preparation 2 - Calcium nitrate and ammonium sulphate:
$$Ca(NO_3)_2.5H_2O_{\ (s)} + (NH_4)_2SO_{4\ (s)} + H_2O_{\ (l)} \rightarrow 2NH_4NO_{3\ (aq)} + CaSO_{4\ (s)}$$

Preparation 3 - Barium nitrate and ammonium sulphate:
$$Ba(NO_3)_{2\ (s)} + (NH_4)_2SO_{4\ (s)} + H_2O_{\ (l)} \rightarrow 2NH_4NO_{3\ (aq)} + BaSO_{4\ (s)}$$
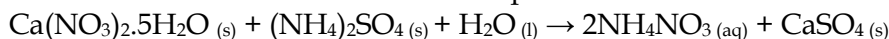
One of these samples of AN (Prep 1) was also heated/melted to simulate the melt procedure which is undertaken during the processing of AN to form prills [48]. The heating temperature profile which was used is shown in Figure 4-10. This simulated melt procedure was undertaken to determine its effect on the $\delta^{15}N$ values of the AN.
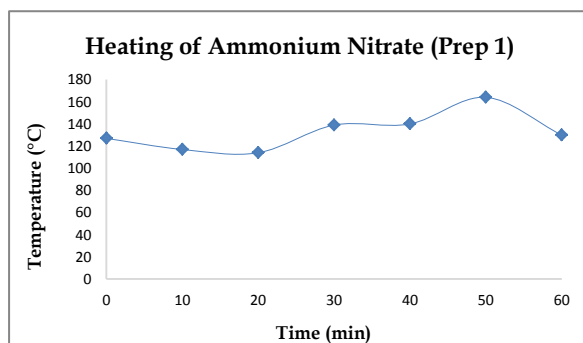
Figure 4-10: Heating profile utilised for melting of AN (Prep 1)

Sample	$\delta^{15}N_{Bulk}$	s.d	$\delta^{15}N_{Nitrate}$	s.d	$\delta^{15}N_{Ammonium}$
KNO_3	-24.87	0.33	N/A	N/A	N/A
NH_4Cl	-0.65	0.17	N/A	N/A	N/A
$Ba(NO_3)_2$	+4.55	0.05	N/A	N/A	N/A
$Ca(NO_3)_2$	+5.95	0.07	N/A	N/A	N/A
$(NH_4)_2SO_4$	-7.09	0.14	N/A	N/A	N/A
Prep 1	-7.17	0.17	-25.46	0.1	+11.12
Prep 1 Heated	-5.3	0.21	-25	0.08	+14.41
Prep 2	-0.4	0.03	+5.95	0.14	-6.76
Prep 3	-3.64	0.51	+4.04	0.05	-11.31

Table 4-7: Details the precursor materials used in the preparation of the AN sample and shows the obtained $\delta^{15}N$ values for the AN samples prepared (These include $\delta^{15}N_{Bulk}$, $\delta^{15}N_{Nitrate}$ and the calculated $\delta^{15}N_{Ammonium}$)
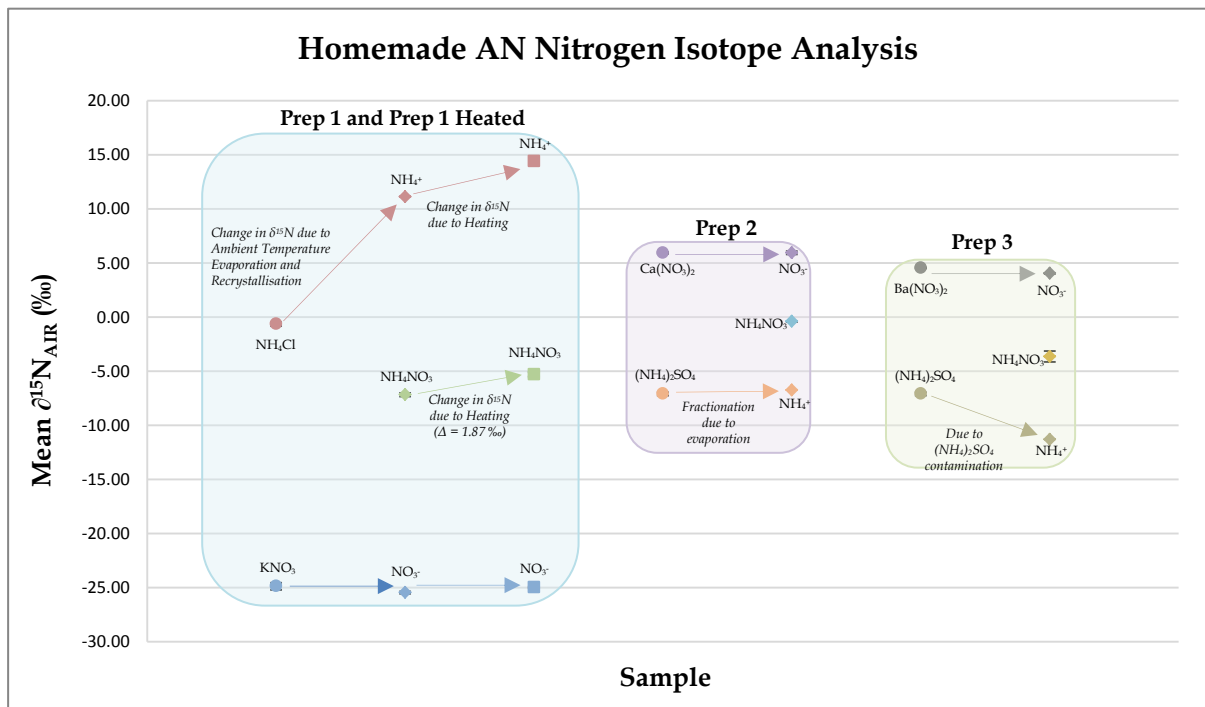
Figure 4-11: Overall $\delta^{15}N$ results for "homemade" AN samples

Figure 4-11 and Table 4-7 details the changes in $\delta^{15}N$ values obtained for the bulk AN, nitrate and ammonium for each of the prepared AN samples. In all three preparations it can be seen that the final $\delta^{15}N_{Nitrate}$ values do not vary from the initial nitrate salt value. This information could be utilised in linking samples together based on the precursors used in the preparation of AN.

Table 4-8 details the theoretical $\delta^{15}N_{Bulk}$ value for each synthesised AN sample. These were calculated based on the $\delta^{15}N$ values obtained for the precursor materials. There are slight differences between the theoretical values and the practically obtained values, due to fractionation effects and contamination (in the case of Prep 3). It can be observed in Prep 1 that there was a large difference between the theoretical and practical values for the $\delta^{15}N_{Bulk}$ AN. It was determined that there was a large amount of isotopic fractionation (loss of ammonia) cause by the evaporation of the water used to prepare the sample (the water was slowly evaporated off over a week at 60°C). This result indicates that if a sample of AN is

subjected to harsh conditions (environmental) it will have a large impact on the $\delta^{15}N_{Bulk}$ value, which makes linking samples together based on isotopic values difficult.

Sample	Mixture	Theoretical Bulk ($\delta^{15}N$)	Measured ($\delta^{15}N$)	Δ ($\delta^{15}N$)	Reason for change in $\delta^{15}N$
Prep 1	KNO_3 + NH_4Cl	-12.76	-7.17	+5.59	Fractionation due to evaporation/purification
Prep 2	$Ca(NO_3)_2$ + $(NH_4)_2SO_4$	-0.57	-0.40	+0.17	Fractionation due to evaporation
Prep 3	$Ba(NO_3)_2$ + $(NH_4)_2SO_4$	-1.27	-3.64	-2.36	Potential $(NH_4)_2SO_4$ contamination (verified using FT-IR)

Table 4-8: details the $\delta^{15}N_{Bulk}$ AN measurements and reasons for observed changes between theoretical and practically obtained values

The isotopic enrichment and fractionation factors can be used to illustrate the average change in δ values between different precursors and products. It can be observed in Figure 4-11 that "Prep 1" and "Prep 1 heated" have different $\delta^{15}N_{Bulk}$ values due to fractionation through loss of ammonia.

$$NH_4NO_3 \rightleftharpoons NH_3 + HNO_3 \qquad \text{(Equation 4-3)}$$

The $\delta^{15}N_{Bulk}$ enrichment and fractionation factors obtained for "Prep 1 Heated" are α = 1.0019 and ε = 1.89. These values indicate that the sample (Prep 1 heated) is enriched in ^{15}N compared to the initial Prep 1 sample. These changes in the $\delta^{15}N$ values for the bulk AN and the ammonium species indicate that they may not be useful for linking samples together due to the high likelihood of the ammonium ions undergoing isotopic fractionation.

The practical value for the bulk $\delta^{15}N$ for Prep 2 also showed some differences in comparison to the theoretical value, this change can be explained by isotopic fractionation due to a loss of ammonia during evaporation of the water. This isotopic fractionation was not as harsh as that seen in Prep 1 due to the fact that it was undertaken at room temperature and in a desiccator. Controlling the evaporation conditions meant that the amount of isotopic fractionation seen was minimised.

Prep 3 also showed differences between theoretical and observed $\delta^{15}N_{Bulk}$ results, and this was more than likely caused by an ammonium sulphate contamination rather than any isotopic fractionation. The samples was analysed and the presence of ammonium sulphate was confirmed by FT-IR.

The main objective of this research task was to identify any possible uses of $\delta^{15}N_{Nitrate}$ analysis in linking samples of AN together. It has been observed that $\delta^{15}N_{Nitrate}$ values can be utilised to link samples of homemade AN to the precursor material used in its preparation (KNO_3).

It was also shown that even under varying conditions (such as heating/evaporation) the $\delta^{15}N_{Nitrate}$ was unaltered, whereas the $\delta^{15}N_{Bulk}$ and $\delta^{15}N_{Ammonium}$ values have been shown to be altered by such variables. The results obtained from this research task indicate that $\delta^{15}N_{Nitrate}$ values would be of great use in linking/discriminating between samples of AN. This methodology has great potential to provide valuable forensic information to aid investigations and provide actionable intelligence.

4.8 Application of Nitrate Separation to AN-based HME Samples

This research involved the preparation and isotopic analysis of 11 different types of AN-based HME (Table 4-9). All HME samples were prepared using a single sample of AN (Orica Nitropril) and the objective of this study was to determine whether HME samples could be linked together based on $\delta^{15}N_{Bulk}$, $\delta^{15}N_{Water\ soluble}$ and $\delta^{15}N_{Nitrate}$ values.

Sample	Composition
HME 1	87% AN & 13% Uncoated Al Powder
HME 2	89% AN & 11% Coated Al Flake
HME 3	88% AN & 12% Sugar
HME 4	77% AN, 13% Coated Al & 10% Sugar
HME 5	90% AN & 10% Diesel
HME 6	71% AN & 29% Nitromethane
HME 7	87% AN & 13% Baby Formula
HME 8	80% AN & 20% Hexamine
HME 9	60% AN & 40% TNT
HME 10	100% AN
HME 11	75% AN, 15% $CaCO_3$ and 10% Coated Al Flake

Table 4-9: Summary of HME compositions

The analysis of the water soluble components is potentially useful for analysis of AN-based HMEs as it may give some information on other nitrogen sources in the mixture. Water extraction was achieved by adding water to a sample in a centrifuge tube which was sonicated for 10 minutes to ensure that all the water soluble components were dissolved. The tube was then centrifuged and the supernatant liquid was removed by pipette. The water soluble fraction was then dried and analysed by IRMS. This analysis is denoted as $\delta^{15}N_{Water\ soluble}$ for nitrogen.

Separation of the nitrate component of each HME was achieved using the procedure used in the previous sections.

Figure 4-12 and Table 4-10 show the results obtained for the $\delta^{15}N_{Bulk}$, $\delta^{15}N_{Water\ soluble}$ and $\delta^{15}N_{Nitrate}$ analysis of the eleven HMEs and nitrogen containing precursors which were utilised in the preparation of the HME samples. It can be noted that the baby formula did not contain sufficient nitrogen for IRMS analysis.
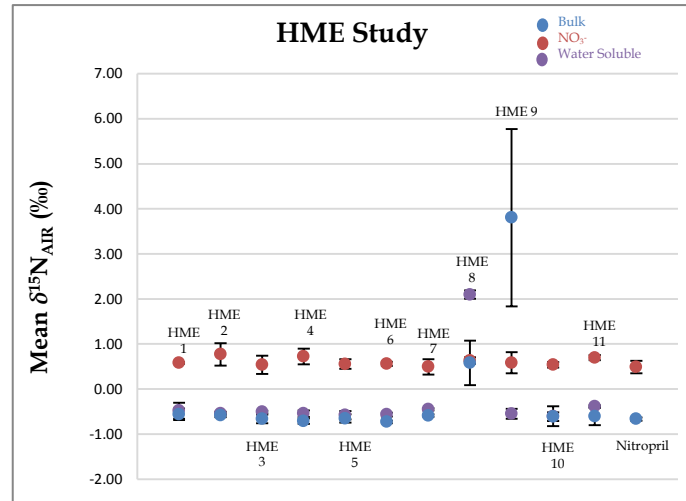
Figure 4-12: Overall δ15N results for eleven AN-based HME samples and their precursors

Sample	$\delta^{15}N_{Bulk}$	s.d	$\delta^{15}N_{Nitrate}$	s.d	$\delta^{15}N_{water\ soluble}$	s.d
HME 1	-0.56	0.13	+0.58	0.02	-0.48	0.18
HME 2	-0.58	0.04	+0.77	0.25	-0.54	0.04
HME 3	-0.66	0.09	+0.54	0.21	-0.51	0.03
HME 4	-0.71	0.06	+0.72	0.17	-0.54	0.07
HME 5	-0.65	0.09	+0.55	0.11	-0.58	0.09
HME 6	-0.73	0.03	+0.56	0.05	-0.57	0.05
HME 7	-0.59	0.03	+0.49	0.17	-0.45	0.03
HM8 8	+0.58	0.49	+0.63	0.07	+2.10	0.09
HME 9	+3.80	1.97	+0.58	0.23	-0.55	0.11
HME 10	-0.61	0.09	+0.54	0.06	-0.60	0.22
HME 11	-0.61	0.19	+0.70	0.06	-0.39	0.02
Hexamine	+0.61	0.02	N/A	N/A	N/A	N/A
Nitromethane	-0.88	0.13	N/A	N/A	N/A	N/A
TNT	-14.31	0.12	N/A	N/A	N/A	N/A
Baby formula	Insufficient Nitrogen		N/A	N/A	N/A	N/A

Table 4-10: IRMS results for HME samples including the fuel sources used in the preparation of the HME samples

The results indicated that bulk $\delta^{15}N$ analysis is able to be utilised in linking the AN used in the preparation of HME samples containing a single source of nitrogen (e.g. AN/Al, AN/S and AN/S/Al) however it is unable to be utilised for samples with dual nitrogen sources (samples which contained hexamine and TNT).

The water soluble $\delta^{15}N$ results can be utilised to gain information about the AN used in the preparation of the HME samples for all samples except those containing hexamine. The water soluble results therefore show that even a simple water extraction can potentially separate dual N-sources (without fractionation if drying is done at room temperature). The result obtained for the AN/hexamine HME solution is unusual as value determined for $\delta^{15}N_{water\ soluble}$ should be identical to that of $\delta^{15}N_{Bulk}$ due to the solubility of hexamine in water. The result obtained was markedly different, which may indicate another process or reaction occurring.

AN and hexamine mixtures are currently used in commercial explosive compositions. A solution of hexamine and AN is utilised as an ingredient for the manufacture of bulk blasting agents used in the mining, quarrying and civil engineering sectors. The hexamine is

139

included within the mixture as it is able to react with nitric acid also present in the formulation to form hexamine nitrate. The proportion of hexamine in a formulation is low (1-9%) [243-246].

The proposed mechanism for the isotopic changes seen is described below. Hexamine accepts a proton in weak acidic media (pH 4-6) and becomes positively charged. In strongly acidic media hexamine is decomposed to formaldehyde and ammonium. The pK_a for hexamine = 4.9 and the pK_a for ammonium = 9.2 [247, 248].

$$(CH_2)_6N_{4\,(s)} + NH_4NO_{3\,(s)} + H_2O_{(aq)} \qquad \text{(Equation 4-4)}$$

$$(CH_2)_6N_{4\,(aq)} + NH_{4\,(aq)}^+ + NO_{3\,(aq)}^- \qquad \text{(Equation 4-5)}$$

$$(CH_2)_6N_{4\,(aq)} + H_{(aq)}^+ + NO_{3\,(aq)}^- + NH_{3\,(g)} \qquad \text{(Equation 4-6)}$$

$$(CH_2)_6N_4H_{(aq)}^+ + NH_{3\,(g)} + NO_{3\,(aq)}^- \qquad \text{(Equation 4-7)}$$
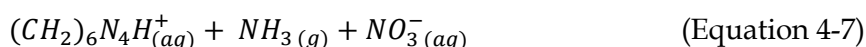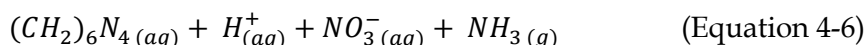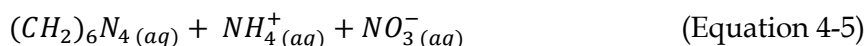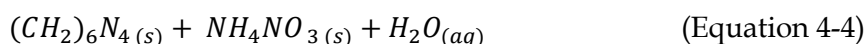
As a solution of AN and hexamine dries, ammonia will be released as shown in Equation 4-7 above. This is the cause of the observed isotopic fractionation from the bulk solid ($\delta^{15}N$ = +0.58‰) to water soluble ($\delta^{15}N$ = +2.09‰).

Nitrate analysis shows potential in linking most of the prepared HME samples together and with the AN source used, however it was identified that there was an unexpected slight enrichment in the $\delta^{15}N_{Nitrate}$ values from the HME samples (HME2/HME4/HME11) which contained Al powder with a coating agent. The effects of coating agents are discussed in further detail in Section 4.8.1.

Table 4-11 gives an overview of all the HME samples and also indicates whether the obtained $\delta^{15}N_{Bulk}$, $\delta^{15}N_{Water\ soluble}$ or $\delta^{15}N_{Nitrate}$ values can be used to link each HME sample to the AN used to prepare each HME. Two tailed t-tests were utilised to determine whether there are significant differences in the means of the measurements of the samples in relation to the original AN source at 95% confidence.

Matching of HME to AN using $\delta^{15}N$				
Code	Description	Bulk	H$_2$O Sol	NO$_3^-$
HME 1	AN/Al	✓	✓	✓
HME 2	AN/Al	✓	✓	✓
HME 3	AN/Sugar	✓	✓	✓
HME 4	AN/Sugar/Al	✓	✓	✓
HME 5	ANFO	✓	✓	✓
HME 6	AN/NM	✓	✓	✓
HME 7	AN/Formula	✓	✓	✓
HME 8	AN/Hexamine	X	X	✓
HME 9	AN/TNT	X	✓	✓
HME 10	Nitropril	✓	✓	✓
HME 11	CAN/Al	✓	✓	X

Table 4-11: Overview of linkages seen between AN-based HME samples.

4.8.1 Aluminium Powder Coating Agent Study

Due to the previously identified anomalies in the $\delta^{15}N_{Nitrate}$ values, a further study was completed to determine the effect of coating agents from aluminium powder on the isolation and $\delta^{15}N$ analysis of the nitrate species from a HME sample.

Figure 4-13 shows the $\delta^{15}N_{Nitrate}$ values for the HME samples previously analysed in this Chapter. The coating agent utilised on the aluminium powder which was incorporated in the HME samples was identified as stearic acid. Therefore a sample of AN (97%) and stearic acid (3%) (AN+SA) also had the nitrate isolated and the result is shown. The original Nitropril $\delta^{15}N_{Nitrate}$ value is also shown for comparison purposes.
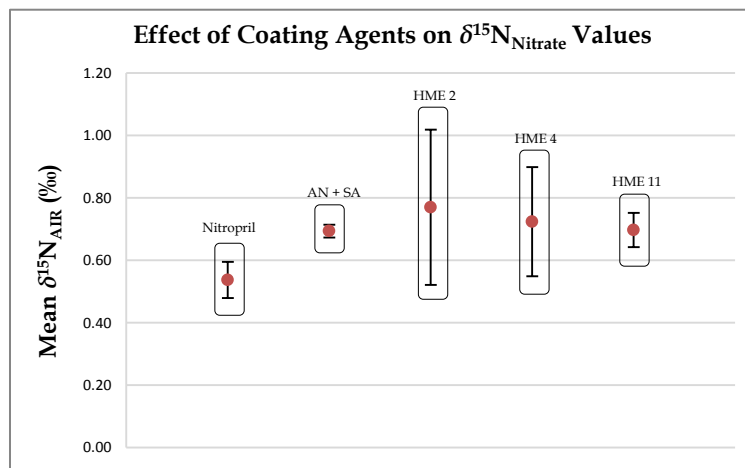
Figure 4-13: Effect of coating agents on $\delta^{15}N_{Nitrate}$ values for HME samples

As stearic acid does not contain any nitrogen (a sample of stearic Acid was analysed by IRMS and there was insufficient nitrogen for analysis), this result was puzzling. Additionally, as the observed shift in the $\delta^{15}N_{Nitrate}$ value was also observed in the AN+SA sample, the shift is not due to the aluminium itself.

One possible explanation for the shift observed in the $\delta^{15}N_{Nitrate}$ value is the adsorption of atmospheric nitrogen or ammonia (due to degradation of the AN) into the coating as governed by the Langmuir adsorption isotherm, which explains the adsorption of molecules on to a solid surface at a fixed temperature [249, 250]. The amount of material adsorbed to a surface can be calculated using Equation 4-8, where θ = the fractional coverage of a surface, b = is a constant and P = gas pressure or concentration.

$$\theta = \frac{bP}{1 + bP}$$

<div align="right">Equation 4-8</div>

The Langmuir adsorption isotherm produces a graph as shown in Figure 4-14, for low concentrations there is a notable rise in the fractional coverage where $\theta \sim P$. However, this flattens out in high concentrations where $\theta \sim 1$, which indicates that all the available sites have been occupied [250].

General Form of the Langmuir Isotherm
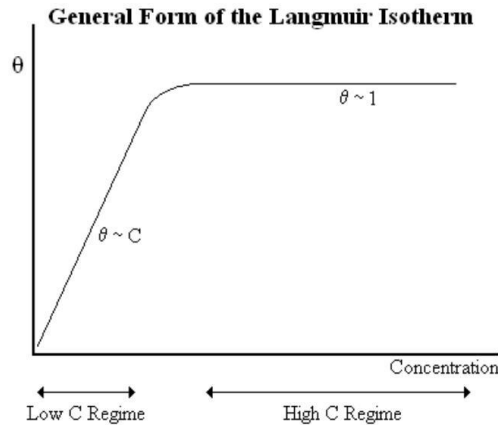
Figure 4-14: Form of the Langmuir isotherm

The fractionation factor (α) and enrichment factor (ε) for each sample in comparison to the original $\delta^{15}N_{Nitrate}$ for the Nitropril is shown in Table 4-12. The enrichment factor was found to be consistent in the three HME and the AN+SA samples containing stearic acid. In the case of the HME samples, the approximate percentage of stearic acid would be ~0.01% of the total sample, whilst in the AN+SA sample, the percentage of stearic acid was 3%. As the enrichment seems to be independent of the amount of stearic acid present in the samples, θ ~ 1 for stearic acid contents above ~0.01%.

	Nitrogen (Nitrate)	
	α	ε
HME 2	1.0003	0.28
HME 4	1.0002	0.24
HME 11	1.0002	0.21
AN + SA	1.0002	0.21

Table 4-12: Calculated enrichment and fractionation factors for HME samples containing aluminium with coating agents

The amount of nitrogen enrichment seen in the samples (due to adsorption of either atmospheric nitrogen or ammonia on the stearic acid) is not considerable due to the relatively low amounts that are adsorbed onto the acid. So the influence may be negligible when attempting to match $\delta^{15}N_{Nitrate}$ values for forensic purposes. However these subtle changes should be taken into consideration when looking at samples that have coated aluminium fuels present, especially in high percentages.

In order to investigate the effect of other coatings commonly used to protect aluminium flake, another four HME samples which were prepared using the Orica Nitropril and different aluminium powders were investigated. The samples prepared are detailed in Table 4-13.

Code	Description	Coating Agent
DSTO-HME-1	10% Silveral 16 Aluminium Flake and 90% AN	Stearic Acid
DSTO-HME-2	10% Silveral 16N Aluminium Flake and 90% AN	Oleic Acid
DSTO-HME-3	10% Silberline DF1667 and 90% AN	Teflon ®
DSTO-HME-4	10% CAP45A Aluminium Powder and 90% AN	Un-coated

Table 4-13: Compositional breakdown of AN/Al HME samples

Table 4-14 and Figure 4-15 details the $\delta^{15}N_{Nitrate}$ and $\delta^{15}N_{Bulk}$ for each of the four HME samples and also the original AN used to prepare the samples.

Ammonium Nitrate Sep - AN-Bulk				
Sample	$\delta^{15}N_{Bulk}$	s.d	$\delta^{15}N_{Nitrate}$	s.d
DSTO-HME-1	+0.66	0.045	+3.22	0.135
DSTO-HME-2	+0.68	0.057	+3.18	0.026
DSTO-HME-3	+0.66	0.102	+3.30	0.030
DSTO-HME-4	+0.66	0.051	+2.99	0.084
DSTO-AN-1	+0.69	0.025	+2.93	0.066

Table 4-14: $\delta^{15}N_{Bulk}$ and $\delta^{15}N_{Nitrate}$ values obtained for AN/Al HME samples
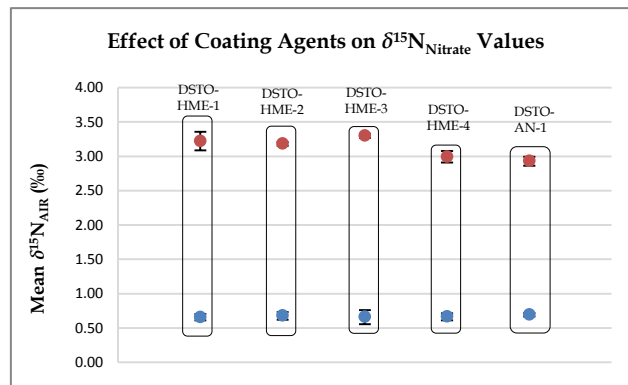
Figure 4-15: $\delta^{15}N_{Bulk}$ (blue) and $\delta^{15}N_{Nitrate}$ (red) values obtained for AN/Al HME samples

The results shown in Figure 4-15 also show a shift in $\delta^{15}N_{Nitrate}$ values for samples that have the presence of a coating agent, this is again believed to be due to the Langmuir adsorption isotherm. The adsorption of nitrogen/ammonia to stearic acid, oleic acid and Teflon® has previously been reported [251-253].

The fractionation factor (α) and enrichment factor (ε) for each sample is shown in Table 4-15. The enrichment factors were similar in samples DSTO-HME-1 and DSTO-HME-2, but slightly higher in the Teflon coated sample (DSTO-HME-3). As a control, the result obtained for the HME sample that used uncoated aluminium flake (DSTO-HME-4) did not shift in the $\delta^{15}N_{Nitrate}$ value.

	Nitrogen (Nitrate)	
	α	**ε**
DSTO-HME-1	1.0003	0.29
DSTO-HME-2	1.0002	0.25
DSTO-HME-3	1.0004	0.37
DSTO-HME-4	1.0001	0.06

Table 4-15: Calculated enrichment and fractionation factors for AN/Al HME samples

Once again the amount of enrichment seen in these samples is not considerable. However this change in isotopic ratio should still be noted and taken into consideration when looking at results where samples have aluminium powder present. It would be optimal, as part of the initial exploitation of HME samples, to identify any coating agents that are present in a sample.

4.8.2 Using a Combination of $\delta^{15}N$ Values to Discriminate Between AN-based HME Samples

This task involved the isotopic analysis of pairs of AN-based HME samples. The objective of this task was to demonstrate the importance of combining $\delta^{15}N_{Bulk}$, $\delta^{15}N_{Water\ soluble}$ and $\delta^{15}N_{Nitrate}$ values to discriminate samples which might otherwise have been thought to be linked using these example HMEs.
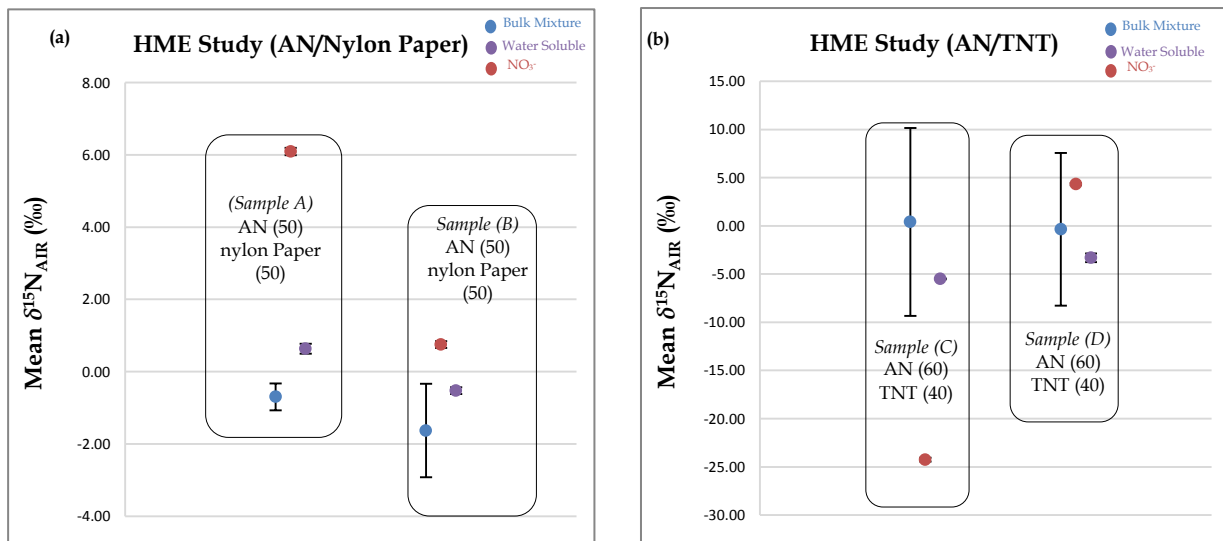
Figure 4-16: a) Overall $\delta^{15}N$ values obtained for two HME samples (AN/nylon Paper) of interest and b) Overall $\delta^{15}N$ values obtained for two HME samples (AN/TNT) of interest.

In Figure 4-16 (a) these HME samples were a mixture of nylon paper and AN. $\delta^{15}N_{Bulk}$ analysis indicates that the two samples are isotopically indistinguishable, $\delta^{15}N_{Water\ soluble}$ analysis shows that the AN within the samples are isotopically different. The $\delta^{15}N_{Nitrate}$ analysis shows that the AN used in each of the samples are isotopically different.

Similarly, in Figure 4-16 (b) these HME samples were a mixture of TNT and AN (Amatol). $\delta^{15}N_{Bulk}$ analysis indicates that the two samples are isotopically indistinguishable. The isotopic spread for the mixtures of approximately 20 ‰ is quite large and implies that the samples are not homogenous which is representative of the poor nature of realistic samples. The $\delta^{15}N_{Water\ soluble}$ analysis shows that the AN within the samples are isotopically different. The $\delta^{15}N_{Nitrate}$ analysis shows that the AN used in each of the samples are isotopically different.

In a final example, Figure 4-17 shows the $\delta^{15}N_{Bulk}$, $\delta^{15}N_{Ammonium}$ and $\delta^{15}N_{Nitrate}$ values obtained for two AN samples. These are two different samples of AN, which have a similar $\delta^{15}N_{Bulk}$ value. However, when the nitrate was isolated and analysed for each sample, the samples are shown to be quite isotopically different.
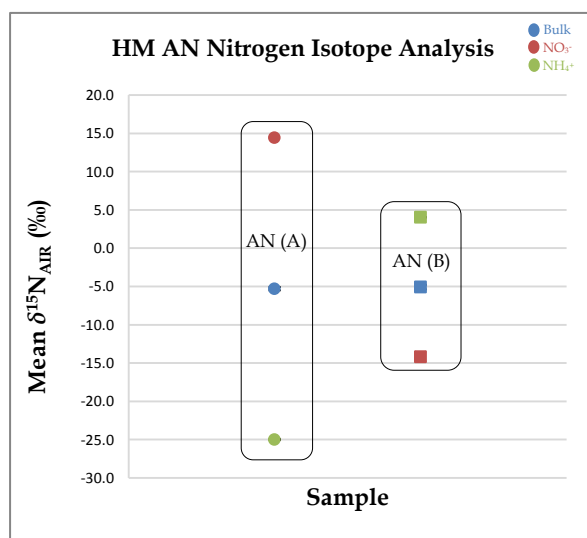
Figure 4-17: Overall $\delta^{15}N$ values obtained for two AN samples of interest.

These examples illustrate the need for a combination of the three $\delta^{15}N$ values ($\delta^{15}N_{Bulk}$, $\delta^{15}N_{Ammonium}$ and $\delta^{15}N_{Nitrate}$) to allow for a greater insight into the isotopic makeup of each AN sample. The more information which can be obtained about each individual sample will allow for a greater comparison of samples and therefore allow for any linkages to be identified or discarded.

4.9 Using $\delta^{15}N_{Nitrate}$ and $\delta^{13}C_{Carbonate}$ to Improve Clustering

As mentioned in Section 4.8 water extractions can be a very useful method to separate mixtures of HME into specific fractions. The insoluble fraction, which remains at the bottom of the centrifuge tube, will generally contain any calcium carbonate from CAN-based samples and insoluble fuels such as aluminium flake. For CAN-based materials, the carbon isotopic ratio of the calcium carbonate may be useful for the source matching. It has been recognised that EA-IRMS is not an particularly precise method for the measurement of carbonates as this attempts to convert CO_3 to CO_2 in an oxidising environment. The preferred methodology is to utilise the reaction with phosphoric acid, however due to resource limitations the EA-IRMS methodology was employed and assessed.

The IRMS determination of the $\delta^{13}C_{Bulk}$ and $\delta^{15}N_{Bulk}$ values may be used to determine batch-to-batch matching of like samples if appropriate care is taken in sampling and IRMS

determination. However, the bulk values do not allow for the source of the AN/CAN to be determined.

It is therefore proposed that the combination of the IRMS results obtained for the two separated species, $\delta^{15}N_{Nitrate}$ and $\delta^{13}C_{Carbonate}$, may allow the formation of tighter clusters when graphically plotted. This will improve the confidence of matching explosive samples to a source material.

4.9.1   Sample Preparation

In order to evaluate the use of $\delta^{15}N_{Nitrate}$ and $\delta^{13}C_{Carbonate}$ IRMS values to improve clustering and thereby improving the ability to source match, 15 samples were analysed. These samples were prepared utilising three different CAN samples. Additionally, some of the source materials were wet processed/cooked prior to blending. CAN/Sugar HME samples were prepared by blending the different AN with two different sugars (either maltose or sucrose), and in order to diversify the HMEs produced, the amount of sugar was added in different ratios. The final sample set produced is shown in Table 4-16.

Sample	Type	AN Source	Fuel	Ratio
1	Source material	DSTO-CAN-1	-	100:0
2	Source material	DSTO-CAN-2	-	100:0
3	Cooked-60 min	DSTO-CAN-2	-	100:0
4	Cooked-60 min	DSTO-CAN-1	-	100:0
5	Source material	BDH AN / Calcium carbonate	-	100:0
6	Cooked-30 min	BDH AN / Calcium carbonate	-	100:0
7	Cooked-60 min	BDH AN / Calcium carbonate	-	100:0
8	HME	Sample 6 + sugar (maltose)	sugar	88:12
9	HME	Sample 5 + sugar (maltose)	sugar	88:12
10	HME	Sample 1 + sugar (maltose)	sugar	95:5
11	HME	Sample 2 + sugar (sucrose)	sugar	87:13
12	HME	Sample 3 + sugar (maltose)	sugar	94:6
13	HME	Sample 4 + sugar (sucrose)	sugar	88:12
14	HME	Sample 7 + sugar (sucrose)	sugar	95:5
15	HME	Sample 5 (cooked 15 min) + sugar (sucrose)	sugar	90:10

Table 4-16: CAN-based HMEs prepared

146

4.9.2   IRMS Analysis

The $\delta^{13}C_{Bulk}$ and $\delta^{15}N_{Bulk}$ values for the prepared HME samples were analysed by IRMS and plotted as shown in Figure 4-18. It can be observed that there are small variations in the $\delta^{15}N_{Bulk}$ values of HME samples prepared using the same source of CAN which is due to uncertainties associated with the instrumentation. The plot obtained appeared similar to the bulk analysis of genuine samples, shown previously in Figure 3-1.
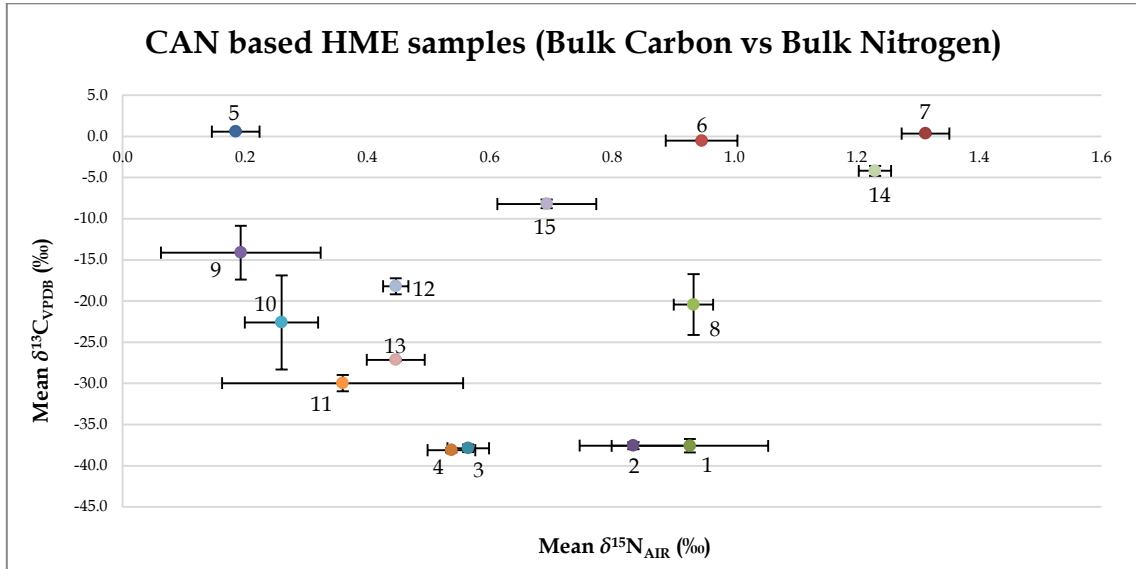
Figure 4-18: The $\delta^{13}C_{Bulk}$ and $\delta^{15}N_{Bulk}$ values obtained for 15 samples of CAN-based HME

The 15 prepared HME samples were then separated by the methods described in this report and the $\delta^{15}N_{Nitrate}$ and $\delta^{13}C_{Carbonate}$ values determined by IRMS. The resulting data were plotted and is shown in Figure 4-19. The graph shows the formation of distinct clusters which directly relate to the two sources of CAN used in their preparation. The advantage of using this technique is that it works independently of the fuel used and that links between seemingly unrelated samples are able to be made with high confidence.
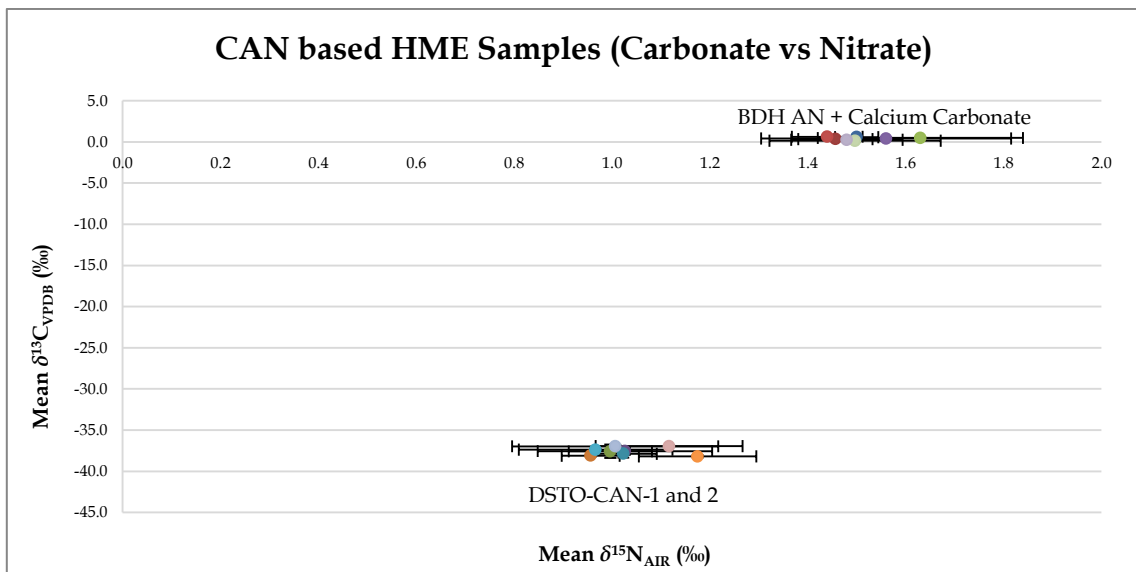
Figure 4-19: Formation of distinct clusters by IRMS analysis of $\delta^{13}C_{Carbonate}$ and $\delta^{15}N_{Nitrate}$

On the basis of the results obtained by using the $\delta^{15}N_{Nitrate}$ and $\delta^{13}C_{Carbonate}$ IRMS values it appears that analysis of separated components is the best method for determining the provenance of materials. For this method to be of widespread use, considerable effort needs to be undertaken to database source materials produced by CAN manufacturers around the world, as reference samples are required to enable comparisons to occur.

4.9.3 Conclusion

The main objective of this research was to develop methodologies which could overcome some of the limitations of IRMS in the forensic analysis of AN and AN-based HME samples.

A suitable method was developed for the $\delta^{15}N$ analysis of the nitrate species isolated from samples of AN and CAN. This included the development of a method to isolate the nitrate species (by removal of the ammonium species). This separation and isolation was verified through the analysis of products by nitrogen-IRMS, FT-IR and FIA.

The variability/verification study showed there was minimum variability within the ten independent separations undertaken (30 individual $\delta^{15}N_{Nitrate}$ analyses) for each AN sample. The small amount of observed intra-variability for each sample indicates that $\delta^{15}N_{Nitrate}$ measurements could be used to discriminate between samples of AN.

The $\delta^{15}N$ analysis of the isolated nitrate appears to contain vast amounts of information concerning the source of nitrate used in the preparation of AN. The isotopic value of the nitrate does not considerably change during synthesis or when subjected to harsh heating processes (as part of evaporation or purification). Samples of homemade AN have been isotopically traced back to their precursor nitrate salt using this analysis method.

The AN and CAN samples which were analysed showed that the combination of three $\delta^{15}N$ values allows for greater discrimination between samples of AN and CAN. This in combination with carbon IRMS would be the preferred analytical methodology to employ in linking or discriminating AN/CAN samples.

It has been identified that $\delta^{15}N_{Bulk}$ values obtained for samples of AN may be isotopically enriched with ^{15}N due to isotopic fractionation. This isotopic fractionation is due to the loss of ammonia (e.g. through purification processes/poor storage) leading to change in the $\delta^{15}N_{Bulk}$ of AN. This isotopic enrichment of the final product AN is due to kinetic isotope effects. Due to this and other identified weaknesses in $\delta^{15}N_{Bulk}$ analysis; $\delta^{15}N_{Nitrate}$ analysis should be incorporated into the overall analysis scheme, as it has been shown that the nitrate is unaffected by the purification (cooking) and poor storage conditions. The isotopic composition of the nitrate species can be used to identify linkages between samples, and also back to the original precursor material.

This research also involved the preparation and isotopic analysis of eleven different types of AN-based HME. All HME samples were prepared using a single sample of AN (ORICA Nitropril) and the objective of this study was to determine whether we could link any HME samples together based on $\delta^{15}N_{Bulk}$, $\delta^{15}N_{Water\ soluble}$ and $\delta^{15}N_{Nitrate}$ values.

The results indicated that $\delta^{15}N_{Bulk}$ analysis is able to be utilised in linking the AN used in the preparation of HME samples containing a single source of nitrogen (e.g. AN/Al, AN/S and AN/S/Al) however it is unable to be utilised for samples with multiple nitrogen sources (samples which contained hexamine and TNT). The $\delta^{15}N_{Water\ soluble}$ results can be utilised to

gain information about the AN used in the preparation of the HME samples for all samples except those containing hexamine. $\delta^{15}N_{Nitrate}$ analysis shows potential in linking most of the prepared HME samples together, however it was identified that there was some unusual isotopic values with HME samples (HME2/HME4/HME11) which contained aluminium powder (with a coating agent). The amount of isotopic enrichment seen in these HME samples was not considerable. However, this change in isotopic ratio should still be noted and taken into consideration when looking at results where samples have aluminium powder present. It would be optimal, as part of the initial exploitation of HME samples to identify any coating agents that are present in a sample.

Separation of HME blends into its various fractions was readily achieved through the use of a simple aqueous wash, this allows for the analysis of $\delta^{15}N_{water\ soluble}$ (the aqueous component) and $\delta^{13}C_{Carbonate}$ (insoluble materials), the determination of the $\delta^{13}C_{Carbonate}$ value is especially important for the characterisation of CAN-based HME. In this study it was found that the isotopic ratio of the insoluble calcium carbonate is characteristic of the source CAN. By combining the $\delta^{15}N_{Nitrate}$ and the $\delta^{13}C_{Carbonate}$ value, tight clusters of material were produced, which were indicative of the source material used. This method is recommended for the analysis of CAN-based HME samples.

In conclusion this research has indicated that $\delta^{15}N_{Bulk}$ analysis is good for batch-to-batch comparison of AN and HME samples and $\delta^{15}N_{Water\ soluble}$ analysis is good for gaining further info about the AN utilised in the preparation of HME samples. This research has identified a number of separation techniques which need to be employed to determine the source of the materials, and by using the described methods, the $\delta^{15}N_{Nitrate}$ and $\delta^{13}C_{Carbonate}$ values enables high confidence identification of the source CAN used in HME mixtures. It should be noted that prior to this isotopic data being utilised, the samples of CAN-based HME must be proven to be physically and chemically identical.

Intentionally Blank

5. Analysis of Sugars

5.1 Historical Used of Sugars as a Fuel in Homemade Explosives

The use of sugar as a fuel source in AN-based HMEs has been reported and detailed in Chapter 3 of this thesis. A number of samples of AN-based HME were analysed by the FEL, DSTL and the typical percentages of sugar observed in these samples ranged between 6-14% [254].

Police on the UK mainland have previously discovered substantial quantities of HME of the fertiliser/sugar type. These include both large quantities in storage and those already made into large devices ready for detonation [255]. Table 5-1 details these various explosive finds on the UK mainland [255].

Location	Date	Container	Quantity	Remarks
London	August 1992	Trailer	12.7 metric tons	Included fifteen partially prepared devices
London	August 1992	Van	1.5 tonnes	One device
London	November 1992	Van	1.6 tonnes	One device
London	December 1992	Van	1.45 tonnes	One device
London	November 1992	Cargo van	3.2 tonnes	One device
Lancashire	July 1994	Flatbed lorry	3.3 tonnes	One device
London	September 1996	Self-storage unit	6.5 tonnes	Included four partially prepared devices

Table 5-1: Summary of finds of fertiliser/sugar mixtures on U.K. mainland between 1992 and 1996

5.2 Use of Sugar in Home Made Explosives on Current ADF Operations

The Australian Defence Force (ADF) is currently supporting the International Security Assistance Forces (ISAF) mission in Afghanistan. Although AN and CAN has been officially banned by the Afghan government [2], nitrate-based fertilisers remain in use all over the country, supported by smuggling operations from adjacent countries. Therefore, this ban has done little to reduce the widespread use of CAN-based explosives.

Historically, the majority of HMEs used in IEDs in Afghanistan have been based on CAN/Al formulations. When supplies of powdered aluminium or other sources of aluminium are in short supply, bomb makers have shown a high degree of resourcefulness in sourcing other viable fuel types. Sugar has typically been one of those fall back fuel sources. Sugar in explosives can be used as a single fuel source, such as CAN/Sugar mixtures, or as part of a multi-fuel blend, such as CAN/Sugar/Al blends.

More recently, bomb makers have been transitioning away from CAN-based formulations to potassium chlorate, so potassium chlorate/sugar blends are becoming increasingly more prevalent.

5.3 Types of Sugar

Sugars or complex carbohydrates are one of the most important components in many foods. Sugar may be present as isolated molecules or they may be physically associated or chemically bound to other molecules.

151

Individual molecules can be classified according to the number of sugar monomers that they contain, i.e. monosaccharides – one sugar monomer, oligosaccharides – 2-10 sugar monomers, and polysaccharides – multiple sugar monomers [256, 257]. The samples of interest to this project are monosaccharides, disaccharides and one sugar alcohol known as erythritol (which is an artificial sweetener), as shown in Figure 5-1.

Monosaccharides are water-soluble crystalline compounds. They are aliphatic aldehydes or ketones which contain one carbonyl group and one or more hydroxyl groups. Most natural monosaccharides have either five (pentoses) or six (hexoses) carbon atoms. Oligosaccharides are relatively low molecular weight polymers of monosaccharides (<20) that are covalently bonded through glycosidic linkages. Disaccharides consist of two monomers, whereas trisaccharides consist of three. Oligosaccharides containing the glucose, fructose and galactose hexose monomers are the most commonly occurring in foods [256, 257]. Common table sugar, or sucrose, is the most commercially important sugar, and is a disaccharide consisting of one glucose and one fructose monomer unit per molecule.
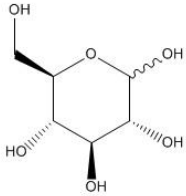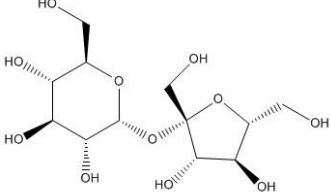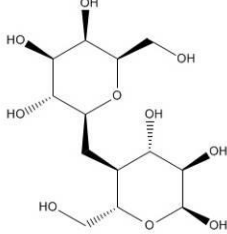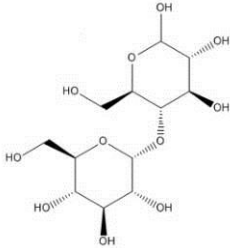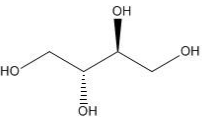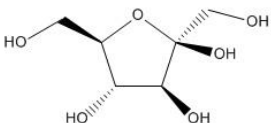
Glucose $C_6H_{12}O_6$ $M_W = 180.16$ % C = 40.00		**Sucrose** $C_{12}H_{22}O_{11}$ $M_W = 342.30$ % C = 42.11	
Lactose $C_{12}H_{22}O_{11}$ $M_W = 342.30$ % C = 42.11		**Maltose** $C_{12}H_{22}O_{11}$ $M_W = 342.30$ % C = 42.11	
Erythritol $C_4H_{10}O_4$ $M_W = 122.12$ % C = 39.34		**Fructose** $C_6H_{12}O_6$ $M_W = 180.16$ % C = 40.00	

Figure 5-1: Common Sugars – properties and molecular projections

5.4 Sugar Production by the C_3, C_4 and CAM Metabolic Pathways

Sugar production in plants is achieved through photosynthesis, where carbon dioxide and water are metabolised to form simple sugars. There are three major photosynthetic pathways available to plants, namely the Calvin–Benson cycle (C_3), the Hatch-Slack cycle (C_4) or the Crassulacen Acid Metabolism (CAM) [258]. The mechanism that a plant uses is largely dependent on the amount of sunlight available, the amount of water and evaporation rates related to the average day/night temperatures of the growing environment.

5.4.1 C_3 Metabolic Pathway

Approximately 95% of all plant species follow the Calvin-Benson cycle (C_3) photosynthetic pathway (Figure 5-2).

It is called the C_3 cycle because the CO_2 absorbed by the plant is converted into a three-carbon molecule, 3-phosphoglycerate, by the enzyme ribulose biphosphate carboxylase oxygenase (RuBisCo). Plants that solely use C_3 fixation tend to thrive in areas where sunlight intensity and temperatures are moderate, ground water is plentiful and CO_2 levels are around 200 ppm or higher [259].

C_3 plants do not typically grow in hot areas due to increased transpiration and competing side reactions of RuBisCo, which incorporates more oxygen as temperature increases and leads to a net loss of carbon and nitrogen from the plant, thus limiting growth. C_3 plants show a higher degree of $\delta^{13}C$ depletion than C_4 plants, typically having isotopic values in the range -22 to -35‰ [259].

5.4.2 C_4 Metabolic Pathway

Three percent of all plants use the Hatch-Slack (C_4) photosynthetic pathway (Figure 5-2) [260], and it is believed to be an evolution of the C_3 pathway. This pathway appears to have evolved to overcome the inefficiencies of the RuBisCo enzyme due to heat and temperature. A different enzyme, phosphoenolpyruvate carboxylase (PEPC) is used to initially fix the carbon dioxide to a four carbon organic acid, which is then transported to the RuBisCo enzyme.

PEPC has a higher affinity for carbon dioxide than RuBisCo and no side reactions due to oxygen occur, however, since every CO_2 molecule has to be fixed twice, the C_4 pathway uses more energy. This energy use is offset by the amount of water needed per CO_2 molecule fixed, i.e. the C_3 pathway uses 833 molecules of water, while the C_4 pathway only uses 277 molecules of water. This conservation of water allows C_4 plants to grow in arid, dry environments. C_4 plants including grasses, sugar cane, desert plants and marine plants, generally have isotopic values in the range of -8 to -20‰. C_4 plants are enriched in ^{13}C compared to C_3 plants [259, 261].
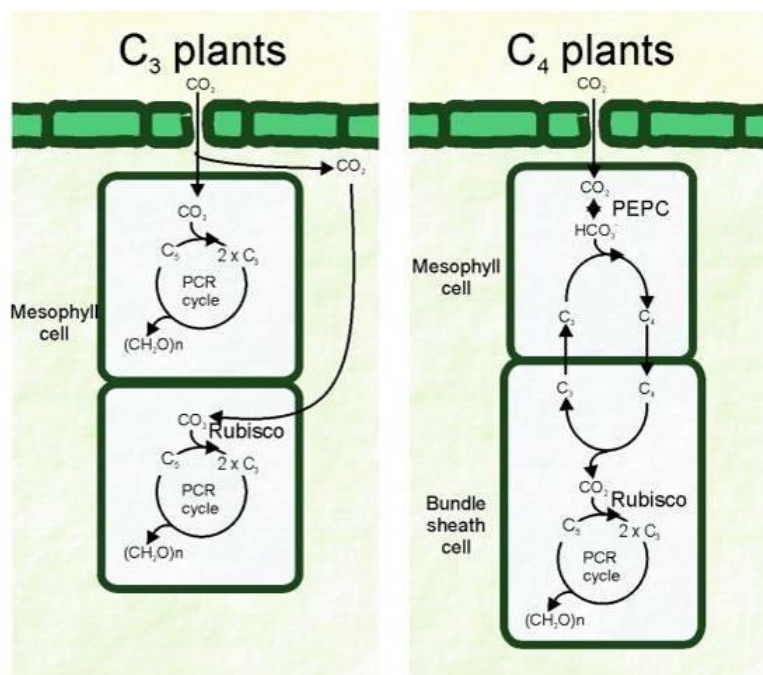
Figure 5-2: Simplified schematics of the C_3 and C_4 pathways

153

5.4.3   CAM Metabolic Pathway

The CAM cycle is an adaption for extreme water efficiency and is typically found in plants inhabiting very arid conditions, and is commonly associated with succulents and cacti. The cycle is based on the C_4 mechanism, however the plant closes its stoma during the day to prevent water loss, only opening during the night to collect carbon dioxide. The carbon dioxide is stored within the plant as the four carbon organic acid is produced by the C_4 pathway, however, this may not be directly transported to the RuBisCo enzyme, but stored in vacuoles. Most CAM plants are also able to use the C_3 or C_4 pathways as well, if conditions allow, and therefore no clear generalised isotopic distributions are able to be made.

5.5 Commercial Production of Sugars

Sucrose is produced in over 120 countries and global production exceeds 1.9 billion tons per year [262]. Approximately 75% is produced from sugar cane (a C_4 plant), a very tall grass largely grown in tropical regions. The remaining 25% is produced from sugar beet (a C_3 plant), a root crop mostly grown in the temperate zone of the northern hemisphere as shown in Figure 5-3 [263]. The major producers and exporters of cane and beet sugar are shown in Table 5-2 [262].

Figure 5-3: Worldwide production of cane and beet sugar

Cane Sugar		Beet Sugar	
Country	**Production (Million Tonne)**	**Country**	**Production (Million Tonne)**
Brazil	717.4	France	31.9
India	292.2	USA	29.1
China	111.4	Germany	23.9
Thailand	68.8	Russian Federation	22.2
Mexico	50.4	Turkey	17.9
Pakistan	49.4	Ukraine	13.7
Colombia	38.5	Poland	9.8
Philippines	34.0	China	9.3
Australia	31.5	Egypt	7.8
Argentina	25.0	United Kingdom	6.5
USA	24.8	Netherlands	5.3
Indonesia	24.4	Belgium	4.5
Guatemala	22.2	Iran	3.9
South Africa	16.0	Italy	3.6
Vietnam	15.9	Spain	3.4

Table 5-2: Top 15 producers of cane and beet sugar worldwide in 2010

154

5.6 IRMS Analysis of Sugars

Natural variations in the abundance of ^{13}C reflect its passage through chemical and/or biological systems in which transformations are accompanied by isotopic fractionation that results in enrichment or depletion of ^{13}C due to the difference in mass, often referred to as the kinetic isotope effect [116]. An example of an important kinetic isotope effect is that which results in selective incorporation of ^{12}C into organic matter during photosynthesis. Living plants assimilate atmospheric CO_2 during photosynthesis [86]. The degree of fractionation depends on various factors, including the specific photosynthetic pathway used for carbon fixation, the rate of diffusion of carbon dioxide into the plant, and the amount of metabolic carbon available [264, 265].

Sugar cane and sugar beet are both able to be processed into sucrose. Isotopic differences are introduced as sugar cane utilises the C_4 metabolic pathway, whereas sugar beet uses the C_3 metabolic pathway. Previous isotopic analyses of cane and beet sugars have yielded the following $\delta^{13}C$ values (Table 5-3) [123, 124, 259]:

Cane sugars (C_4)	Beet sugars (C_3)
-11.5 ‰	-24.2 ‰
-11.7 ‰	-24.98 ‰
-11.99 ‰	-25.62 ‰

Table 5-3: Summary of $\delta^{13}C$ values for cane and beet sugars

In C_3 plants, RuBisCo brings about the enrichment of ^{12}C in its products because it fixes $^{12}CO_2$ faster than it fixes $^{13}CO_2$ per unit of isotope available. However, in C_4 plants, virtually all of the CO_2 which is offered as a result of the decarboxylation is fixed. These processes are shown in Figure 5-4 [105, 111, 124, 259].
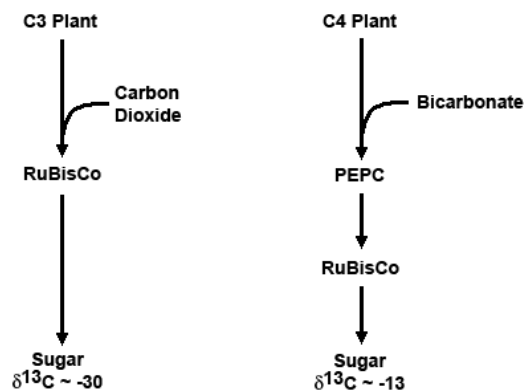
Figure 5-4: Illustration of Carbon dioxide fixation in C_3 and C_4 plants

The possibility of characterising plants by their $\delta^{13}C$ value has led to some interesting applications in food regulation relevant to forensic science. These studies have been focused on quality control and proof of authenticity of various food and beverage products. Numerous publications cover the analysis of substances such as wine, fruit juices, sweeteners and honey [123, 124, 266, 267].

Overall carbon isotopic ratio values can be used to differentiate between C_3 and C_4 sugars. This type of information may prove useful for potentially discriminating between sugars found in explosive mixtures.

5.7 Analysis of Sugar by ICP-MS

Differences in elemental concentrations between cane and beet sugars are likely due to several factors. Variations in impurities originating from processing and packaging may be partially responsible. However the concentration difference appears to be mostly due to the degree of refinement of the samples [123].

In a recent report, an interlaboratory program was tasked to determine the concentrations of 63 elements in a standard set of sugar samples (14 in total) from beet sugar (eight samples) and cane sugar (six samples) from different geographical origins [123]. Laboratories participating in this study used a variety of techniques including: ICP-MS, ICP-OES, Thermal Ionisation Mass Spectrometry (TIMS) and IRMS. Unrefined sugars were found to contain much higher amounts of most elements when compared to the corresponding refined sugar, independent on whether it was of cane or beet origin [123]. The authors have suggested that determining the geographical origin of sugars appeared to be feasible by using elemental fingerprinting, the results shown in Table 5-4 compare two sugar samples (a refined beet sugar and an unrefined cane sugar) contrasting the concentration of 29 elements [123].

Element	Units	Refined Beet Sugar (SD)	Unrefined Cane Sugar (SD)
K	µg/g	25 (4-38)	600 (250-1100)
Ca	µg/g	6.8 (0.05-29)	230 (100-500)
Mg	µg/g	0.08 (0.005-0.39)	76 (40-110)
Na	µg/g	6.4 (0.6-18)	25 (4-60)
P	µg/g	0.8 (0.1-3.0)	27 (18-42)
Fe	µg/g	0.08 (0.02-0.25)	11 (4-25)
Al	µg/g	0.06 (0.006-0.24)	2.2 (0.4-2.0)
Mn	ng/g	25 (0.2-83)	1100 (400-2000)
Cu	ng/g	33 (4-78)	520 (100-1200)
Sr	ng/g	24 (0.4-160)	650 (190-1400)
Zn	ng/g	29 (2-80)	340 (170-620)
Ba	ng/g	3 (0.1-20)	190 (50-300)
B	ng/g	110 (10-400)	70 (40-120)
Se	ng/g	<5	29 (<5-100)
Ni	ng/g	1.7 (0.1-4.5)	31 (8-60)
V	ng/g	0.5 (0.1-0.8)	21 (4-60)
As	ng/g	0.6 (<0.5-0.9)	19 (8-50)
Cr	ng/g	0.5 (0.2-1.1)	18 (10-30)
Co	ng/g	0.7 (0.04-3.3)	16 (1-25)
Mo	ng/g	0.28 (0.02-0.80)	14 (3-30)
Pb	ng/g	4 (0.06-30)	29 (9-100)
Li	ng/g	0.6 (<0.2-2.7)	7 (1-22)
Zr	ng/g	0.38 (0.07-1.3)	3 (1-7)
Cd	ng/g	0.86 (0.01-4.8)	1.0 (0.3-2.0)
Y	ng/g	0.018 (<0.01-0.10)	1.5 (0.3-3.0)
Tl	ng/g	0.09 (0.01-0.28)	1.3 (0.2-3.3)
Sc	ng/g	0.009 (<0.01-0.019)	0.5 (0.1-1.3)
Sb	ng/g	1.9 (0.3-2.2)	1.3 (0.4-3.0)
U	pg/g	100 (5-400)	510 (90-1600)

Table 5-4: Summary of elemental content average (range) of two sugar samples

Advanced statistical analyses such as principal component analysis (PCA) has been used to demonstrate that geographic origin can be determined. PCA is a widely used statistical technique for unsupervised dimension reduction. The main basis of PCA-based dimension reduction is that PCA picks up the dimensions with the largest variances [268]. The principal components may then be used as predictor or criterion variables in subsequent analyses [269].

The example shown in Figure 5-5 shows distinct groupings that can be used to identify geographical origin [123]. Group 1 – IAEA-C6 (cane sugar); group 2 - ultrex (cane sugar); group 3 - Moldova (beet sugar); group 4 - Poland (beet sugar); group 5 – Idaho USA (beet sugar); group 6 – Netherlands (beet sugar); group 7 – France (beet sugar); group 8 – Germany (beet sugar); group 9 – Hungary (beet sugar) and group 10 – Michigan, USA (beet sugar).

These results were obtained for ten refined sugar samples, in which 22 trace elements were identified, namely: Al, B, Ba, Ca, Co, Cr, Cs, Cu, Fe, Li, K, Mg, Mn, Na, Ni, Pb, Rb, Sn, Sr, Ti, V and Zn.
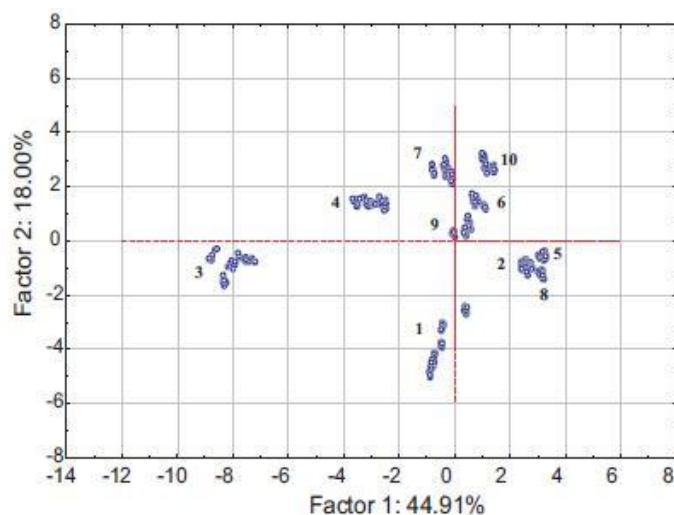
Figure 5-5: Results of PCA using 22 elements and 10 refined sugar samples

5.8 Analysis of Sugars by Gas Chromatography/Mass Spectrometry

GC/MS is a sensitive technique, which can be utilised to identify organic compounds in a mixture. A well-established technique for the analysis of sugars by GC/MS is to first convert the sugar to its trimethylsilyl (TMS) derivative. Nowicki and Pauling were able to derivatise six common sugars (fructose, dextrose, mannitol, lactose, sucrose and maltose) and analyse them by GC/MS. The lactose-TMS derivative had the same retention time as the sucrose-TMS derivative under the chromatographic conditions that they employed, however they were differentiated by their mass spectra [270].

Goodpaster and Keto published a paper looking at the identification of ascorbic acid and its degradation products in black powder substitutes [271]. From GC/MS results one of the samples (Clear shot powder) contained an alternative fuel source which included a variety of simple sugars such as fructose, glucose and galactopyranose. This produce was unique

157

from the other ascorbic acid containing products due to the presence of intact sugars such as fructose [271].

5.9 Analysis of Sugars by High Performance Liquid Chromatography

While sugars can be analysed by gas chromatography (GC) techniques, alternative chromatographic techniques have been explored based on liquid techniques, such as High Performance Liquid Chromatography (HPLC) [272]. In order to analyse sugars, refractive index (RI) or evaporative light scattering (ELS) detectors must be used as sugars have no ultraviolet active chromaphore. Sellers and Morehead were able to separate five sugars (fructose, glucose, sucrose, maltose and lactose) using HPLC-RI and this technique has also been used to identify and quantify sugar adulterants in seized cocaine samples [272]

5.10   Aim

The aim of this research was to determine whether advanced analytical techniques such as IRMS and ICP-MS could be used to obtain isotopic and elemental information about a series of CAN/sugar samples.

IRMS will be used to determine of the $\delta^{13}C_{Bulk}$ value for a series of sugars and CAN/Sugar mixtures to identify the metabolic pathway used to produce sugar, i.e. beet sugar (C_3) or cane sugar (C_4).

A HPLC method will be developed that enables the identification of sugars present and their approximate ratio in an explosive mixture.

5.11   Experimental

5.11.1 Samples

Fifteen sugar samples were obtained from a variety of sources, such as chemical suppliers or purchased from local retail stores. Table 5-5 details the sugar samples under investigation.

A number of CAN/Sugar samples in which the ratio of CAN:Sugar were also prepared, the mixtures prepares are summarised in Tables 5-6 to 5-10 . The CAN and sugar used in the preparation of these materials is listed below:

- CAN 1 is a simulated CAN sample that was prepared by mixing pure AN (75%) to pure calcium carbonate (25%).
- CAN 2 is a commercially obtained CAN from Incitec Pivot. The calcium carbonate percentage in this CAN was determined to be 9.9%.
- Sugar 2 is sucrose refined from Australian cane sugar produced by Bundaberg sugar (North Queensland).
- Sugar 8 is maltose purchased from Sigma Aldrich, Japan.

NOTE: Prior to blending CAN with sugar, the CAN was dissolved in a minimal amount of water and heated until the CAN dissolved, the material was then decanted and evaporated to dryness, this introduces some fractionation and is analogous to the purification methods employed by bomb makers.

Code	Description	Country of Origin	Source	Batch Number
Sugar-1	CSR Smart (Sucrose and Stevia)	-	CSR	-
Sugar-2	Bundaberg Cane Sugar	Australia	Bundaberg Sugar	M11060410:55
Sugar-3	AR grade Lactose	England	BDH Laboratories	302629U
Sugar-4	D(-) Fructose	-	BDH Laboratories	-
Sugar-5	Dextrose	-	Evans Medical	-
Sugar-6	Sucrose	USA	Sigma Aldrich	110M01351V
Sugar-7	D(-) Fructose	USA	Sigma Aldrich	090M0128V
Sugar-8	D(+) Maltose Monohydrate	Japan	Sigma Aldrich	020M15881V
Sugar-9	D(+) Glucose	USA	Sigma Aldrich	080M0142V
Sugar-10	Sucrose	-	AFP-C3	-
Sugar-11	Sucrose (99.9%)	-	Eurovector	E11017
Sugar-12	Vanilla Favour Sugar	Germany	RUF Lebensmittelwerk KG	L3353972
Sugar-13	100% Natural Sweetener (Erythritol and Stevia)	Australia	Natvia Pty Ltd	-
Sugar-14	Palm Sugar	Malaysia	Jeeny's Oriental Foods Palm Sugar	-
Sugar-15	Raw Sugar	-	Cibo	-

Table 5-5: Summary of sugar samples

Sample	Mass of CAN (mg)	Mass of Sugar (mg)	% Sugar
CAN/Sugar (98:2) (CAN 1/Sugar2)	98	2	2
CAN/Sugar (95:5) (CAN 1/Sugar2)	95	5	5
CAN/Sugar (90:10) (CAN 1/Sugar2)	90	10	10
CAN/Sugar (88:12) (CAN 1/Sugar2)	88	12	12
CAN/Sugar (85:15) (CAN 1/Sugar2)	85	15	15

Table 5-6: CAN/Sugar mixtures containing CAN 1 and Sugar 2

Sample	Mass of CAN (mg)	Mass of Sugar (mg)	% Sugar
CAN/Sugar (98:2) (CAN 1/Sugar8)	98	2	2
CAN/Sugar (95:5) (CAN 1/Sugar8)	95	5	5
CAN/Sugar (90:10) (CAN 1/Sugar8)	90	10	10
CAN/Sugar (88:12) (CAN 1/Sugar8)	88	12	12
CAN/Sugar (85:15) (CAN 1/Sugar8)	85	15	15

Table 5-7: CAN/Sugar mixtures containing CAN 1 and Sugar 8

Sample	Mass of CAN (mg)	Mass of Sugar 2 (mg)	Mass of Sugar 8 (mg)	% Sugar
CAN 1-S2-S8	88	6	6	12

Table 5-8: CAN/Sugar mixture containing CAN 1, Sugar 2 and Sugar 8

Sample	Mass of CAN (mg)	Mass of Sugar (mg)	% Sugar
CAN/Sugar (98:2) (CAN 2/Sugar2)	98	2	2
CAN/Sugar (95:5) (CAN 2/Sugar2)	95	5	5
CAN/Sugar (90:10) (CAN 2/Sugar2)	90	10	10
CAN/Sugar (88:12) (CAN 2/Sugar2)	88	12	12
CAN/Sugar (85:15) (CAN 2/Sugar2)	85	15	15

Table 5-9: CAN/Sugar mixtures containing CAN 2 and Sugar 2

Sample	Mass of CAN (mg)	Mass of Sugar (mg)	% Sugar
CAN/Sugar (98:2) (CAN 2/Sugar8)	98	2	2
CAN/Sugar (95:5) (CAN 2/Sugar8)	95	5	5
CAN/Sugar (90:10) (CAN 2/Sugar8)	90	10	10
CAN/Sugar (88:12) (CAN 2/Sugar8)	88	12	12
CAN/Sugar (85:15) (CAN 2/Sugar8)	85	15	15

Table 5-10: CAN/Sugar mixtures containing CAN 2 and Sugar 8

5.11.2 Isotope Ratio Mass Spectrometry

An IsoPrime (GV Instruments) stable isotope ratio mass spectrometer with a EuroEA3000 Series (EuroVector) elemental analyser, was utilised for the measurement of carbon isotopes. The system utilised Waters MassLynx mass spectrometry software.

The sampling technique utilised was continuous flow IRMS (CF-IRMS), consisting of a helium carrier gas to carry the analyte gas into the ion source of the IRMS.

For the analysis of pure sugar approximately 100 μg of sample was weighed into a tin capsule (5 x 9 mm, EuroVector).

Samples were prepared by dissolving CAN/Sugar (20 mg, 85% CAN/15% Sugar) into 400 μL of water, which was subsequently sonicated to ensure the sample was mixed. The sample was left to stand for 10 min, which allowed for the insoluble calcium carbonate to settle at the bottom of the vial. A syringe was used to extract 10 μL of the aqueous layer to the IRMS tin capsule, was dried prior to $\delta^{13}C$ analysis. All analyses were performed in triplicate.

5.11.3 High Performance Liquid Chromatography (HPLC)

A Shimadzu prominence UFLC with Refractive Index Detector was used for the qualitative and quantitative analysis of sugars. The method used for this analysis is detailed below:

- Column: Phenomenex ® Luna ® 5 μm NH2 100 Å LC Column 250 x 4.6 mm (with Guard Cartridge)
- Dimensions: 250 x 4.6 mm ID
- Order No: 00G-4378-E0
- Elution type: Isocratic

160

- Eluent A: Acetonitrile (80%) – Scharlau Acetonitrile, Supragradient HPLC Grade (Ref: AC03312500) (Batch 83188)
- Eluent B: Water (20%) – MilliQ water (18.2 MΩ @ 25°C) obtained from a Merck Synergy UV Millipore System
- Flow rate: 2 mL/min
- Column temperature: 40°C
- Pressure: 1480 psi
- Detection: Refractive Index (RI) @ 40°C
- Sample injection volume: 10 μL
- Solvent: mobile phase

Refractive Index (RI) detectors work by measuring changes in the bulk properties of the solvent and the solutes under investigation, exploiting the improbability that solvents and solutes would share the identical refractive index. It should be noted that positive and negative peaks can occur during a single analysis due to the following factors *[273-275]*:

- Changes in solvent temperature and pressure (which can cause baseline instability);
- If sample solvent properties don't perfectly match with the mobile phase properties;
- Differences in the nature of analytes and eluents; and
- A negative air/solvent peak from the injection can be caused if a non-degassed sample is injected into degassed solvent.

5.11.3.1   *Sugar Calibration*

Two sugar standards for sucrose and maltose were prepared. The standards ranged in concentration from 0.26 mg/mL to 2.65 mg/mL. The preparation of these sugar standards allow for the areas below the peaks to be integrated, which can be used to calculate the relative amounts of sugar present and their ratio when analysing unknown samples. Table 5-11 details the preparation of sugar standards and the resulting calibration plots are shown in Figure 5-6 and 5-7.

Sucrose Conc. (mg/mL)	Maltose Conc. (mg/mL)	Volume of Sugar standard solution (μL)	Volume Mobile phase (μL)
2.6	2.65	250	750
2.08	2.12	200	800
1.04	1.06	100	900
0.52	0.53	50	950
0.26	0.265	25	975
0	0	0	1000

Table 5-11: Summary of calibration standards
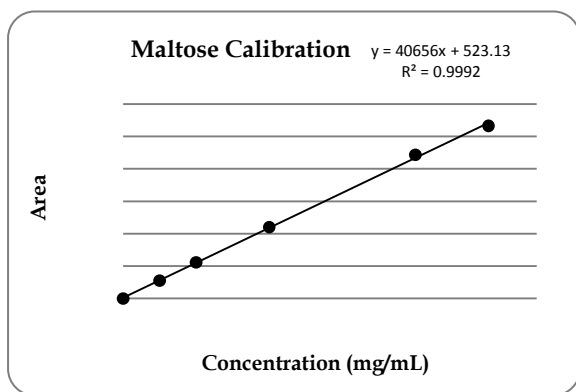
Figure 5-6: Maltose calibration
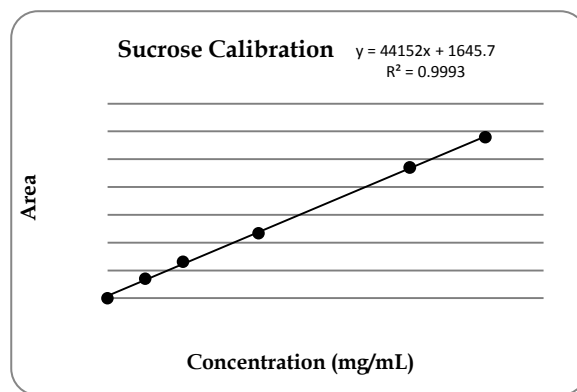
Figure 5-7: Sucrose calibration

5.11.3.2 Sugar Sample Preparation

Sugar solutions for the 15 sugars listed in Table 5-5 were prepared by dissolving ≈1 mg of sample in 1 mL of an acetonitrile/water (4:1) solution. The resulting solution was then sonicated for 30 minutes to ensure that the sugar had completely dissolved.

Additionally, a reference sample containing six sugars (sucrose, maltose, lactose, fructose, glucose and erythritol) was prepared by dissolving ≈ 10 mg of each sugar in water (1 mL) to create a bulk standard solution. The standard was then further diluted to a 1 mg/mL solution.

5.11.3.3 CAN/Sugar Sample Preparation

Multiple CAN/Sugar samples were prepared that contained varying sugar percentages, namely 2, 5, 10, 12 and 15%. For HPLC analysis, the goal was to achieve a sugar concentration of approximately 1 mg/mL in each sample, which required a calculation to be performed to determine the amount of CAN/Sugar that needs to be added. The mass of CAN/Sugar needed to achieve the desired concentration for each sugar percentage is shown in Table 5-12.

Percentage of Sugar in Sample	Mass needed for HPLC sample (mg)
2	27
5	15
10	10
12	8
15	7

Table 5-12: Masses of CAN/Sugar required to produce a sugar concentration of 1 mg/mL for each sugar percentage

CAN/Sugar solutions, with a sugar concentration of 1 mg/mL, were prepared by dissolving the calculated mass for each sugar percentage in 1 mL of an acetonitrile/water (4:1) solution. The resulting solution was then sonicated for 30 minutes to ensure that the sugar had completely dissolved.

5.12   Results

5.12.1 IRMS Results

The fifteen sugar samples were analysed by IRMS to determine their $\delta^{13}C_{Bulk}$ value. The results obtained are shown in Table 5-13. The results indicate that it is possible to determine the metabolic pathway from which the sugar was produced.

Eleven out of the fifteen samples were determined to be C_4 sugars, based on a $\delta^{13}C_{Bulk}$ values between -9 and -13‰. These samples comprised sucrose, glucose, fructose and also erythritol, which is a precursor to the explosive erythritol tetranitrate (ETN).

Four of the samples were identified as C_3 sugars, having a $\delta^{13}C_{Bulk}$ values between -23 and -27‰ and were comprised of lactose, maltose, fructose and a vanilla sugar (vanilla sugar is usually sugar mixed with vanilla extract (or could be sugar mixed with vanilla beans) [276].

This result shows that it is quite easy to differentiate between sugars produced by the C_3 and C_4 metabolic pathways, as shown graphically in Figure 5-8.

Code	Pathway	Mean $\delta^{13}C$ (‰)	S.D $\delta^{13}C$ (‰)
Sugar-1	C_4	-12.00	0.13
Sugar-2	C_4	-12.00	0.12
Sugar-3	C_3	-25.62	0.15
Sugar-4	C_3	-23.66	0.09
Sugar-5	C_4	-9.35	0.19
Sugar-6	C_4	-11.72	0.09
Sugar-7	C_4	-10.81	0.06
Sugar-8	C_3	-26.65	0.03
Sugar-9	C_4	-10.75	0.03
Sugar-10	C_4	-11.45	0.06
Sugar-11	C_4	-11.63	0.10
Sugar-12	C_3	-26.81	0.02
Sugar-13	C_4	-12.88	0.06
Sugar-14	C_4	-11.81	0.02
Sugar-15	C_4	-11.79	0.02

Table 5-13: $\delta^{13}C$ values for sugar samples of interest
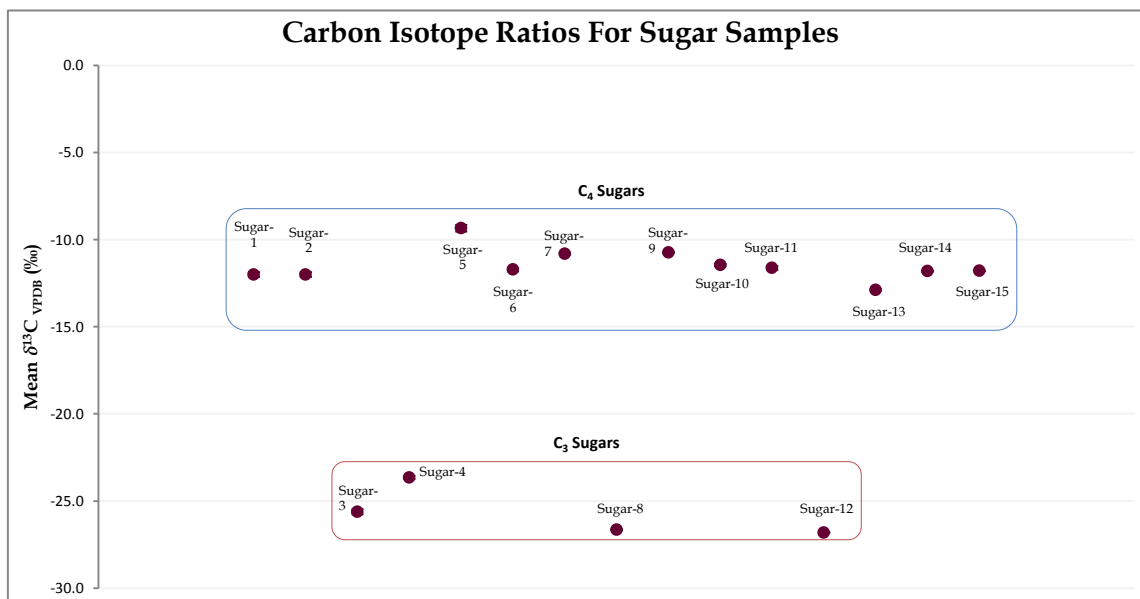
Figure 5-8: Carbon isotope ratios obtained for the 15 sugar samples

5.12.2 Percentage of Sugar and its effect on the $\delta^{13}C$ of CAN/Sugar mixtures

The $\delta^{13}C$ isotopic values for the CAN/Sugar mixtures (containing 2, 5, 10, 12 or 15% sugar) and the corresponding precursor materials were determined by IRMS.

The results obtained for the precursor materials are shown in Table 5-14. The two CAN samples used in the preparation of the CAN/Sugar mixtures were quite different in composition and $\delta^{13}C$ value. CAN 2 had a $\delta^{13}C$ = -37.87 ‰ ± 0.46 and a calcium carbonate content of approximately 9%. CAN 1 had a $\delta^{13}C$ = +0.39‰ ± 1.34 and a calcium carbonate content of approximately 25%. The standard deviations observed in these two samples of CAN indicate that the samples are not especially homogeneous (which is representative of real world samples) and this factor was noted prior to the preparation of the CAN/sugar mixtures. The two sugar samples were also quite different with sugar 2 (sucrose) being a C_4 sugar and having a $\delta^{13}C$ = -12.00 ‰ ± 0.12. Sugar 8 (maltose) was identified as a C_3 sugar and had a $\delta^{13}C$ = -26.65 ‰ ± 0.03.

Sample	Mean $\delta^{13}C$ (‰)	S.D $\delta^{13}C$ (‰)
Sugar-2	-12.00	0.12
Sugar-8	-26.65	0.03
CAN 2	-37.87	0.46
CAN 1	+0.39	1.34

Table 5-14: $\delta^{13}C$ values for precursor materials

The values obtained for the CAN/Sugar mixtures based on CAN 1, CAN 2, Sugar 2 and Sugar 8 are shown in Tables 5-15 and 5-16. The tables show how the $\delta^{13}C$ value changes as a percentage of the sugar present. This is shown graphically in Figure 5-9.

CAN 1- Sugar 2					CAN 2- Sugar 2				
CAN/Sugar Ratio	98/2	95/5	90/10	88/12	85/15	98/2	95/5	90/10	88/12	85/15
Mean δ^{13}C (‰)	-3.03	-5.68	-7.8	-8.78	-9.29	-23.61	-16.65	-16.13	-15.21	-14.92
S.D δ^{13}C (‰)	0.25	0.72	0.57	0.66	0.76	0.62	0.25	1.11	0.72	0.23

Table 5-15: δ^{13}C values for CAN/Sugar mixtures based on sugar 2

CAN 1- Sugar 8					CAN 2- Sugar 8				
CAN/Sugar Ratio	98/2	95/5	90/10	88/12	85/15	98/2	95/5	90/10	88/12	85/15
Mean δ^{13}C (‰)	-5.27	-10	-14.86	-18.1	-19.71	-30.21	-28.06	-27.71	-27.66	-27.4
S.D δ^{13}C (‰)	0.51	0.62	0.92	1.19	1.26	0.27	0.75	0.43	0.19	0.42

Table 5-16: δ^{13}C values for CAN/Sugar mixtures based on sugar 8
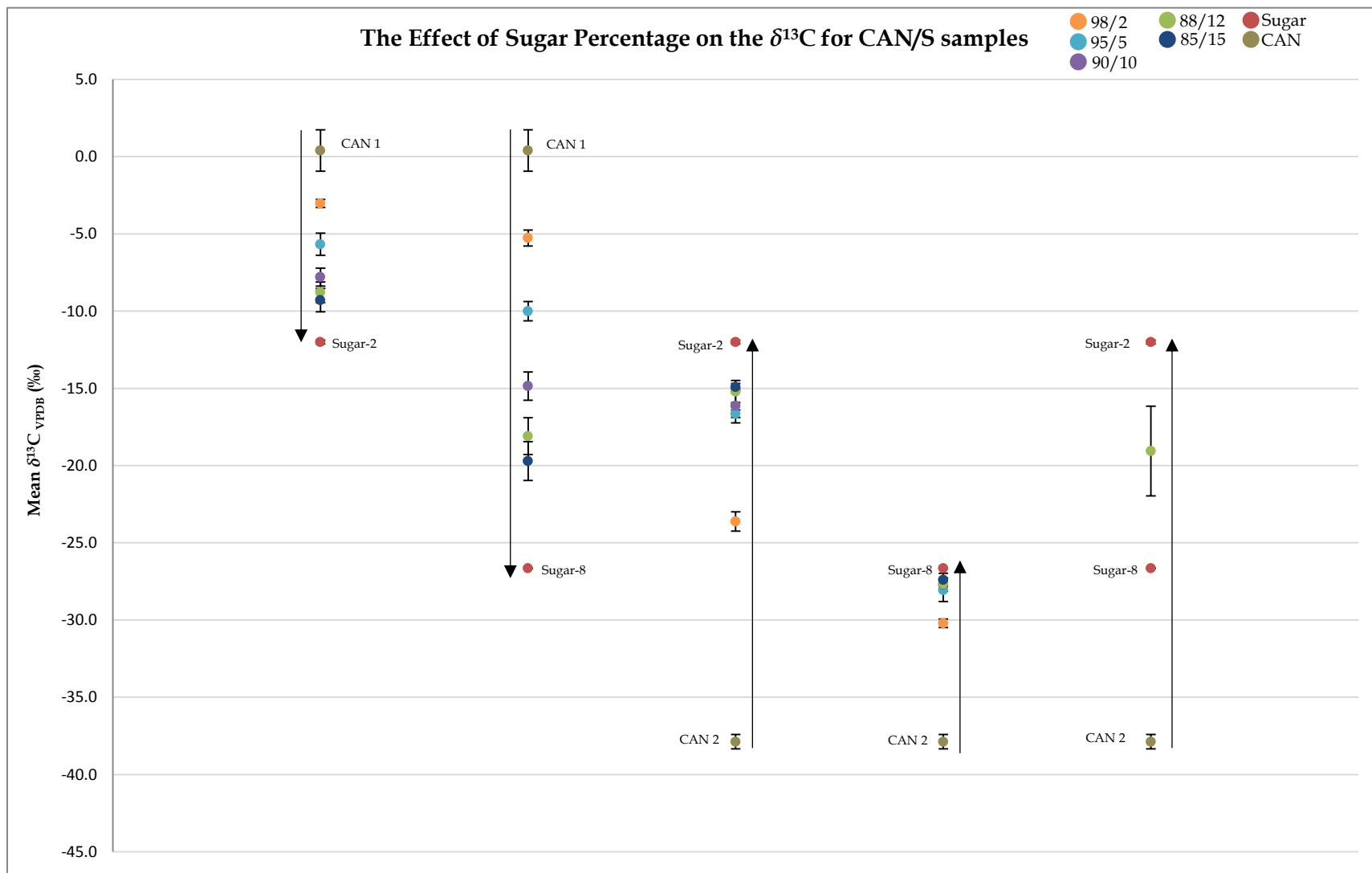
Figure 5-9: A plot of δ¹³C values for various CAN/Sugar mixtures

From this plot it can be seen that as the percentage of sugar increases, the $\delta^{13}C$ value approaches the value of the sugar used, however, the $\delta^{13}C$ value never reaches the absolute value of the sugar which is due to the presence of another source of carbon from the CAN, such as a coating.

The mixed sugar CAN/Sugar sample that contained twelve percent sugar (6% sugar 2 and 6% sugar 8) has three sources of carbon, the $\delta^{13}C$ value was determined to be -19.06 ‰ ± 2.90, which lies between the carbon isotope values for the two sugars. There is a larger amount of variability with the results for this sample mainly due to sampling issues, where a non-homogeneous mixture may result in inconsistent sampling of each sugar.

Figure 5-9 provides valuable information as it shows that altering the sugar percentage in various CAN/Sugar mixtures may effect on the overall $\delta^{13}C$ value for the sample. These results support the need for the development of methods to gain more information about the sugar used in the HME mixture, as more information may allow better use of these IRMS values for intelligence purposes (especially in samples which have overlapping $\delta^{13}C$ values).

Figures 5-10 and 5-11 are derived from experimental data and shows the change in $\delta^{13}C$ of CAN/Sugar mixtures as the percentage of sugar increases (for CAN 2 and both types of sugar). In both plots it can be seen that there is a sharp change in the $\delta^{13}C$ value up to approximately 5% sugar. From 5% and above the $\delta^{13}C$ value levels off quite evenly, with a slight kink observed between 10 and 12% sugar in Figure 5-10.

The initial large change in $\delta^{13}C$ value is mainly due to the large amount of carbon added by the addition of sugar (2% sugar adds 0.84% carbon, which is quite a large amount of carbon (when the CAN in a 98/2 mixture is contributing 1.18% carbon). This carbon percentage contribution for samples which contain CAN 2 mixed with sugar 2 or sugar 8 is summarised in Table 5-17.
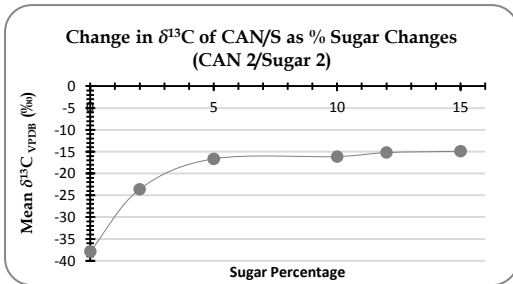
Figure 5-10: Change in $\delta^{13}C$ as % sugar changes (CAN 2/Sugar 2)
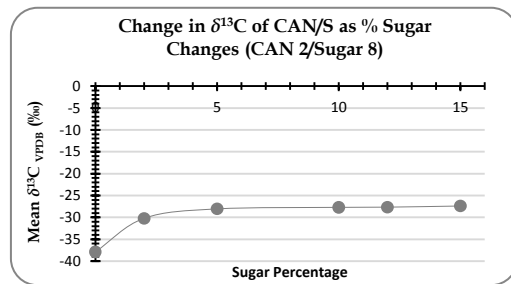
Figure 5-11: Change in $\delta^{13}C$ as % sugar changes (CAN 2/Sugar 8)

CAN 2 mixed with Sugar 2 or Sugar 8		
% Sugar	% Carbon (From Sugar)	% Carbon (From CAN)
2	0.84	1.18
5	2.11	1.14
10	4.21	1.08
12	5.05	1.06
15	6.32	1.02

Table 5-17: Carbon percentage contributions from CAN 2 and sugar in CAN/Sugar mixtures

Figures 5-12 and 5-13 are derived from experimental data and highlight the change in $\delta^{13}C$ of CAN/Sugar mixtures as the percentage of sugar increases (for CAN 1) and both types of sugar. In both plots it can be seen that there is a sharp change in the $\delta^{13}C$ value up to approximately 5% sugar. For the mixtures which contain sugar 2, from 5% to 10% it is a moderate change and above 10% the $\delta^{13}C$ value starts to level off. For the mixtures which contain sugar 8, there is still a fairly linear change in $\delta^{13}C$ value until about 12% sugar where the $\delta^{13}C$ value starts to level off.

The initial large change in $\delta^{13}C$ value is mainly due to the large amount of carbon added by the addition of sugar (2% sugar adds 0.84% carbon, which is quite a large amount of carbon (when the CAN in a 98/2 mixture is contributing 2.94% carbon). This carbon percentage contribution for samples which contain CAN 1 mixed with sugar 2 or sugar 8 is summarised in Table 5-18.
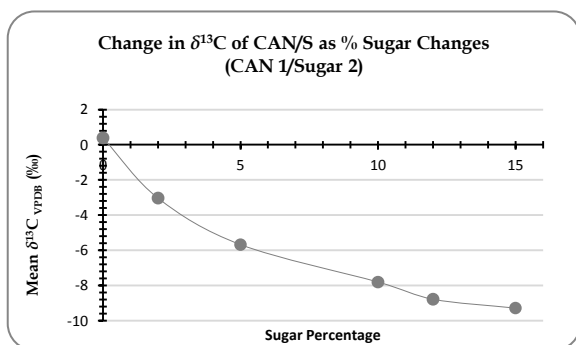
Figure 5-12: Change in $\delta^{13}C$ as % sugar changes (CAN 1/Sugar 2)
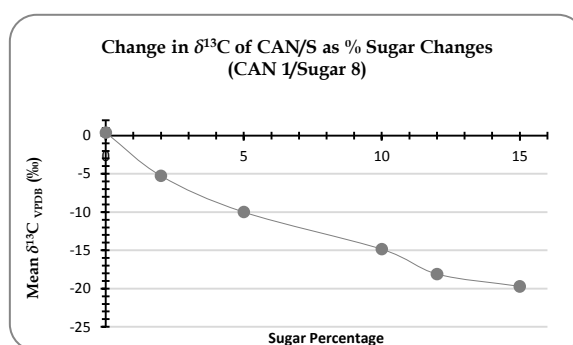
Figure 5-13: Change in $\delta^{13}C$ as % sugar changes (CAN 1/Sugar 8)

CAN 30 mixed with Sugar 2 or Sugar 8		
% Sugar	% Carbon (From Sugar)	% Carbon (From CAN)
2	0.84	2.94
5	2.11	2.85
10	4.21	2.70
12	5.05	2.64
15	6.32	2.55

Table 5-18: Carbon percentage contributions from CAN 1 and sugar in CAN/Sugar mixtures

5.12.3 Separation of Sugar from CAN/Sugar

A method was developed to separate the sugar component from the other carbon containing components (e.g. calcium carbonate) in the CAN/Sugar mixture. The aim was to separate the sugar from the bulk to enable the determination of the $\delta^{13}C$ value of the sugar used. The separation of the sugar from the bulk material allows for the determination of the metabolic pathway.

The sugar was extracted by dissolving approximately 20 mg of the CAN/Sugar sample in water (400 ml), the resulting solution was sonicated to ensure complete dissolution. Any undissolved material was calcium carbonate, which was allowed to settle at the bottom of the container. A sample was prepared by pipetting a 10 µl aliquot of the solution into a tin capsule, which was dried prior to $\delta^{13}C$ IRMS analysis. Analyses were performed in triplicate.

The results obtained from this experiment are shown in Table 5-19.

The $\delta^{13}C$ value of the sugar extracted from the CAN/Sugar mixture was indicative of the source sugar $\delta^{13}C$ value which can be utilised to determine if the sugar is of C_3 or C_4 origin. These results indicate that a simple aqueous wash of a CAN/Sugar explosive is viable for extracting sugar. A slight isotopic shift (depletion) in the recovered sugars is noted and this may be due to a slight contamination of $CaCO_3$ in the sample.

It is worth noting that the aqueous wash also extracts the AN, however as this material contains no carbon it does not appear to interfere with the analysis.

	Separated Sugar ($\delta^{13}C$ (‰))	Initial Sugar ($\delta^{13}C$ (‰))
CAN/Sugar (85:15) (CAN 2/Sugar 2)	-12.23 ± 0.07	-12.00 ± 0.12
CAN/Sugar (85:15) (CAN 2/Sugar 8)	-26.67 ± 0.09	-26.65 ± 0.03
CAN/Sugar (85:15) (CAN 1/Sugar 2)	-12.66 ± 0.30	-12.00 ± 0.12
CAN/Sugar (85:15) (CAN 1/Sugar 8)	-26.71 ± 0.01	-26.65 ± 0.03

Table 5-19: IRMS results for separated sugar samples

5.12.4 Problems with the Isotopic Analysis of Bulk Samples

IRMS has been used to demonstrate that it is possible to link identical materials based on the $\delta^{13}C$ value.

However, analyses should be performed prior (and typically are) to IRMS analysis to ensure that the samples are in fact compositionally identical, as there is the potential to identify a link based on just the $\delta^{13}C$ value, when in fact the samples are not the same.

To demonstrate this, IRMS bulk analysis was conducted on two materials that were compositionally different, but were prepared in an AN:sugar ratio that produced an identical $\delta^{13}C_{Bulk}$ value. The samples prepared are shown in Table 5-20.

Mixture	Ratio	$\delta^{13}C_{Bulk}$
CAN 1 / Sugar 8	90:10	-14.86 ‰ ± 0.92
CAN 2 / Sugar 2	85:15	-14.92 ‰ ± 0.23

Table 5-20: Prepared CAN/Sugar mixtures with identical $\delta^{13}C_{Bulk}$ values.

Despite the $\delta^{13}C_{Bulk}$ values for these samples are identical, no link should be assigned as the materials used are different.

What this example demonstrates is that it is not simply a case of looking for similar isotopic values when determining whether two samples are linked, and highlights the need to further analyse the sample to gain more information on the individual components.

In this case, further analysis of the samples by HPLC-RI determined the sugar type and the percentage of sugar present, this is shown in Figure 5-14.
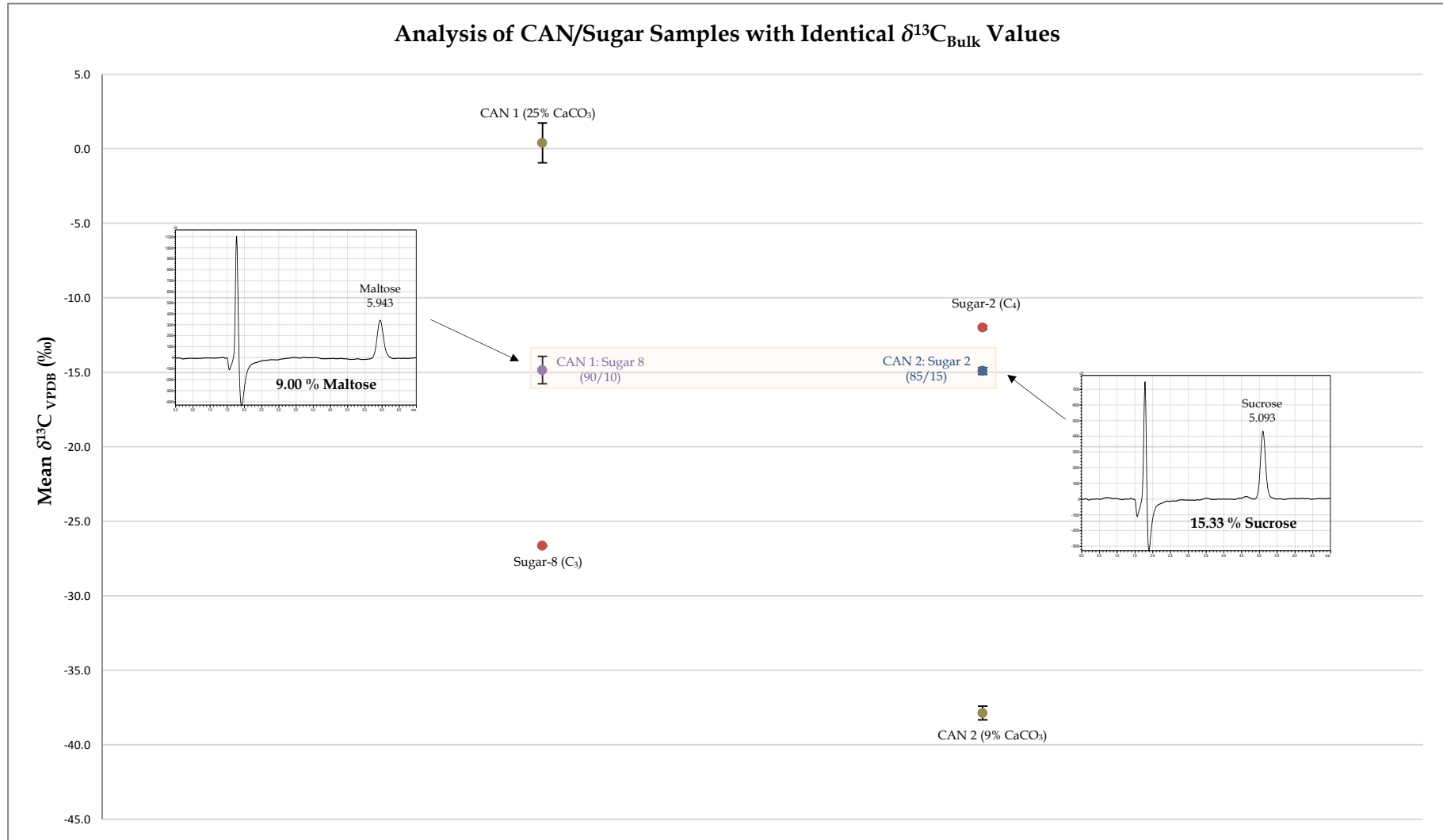
Figure 5-14: Differentiation of two different CAN/Sugar mixtures that have identical $\delta^{13}C_{Bulk}$ values, inset are HPLC chromatograms identifying the sugar type and ratio

5.12.5 Inductivity Couples Plasma Mass Spectrometry

ICP-MS analysis was not undertaken on any sugar or CAN/Sugar samples for two main reasons:

1) There is a low percentage of sugar in any HME sample (maximum 15%). This is equivalent to 7.5 mg out of 50 mg which is normally needed for the current routine ICP-MS analysis of HME samples.
2) Concentrations of elements in sugar samples have been previously determined [123]. In this report, the researchers identified that sugar has a relatively low concentration of detectable trace elements (in the low mg/kg to ng/kg range). When this is compared to the levels seen in a typical HME sample, the contribution of the trace elements due to the sugar are likely not to make a noticeable difference in overall elemental profile.

Therefore the ICP/MS characterisation of sugars are not likely to provide any useful sourcing or batch matching information that can be used for chemical intelligence.

5.12.6 High Performance Liquid Chromatography

HPLC was identified as a technique, which may be able to provide a significant amount of information about the sugars used in HME samples such as the identity of the sugar (i.e. sucrose or fructose) and the percentage of sugar present in an unknown sample.

The 15 sugar samples listed in Table 5-5 were analysed by HPLC-RI to determine their respective retention times, which is shown in Table 5-21.

Most of the sugar tested contained a single sugar type, however in Sugar 14 (palm sugar) three different sugars were identified, namely sucrose, fructose and glucose. The chromatogram for Sugar 14 is shown in Figure 5-15.

Sample (Code)	Retention Time (min)	Sugar Type
Sugar 1	5.102	Sucrose and Stevia
Sugar 2	5.103	Sucrose
Sugar 3	5.892	Lactose
Sugar 4	3.286	Fructose
Sugar 5	3.903	Dextrose
Sugar 6	5.101	Sucrose
Sugar 7	3.284	Fructose
Sugar 8	5.982	Maltose
Sugar 9	3.905	Glucose
Sugar 10	5.103	Sucrose
Sugar 11	5.102	Sucrose
Sugar 12	5.101	Vanilla Flavour Sugar (Sucrose)
Sugar 13	2.755	Erythritol and Stevia
Sugar 14	3.288	Palm Sugar (contained Fructose, Glucose and Sucrose)
	3.900	
	5.103	
Sugar 15	5.102	Raw Sugar (Sucrose)

Table 5-21: Summary of the retention times for the sugars of interest
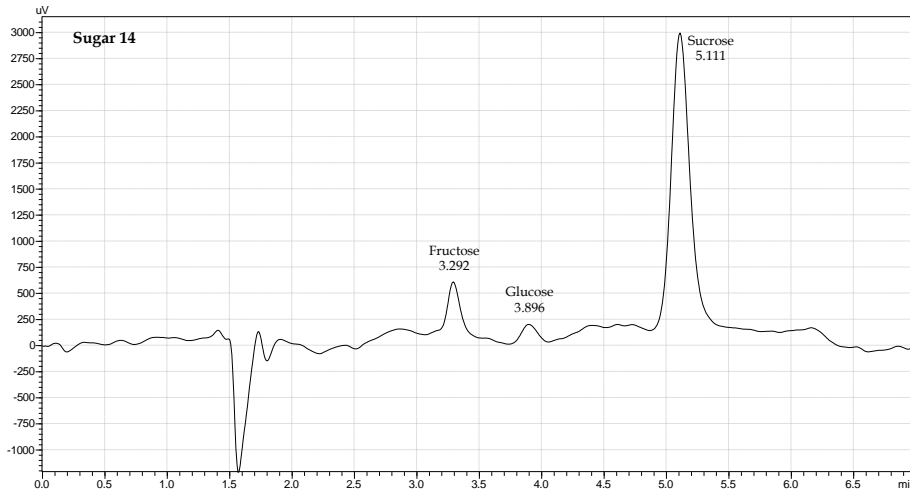
Figure 5-15: HPLC chromatogram of sugar-14 (palm sugar) showing the three sugars present

A mixture of six sugars (erythritol, fructose, glucose, sucrose, maltose and lactose) was also analysed to determine the retention time of each sugar, and identify any possible problems due to co-elution of two or more sugars, i.e. sugars with the same retention times. This proved to be the case with maltose and lactose both being eluted with the same retention time. Figure 5-16 shows the chromatogram obtained for the six-sugar mixture.
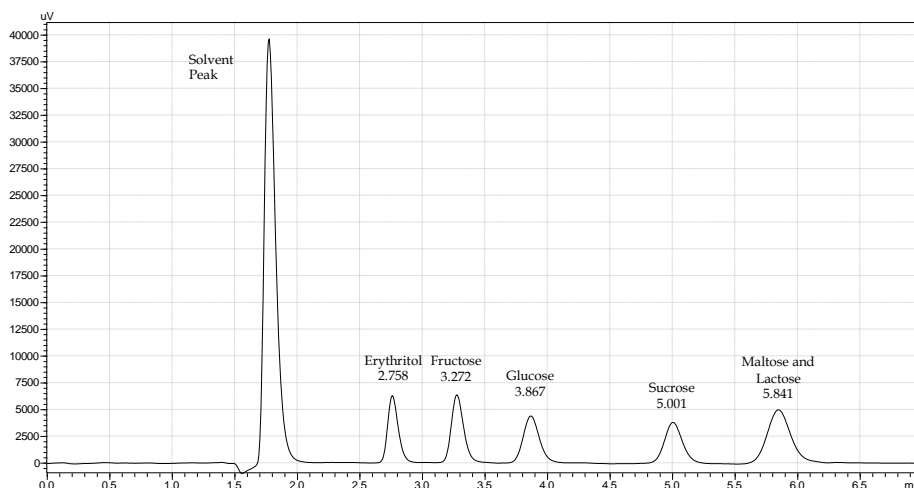
Figure 5-16: HPLC-RI chromatogram of the analysis of the six-sugar mix

Having the ability to identify sugars is of great advantage but being able to also determine the percentage of sugar in a HME sample offers another level of information to potentially link samples to each other. The 21 explosive mixtures which were analysed by IRMS (Table 5-6 to Table 5-10) were also analysed by HPLC-RI to determine the type of sugar used in each preparation and the percentage of sugar used. Each sample was analysed in triplicate and percentages were calculated using sucrose and maltose calibrations. Tables 5-22 to 5-25 detail the type of sugar identified and percentage of sugar for each of the CAN/Sugar mixtures. It should be noted that the presence of AN did not interfere with the chromatographic separation of sugars via HPLC-RI as highlighted in Figure 5-17.

Sample	Identified Sugar	% of Sugar	Std Deviation (%)
CAN/Sugar (98:2) (CAN 2/ Sugar 2)	Sucrose	2.05	0.04
CAN/Sugar (95:5) (CAN 2/ Sugar 2)	Sucrose	6.38	0.92
CAN/Sugar (90:10) (CAN 2/ Sugar 2)	Sucrose	9.22	0.75
CAN/Sugar (88:12) (CAN 2/ Sugar 2)	Sucrose	11.46	1.22
CAN/Sugar (85:15) (CAN 2/ Sugar 2)	Sucrose	15.33	0.28

Table 5-22: CAN/Sugar mixtures made with CAN 2 and sugar 2 (sucrose)

Sample	Identified Sugar	% of Sugar	Std Deviation (%)
CAN/Sugar (98:2) (CAN 2/ Sugar 8)	Maltose	2.16	0.44
CAN/Sugar (95:5) (CAN 2/ Sugar 8)	Maltose	4.17	0.51
CAN/Sugar (90:10) (CAN 2/ Sugar 8)	Maltose	7.59	0.05
CAN/Sugar (88:12) (CAN 2/ Sugar 8)	Maltose	10.17	1.36
CAN/Sugar (85:15) (CAN 2/ Sugar 8)	Maltose	11.46	1.22

Table 5-23: CAN/Sugar mixtures made with CAN 2 and sugar 8 (maltose)

173

Sample	Identified Sugar	% of Sugar	Std Deviation (%)
CAN/Sugar (98:2) (CAN 1/ Sugar 2)	Sucrose	1.96	0.10
CAN/Sugar (95:5) (CAN 1/ Sugar 2)	Sucrose	4.87	0.62
CAN/Sugar (90:10) (CAN 1/ Sugar 2)	Sucrose	11.06	1.01
CAN/Sugar (88:12) (CAN 1/ Sugar 2)	Sucrose	12.05	1.33
CAN/Sugar (85:15) (CAN 1/ Sugar 2)	Sucrose	14.97	1.20

Table 5-24: CAN/Sugar mixtures made with CAN 1 and sugar 2 (sucrose)

Sample	Identified Sugar	% of Sugar	Std Deviation (%)
CAN/Sugar (98:2) (CAN 1/ Sugar 8)	Maltose	2.39	0.54
CAN/Sugar (95:5) (CAN 1/ Sugar 8)	Maltose	4.37	0.58
CAN/Sugar (90:10) (CAN 1/ Sugar 8)	Maltose	9.00	0.55
CAN/Sugar (88:12) (CAN 1/ Sugar 8)	Maltose	10.49	0.52
CAN/Sugar (85:15) (CAN 1/ Sugar 8)	Maltose	13.53	2.45

Table 5-25: CAN/Sugar mixtures made with CAN 1 and sugar 8 (maltose)

Overall the results obtained from the HPLC analyses show that the types of sugar present (by comparison against a reference standard) and its percentage of the bulk (by integrating the area under the peaks) was correctly identified in all of the samples tested. The results obtained were all within experimental error of the technique, thus HPLC appears to be a valid technique for the identification of sugar-based fuels present in HMEs.

In order to demonstrate the utility of this technique a CAN/Sugar mixture was prepared that contained two different sugars (6% sugar 2 and 6% sugar 8). The HPLC chromatogram obtained when this sample was analysed is shown in Figure 5-17.
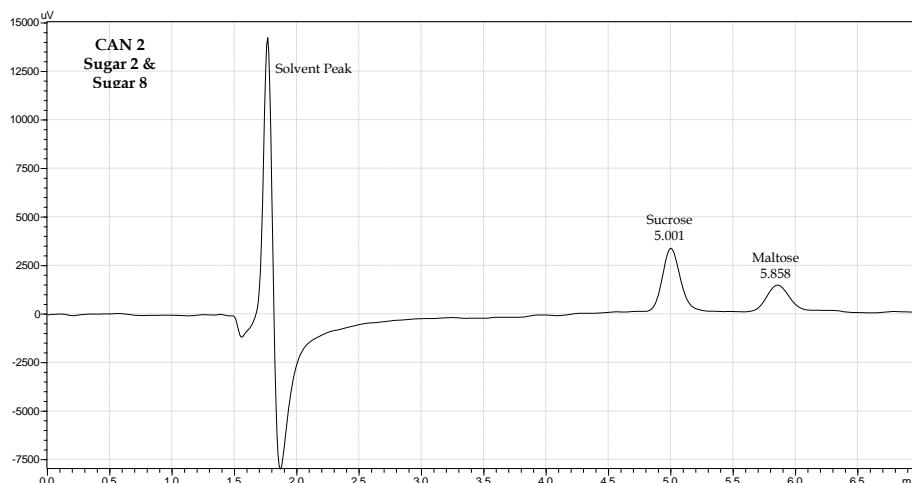
Figure 5-17: HPLC trace of CAN/Sugar sample containing a sugar mix (sucrose and maltose)

HPLC was able to correctly identified both of the sugars used in the preparation of this material. The peak areas were then integrated to determine the area under the peaks, integration showed that the sugars were present in an approximately 1:1 ratio. Comparison against the calibration curves for each sugar indicated the percentage to be 6.39 and 5.76% for sucrose and maltose respectively, as shown in Table 5-26.

174

Sample	Identified Sugar	Percentage of Sugar (%)	Std Deviation (%)
CAN 2, Sugar 2 and Sugar 8	Sucrose	6.39	2.03
	Maltose	5.76	0.81
		12.15	**1.79**

Table 5-26: Analysis of CAN/Sugar sample containing a sugar mix (sucrose and maltose)

NOTE: A possible source of error with this technique that may be introduced is sampling errors due to a lack of homogeneity within a sample. This effect may be minimised by performing the analysis in triplicate, or ensuring that sufficient sample is adequately mixed prior to analysis.

5.13   Conclusion

The results described in this Chapter indicate that the analysis of sugar present as the fuel in explosive mixtures by advanced chemical analytical techniques may provide some intelligence value.

IRMS was used to analyse a series of cane and beet derived sugars to determine their $\delta^{13}C$ values, for Beet sugars the $\delta^{13}C_{Bulk}$ value was between -23 and -27‰, while for Cane sugars the value was between -9 and -13‰. These differences are due to the metabolic pathways used in the synthesis of sugar, i.e. C_3 vs. C_4, respectively.

The separation of the water soluble component from an aqueous wash of a CAN/Sugar explosive mixture enabled the $\delta^{13}C$ value for the sugar to be determined. It is worth noting that although this aqueous wash contains dissolved AN, the AN does not appear to effect the $\delta^{13}C$ result obtained. The ease at which sugar can be extracted from CAN/Sugar explosive mixtures enables the $\delta^{13}C$ value of the sugar to be determined, which can be used to distinguish between explosives, allowing for the batch-matching of materials. The $\delta^{13}C$ value for the sugar can also be used to determine metabolic origin.

For CAN/Sugar samples that contain >10% sugar, the $\delta^{13}C_{Bulk}$ value is reflective of the sugar used, as pure CAN contains very little carbon (only present as calcium carbonate). A potential problem of different samples that have the same $\delta^{13}C_{Bulk}$ value was identified, this was easily solved by the use of other analytical techniques to determine the identity of the components present, to ensure that the samples are indeed similar.

A HPLC method was developed demonstrating that it is possible to separate and identify the type of sugar present. The percentage of sugar in a CAN/Sugar mixture was able to be determined by integrating the peak area and comparing against a calibration curve produced from stock solutions.

The techniques described in this Chapter therefore have the potential to batch match samples based on the analysis of the components present. Where source materials are identified it may be possible to determine the origins or point of manufacture. Such information is of increasing interest for Defence and National Security organisations, as it has the potential to provide actionable intelligence.

Intentionally Blank

6. Analysis of Plastic Particulates Recovered from HME Samples

In recent times, the exploitation of HME has focused on the provision of chemical intelligence to the wider intelligence community, as the analyses performed may provide information on where explosive precursors are sourced, where explosives are manufactured and how widespread materiel is distributed by insurgent networks.

Typically, it is not possible to link directly an event to another, or an event to a source based on a single analysis of recovered evidence. Forensic investigations usually employ multiple analysis techniques over several sub-components in order to fully characterise the material. Analysis of multiple sub-components improves the confidence levels when determining whether similar samples are linked.

Evidence that belongs to a small, distinct group based on shared characteristics is described as class evidence. Class evidence does not necessarily point to the exact individual or object, it can be used to narrow the search and indicate similarities. If several types of class evidence are combined then the size of that group is narrowed to the point where only a few alternatives persist [277].

Most of the explosive samples recovered in recent conflict zones are multi-component materials, comprising an oxidiser/fuel blend, e.g. AN/Al and AN/S. These explosives are described as HME, which may have a number of potentially unique or distinguishing features. Differences arise due to the nature of the materials used, introduction of impurities, variations in precursor source and the methods used during manufacture.

In order to fully identify the composition of an explosive it may be necessary to separate the various components. The ability to analyse each component has a number of useful implications, e.g. consider two different explosive mixtures, AN/Al and AN/S. Separation and analysis of the AN component may indicate that the same AN was used in two seemingly different explosives. This information could be used to identify the AN source, a possible AN distribution network, or indicate the supply shortages of aluminium e.g. why would bomb makers change to sugar as a fuel, or it may reveal the relative skill level of the bomb maker.

6.1 Analysis Types

Visual, physical and chemical analysis of an evidentiary sample is often used to reveal similarities and differences between samples. One of the goals of any exploitation activity is to link a sample from an event, to other samples or source. The presence of unique sub-components, especially if foreign to the source materials, may be a vital in order to establish links.

6.1.1.1 Visual Analysis
Visual inspections can be done with the naked eye, or enhanced through the use of advanced optical microscopes. Visual techniques enable the identification of colour, the presence of foreign materials or any other material that may have been added during the manufacturing process.

Optical microscopy allows the analyst to observe, in detail, the physical composition of the sample and allows for the measurement of the size and shape of the various components. Microscope imaging may be used to identify multi-component mixtures and determine their approximate ratios. The physical form of the components also provides insight into how the sample was prepared, i.e. level of mixing and processes used.

Scanning electron microscopy coupled with energy dispersive X-ray (SEM/EDX) is an advanced technique that can form images based on the analysis of secondary electrons. The elemental composition of each component can be determined by analysing the back scattered X-rays produced, which are characteristic of the elements present.

6.1.1.2 Physical Analysis
Physical analysis is any technique that can give information based on the measurement of some physical property of the evidence, e.g. size, shape and colour.

6.1.1.3 Chemical Analysis
Chemical analytical techniques fall into two main categories, bulk and trace analysis.

- Bulk analysis informs the analyst what the major component is, this information can then be used to determine the identity, inform safe handling measures and the approximate composition ratio if multiple components are present.
- Trace analysis techniques can also be used to determine the major component, but also inform 'what else is there'. At the trace level, contaminants are often present - these come from the starting material, the manufacturing process and/or methods used during refinement/purification process. Analysis of trace materials may therefore enable the gathering of intelligence by comparing the levels of trace materials within samples, thus enabling source and batch matching of like materials.

6.2 Analysis of Authentic Samples

With the use of advanced analytical techniques, such as IRMS and ICP-MS, it becomes possible to examine an explosive sample at the isotopic and elemental level, meaning that it is now possible to determine differences between the same explosive type, i.e. between two AN samples. The information obtained by these techniques is valuable as it can be used to identify batch-matched materials, or link an explosive back to where component were sourced.

Analyses typically performed on explosive material include the identification of the oxidiser, e.g. AN or potassium chlorate (PC); identification of the fuel, e.g. aluminium, sugar or diesel; analysis of miscellaneous objects present, e.g. glitter; or any foreign matter introduced during processing, transport or emplacing the explosive, e.g. fibres, grains and dirt. The results obtained from the chemical analyses are then combined with operational data, such as location, the device it was employed in and the various bomb maker tactics, techniques and procedures (TTP) used to inform the current and evolving threat.

The aluminium found in explosive compositions comes from a number of sources, such as: finely shredding aluminium foil, spraying metallic paint on a surface then scraping off the metallic residue, or more commonly, using paint grade aluminium flake that is used in the

vehicle paint industry. Each source of aluminium will have characteristics that can be used to determine aluminium origin. The shape and size of the aluminium particles is perhaps the easiest to identify, as shown in the examples in Figure 6-1.

Aluminium is an ideal fuel for bomb makers, as it is relatively cheap, distributed widely, and comes in a form (i.e. small particle size) that enables intimate mixing with an oxidiser to produce an effective explosive.

The aluminium flake that is used in vehicle paint often contains a number of additives that produce a visual effect, the metallic lustre or shimmer seen in modern cars can produced by the inclusion of glitter particles in the paint medium, and as such they can be found in homemade explosive formulations.

| Shredded foil | Sprayed paint scraping | Glitter |
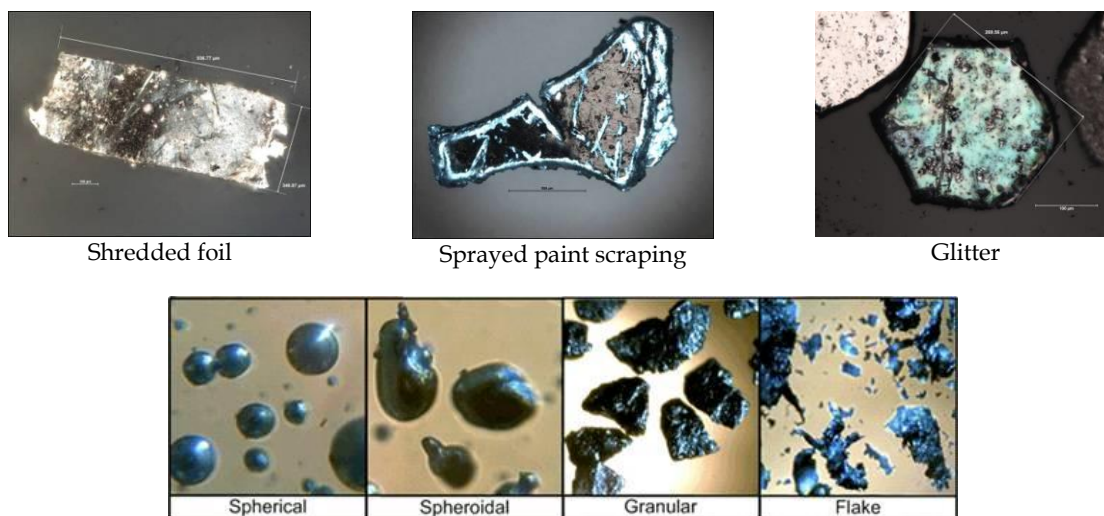
Figure 6-1: Aluminium varieties used in explosive formulations

A microscope image of glitter present in paint grade aluminium, extracted from a real AN/Al HME sample, is shown in Figure 6-2A. The glitter in the sample was generally hexagonal in shape, but has a number of distinguishing features and imperfections [278-280]. The diagram shown in Figure 6-2B shows a cross section of a glitter particle, where an aluminium layer (grey) is applied to a plastic backing, typically polyethylene terephthalate (PET) represented by the blue layer.

A (Width ≈ 26.29 μm)   B
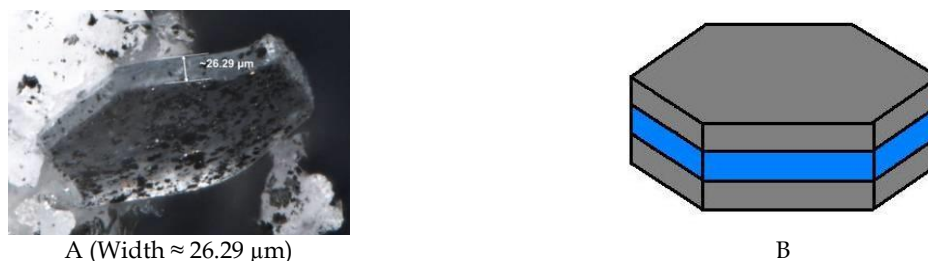
Figure 6-2: Glitter recovered from a real HME sample. (A) Microscope image (B) Schematic representation showing the various layers

Several different types of glitter particle have been recovered from real HME samples, therefore it may be possible to identify bomb maker groups and their explosive distribution networks based on the type of glitter particles present in recovered samples, i.e. samples that

have glitter of the same physical and chemical characteristics may have been produced by the same person, using the same source of materials.

6.3 Glitter

6.3.1   Glitter Production

Glitter is an entirely man-made product that is likely to have a number of unique and distinguishing features due to the different materials and manufacturing processes used. These variations may allow for the differentiation of glitter particles, there have been a number of legal cases where convictions have been recorded due to the analysis of evidential glitter samples [281, 282].

Glitter can be produced a number of ways. The most widespread and simplest method is by feeding a roll of metallised plastic sheet through a set of cutting blades, consisting of a rotary cutting blade and a stationary bed knife (Figure 6-3A). A roll of metallised foil is fed into the blades where it is cut to produced glitter (Figure 6-3B). The size and shape of the glitter particles is dependent on the grooves machined on the bed knife and the rotating cutting blade. Glitter is mainly produced in the USA, Germany, India, Pakistan, Korea and Taiwan [281].

A   **B**

Figure 6-3: Glitter manufacturing process. A) Close-up of the rotary blade and a stationary bed knife. B) Metallised plastic film being fed into the cutting blade

6.3.2   Characterisation of Glitter

The blade setup and maintenance of these cutting machines has a dramatic impact on the quality of the glitter produced. Worn cutting teeth or misalignment of the blades are likely to produce imperfections in the final glitter product, which will be consistently repeated during the entire cutting process, producing a batch of characteristically similar glitter particles.

Common imperfections seen in glitter include surface marks, irregular shape, cuts and tears. These slight imperfections can be used to differentiate one type of glitter from another. Imperfections are produced if the machine is incorrectly configured, the cutting teeth on the blades are not fully formed or have dulled from overuse and need re-machining, or if the stationary bed knife is set below the plane of the rotary knife.

An extreme example of the material produced from an incorrectly configured machine is "Glitter grass" (Figure 6-4A) which gives long needle-like strands of the metallised plastic film. Despite glitter grass being generally seen as a waste product, numerous companies sell multiple tons of this material online for use in the arts and craft industry [283]. It is worth noting that material in this form is not likely to produce a viable explosive. Similarly, dull and poorly aligned blades may result in glitter particles that have tears, is poorly cut, remain joined or are unsymmetrical in shape (Figure 6-4B).

A

B

Figure 6-4: Glitter imperfections. A) Formation of "glitter grass". B) Tears, poor cuts and unsymmetrical glitter

A shortlist of possible identifying features that may be present on glitter particles include [282]:

Shape: The physical shape of the glitter.
Size: The physical size of the glitter and its uniformity.
Thickness: The thickness of the plastic layer and metallic coating (cross-section).
Morphology: Although glitter products have no distinctive surface appearance and appear the same on both sides, some have an added pigment on one side that is distinctive in both colour and morphology.
Number of layers: Individual glitter particles may be cross sectioned and separate layers counted and thickness measured.
Chemistry of each layer: Chemical composition of each layer may be determined.
Colour: Different colours or effects (fluorescence, holographic, pearlescent)
Suspension medium: Identification of liquids (such as solvents, oils and glues) that are used to suspend the glitter particles, often seen for glitter used in cosmetic products; arts and crafts; and paints.

6.4 Materials and Methods

6.4.1 Samples

A table summarising the samples analysed in this Chapter are shown in Table 6-1.

PET plastic samples were obtained by cutting a small section from two commercial drink containers, namely a Coca Cola® bottle (PET-1) and a Lipton ice tea® bottle (PET-2).

Five commercial glitter samples (Samples G1-G5) were obtained from an Australian based arts and craft supplier, Spotlight. These glitter samples were all different with variations in

181

colour, shape and size. The glitter samples purchased were produced by different manufacturers; this was done to ensure variation between the samples.

Glitter was also obtained by extraction from four HME samples of AN/Al which were provided by DSTO. The bulk explosive composition of these samples had previously been analysed and the results obtained indicated that they may be linked [278]. Analysis of the glitter in these samples may increase the confidence in the previously determined link.

Sample Type	Physical Description	Source	Code
Plastic bottle	Clear plastic	Coke Cola®	PET-1
Plastic bottle	Clear plastic	Lipton Ice Tea®	PET-2
Glitter	Green squares	Spotlight	G-1
Glitter	Red hexagons	Spotlight	G-2
Glitter	Blue hexagons	Spotlight	G-3
Glitter	Red hexagons	Spotlight	G-4
Glitter	Silver hexagons	Spotlight	G-5
Glitter	Silver hexagons	real AN/Al HME	16-23
Glitter	Silver hexagons	real AN/Al HME	16-25
Glitter	Silver hexagons	real AN/Al HME	16-27
Glitter	Silver hexagons	real AN/Al HME	16-28

Table 6-1: Summary of subcomponent samples analysed

6.4.2   Instrumentation, Techniques and Sample Preparation

6.4.2.1 Visual Microscopy

The microscope used for the imaging of the glitter particles was a Nikon AZ100M. Software used for image capture, manipulation and measurement was 'NIS-Elements' [284]. "The AZ100M offers the combined advantages of a stereoscopic microscope with a wide field of view and long working distance, and a compound microscope boasting high-resolution images. The AZ100M also allows secure and efficient image acquisition in conjunction with a PC and a digital camera. This system supports a broad range of applications including developmental biology and the study of biological structures" [285].

Each glitter sample was placed on a glass microscope slide and imaged under the microscope. The glitter sample was positioned at the centre of the field of view, the magnification and focus was adjusted till a suitable image was obtained. A completely in focus image was captured with a technique called 'composite sectioning'. In this technique several images are taken at different 'Z-levels', these images are then merged to produce a single all in-focus image, or 'Z-series' by the software. The size of each glitter particle was determined using the calibrated ruler tool.

6.4.2.2 Scanning Electron Microscopy/Energy Dispersion X-ray

In SEM/EDX, an energetic, finely focused electron beam is scanned over the surface of a sample, this electron beam interacts with the sample causing the ejection of an inner shell electron, higher energy electrons relax to the inner shell, causing the emission of an X-ray. The X-rays produced have an energy that is characteristic of the elements present; analysis of these X-rays therefore allows for the composition of the sample to be determined.

When the electron beam interacts with the sample, the electrons may undergo two different types of collision:

1) Elastic collisions – in which the energy of the incident electrons is unchanged, and
2) Inelastic collisions – incident electrons lose energy due to collisions.

Elastic collisions give rise to a back scattered electron (BSE) imaging which can be used to determine the effective atomic number of the elements present on the surface of the sample.

Inelastic collisions produce a secondary electron (SE) imaging which displays surface detail and particle morphology in great detail.

The main advantage of the SEM/EDX technique is that detailed spatial and compositional analysis can be acquired at any point on the sample, microscopic features can be investigated and high-resolution images are obtained.

SEM/EDX was performed on a CamScan MX2500 SEM fitted with an energy dispersive x-ray microanalyser (Flinders University). Analyses were performed using a primary electron beam of 20 keV, utilising various spot sizes and magnifications depending on the size of the glitter particle. The output from the EDX was analysed by the Maxim 4 software. Images and spectra were obtained for each sample.

Analyses were performed by mounting several glitter particles on to a SEM stub. The glitter was then coated in carbon using a high vacuum evaporator (HITACHI HUS-5GB) to ensure an electrically conductive surface.

6.4.2.3 Infrared

IR spectroscopy is a technique based on the absorption of light by a molecule at specific frequencies that are characteristic of the function groups and bonds present. The energies are dependent on the mass of the atoms, vibrational coupling and the potential energy surface of the molecule. Many IR spectral libraries exist that automate the identification of pure materials, though identification is difficult for non-pure materials and mixtures. The analysis of glitter particles by IR has been reported previously [286, 287].

Spectra were obtained on a Perkin Elmer Spectrum 400 Fourier Transform-Infrared (FT-IR)/ Fourier Transform-Near Infrared (FT-NIR) spectrometer with a universal attenuated total reflectance (ATR) sampling accessory. This instrument utilised Perkin Elmer Spectrum software version 6.3.4. An IR spectrum was recorded and compared against reference spectra utilising the Hummel polymer sample library [288].

6.4.2.4 Pyrolysis Gas Chromatography/Mass Spectrometry

Pyrolysis gas chromatography/mass spectroscopy (py-GC/MS) is a technique where a sample is heated to decomposition (~600-650 °C), causing cleavage at the weakest point in the molecule. This generates smaller more volatile fragments that can be separated and characterised by traditional GC/MS. This technique is best suited for the identification of polymeric materials which generally have high molecular weights, e.g. plastics. The decomposition of plastics by py-GC/MS allows for the characterisation of the individual monomeric units.

A Fischer GSG Curie Point Pyrolyser 1040PSC with a Perkin Elmer Clarus500 gas chromatograph and Perkin Elmer quadrupole mass spectrometer (Forensic Science, South Australia) was used.

The plastic samples, PET-1 and PET-2, were placed on a ferromagnetic pyrolysis wire (GSG Analytical) and crimped, while glitter samples needed to be suspended in ethanol before being deposited on the ferromagnetic pyrolysis wire (GSG Analytical). The ethanol was then air dried before the wire was crimped and the analysis performed.

6.4.2.5 IRMS
IRMS is a specialised mass spectrometer that measures the variations in the natural isotopic abundance of light and heavy elements, e.g. ^{12}C vs. ^{13}C. IRMS instruments differ from conventional mass spectrometers, as they do not scan a mass range for characteristic fragment ions (in order to provide structural information), instead each isotope is separated out and their ratios compared. The advantage of this technique is that it is possible to identify samples based on their isotopic ratio. This technique can be used to determine whether samples originate from the same batch or source, as these materials share similar isotopic ratios [289, 290].

IRMS data were obtained on an IsoPrime (GV Instruments) stable isotope ratio mass spectrometer with a EuroEA3000 Series (EuroVector) elemental analyser (EA) operated by Waters MassLynx mass spectrometry software.

Continuous flow IRMS was used to determine the carbon ratios of the plastic and glitter samples. As IRMS is a relative technique, comparisons are usually made against Vienna Pee Dee Belemnite (VPDB). This was achieved with a calibrated laboratory sample of sucrose (99.9% EuroVector, product code. E11017) which equated to $\delta^{13}C_{VPDB}$ = -11 ‰.

Analyses were performed by weighing 100 µg of the sample in a tin capsule (5 x 9 mm, EuroVector). The tin capsules are then placed in an auto-sampler and analysed, each sample is analysed in triplicate.

Caveat – Due to the nature of the samples analysed and limitations with the analytical instrumentation used, the isotopic data presented in this research is fit for the purpose of a comparative exercise (proof of concept) but should not be compared to data from other laboratories. All of the δ values displayed within this research have an associated error range (error bars) of ± 1 standard deviation.

6.4.2.6 ICP-MS
ICP-MS is a powerful technique that enables the simultaneous analysis of multiple elements in a sample at the ultra-trace level, i.e. parts per trillion (ppt).

Analyses were performed on an Agilent 7500 Series ICP-MS instrument (Flinders Analytical). Between 50 µg and 1.5 mg of plastic/glitter was weighed out into a 15 mL polypropylene digestion vial. Samples were digested by adding 100 µL of water followed by 300 µL of nitric acid, the samples were than heated for three hours at 60°C, then shaken for 24 hours.

The digested samples were then diluted with water to a volume of 15 mL, samples were then further diluted before analysis by ICP-MS to limit possible matrix interferences.

6.5 Results and Discussion

6.5.1   Glitter Analysis

6.5.1.1 Visual Microscopy

Visual microscopy was undertaken on all of the glitter samples. The images obtained for the glitter obtained from Spotlight (G-1 to G-5) and glitter extracted from the real HME sample provided by DSTO (16-23 to 16-28) is shown in Figure 6-5 and Figure 6-6, respectively. Measurement of the dimensions of each glitter sample is shown in Table 6-2.

The Spotlight glitter samples were larger in size and the plastic appeared to be more flexible than the genuine glitter samples, this may be due to the intended purpose of the glitter, namely for arts and crafts as opposed to 'sparkle' effect in vehicular paint. The Spotlight glitter also appeared to be more regular in size and shape (dimension and cleanness of cut), with the exception of glitter sample, G-5, which was quite irregular.

Microscope images for the four glitter samples extracted from real HME samples were all visually similar, silver in colour and hexagonal in shape. On average, the dimensions were ~270 μm at the short axis and ~320 μm at the long axis. It was noteworthy that a high percentage of the glitter in each sample was badly cut, malformed or had some imperfection this is probably due to poor maintenance of the manufacturing equipment. The metal foil coating on the glitter particle was also easy to remove from the plastic backing by the use of a solvent or by the application of slight mechanical force. The underlying plastic was colourless, transparent but relatively firm when compared to the Spotlight glitter samples.

Analysis of the glitter samples by microscopy allows size and shape comparisons to be made. The results obtained from the real HME glitter samples show that their size was consistent over the four samples analysed.

Sample	Shape	Size (length, mm)	Size (width, mm)
G-1	Square/Rectangle	0.63 ± 0.05	0.59 ± 0.05
G-2	Hexagonal	0.95 ± 0.05	0.80 ± 0.05
G-3	Hexagonal	0.95 ± 0.05	0.75 ± 0.05
G-4	Hexagonal	0.50 ± 0.05	0.42 ± 0.05
G-5	Crude Hexagonal	0.50 ± 0.05	0.42 ± 0.05
16-23	Hexagonal	0.32 ± 0.05	0.27 ± 0.05
16-25	Hexagonal	0.32 ± 0.05	0.27 ± 0.05
16-27	Hexagonal	0.32 ± 0.05	0.27 ± 0.05
16-28	Hexagonal	0.32 ± 0.05	0.27 ± 0.05

Table 6-2: Summary of glitter samples

G-1

G-2

G-3

G-5
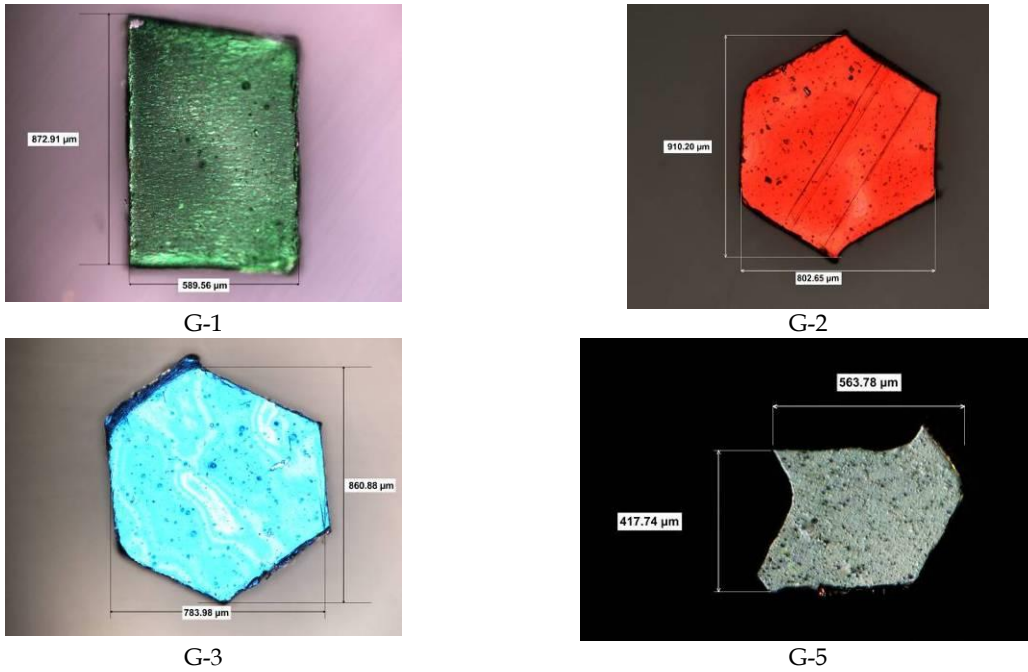
Figure 6-5: Microscope images of glitter samples G-1, G-2, G-3 and G-5

16-23

16-25

16-27

16-28
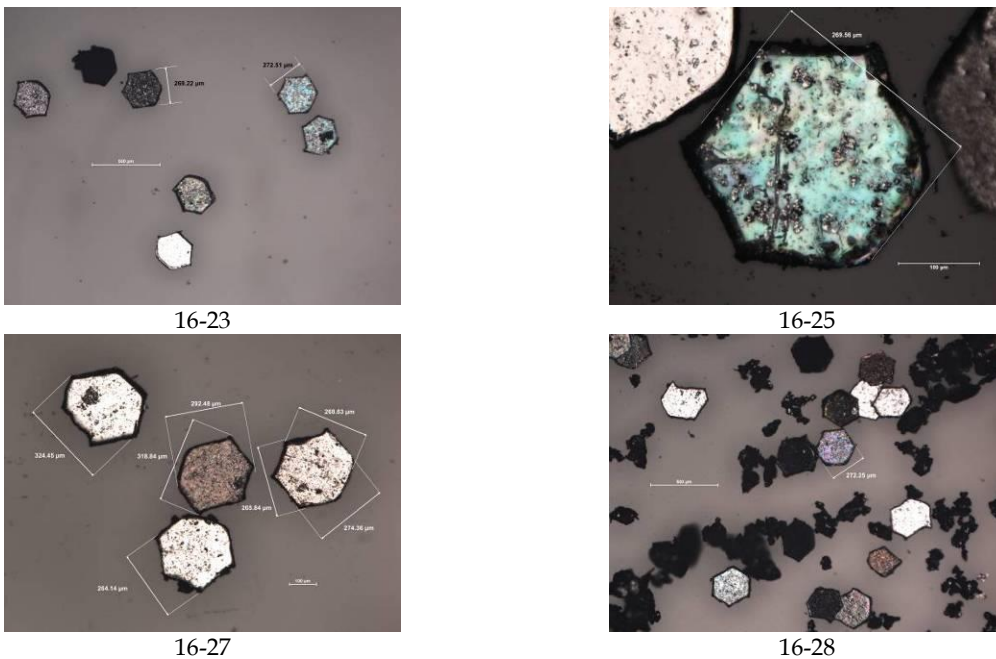
Figure 6-6: Glitter samples extracted from the real HME AN/Al explosive samples

6.5.1.2 Scanning Electron Microscopy/Energy Dispersion X-ray

Each glitter sample was mounted on a SEM stub and carbon coated to prevent charge build-up. An overview image of the glitter sample was captured by the SEM, whilst a representative surface of the glitter was interrogated by the EDX. A typical image and spectra obtained by SEM/EDX analysis is shown in Figure 6-7.

SEM Image	EDX Spectra	Elements:
		Aluminium Sodium Magnesium Chlorine Silicon Phosphorus Chromium
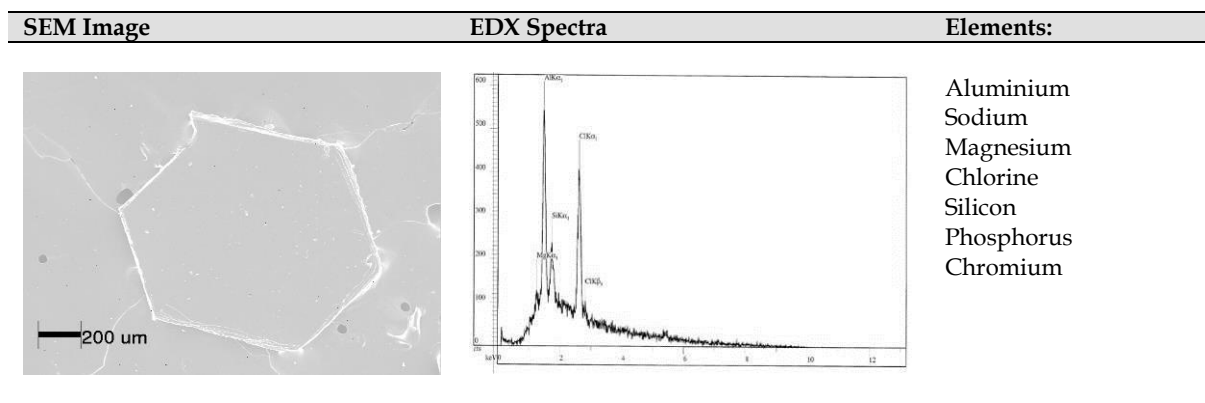
Figure 6-7: SEM image and EDX spectrum for G-2

The EDX spectra for the Spotlight glitter samples differed from the samples of glitter obtained from the four HME samples; this was due to the different elements present in the outer foil layer. The inclusion of different elements into the foil is what determines the colour of the glitter.

The four real HME glitter samples produced similar EDX spectra, with only aluminium and silicon identified. A calcium peak was observed in the EDX for 16-27, this peak is believed to be from residual calcium carbonate which is present in CAN.

SEM/EDX was used to confirm the size measurements of each glitter sample similar to that achieved with the visual microscope, additionally the EDX attachment can be used to give an indication as to what elements are present. It should be noted that although EDX can be used to determine a 'bulk' composition, the technique is not sensitive enough for trace analysis.

6.5.1.3 Infrared
The aim of analysing the glitter samples using IR spectroscopy was not only to determine the type of plastic used in each glitter, but also to "match" samples based on their IR spectrum. There are a number of reference spectra libraries that can be used to correlate samples from authentic known materials, an example is the Hummel polymer sample library [288].

PET is the most common polymer used for the production of glitter [281, 282]. However, other materials are sometimes used, e.g. a layer of polyester co-polymer or nylon-6. These different plastics are able to be readily differentiated by IR.

The offset IR spectra obtained for the sections obtained from plastic bottles are shown below in Figure 6-8. The spectra obtained were identified as PET.
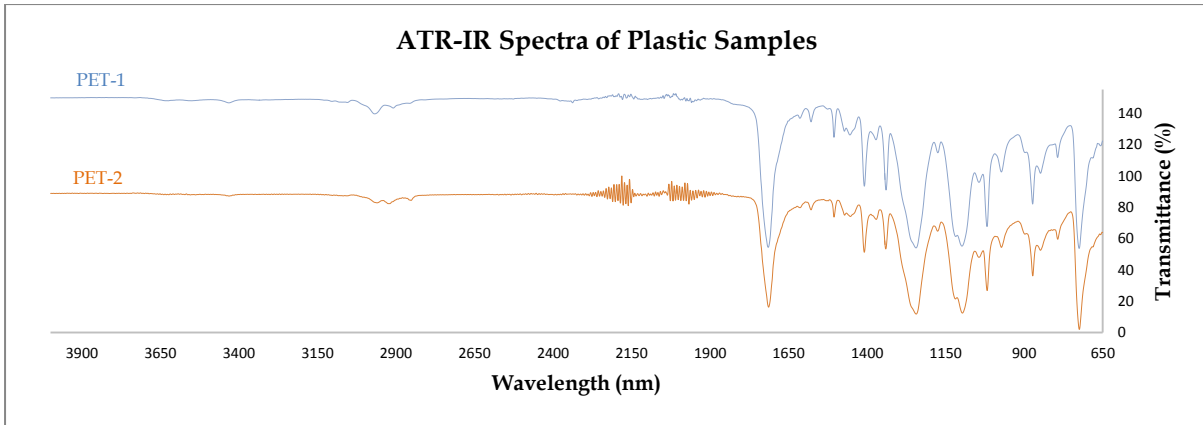
Figure 6-8: Infrared spectra of PET-1 and PET-2 which were identified as PET

Similarly, IR spectra were acquired for the real HME glitter samples as shown in Figure 6-9. The offset spectra of all four were similar and a search of the Hummel Polymer Sample Library indicated the plastic was PET [288].
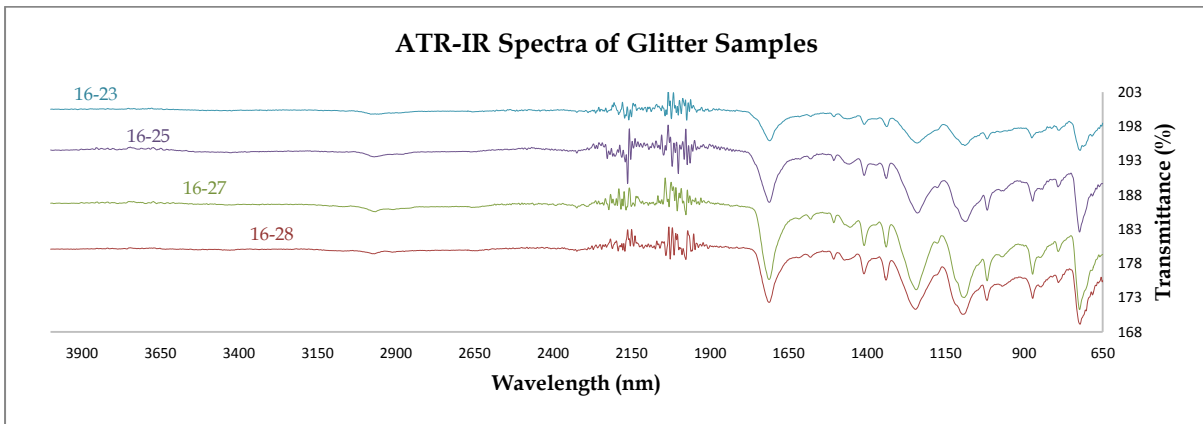
Figure 6-9: Infrared spectrum obtained for 16-23, 16-25, 16-27 and 16-28 also identified as PET

The spectra obtained for the glitter purchased from Spotlight was different to the PET spectra obtained for the plastic bottle sections and the real HME glitter samples, suggesting that a different plastic was used. A search of the Hummel polymer sample library indicated that the plastic was nylon-6 [288]. It should be noted that it is quite hard to discriminate between nylon-6 and nylon-6,6 by IR analysis (especially ATR) as the only difference between the two is a tiny band due to crystallinity. The offset spectra obtained are shown in Figure 6-10.
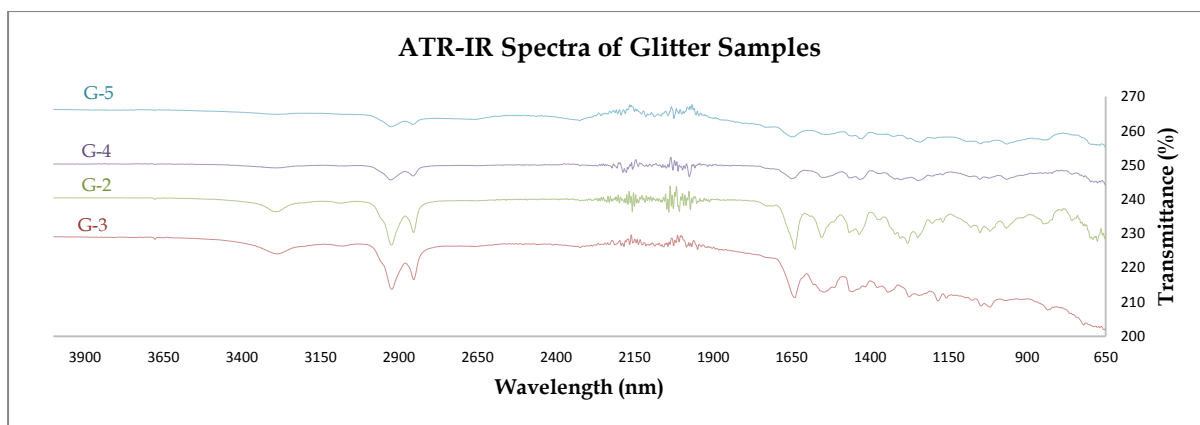
Figure 6-10: Comparison of infrared spectra obtained for G-2, G-3, G-4 and G-5 matched as nylon-6

Analysis of the glitter samples by IR demonstrates the ease with which it is possible to differentiate glitter samples into two distinct classes based on the plastic backing.

6.5.1.4 Pyrolysis Gas Chromatography/Mass Spectrometry

Py-GC/MS was undertaken on plastic and glitter samples as an additional method to confirm the type of polymer used in each sample. Figure 6-11 is the chromatograms obtained for the sections obtained from PET-1 and the real HME glitter 16-28.

These chromatograms show that the peaks occur at the same retention times and have a similar shape, which is indicative of the two materials being the same. These results confirm the results obtained from IR analysis.
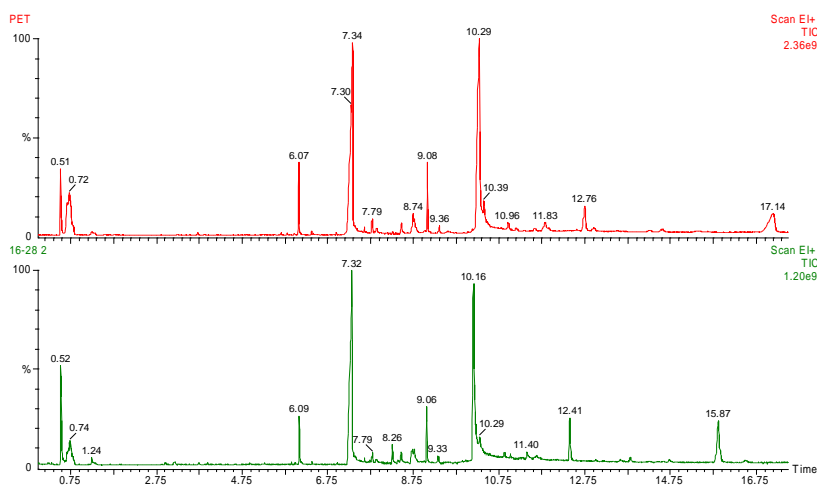
Figure 6-11: Total ion chromatogram comparing PET plastic and glitter samples (16-28)

6.5.1.5 IRMS

The $\delta^{13}C$ isotopic ratio for each of the glitter samples was determined by IRMS analysis. Generally, materials that originate from the same source will have the same isotopic ratio, thus this technique is able to be employed to determine whether samples have a common origin or manufacturer. The results obtained are shown graphically in Figure 6-12. The error

189

bars correspond to ± 1 standard deviation, the data points represent the mean value obtained from three analyses.

All samples of PET and nylon-6 were found to be isotopically depleted and from the plot it can also be seen that there is very good reproducibility in the values obtained for each sample, indicating the coating on the glitter particles is homogenous.

While IRMS analysis of the commercially acquired nylon-6 backed glitter samples confirmed that they are distinguishable from each other based on their carbon isotope values, G-2 and G-4 had very similar values and therefore cannot be distinguished based on this data alone.

Conversely, the two plastic PET bottle samples were shown to be indistinguishable based on carbon isotope values. This may be due to the fact that the bottles originate from the same PET material or bottler.
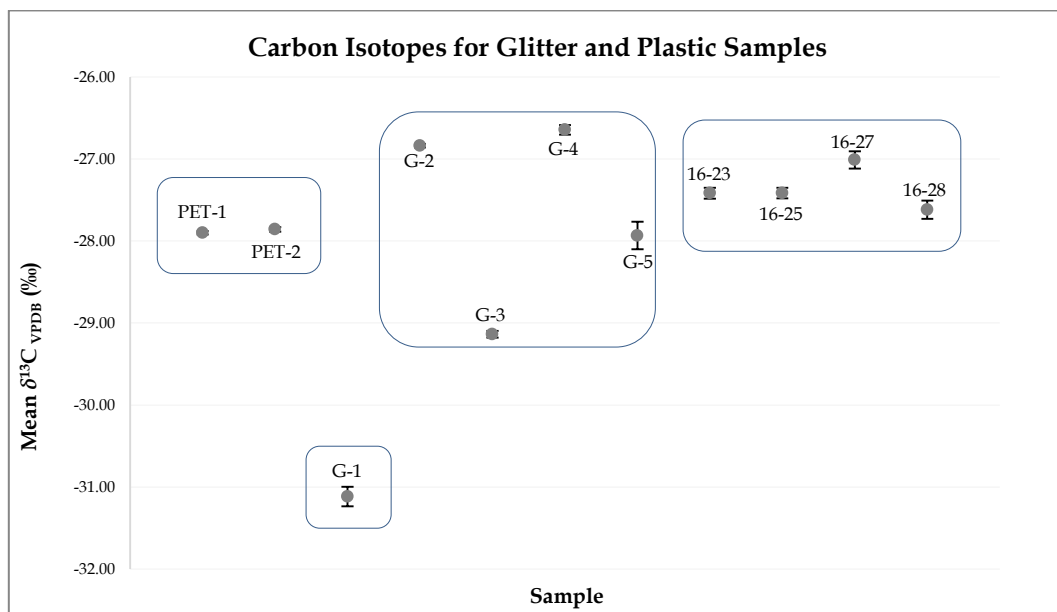
Figure 6-12: δ¹³C Isotope ratios for the glitter and plastic samples

The four real HME glitter samples (PET backed glitter) could potentially be linked together based on their carbon isotope value. There is an indication that the glitter present in each of these samples is likely to have originated from the same source, as they are isotopically indistinguishable from each other. However to further validate this finding, a larger number of PET backed glitter samples need to be analysed to determine the variation in carbon isotope values for these types of materials.

The range of δ^{13}C isotopic values obtained, indicate that IRMS has the ability to differentiate between the samples of nylon-6 backed glitter and conversely show similarities in the samples of PET backed glitter. This research task was not focussed on comparing the isotopic ratios of glitter which were manufactured using different plastics. Improved accuracy and discrimination of samples could be achieved by analysing additional elemental isotopic ratios, such as hydrogen (δ^2H) and oxygen (δ^{18}O).

6.5.1.6 ICP-MS

Analysis of the glitter samples by ICP-MS was conducted to determine the presence and amount of trace elements within each sample. ICP-MS is a sensitive technique that is able to detect elements present in the range of parts per million down to parts per trillion. This sensitivity allows for the detection of trace elements that may be introduced during manufacture or handling. It is postulated that samples with a similar ICP-MS fingerprint may have been produced in the same batch, however to full validate this theory a larger number of comparative samples will need to be analysed.

The overlapped radial plot for the Spotlight glitter samples are shown in Figure 6-13A, while the individual radial plots for each sample is shown in Figure 6-13B to 6-13F.
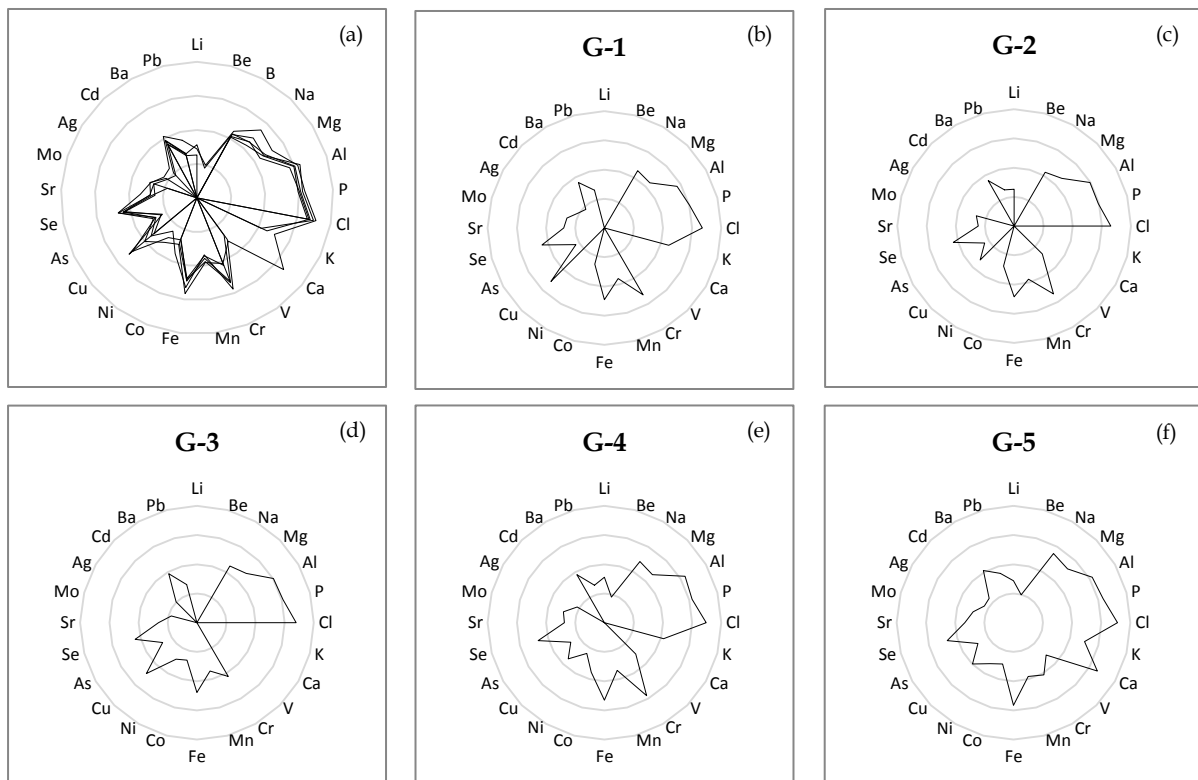
Figure 6-13: Radial plots of ICP-MS data for commercial glitter samples

The ICP-MS results obtained for the Spotlight glitter samples highlights the potential for matching and discriminating samples of glitter. The variations observed between the Spotlight glitter samples arise due to the different elements used to give the metal foil its colour, e.g. metals such as iron, cadmium, chromium and lead were found in red coloured foils; copper, cobalt and calcium were found in blue foils; and chromium and copper were found in green foils. These observations were also seen from the SEM/EDX results, but were unable to be sufficiently quantified.

The real HME glitter samples (16-23, 16-25, 16-27 and 16-28) were also analysed, results obtained are shown in Figure 6-14. Due to possible contamination by residual explosive material (AN and CAN), the number of elements were reduced on the radial plots to only include those likely to have been present in the glitter. It should be noted that in the case of the Spotlight samples if the number of elements presented on the radial plots were also

reduced to 10 (only Al, V, Cr, Mn, Co, Ni, Cu, se, Ag and Cd), the discriminating ability of this analysis method would not be severely reduced.
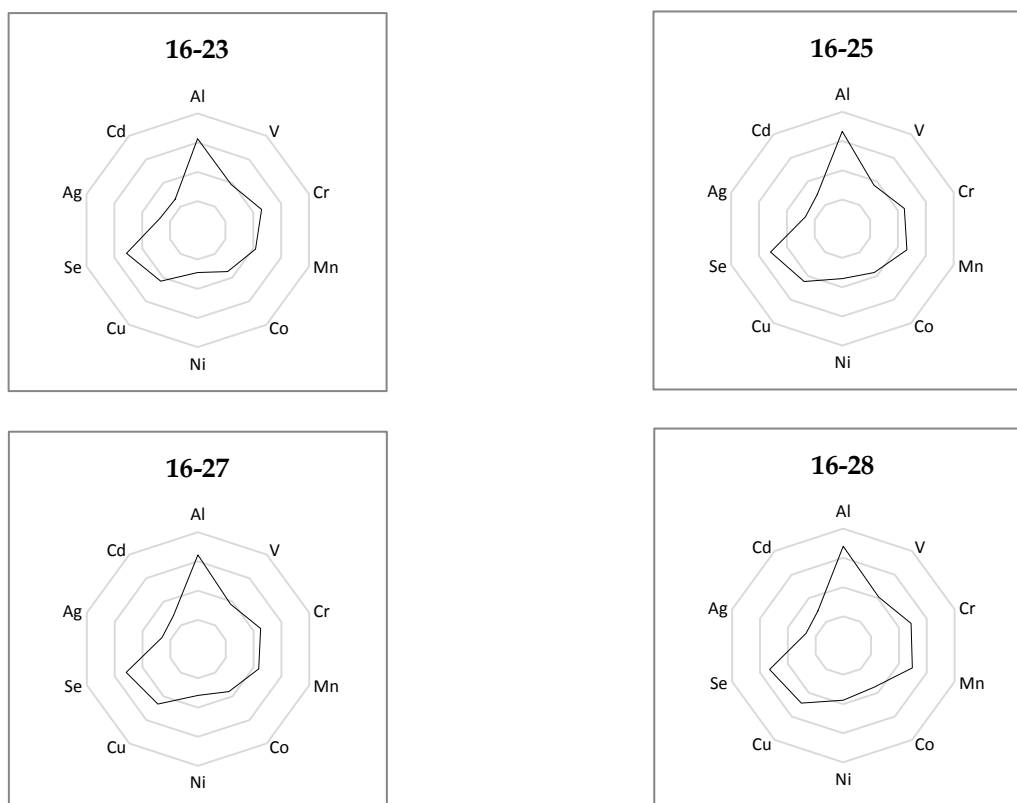
Figure 6-14: Radial log plots of the ICP-MS data obtained for the four real HME glitter particles

The absolute value for each element across the real HME glitter samples shows some variability. This may be a function of sampling errors or due to variations in the material brought about due to manual handling, differences in shape, thickness and size, or the presence of residual explosive contamination.

Despite these differences, visualising the data on a logarithmic radial plot does appear to minimise these variations, producing radial plots of essentially the same basic shape for the real HME glitter samples.

6.6 Statistical Analysis

It is possible to do simple manual pair-wise comparisons of the chemical analyses for small sample sets, however it rapidly becomes unfeasible when many hundreds or thousands of samples need to be compared. A possible solution is through the use of automated statistical analysis.

Statistical analysis was undertaken using CAMO softwares "Unscrambler X" [291]. Using this program, we attempted to determine whether it is possible to use a simple statistical method to compare the analyses of the glitter samples to determine which samples were the most alike and which samples were different. The method used was hierarchal cluster analysis using complete linkage clustering and Spearman's rank correlation.

The variables used for statistical analysis were:

1) ICP-MS results for: Al, V, Cr, Mn, Co, Ni, Cu, Se, Ag and Cd;
2) Physical dimensions of the glitter; and
3) Carbon isotope ratio value obtained from IRMS.

The plastic type (PET or nylon-6) and the colour of the glitter were not included as variables in this statistical analysis.

The results are displayed as a dendogram, this is shown in Figure 6-15. The four real HME glitter samples form a tight cluster on the dendogram, with a short 'relative distance' between the samples, this indicates that the glitter used has numerous similar properties and are more likely to be linked or originate from a common source.

The clustering of the Spotlight glitter samples is less tightly defined than the real HME glitter samples, as the relative distance between samples is between two and three. This difference is probably due to the variables used, namely, the ICP-MS results, which is largely dependent on the foil colour used.

In this example provided, it appears that a simple Spearman's rank correlation with hierarchal cluster analysis allowed for the differentiation of real HME glitter and Spotlight glitter samples. A drawback of this technique is that it is unable to 'weight' the analysis, i.e. in the above example, the carbon isotope was only one variable, whilst ICP-MS provided ten variables, therefore the ICP-MS data had a greater impact on determining similarities between the samples.

This technique is also not suitable for comparisons of large sample sets and a more robust statistical method would need to be employed, namely some form of multivariate analysis, such as principle component analysis. This forms the basis of "Chemometrics" which is an area of increasing demand.
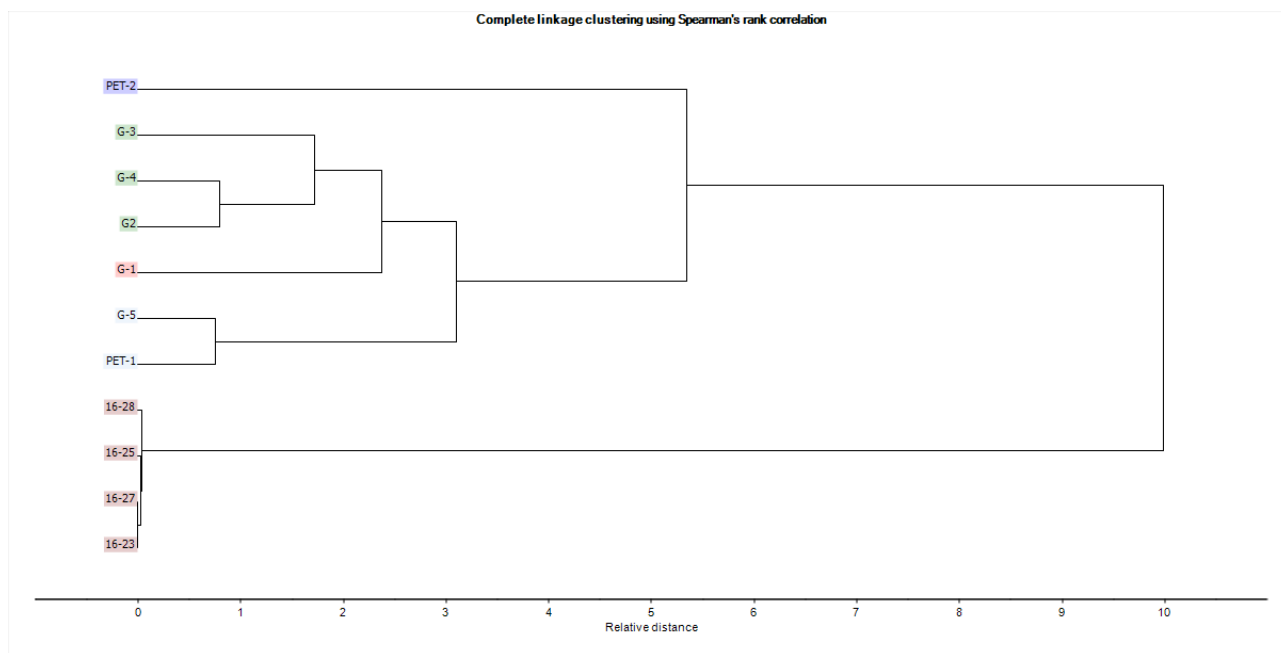
Figure 6-15: Hierarchal cluster analysis using Spearman's rank to show the similarity between the glitter samples analysed

6.7 Conclusions

The visual, physical and chemical analysis of the real HME glitter samples analysed in this report was shown to share a number of similar characteristics. This indicates that the explosive compositions they were extracted from are highly likely to have used the same source of aluminium or originate from the same batch. This result not only confirms the previous analyses conducted on the AN explosive component, but also provides a higher level of confidence in the linkage of these samples.

The analysis techniques employed were able to differentiate between glitter samples obtained from commercial suppliers in Australia and those obtained from real HME. This demonstrates that the characterisation techniques used were sufficient to differentiate between glitter samples.

Visual microscopy was used to determine the colour, dimensions and shape of each glitter, imperfections due to manufacturing errors were also able to be observed. Similarly, analysis by SEM/EDX was also able to produce detailed visual images of the glitter. EDX was then able to be used to determine the bulk compositional elements present.

Using a spectroscopic technique, such as infrared, the composition of the plastic backing was able to be determined. For the real HME glitter samples the plastic was determined to be PET, while for the Australian sourced glitter samples this plastic was identified as nylon-6. This was confirmed by py-GC/MS, where the plastic samples are heated to decomposition, allowing for the individual monomer units to be separated by gas chromatography and analysed by mass spectrometry.

194

While the above mentioned techniques were able to differentiate glitter samples based on compositional differences in the materials used, for batch and source matching of materials that have the same composition, characterisation needs to occur at the ultra-trace level. Two techniques were explored, namely IRMS and ICP-MS.

IRMS is able to distinguish chemically identical materials based on the ratio of light and heavy isotopes for a given element, where differences arise due to fractionation. It is postulated that materials from the same batch may have similar isotopic ratios, however this would need to be validated via further studies on PET and nylon-6 backed glitters. The $\delta^{13}C$ IRMS results obtained for the plastic samples of interest has shown the potential for this technique to be incorporated into the overall analytical methodology utilised to either link or distinguish between samples of glitter.

During manufacture, trace level contaminants are introduced from the source materials and processes used, and thus may differ from location-to-location and from manufacturer-to-manufacturer, however the level of these potential variations will need to be further investigated, possibly through engagement with manufacturers. ICP-MS analysis of the real HME glitter samples produced similar radial plots which are a strong indication that the glitter originated from the same source. The ICP-MS results obtained for the Australian glitter samples showed a higher degree of variation, due to different elements present in the foil to produce the desired colour.

Statistical analysis of the results was performed using the Unscrambler X software program. By using hierarchical cluster analysis and Spearmans Rank, the results obtained from chemical analysis were reduced to a simple dendrogram which could be used to show potential linkages between the glitter particles based on their similarity. In this limited sample size, the technique employed seemed quite effective, however for larger sample sets, a more robust statistical method would need to be employed.

Intentionally Blank

7. Chemical Exploitation of Organic-based HME

7.1 Objective

The objective of this research was to develop a method for the measurement of bulk nitrogen and carbon isotope ratios of organic-based HME. This objective was set in order to work towards an overall goal of determining whether IRMS would assist in discriminating and/or linking samples of organic-based homemade explosives, which cannot be achieved using traditional forensic techniques.

The samples of interest underwent analysis using various other analytical techniques (such as Raman, FT-IR, IC, Headspace-GC/MS and HPLC) however; those results will not be discussed in this Chapter.

7.1.1 Instrumentation

An IsoPrime (GV Instruments) Stable Isotope Ratio Mass Spectrometer was coupled to a EuroEA3000 Series (EuroVector) Elemental Analyser. The system utilised GV Instruments Micromass MassLynx mass spectrometry software. The sampling technique utilised was continuous flow (CF-IRMS), which consisted of a helium carrier gas to carry the analyte gas into the IRMS ion source.

Caveat – Due to the nature of the samples analysed and limitations with the analytical instrumentation used, the isotopic data presented in this research is fit for the purpose of a comparative exercise (proof of concept) but should not be compared to data from other laboratories. All of the δ values displayed within this research have an associated error range (error bars) of ± 1 standard deviation.

7.1.2 Nitrogen Isotope Analysis

Samples were weighed into a tin capsule (5 x 9 mm Sercon) using a microbalance and then sealed for subsequent IRMS analysis. Each sample was analysed in triplicate for nitrogen IRMS analysis.

Sample sizes needed for nitrogen IRMS analysis of organic-based explosive samples are detailed in Table 7-1.

Nitrogen IRMS Analysis			
Sample	Description	% Nitrogen	Sample Mass (µg)
TNT	$C_7H_5N_3O_6$ (M.W = 227.13)	18.50	433
PETN	$C_5H_8N_4O_{12}$ (M.W = 316.14)	17.72	451
RDX	$C_3H_6N_6O_6$ (M.W = 222.12)	37.84	212
HMX	$C_4H_8N_8O_8$ (M.W = 296.16)	37.48	212
Nitro-glycerine (NG)	$C_3H_5N_3O_9$ (M.W = 227.08)	18.50	433
Amatol	60% AN and 40% TNT	28.40	282
Dynamite	80% TNT, 10% AN and 10% NG	16.66	481
Comp B	60% RDX and 40% TNT	30.10	266

Table 7-1: Proposed sample sizes needed for nitrogen IRMS analysis

7.1.3   Carbon Isotope Analysis

Samples were weighed into a tin capsule (5 x 9 mm Sercon) using a microbalance and then sealed for subsequent IRMS analysis. Each sample was analysed in triplicate for carbon IRMS analysis.

Sample sizes needed for carbon IRMS analysis of organic-based explosive samples are detailed in Table 7-2

Carbon IRMS Analysis			
Sample	**Description**	**% Carbon**	**Sample Mass (μg)**
TNT	$C_7H_5N_3O_6$ (M.W = 227.13)	37.02	82
PETN	$C_5H_8N_4O_{12}$ (M.W = 316.14)	19.00	158
RDX	$C_3H_6N_6O_6$ (M.W = 222.12)	16.22	185
HMX	$C_4H_8N_8O_8$ (M.W = 296.16)	16.22	185
NG	$C_3H_5N_3O_9$ (M.W = 227.08)	15.87	190
Amatol	60% AN and 40% TNT	14.87	202
Dynamite	80% TNT, 10% AN and 10% NG	31.21	97
Comp B	60% RDX and 40% TNT	24.54	123

Table 7-2: Proposed sample sizes needed for carbon IRMS analysis

7.2 Results

Various samples of organic-based HME were analysed as part of this research task. These samples may have been of commercial origin (dynamite/military ordinance) or they may have been prepared within a clandestine HME laboratory. The samples included dynamite, Amatol, RDX, TNT, PETN and various compositions made up of multiple explosives. The obtained carbon and nitrogen isotope results for the 51 samples of interest are displayed in Figure 7-1. The IRMS values obtained for all of the organic based HME samples are displayed in Figure 7-1 to highlight the large range of isotopic values obtained as part of this research and not displayed for the comparison of chemically different materials.

It can be observed from Figure 7-1 that both the carbon and nitrogen isotope values obtained for samples of HME can be utilised to show linkages between samples of a similar type (in the case of the two semtex samples – grey coloured). This data can also be utilised to discriminate between samples of a similar type (as seen in the five samples of Comp B – red coloured).
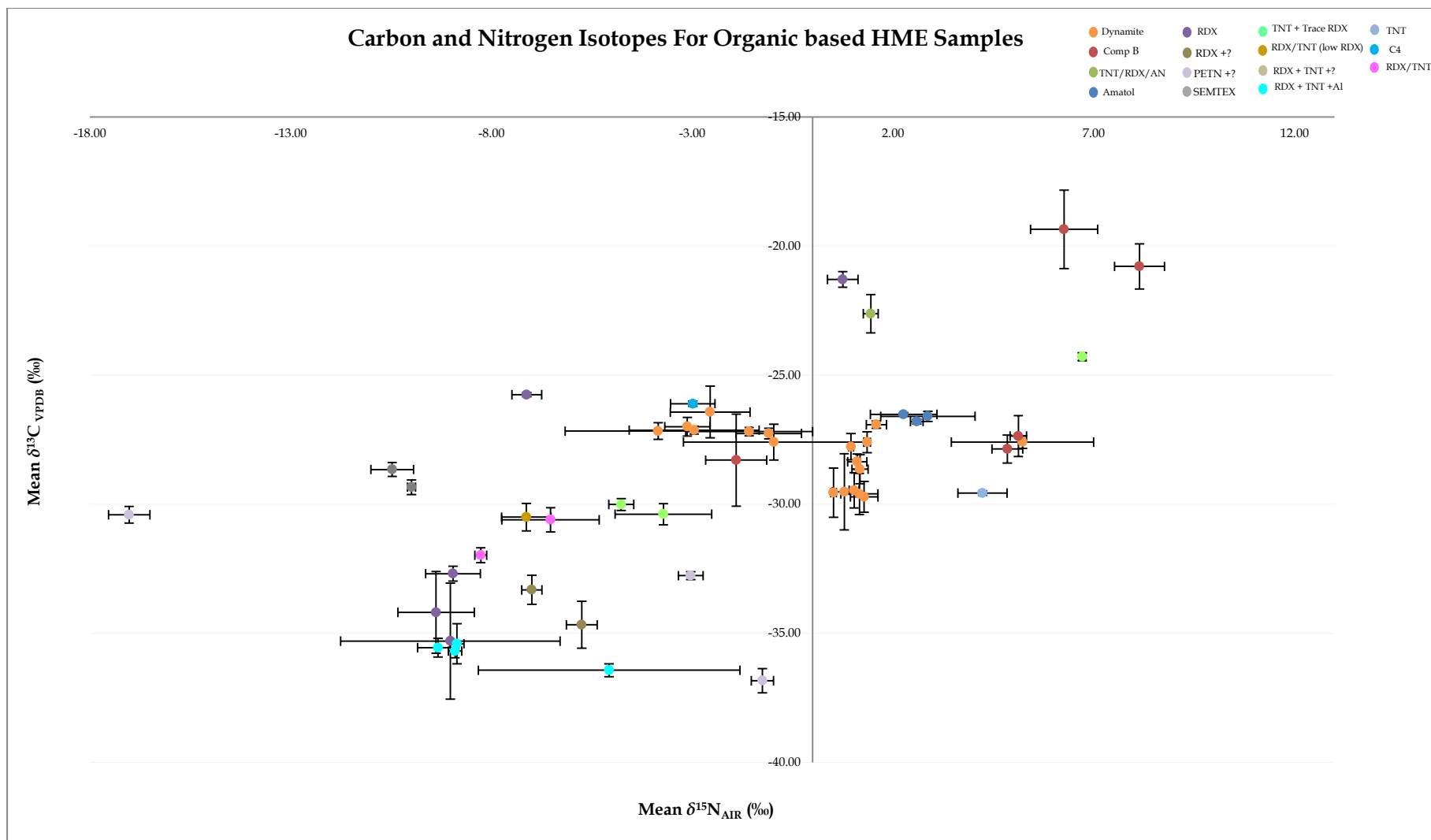
Figure 7-1: Carbon and nitrogen IRMS results for various organic-based HME samples

There are two notable batches of samples observed in Figure 7-1, which are related to the samples known as dynamite (●). This is an explosive, which is suitable for all types of rock blasting operations and is manufactured in various grades (namely 40, 60 and 80%). The composition of this material is unknown; however, it is thought to consist of TNT, NG, AN and multiple mono- and di-nitro toluenes.

The bulk isotopic analysis (nitrogen and carbon) of the dynamite samples indicates that there are two distinct types of the material. This distinction is further verified by the interpretation of the nitrogen and carbon contents for each of the samples as seen in figure 7-2. As part of this research two batches of dynamite were analysed and were labelled A and B.
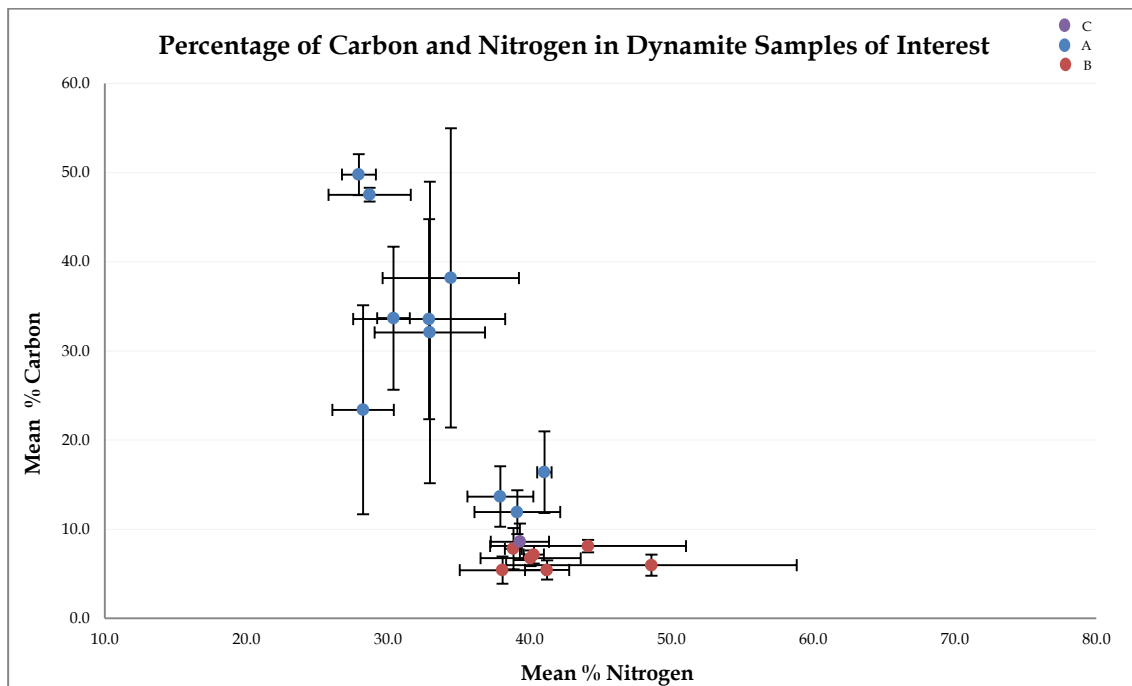
Figure 7-2: Carbon and nitrogen content for dynamite samples of interest

From Figure 7-2 it can be observed that all of the samples from B batch together (Carbon ~ 6.7% and Nitrogen ~ 41.6%). The sample known as C (analysed separately) also batches with the Batch B samples.

The samples from batch A show two distinct groupings. The first grouping was all batch A, which had an average percentage of carbon ~ 14.0% and an average percentage of nitrogen ~ 39.4%. This grouping was similar to the grouping seen for the batch B samples. The second Batch A grouping had an average percentage of carbon ~ 36.9% and an average percentage of nitrogen ~ 30.8%.

The carbon and nitrogen content results show a similar pattern as seen in the dynamite samples within Figure 7-1 where two distinct groupings can be observed in the data.

These groupings may be related to the composition of the material, as it was previously stated that this dynamite could be manufactured as three different grades (40, 60 and 80%). There are currently no specific details as to what these grade values refer to in regards to the composition of the explosive.

These explosive mixtures reportedly contain a mixture of TNT, NG, AN and various other components as previously detailed. The carbon/nitrogen content results lead to the possibility that the samples, which had a higher carbon content and lower nitrogen content may have contained a higher portion of TNT in the mixture. The samples which had a lower carbon content but a higher nitrogen content may contain a higher concentration of AN in the mixture.

Analysis of the aqueous component isolated from each of the dynamite samples was undertaken to determine if the source of the AN in the dynamite was similar. This comparison was completed using nitrogen isotope values. Figure 7-3 illustrates the results obtained for each of the AN samples and it can be deduced that all of the AN samples are isotopically indistinguishable, and therefore could have originated from the same source.
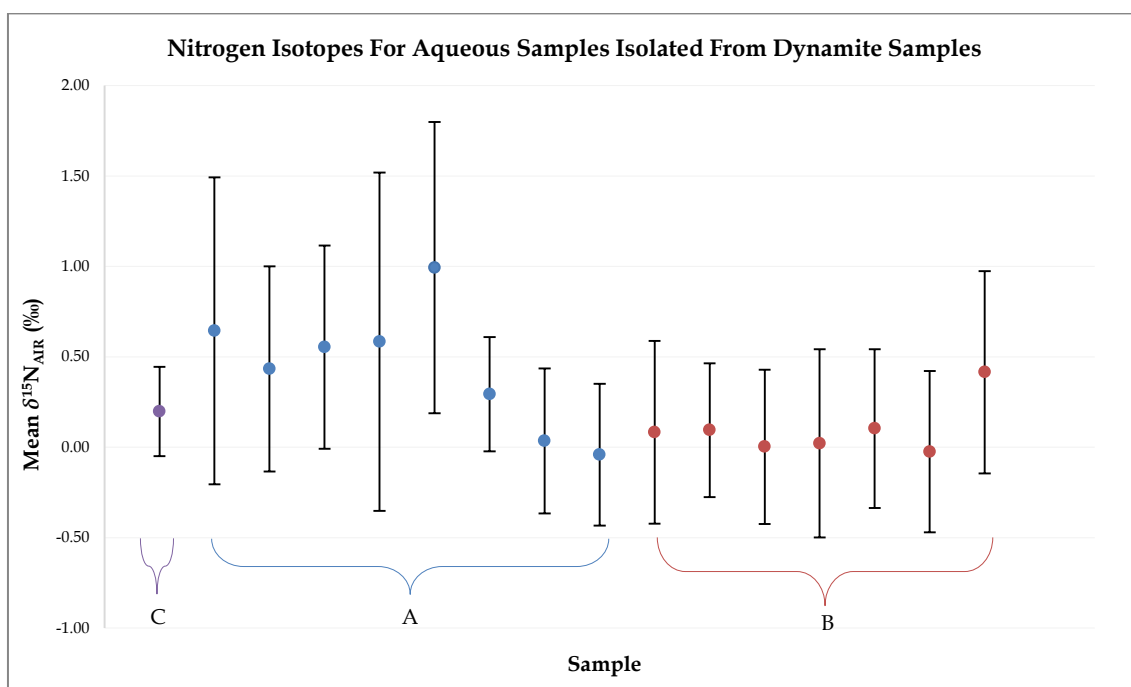
Figure 7-3: Nitrogen isotope results for dynamite samples of interest

The combination of bulk IRMS (nitrogen and carbon), the nitrogen and carbon content and the independent analysis of the AN (nitrogen IRMS of aqueous fraction) indicates that the two batches related to the dynamite samples observed in Figure 7-1 may in fact originate from a similar source. It should be stated that the bulk IRMS results are potentially skewed by the fact that this explosive material could have been one of three different compositions (The results shown in Figures 7-1 and 7-2 potentially indicate that there was two different compositions).

A third notable batch of samples observed in Figure 7-1, relates to the samples known as amatol (•). Amatol is an explosive material made from a mixture of TNT and AN.

The bulk IRMS (nitrogen and carbon) results (Figure 7-1) have indicated that the samples potentially originate from the same source. This initial finding led to further investigation and analysis of these samples. ICP-MS analysis of each of the explosive materials was undertaken to determine if any similarities in the trace elemental profiles could be identified.

ICP-MS analysis was performed using an Agilent 7500 Series ICP-MS instrument. The analysis method utilised is detailed in Chapter two of this thesis with the following modifications:

Note: These modifications should be viewed as a guide only, as full method validation has not been performed to determine the effect of sample matrix on MDL, working ranges and MUs.

It was determined that the digest of organic-based samples should be conducted with a mixture of 69% HNO_3 and 36% hydrochloric acid. This mixture contained a ratio of 3:1 (HNO_3:HCl) which is known more commonly as aqua regia. Approximately 50 mg of sample was weighed (accurately and with the weight recorded) into a 15 mL polypropylene digestion vial. The samples were digested by adding 1000 µL of aqua regia to the vial. Samples were then heated in an oil bath for 6 hours at 100°C and then shaken overnight. Samples were then made up to 15 mL with MilliQ water and allowed to settle.

It should be noted that the digestion of the organic-based explosives was not complete. Due to safety considerations, the samples could not be subjected to any harsher digestion conditions and as such some solids precipitated out (i.e., TNT) after the solutions were made up to volume for ICP-MS analysis. This factor has been taken into account when observing any ICP-MS results, and as all of the organic-based samples were "digested" in the same way, the samples are able to be compared to each other.

Figure 7-4 shows the "chemical fingerprints" obtained for the three-amatol samples of interest.
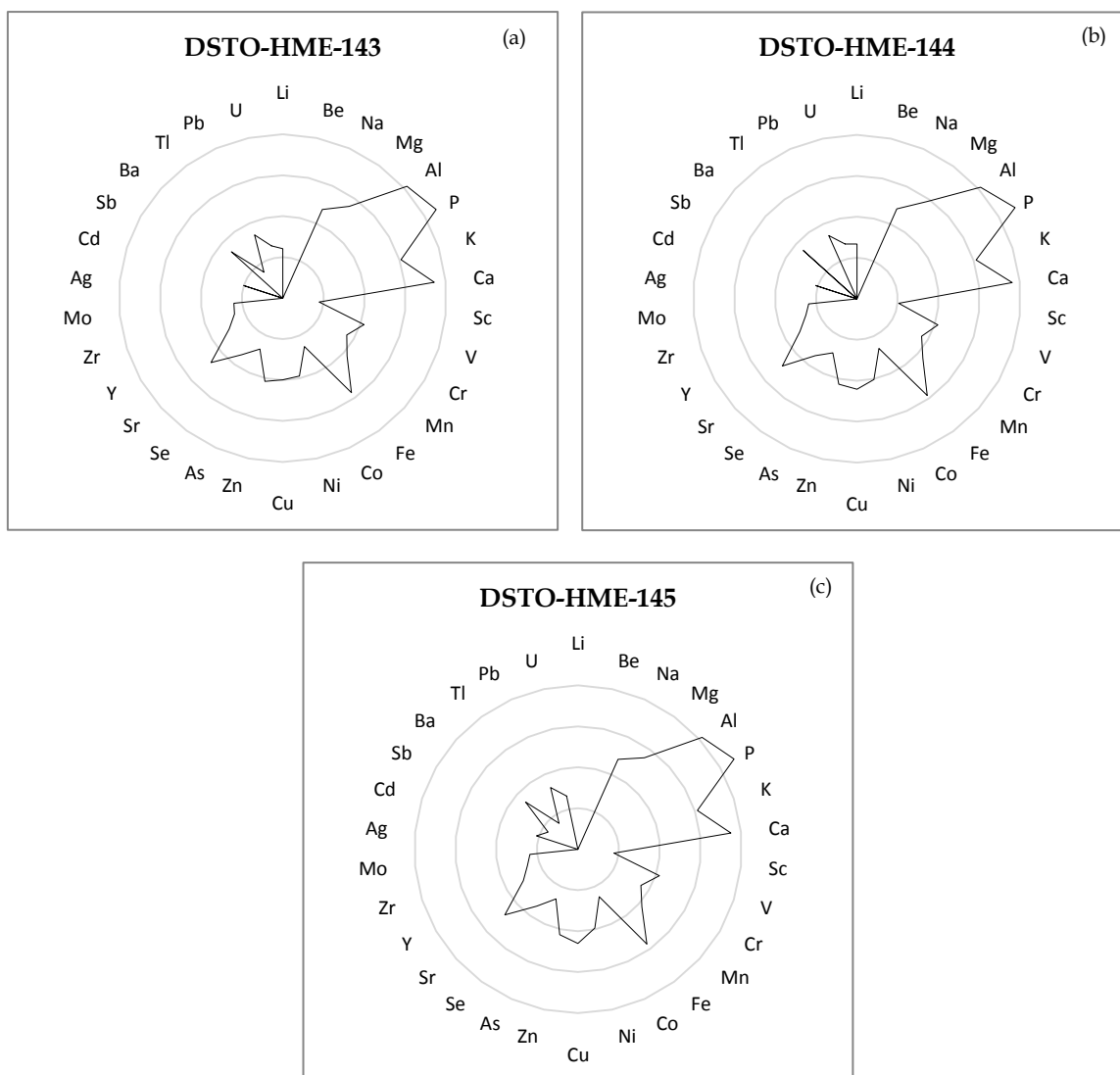
Figure 7-4 (a/b/c): Trace element profiles for three amatol samples of interest

The trace element fingerprints for the three samples of interest are quite similar and as such further confirm the suspicion that the three explosives may have originated from the same source. The trace element profiles have also revealed that the material most likely contained a mixture of CAN (the presence of calcium, phosphorous, strontium, and barium are markers for CAN) and aluminium powder.

It should be noted that during the sample preparation for ICP-MS, the digestion of the amatol may not have been complete and as such, the trace element profile may only be indicative of the CAN/Al in the sample not the TNT.

The results obtained from the bulk IRMS and ICP-MS analyses have highlighted the need for further investigation of these three materials.

203

This has resulted in the chemical breakdown of these samples to determine what/if any information could be gathered by further exploitation of these materials.

The chemical breakdown of the Amatol samples consisted of collecting the TNT (using an acetone wash), and subsequently collecting the acetone insoluble CAN/Al as a second fraction. Figure 7-5 details the analysis undertaken for each of the two collected fractions.
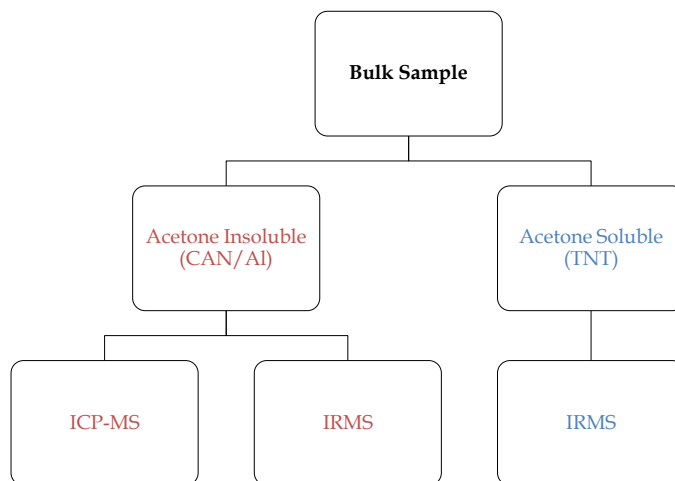
Figure 7-5: Flowchart detailing the analysis scheme for the analysis of collected fractions from three amatol samples

The "chemical fingerprints" for each of the acetone insoluble fractions is shown in Figure 7-6. These results confirm the suspicions that the three materials were prepared using the same source of CAN/Al. The trace element profiles obtained from the acetone insolubles are quite similar to the profiles in Figure 7-4 (which indicates that the profiles in Figure 7-4 were indicative of the CAN/Al in the sample).
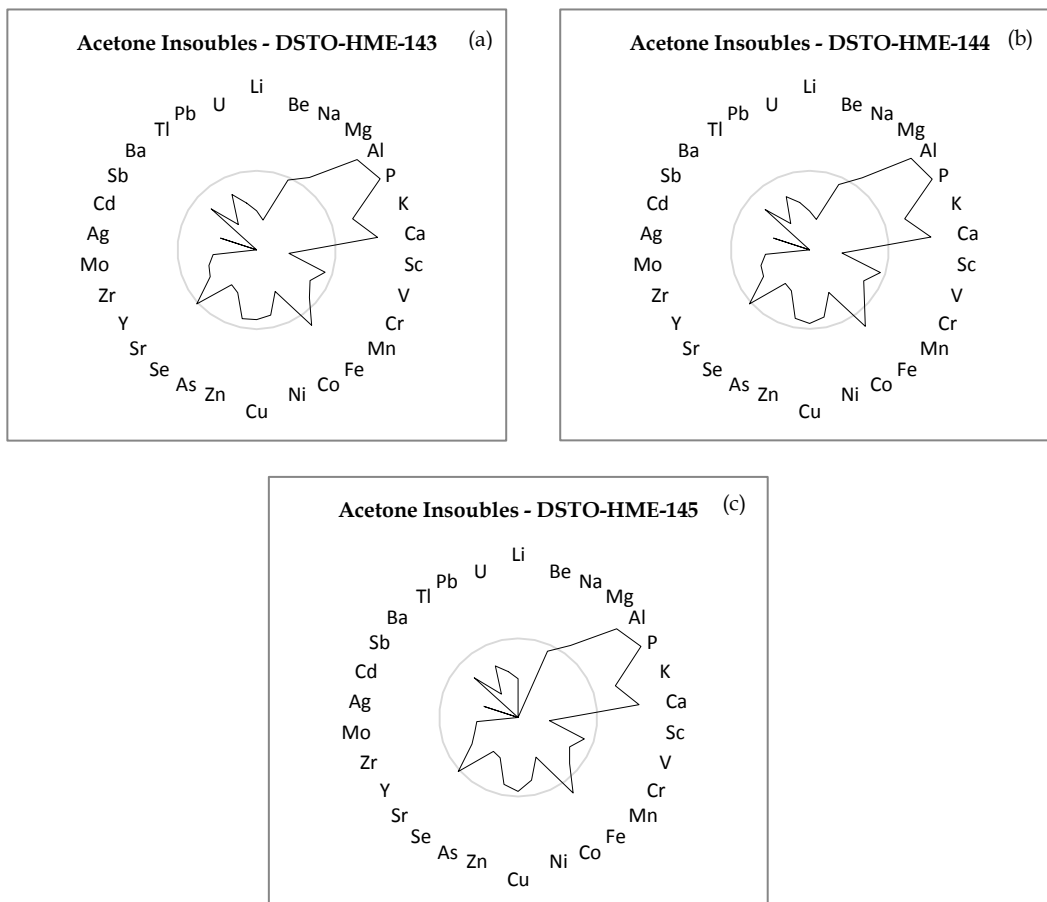
Figure 7-6 (a/b/c): Trace element profiles for the acetone insolubles recovered from three amatol samples of interest.

Figure 7-7 illustrates the carbon and nitrogen isotopic results obtained for the breakdown samples recovered from the three-amatol explosives.
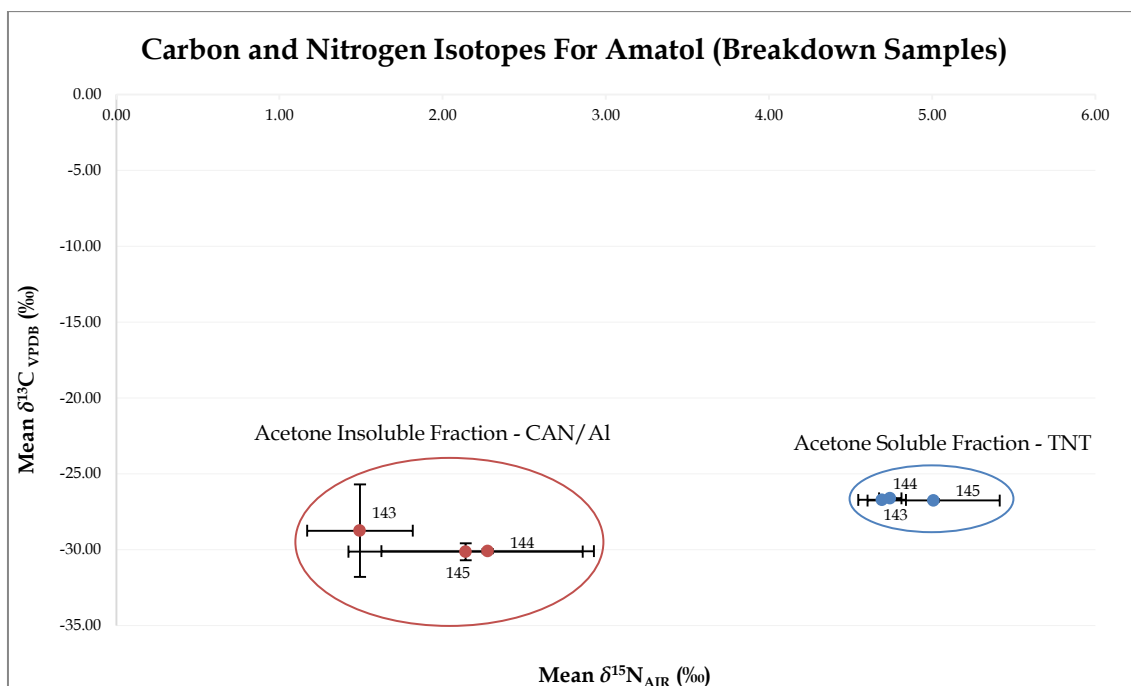
Figure 7-7: Carbon and nitrogen isotope ratios for amatol samples (breakdown analysis)

The nitrogen and carbon results obtained from the three TNT extracts are isotopically indistinguishable and as such are indicative of the fact that a similar source of TNT may have been utilised in the preparation of these three explosive materials. It can also be observed (in Figure 7-7) that the analysis of the acetone insoluble fractions using IRMS indicates that a similar source of CAN/Al may have been utilised in the preparation of these materials.

The bulk analysis of explosive materials using IRMS and ICP-MS potentially provides a batch-to-batch matching capability, and this was highlighted through the analysis of the three-amatol samples. The subsequent breakdown and analysis of these three explosives indicates that the same precursor materials (CAN/Al and TNT) were utilised in the preparation of these HME. This analysis leads to the confirmation that these three explosive samples were homemade amatol's, which were prepared using the same source of CAN/Al and TNT.

7.3 Conclusions

This series of experiments performed in this Chapter has illustrated the fact that isotopic ratios and trace metal analysis can both be utilised to exploit information from samples of organic-based homemade explosives. This information can be used for not only batch-matching samples but also potentially identifying and linking precursor materials used in the preparation of these materials, and this was illustrated throughout the analysis of dynamite and amatol samples.

Intentionally Blank

8. Conclusions and Recommendations

The overall conclusions and recommendations from this thesis are as follows:

The application of IRMS and ICP-MS is suitable for discriminating and/or identifying linkages between samples of AN/CAN.

A number of problems were identified and need to be taken into consideration when utilising either IRMS or ICP-MS for the analysis of CAN-based HME. These identified problems were encountered when analysing the HME in bulk and include factors such as dual nitrogen/carbon sources, storage/purification of CAN and sampling/contamination issues. These identified issues result in the fact that Bulk IRMS/ICP-MS is suitable for batch-to-batch matching of samples (not sourcing precursor materials). Chapters 4 and 5 detail a series of new methods which were developed to further capabilities which can be utilised for identifying linkages in the precursors used in the preparation of HME. These methodologies are illustrated in Figures 8-1 and 8-2.
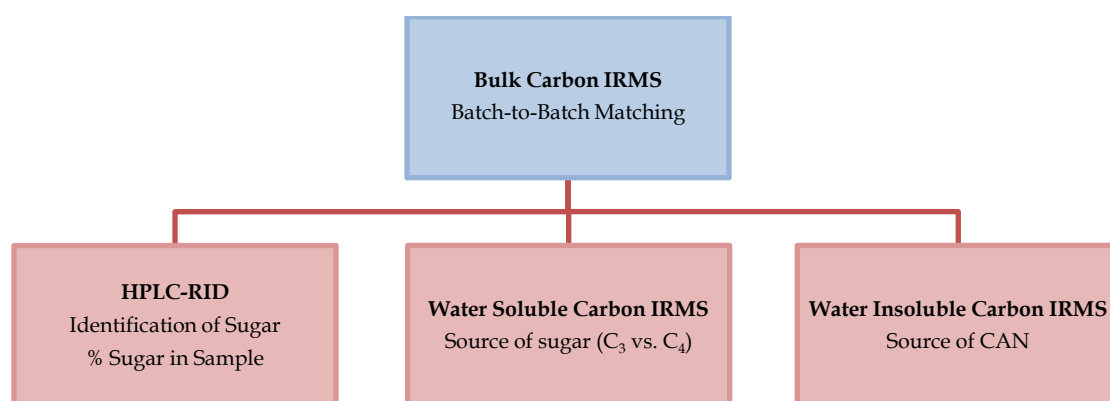
Figure 8-1: Flow diagram for $\delta^{13}C$ analysis methods
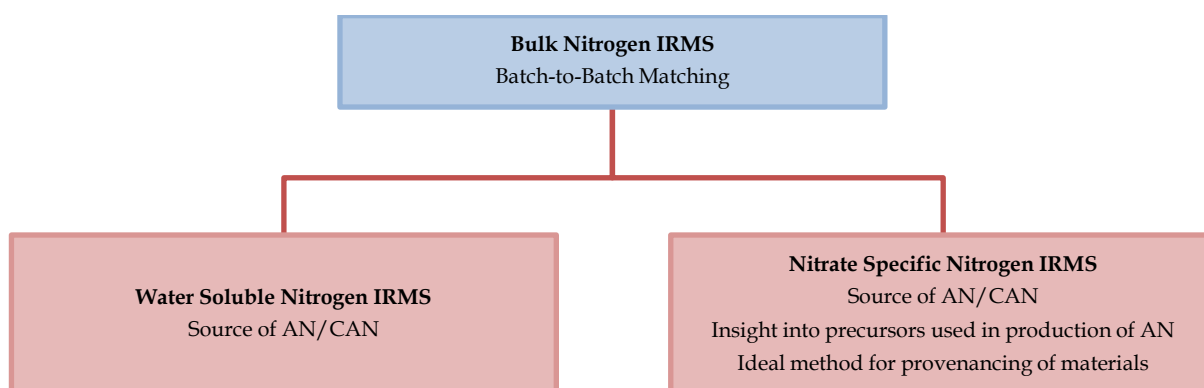
Figure 8-2: Flow diagram for $\delta^{15}N$ analysis methods

As previously stated the bulk analysis of CAN-based HME allows for batch-to-batch matching of sample. Figure 8-3 details the bulk of $\delta^{13}C$ and $\delta^{15}N$ values obtained for 16 samples of CAN-based HME. The data in Figure 8-3 is widespread and unfortunately does not provide much insight into the source materials used in the preparation of the HME samples (similar to Figure 3-1 in Chapter 3).
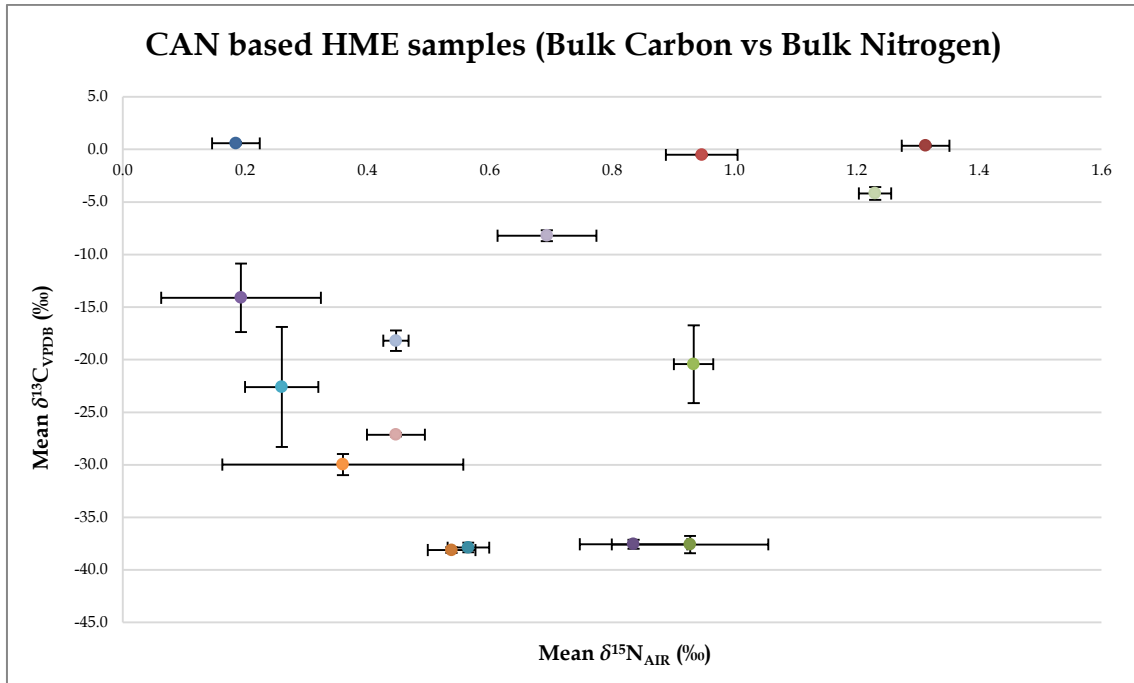
Figure 8-3: Plot of $\delta^{13}C$ and $\delta^{15}N$ values obtained for 15 samples of CAN-based HME.

Analysis of individual components (carbonate and nitrate) allows for the identification of similar sources of CAN used to prepare HME mixtures. The 15 CAN-based HME samples shown in Figure 8-3 were subsequently broken-down and each component independently analysed. It can be observed in Figure 8-4 that three sources of CAN were utilised in the preparation of the 15 HME samples.

209
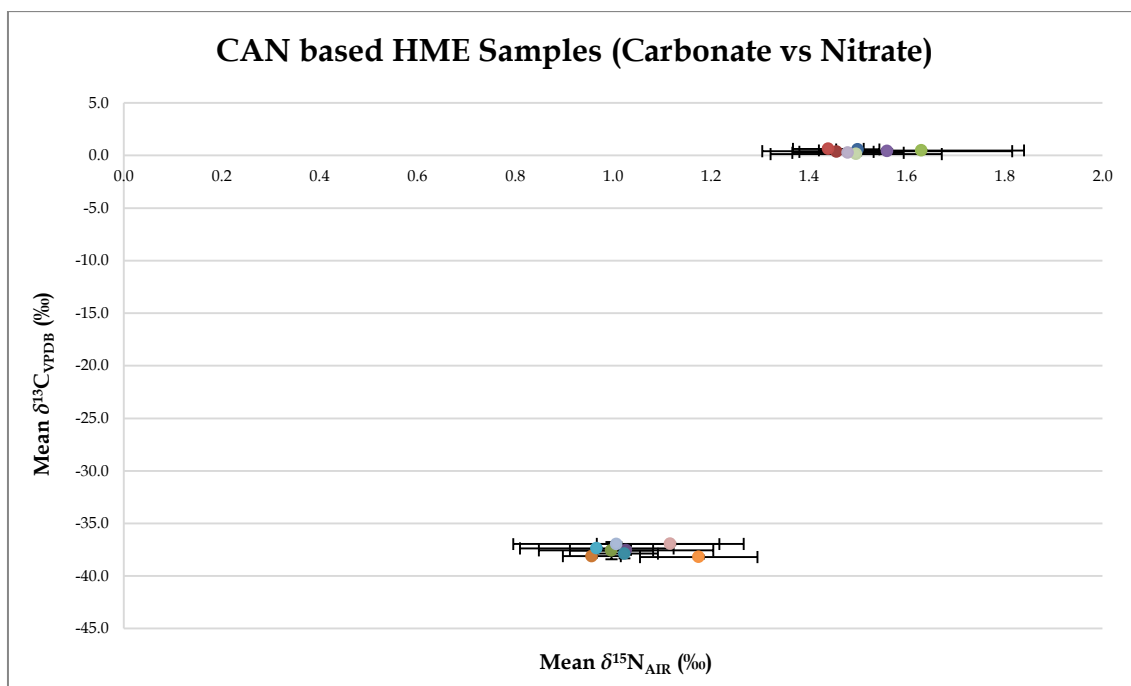
Figure 8-4: Plot of δ¹³C and δ¹⁵N values obtained for the breakdown products from 15 samples of CAN-based HME.

These two new analytical schemes (Figure 8-1 and 8-2) are now the suggested methods for exploiting chemical and forensic intelligence from HME samples. It allows for the collection of analytical data for batch-to-batch matching but also gives insight into precursor materials.

Visual, physical and chemical analysis of evidentiary samples is often used to reveal similarities and difference between samples. One of the goals of any exploitation activity is to link a sample from an event, to other samples or source. The presence of any unique sub-components, especially if foreign to the source materials, may be vital in order to establish links. One such sub-component, which was the focus of analysis, was glitter particles (which can be present in vehicle paint grade aluminium).

Several different types of glitter particle have been observed in samples received, and it may be possible to identify groups and distribution networks based on the type of glitter particles present in recovered samples.

The visual, physical and chemical analysis of the seized glitter samples (as detailed in Chapter 6) were shown to share a number of similar characteristics. This indicates that the explosive compositions they were extracted from are highly likely to have used the same source of aluminium or originate from the same batch. This result not only confirms the previous analyses conducted on the ammonium nitrate explosive component, but also provides a higher level of confidence in the linkages of these samples.

A series of organic-based HME were subjected to IRMS and ICP-MS analyses to determine what/if any exploitable information could be gathered using these two techniques. The obtained results indicate that both isotopic ratios and trace metal fingerprints can be utilised for batch-to-batch matching purposes when analysing the bulk material. It was also determined that isotopic analysis of the individual components isolated from HME samples could be utilised for linking precursor materials.

Overall, this research task has highlighted a number of positives and potential limitations in applying a number of analytical techniques to the analysis of homemade explosives for forensic purposes. The vast amount of actionable intelligence, which can be procured using techniques such as IRMS and ICP-MS, has been highlighted. The extra nine layers of data, which can now be gathered using these analytical techniques may feed into the general intelligence picture and in combination with other intelligence collection methods allow to the continuing effort of "attacking the network".

Intentionally Blank

9. Reference List

1.   *Af-Pak IED supply lines*. 2010, IHS Jane's.
2.   Cullison, A. and Y. Trofimov, *Karzai Bans Ingredient of Taliban's Roadside Bombs*, in *The Wall Street Journal*. 2010.
3.   GAO, *Counterterrorism - U.S. Agencies Face Challenges Countering the Use of Improvised Explosive Devices in the Afghanistan/Pakistan Region*, GAO, Editor. 2012.
4.   GAO, *Combating Terrorism - State Should Enhance Its Performance Measures for Assessing Efforts in Pakistan to Counter Improvised Explosive Devices*, GAO, Editor. 2012.
5.   JIEDDO, *Joint IED Defeat Organisation HME Profile: Calcium Ammonium Nitrate (CAN-26)*, JIEDDO, Editor. 2011: Virginia.
6.   JIEDDO, *Homemade Explosive (HME) / Bulk Explosive (BE) Recognition Guide*, JIEDDO, Editor. 2011.
7.   *Explosive reaction - Afghan insurgents make IED adjustments*. 2010, IHS Jane's.
8.   Brummitt, C., *Pakistani fertilizer fuels Afghan bombs, US troop deaths*, in *Associated Press*. 2011.
9.   JIEDDO, *Joint IED Defeat Organisation BAA-12-01-HME Rapid Development of New Formulations to enable Counter-HME operations*. 2012: Virginia.
10.   Zygmunt, B. and D. Buczkowski, *Agriculture Grade Ammonium Nitrate as the Basic Ingredient of Massive Explosive Charges.* Propellants, Explosives, Pyrotechnics, 2012. **37**(6): p. 685-690.
11.   *Joint Publication 1-02: Department of Defense Dictionary of Military and Associated Terms*. Director for Joint Force Development.
12.   FBI. *Intelligence Collection Disciplines (INTs)*.   23/07/2013]; Available from: http://www.fbi.gov/about-us/intelligence/disciplines.
13.   CIA. *INTelligence: Human Intelligence*. 2010   23/07/2013]; Available from: https://www.cia.gov/news-information/featured-story-archive/2010-featured-story-archive/intelligence-human-intelligence.html.
14.   CIA. *INTelligence: Signals Intelligence*. 2010   23/07/2013]; Available from: https://www.cia.gov/news-information/featured-story-archive/2010-featured-story-archive/intelligence-signals-intelligence-1.html.
15.   CIA. *INTelligence: Open Source Intelligence*. 2010   23/07/2013]; Available from: https://www.cia.gov/news-information/featured-story-archive/2010-featured-story-archive/open-source-intelligence.html.
16.   CIA. *INTelligence: Geospatial Intelligence*. 2010   23/07/2013]; Available from: https://www.cia.gov/news-information/featured-story-archive/2010-featured-story-archive/geospatial-intelligence.html.
17.   Morelato, M., et al., *The use of forensic case data in intelligence-led policing: The example of drug profiling.* Forensic Science International, 2013. **226**(1-3): p. 1-9.
18.   Ratcliffe, J.H., *Integrated Intelligence and Crime Analysis: Enhanced Information for Law Enforcement Leaders*. 2007, U.S. Department of Justice: Washington.
19.   Stringer, M., *An Introduction To Energetic Materials Safety*, DSTO, Editor. 2009, Defence Science Technology Organisation: Adelaide.
20.   Beveridge, A., ed. *Forensic Investigation of Explosions*. 1998, Taylor & Francis Ltd: London.

21. Thurman, J., *Identification and Recognition of Commercial, Improvised and Military Explosives*, in *Practical Bomb Scene Investigation, 2nd Edition*. 2011, Taylor & Francis. p. 41-115.

22. Marshall, M. and J.C. Oxley, eds. *Aspects of Explosives Detection*. 2009, Elsevier.

23. Hurley, C., et al., *Properties of Alternativley Fueled Ammonium Nitrate Explosives*, in *9th International Symposium on Rock Fragmentation by Blasting - FRAGBLAST9*. 2009: Granada, Spain.

24. Tatiya, R.R., *Explosives and blasting*, in *Surface and Underground Excavations, 2nd Edition*. 2013, CRC Press. p. 904.

25. Davies, P.J., *Personal Communication (Email) - Percentage of Aluminum Powder in AN/Al HME*, P. McCurry, Editor. 2013.

26. Royds, D., S.W. Lewis, and A.M. Taylor, *A case study in forensic chemistry: The Bali bombings*. Talanta, 2005. **67**(2): p. 262-268.

27. Johns, C., et al., *Identification of homemade inorganic explosives by ion chromatographic analysis of post-blast residues*. Journal of Chromatography A, 2008. **1182**(2): p. 205-214.

28. Sleeman, R. and J.F. Carter, *FORENSIC SCIENCES | Explosives*, in *Encyclopedia of Analytical Science*, W. Paul, T. Alan, and P. Colin, Editors. 2005, Elsevier: Oxford. p. 400-406.

29. Beveridge, A.D. and S.J. Benson, *Investigation of explosions*, in *Expert Evidence*, S. Freckelton, Editor. 2009, Thomson Reuters Australia.

30. Aranda Iv, R., et al., *Forensic utility of isotope ratio analysis of the explosive urea nitrate and its precursors*. Forensic Science International, 2011. **206**(1-3): p. 143-149.

31. Tamiri, T., et al., *Urea nitrate, an exceptionally easy-to-make improvised explosive: studies towards trace characterization*. Analytical and Bioanalytical Chemistry, 2009. **395**(2): p. 421-428.

32. *Congressional Hearings Intelligence and Security-Foreign Terrorists in America: Foreign Terrorists in America: Five Years After the World Trade Center*, in *Senate Judiciary*. 1998: Washington DC.

33. Benson, S.J., et al., *Forensic analysis of explosives using isotope ratio mass spectrometry (IRMS) -- Preliminary study on TATP and PETN*. Science & Justice, 2009. **49**(2): p. 81-86.

34. *Profile: Umar Farouk Abdulmutallab*, in *BBC News*. 14th October 2010, http://www.bbc.co.uk/news/world-us-canada-11545509.

35. *'Bomb plotter' studied chemistry*, in *BBC News*. 2007.

36. *Al Qaeda in Yemen claims parcel bomb plot*. ABC News 6/11/2010 Accessed - 9/03/2011].

37. Productivity-Commission, *Chemicals and Plastics Regulation Research Report*. 2008: Melbourne. p. 267-294.

38. Shea, D., L. Schierow, and S. Szymendera, *Regulation of Fertilisers: Ammonium Nitrate and Anhydrous Ammonia*, C.R. Service, Editor. 2013.

39. Oxley, J.C., et al., *Ammonium nitrate: thermal stability and explosivity modifiers*. Thermochimica Acta, 2002. **384**(1-2): p. 23-45.

40. Benson, S.J., et al., *Forensic analysis of explosives using isotope ratio mass spectrometry (IRMS) -- Discrimination of Ammonium Nitrate Sources*. Science & Justice, 2009. **49**(2): p. 73-80.

41. http://www.breakingnews.ie/archives/2004/1208/ireland/kfqlsnojmhcw/. *Three jailed in Continuity IRA trial*. 2004 2/08/2012].

42. OSAC, *Spain 2011 Crime and Safety Report*, U.S.D.o. State and B.o.D. Security, Editors. 2011. p. 8.

43. Simon, J.D., *Ahead of the pack - Lone wolf terrorist attacks increase*. 2013, IHS Jane's.

44. Benson, S.J., et al., *Forensic Analysis of Explosives Using Isotope Ratio Mass Spectrometry (IRMS) -- Part 2: Forensic Inter-Laboratory Trial: Bulk Carbon and NItrogen Stable Isotopes in a Range of Chemical Compounds (Australia and New Zealand)*. Journal of Forensic Sciences, 2009.

45. *Fertilizer that fizzles in a homemade bomb could save lives around the world*. 2013 24/04/2013]; Available from: https://share.sandia.gov/news/resources/news_releases/ied_fertilizer/.

46. Dorsey Jr, J.J., *Pilot Plant - Ammonium Nitrate by the Stengel Process*. Industrial & Engineering Chemistry, 1955. **47**(1): p. 11-17.

47. Lauchard, D. and M.-A. Kordek, *Granulation KT's progress using fluidized drum granulation (FDG) technology*, in *IFA Technical Conference*. 2000, International Fertilizer Industry Association: New Orleans, Louisiana, USA.

48. ORICA, *The Plant and Process: Orica mining services - Kooragang Island*. 2007, ORICA.

49. Benson, S., *Introduction of Isotope Ratio Mass Spectrometry (IRMS) for the Forensic Analysis of Explosives*. 2009, University of Technology. **PhD Thesis**: Sydney.

50. EFMA, *Production of Ammonium Nitrate and Calcium Ammonium Nitrate*, in *Best Available Techniques for Pollution Prevention and Control in the European Fertilizer Industry*. 2000.

51. EPA, *Ammonium Nitrate Manufacturing Industry - Technical Document*. 1981, U.S. Environmental Protection Agency: North Carolina.

52. Wiesenberger, H., *State-of-the-art for the production of fertilisers with regard to the IPPC-directive*, U. GmbH, Editor. 2002, The Federal Environment Agency – Austria.

53. Engelmann, J.L. and R.E. Nitzschmann, *Production of Calcium Ammonium Nitrate*, in *1990 IFA Technical Conference*. 1990, BASF: Venice, Italy.

54. Patwa, M.R. and M.I. Shamsi, *Technology Upgradation by Breakthrough Innovations GNFC Experience with Nitrophosphate ODDA Process*, in *1998 IFA Technical Conference*. 1998, Gujarat Narmada Valley Fertilizers Co. Ltd., India Marrakech, Morocco.

55. Joshi, V.S. and P.A. Shah, *Operating Experience with Different Rock Phosphates In Nitrophosphate Complex*, in *2000 IFA Technical Conference*. 2000, Gujarat Narmada Valley Fertilizers Co. Ltd., India: New Orleans, Louisiana, USA.

56. Uhde, *Nitrate Fertilisers*, Uhde, Editor. 2009.

57. IFA, *World Phosphate Rock (PR) Statistics by Country in '000 Tonnes Product*, IFA, Editor. 2010, Production and International Trade Committee.

58. PotashCorp. *2011 Online Overview - Phosphate*. 2011 13/12/2012]; Available from: http://www.potashcorp.com/industry_overview/2011/nutrients/25/.

59. Kamermann, P. and A. Erben, *The Uhde Pugmill Granulation - The Process for Safe and Reliable Production of CAN and Other AN Based Fertilisers* in *2006 IFA Technical Symposium*. 2006, Uhde GmbH: Vilnius, Lithuania.

60. Franzrahe, H. and P. Niehues, *Pugmill Granulation: A State of The Art Process for CAN and Other Ammonium Nitrate Based Fertilsers*, in *2002 IFA Technical Conference*. 2002, Uhde GmbH: Chennai, India.

61.   Sharma, R.K., *Caking Mechanisms of Phosphatic Fertilizers and its Control at GNFC by the Application of Anticaking Agents and Their Mode of Actions* in *1998 IFA Technical Conference*. 1998, Gujarat Narmada Valley Fertilizers Co. Ltd., India: Marrakech, Morocco.

62.   *Sciencemadness Discussion Board*. Available from: http://www.sciencemadness.org/talk/.

63.   CrEaTiVePyroScience. *Make/Obtain Ammonium Nitrate (from instant cold packs)*. Available from: http://www.youtube.com/watch?v=e5hhdP7W8HY.

64.   Meyer, R., J. Kohler, and A. Homburg, *Explosives*. 2007, Wiley-VCH Verlag GmbH: Weinheim.

65.   Akhavan, J., *The Chemistry of Explosives* 3rd edition ed. 2011: RSC Publishing.

66.   Saferstein, R., *Criminalistics: An Introduction to Forensic Science*. 8th Edition ed. 2004, New Jersey: Pearson Prentice Hall.

67.   Smiths-Detection. *Ion Mobility Spectrometry (IMS)*. [cited 2009 12th November]; Available from: http://www.smithsdetection.com/eng/IMS.php.

68.   Sheble, N. *Ion Mobility Spectrosocopy*. 2002 [cited 2009 10th November]; Available from: http://www.isa.org/InTechTemplate.cfm.

69.   Weaver, J.W., ed. *Reference Analytical Methods for a Textile Laboratory*. 1984, American Association of Textile Chemists and Colourists.

70.   TWGFEX, *Recommended Guidelines for Forensic Identification of Post-Blast Explosive Residues*. 2009, TWGFEX Laboratory Group Standards & Protocols Commitee.

71.   Esseiva, P., et al., *Forensic drug Intelligence: An important tool in law enforcement.* Forensic Science International, 2007. **167**(2-3): p. 247-254.

72.   Esseiva, P., et al., *Illicit drug profiling, reflection on statistical comparisons.* Forensic Science International, 2011. **207**(1-3): p. 27-34.

73.   Dams, R., et al., *Heroin impurity profiling: trends throughout a decade of experimenting.* Forensic Science International, 2001. **123**(2-3): p. 81-88.

74.   NicDaéid, N. and R.J.H. Waddell, *The analytical and chemometric procedures used to profile illicit drug seizures.* Talanta, 2005. **67**(2): p. 280-285.

75.   Krawczyk, W. and A. Parczewski, *Application of chemometric methods in searching for illicit Leuckart amphetamine sources.* Analytica Chimica Acta, 2001. **446**(1-2): p. 107-114.

76.   Lociciro, S., et al., *Cocaine profiling for strategic intelligence, a cross-border project between France and Switzerland: Part II. Validation of the statistical methodology for the profiling of cocaine.* Forensic Science International, 2008. **177**(2-3): p. 199-206.

77.   Lociciro, S., et al., *Cocaine profiling for strategic intelligence purposes, a cross-border project between France and Switzerland: Part I. Optimisation and harmonisation of the profiling method.* Forensic Science International, 2007. **167**(2-3): p. 220-228.

78.   Perillo, B.A., R.F.X. Klein, and E.S. Franzosa, *Recent advances by the U.S. Drug Enforcement Administration in drug signature and comparative analysis.* Forensic Science International, 1994. **69**(1): p. 1-6.

79.   Andersson, K., et al., *Development of a harmonised method for the profiling of amphetamines VI: Evaluation of methods for comparison of amphetamine.* Forensic Science International, 2007. **169**(1): p. 86-99.

80.   Johnston, A. and L.A. King, *Heroin profiling: Predicting the country of origin of seized heroin.* Forensic Science International, 1998. **95**(1): p. 47-55.

81. Perkal, M., Y.L. Ng, and J.R. Pearson, *Impurity profiling of methylamphetamine in Australia and the development of a national drugs database.* Forensic Science International, 1994. **69**(1): p. 77-87.

82. Marquis, R., et al., *Drug intelligence based on MDMA tablets data: 2. Physical characteristics profiling.* Forensic Science International, 2008. **178**(1): p. 34-39.

83. Weyermann, C., et al., *Drug intelligence based on MDMA tablets data: I. Organic impurities profiling.* Forensic Science International, 2008. **177**(1): p. 11-16.

84. Jonson, C.S.L. and L. Strömberg, *Two-level classification of Leuckart amphetamine.* Forensic Science International, 1994. **69**(1): p. 31-44.

85. NicDaéid, N., et al., *Recent Advances in the Application of Stable Isotope Ratio Analysis in Forensic Chemistry.* Australian Journal of Chemistry, 2010. **63**(1): p. 3-7.

86. Benson, S., et al., *Forensic applications of isotope ratio mass spectrometry--A review.* Forensic Science International, 2006. **157**(1): p. 1-22.

87. UN, *Methods For Impurity Profiling of Heroin and Cocaine.* 2005, Office on Drugs and Crime - United Nations: Vienna.

88. Magalhães, E.J., et al., *Evaluation of the composition of street cocaine seized in two regions of Brazil.* Science & Justice, 2013. **53**(4): p. 425-432.

89. Nageswara Rao, R. and M.V.N. Kumar Talluri, *An overview of recent applications of inductively coupled plasma-mass spectrometry (ICP-MS) in determination of inorganic impurities in drugs and pharmaceuticals.* Journal of Pharmaceutical and Biomedical Analysis, 2007. **43**(1): p. 1-13.

90. Koper, C., et al., *Elemental analysis of 3,4-methylenedioxymethamphetamine (MDMA): A tool to determine the synthesis method and trace links.* Forensic Science International, 2007. **171**(2-3): p. 171-179.

91. Chan, K.-W., G.-H. Tan, and R.C.S. Wong, *ICP-MS Method Validation for the Analysis of Trace Elements in Illicit Heroin.* Analytical Letters, 2012. **45**(9): p. 1122-1132.

92. Chan, K.-W., G.-H. Tan, and R.C.S. Wong, *Investigation of trace inorganic elements in street doses of heroin.* Science & Justice, 2013. **53**(1): p. 73-80.

93. Collins, M., et al., *δ13C, δ15N and δ2H isotope ratio mass spectrometry of ephedrine and pseudoephedrine: application to methylamphetamine profiling.* Rapid Communications in Mass Spectrometry, 2009. **23**(13): p. 2003-2010.

94. Collins, M., et al., *δ13C and δ2H isotope ratios in amphetamine synthesized from benzaldehyde and nitroethane.* Rapid Communications in Mass Spectrometry, 2010. **24**(11): p. 1653-1658.

95. Ehleringer, J.R., et al., *Tracing the geographical origin of cocaine.* Nature, 2000. **408**(6810): p. 311-312.

96. Marclay, F., et al., *Potential of IRMS technology for tracing gamma-butyrolactone (GBL).* Forensic Science International, 2010. **198**(1-3): p. 46-52.

97. David, G.E., et al., *Isotope fractionation during precipitation of methamphetamine HCl and discrimination of seized forensic samples.* Forensic Science International, 2010. **200**(1-3): p. 123-129.

98. Buchanan, H.A.S., et al., *Emerging use of isotope ratio mass spectrometry as a tool for discrimination of 3,4-methylenedioxymethamphetamine by synthetic route.* Analytical Chemistry, 2008. **80**(9): p. 3350-3356.

99. Cawley, A.T., et al., *Carbon isotope ratio (δ13C) values of urinary steroids for doping control in sport.* Steroids, 2009. **74**(3): p. 379-392.

100. West, J.B., J.M. Hurley, and J.R. Ehleringer, *Stable Isotope Ratios of Marijuana. I. Carbon and Nitrogen Stable Isotopes Describe Growth Conditions.* Journal of Forensic Sciences, 2009. **54**(1): p. 84-89.

101. Muccio, Z. and G.P. Jackson, *Isotope ratio mass spectrometry.* Analyst, 2009. **134**(2): p. 213-222.

102. Phillips, S.A., et al., *Network developing forensic applications of stable isotope ratio mass spectrometry Conference 2002.* Science & Justice, 2003. **43**(3): p. 153-160.

103. Wakelin, D., et al., *Network developing forensic applications of stable Isotope Ratio Mass Spectrometry conference 2005.* Science & Justice, 2008. **48**(2): p. 79-90.

104. Carter, J.F., et al., *Isotope ratio mass spectrometry as a tool for forensic investigation (examples from recent studies).* Science & Justice, 2005. **45**(3): p. 141-149.

105. Yinon, J., ed. *Advances in Forensic Applications of Mass Spectrometry.* 2004, CRC Press LLC: Florida.

106. Ribaux, O., et al., *Intelligence-led crime scene processing. Part II: Intelligence and crime scene examination.* Forensic Science International, 2010. **199**(1-3): p. 63-71.

107. Ribaux, O., et al., *Intelligence-led crime scene processing. Part I: Forensic intelligence.* Forensic Science International, 2010. **195**(1-3): p. 10-16.

108. Ribaux, O., S.J. Walsh, and P. Margot, *The contribution of forensic science to crime analysis and investigation: Forensic intelligence.* Forensic Science International, 2006. **156**(2-3): p. 171-181.

109. Rossy, Q., et al., *Integrating forensic information in a crime intelligence database.* Forensic Science International, 2013. **230**(1-3): p. 137-146.

110. Wiggett, A.E., et al., *Forensic Science Society Spring Meeting 2002 Intelligence.* Science & Justice, 2003. **43**(2): p. 109-118.

111. Coplen, T.B., et al., *Isotope-Abundance Variations of Selected Elements (IUPAC Technical Report).* Pure and Applied Chemistry, 2002. **74**(10): p. 1987-2017.

112. Carter, J.F. and V.J. Barwick, eds. *Good practice guide for isotope ratio mass spectrometry* 2011, FIRMS.

113. Coplen, T.B., *Guidelines and recommended terms for expression of stable-isotope-ratio and gas-ratio measurement results.* Rapid Communications in Mass Spectrometry, 2011. **25**(17): p. 2538-2560.

114. Brand Willi, A., et al., *Assessment of international reference materials for isotope-ratio analysis (IUPAC Technical Report)*, in *Pure and Applied Chemistry*. 2014. p. 425.

115. Coplen, T.B., et al., *New Guidelines for $\delta^{13}C$ Measurements.* Analytical Chemistry, 2006. **78**(7): p. 2439-2441.

116. Meier-Augenstein, W., *Stable isotope analysis of fatty acids by gas chromatography-isotope ratio mass spectrometry.* Analytica Chimica Acta, 2002. **465**(1-2): p. 63-79.

117. Santrock, J. and J.M. Hayes, *Adaptation of the Unterzaucher procedure for determination of oxygen-18 in organic substances.* Analytical Chemistry, 1987. **59**(1): p. 119-127.

118. EuroVector, *Elemental Analyser User Guide.* EuroVector. 20-21.

119. NicDaéid, N., et al., *Using Isotopic Fractionation to Link Precursor to Product in the Synthesis of (±)-Mephedrone: A New Tool for Combating "Legal High" Drugs.* Analytical Chemistry, 2012. **84**(20): p. 8691-8696.

120. Ovenden, S.P.B., et al., *A Study of the Metabolome of Ricinus communis for Forensic Applications.* Australian Journal of Chemistry, 2010. **63**(1): p. 8-21.

121.   Kreuzer, H.W., J.B. West, and J.R. Ehleringer, *Forensic Applications of Light-Element Stable Isotope Ratios of Ricinus communis Seeds and Ricin Preparations.* Journal of Forensic Sciences, 2013. **58**: p. S43-S51.

122.   Pilgrim, T.S., R.J. Watling, and K. Grice, *Application of trace element and stable isotope signatures to determine the provenance of tea (Camellia sinensis) samples.* Food Chemistry, 2010. **118**(4): p. 921-926.

123.   Rodushkin, I., et al., *Elemental and isotopic characterization of cane and beet sugars.* Journal of Food Composition and Analysis, 2011. **24**(1): p. 70-78.

124.   Jahren, A.H., et al., *An isotopic method for quantiying sweeteners derived from corn and sugar cane.* American Journal of Clinical Nutrition, 2006(84): p. 1380-4.

125.   Tosun, M., *Detection of adulteration in honey samples added various sugar syrups with $^{13}C/^{12}C$ isotope ratio analysis method.* Food Chemistry, 2013. **138**(2–3): p. 1629-1632.

126.   Rodrigues, C.I., et al., *Stable isotope analysis for green coffee bean: A possible method for geographic origin discrimination.* Journal of Food Composition and Analysis, 2009. **22**(5): p. 463-471.

127.   Heaton, K., et al., *Verifying the geographical origin of beef: The application of multi-element isotope and trace element analysis.* Food Chemistry, 2008. **107**(1): p. 506-515.

128.   Kelly, S., K. Heaton, and J. Hoogewerff, *Tracing the geographical origin of food: The application of multi-element and multi-isotope analysis.* Trends in Food Science & Technology, 2005. **16**(12): p. 555-567.

129.   Primrose, S., M. Woolfe, and S. Rollinson, *Food forensics: methods for determining the authenticity of foodstuffs.* Trends in Food Science & Technology, 2010. **21**(12): p. 582-590.

130.   Dietz, M.E., et al., *Forensic utility of carbon isotope ratio variations in PVC tape backings.* Science & Justice, 2012. **52**(1): p. 25-32.

131.   Farmer, N., et al., *Stable isotope profiling of burnt wooden safety matches.* Science & Justice, 2009. **49**(2): p. 107-113.

132.   Farmer, N.L., W. Meier-Augenstein, and R.M. Kalin, *Stable isotope analysis of safety matches using isotope ratio mass spectrometry-a forensic case study.* Rapid Communications in Mass Spectrometry, 2005. **19**(22): p. 3182-3186.

133.   Farmer, N.L., et al., *Forensic analysis of wooden safety matches -- A case study.* Science & Justice, 2007. **47**(2): p. 88-98.

134.   Quirk, A.T., et al., *An initial evaluation of stable isotopic characterisation of post-blast plastic debris from improvised explosive devices.* Science & Justice, 2009. **49**(2): p. 87-93.

135.   Nissenbaum, A., *The Distribution of Natural Stable Isotopes of Carbon As a Possible Tool for the Discrimination of Samples of TNT.* Journal of Forensic Sciences, 1975. **20**: p. 455-459.

136.   Lock, C., S. Doyle, and D. Wakelin, *IRMS - A Technique with a Future in Forensics: The "DNA" of Explosives*, in *Network developing forensic applications of stable Isotope Ratio Mass Spectrometry conference* 2005.

137.   Beardah, A.M., *Isotopic ratio analysis of explosives traces – a new type of evidence (Part 3).* 2002, United Kingdom Defence Science and Technology Laboratory report DSTL/CR05104.

138.   Wakelin, D., *Isotopic ratio analysis of explosives traces – a new type of evidence Part 2.* 2001, United Kingdom Defence Evaluation and Research Agency report DERA/DSTL/CR00569.

139.   Wakelin, D., *Isotopic Ratio Analysis of Explosives Traces - A New Type of Evidence* 2000, Defence Evaluation and Research Agency UK Report DERA/CES/CS/CR000294.

140.   Lock, C.M. and W. Meier-Augenstein, *Investigation of isotopic linkage between precursor and product in the synthesis of a high explosive.* Forensic Science International, 2008. **179**(2-3): p. 157-162.

141.   Lock, C.M., et al., *Investigation of Isotopic Linkages between Precursor Materials and the Improvised High Explosive Product Hexamethylene Triperoxide Diamine.* Analytical Chemistry, 2012.

142.   Pierrini, G., et al., *Evaluation of preliminary isotopic analysis (^{13}C and ^{15}N) of explosives A likelihood ratio approach to assess the links between semtex samples.* Forensic Science International, 2007. **167**(1): p. 43-48.

143.   Belanger, C. *The application of EA-C-IRMS in the Analysis of Explosives.* in *FIRMS network conference 2002 (16-17 September 2002).* 2002.

144.   Lott, M.J., J.Howa, and J.R. Ehleringer. *Locating the origins of explosives through stable isotope ratio analysis (Poster).* in *Isotope Ratio Mass Spectrometry (FIRMS) Conference (16–17 September 2002)* *http://www.forensic-isotopes.rdg.ac.uk/conf/conf.htm*. 2002.

145.   Vitoria, L., et al., *Fertilizer Characterization: Isotopic Data (N, S, O, C, and Sr).* Environmental Science and Technology, 2004(38): p. 3254-3262.

146.   Widory, D., J.-J. Minet, and M. Barbe-Leborgne, *Sourcing explosives: A multi-isotope approach.* Science & Justice, 2009. **49**(2): p. 62-72.

147.   McCurry, P., *The Detection, Analysis and Characterisation of Various Ammonium Nitrate Explosives,* in *School of Chemical and Physical Sciences.* 2009, Flinders University: Adelaide. p. 40.

148.   Gentile, N., R.T.W. Siegwolf, and O. Delémont, *Study of isotopic variations in black powder: reflections on the use of stable isotopes in forensic science for source inference.* Rapid Communications in Mass Spectrometry, 2009. **23**(16): p. 2559-2567.

149.   Brust, H., et al., *Isotopic and elemental profiling of ammonium nitrate in forensic explosives investigations.* Forensic Science International, 2014. **248**: p. 101-112.

150.   Agilent Technologies, *ICP-MS. Inductively Coupled Plasma Mass Spectrometry. A Primer.* 2005, Agilent Technologies: Santa Clara, California, USA.

151.   PerkinElmer, *The 30 Minute Guide to ICP-MS.* 2004, PerkinElmer: Waltham, Massachussetts, USA.

152.   McCurdy, E., G. Woods, and D. Potter, *Unmatched Removal of Spectral Interferences in ICP-MS Using the Agilent Octopole Reaction System with Helium Collision Mode.* 2006, Agilent Technologies: Cheadle Royal, Cheshire, UK.

153.   Lane, D.W. and D.C. Wicks, *PIXE, a New Technique for the Trace Element Analysis of High Explosives.* Nuclear Instruments and Methods in Physics Research Section B: Beam Interactions with Materials and Atoms, 2000. **161–163**: p. 792-796.

154.   Husáková, L., et al., *Characterization of Industrial Explosives Based on the Determination of Metal Oxides in the Identification Particles by Microwave Digestion and Atomic Absorption Spectrometry Method.* Forensic Science International, 2008. **178**: p. 146-152.

155.   Turillazzi, E., et al., *Collection of Trace Evidence of Explosive Residues from the Skin in a Death Due to a Disguised Letter Bomb. The Synergy Between Confocal Laser Scanning Microscope and Inductively Coupled Plasma Atomic Emission Spectrometer Analyses.* Forensic Science International, 2010. **197**: p. e7-e12.

156. Bakowska, E., P.B. Harrsch, and J. Gluodenis, Thomas J., *Analysis of Gunshot Residue by ICP-MS*. 2001, Agilent Technologies: Santa Clara, California, USA.

157. Steffen, S., et al., *Chemometric Classification of Gunshot Residues Based on Energy Dispersive X-Ray Microanalysis and Inductively Coupled Plasma Analysis with Mass-Spectrometric Detection.* Spectrochimica Acta Part B: Atomic Spectroscopy, 2007. **62**: p. 1028-1036.

158. Udey, R.N., B.C. Hunter, and R.W. Smith, *Differentiation of Bullet Type Based on the Analysis of Gunshot Residue Using Inductively Coupled Plasma Mass Spectrometry*.* Journal of Forensic Sciences, 2011. **56**: p. 1268-1276.

159. Turillazzi, E., et al., *Analytical and Quantitative Concentration of Gunshot Residues (Pb, Sb, Ba) to Estimate Entrance Hole and Shooting-Distance Using Confocal Laser Microscopy and Inductively Coupled Plasma Atomic Emission Spectrometer Analysis: An Experimental Study.* Forensic Science International, 2013. **231**: p. 142-149.

160. Meng, H.-H. and H.-C. Lee, *Elemental Analysis of Primer Mixtures and Gunshot Residues from Handgun Cartridges Commonly Encountered in Taiwan.* Forensic Science Journal, 2007. **6**: p. 39-54.

161. Rodrigues, S.M., et al., *Elemental analysis for categorization of wines and authentication of their certified brand of origin.* Journal of Food Composition and Analysis, 2011. **24**(4-5): p. 548-562.

162. United Nations Office on Drugs and Crime Vienna, *Methods For Impurity Profiling of Heroin and Cocaine. Manual for Use by National Drug Testing Laboratories*. 2005, United Nations Office: New York, New York, USA.

163. Johnston, A. and L.A. King, *Heroin Profiling: Predicting the Country of Origin of Seized Heroin.* Forensic Science International, 1998. **95**: p. 47-55.

164. Chan, K.-W., G.-H. Tan, and R.C.S. Wong, *ICP-MS Method Validation for the Analysis of Trace Elements in Illicit Heroin.* Analytical Letters, 2012. **45**: p. 1122-1132.

165. NicDaéid, N., S. Jayaram, and W.J. Kerr, *Elemental Profiling Using ICP-MS of Methylamphetamine Hydrochloride Prepared from Proprietary Medication Using the Moscow and Hypophosphorous Synthesis.* Science and Justice, 2012.

166. Engelmann, J.L. and R.E. Nitzschmann, *Production of Calcium Ammonium Nitrate*, in *IFA Technical Conference*. 1990, International Fertilizer Industry Association: Venice, Italy. p. 3A.

167. Sabiha-Javied, et al., *Heavy Metal Pollution from Phosphate Rock Used for the Production of Fertilizer in Pakistan.* Microchemical Journal, 2009. **91**: p. 94-99.

168. Otero, N., et al., *Fertiliser Characterisation: Major, Trace and Rare Earth Elements.* Applied Geochemistry, 2005. **20**: p. 1473-1488.

169. Bech, J., et al., *Selenium and Other Trace Elements in Phosphate Rock of Bayovar-Sechura (Peru).* Journal of Geochemical Exploration, 2010. **107**: p. 136-145.

170. Bech, J., et al., *Selenium and Other Trace Elements in Phosphorites: A Comparison Between Those of the Bayovar-Sechura and Other Provenances.* Journal of Geochemical Exploration, 2010. **107**: p. 146-160.

171. Aydin, I., et al., *Hazardous Metal Geochemistry of Sedimentary Phosphate Rock Used for Fertilizer (MazIdag, SE Anatolia, Turkey).* Microchemical Journal, 2010. **96**: p. 247-251.

172. Chauhan, P., R.P. Chauhan, and M. Gupta, *Estimation of Naturally Occurring Radionuclides in Fertilizers Using Gamma Spectrometry and Elemental Analysis by XRF and XRD Techniques.* Microchemical Journal, 2013. **106**: p. 73-78.

173. Wilson, L., *The Analysis of Aluminium Alloys by Atomic Absorption Spectroscopy with Special Reference to the Determination of Chromium and Zirconium.* Analytica Chimica Acta, 1968. **40**: p. 503-512.

174. Akhtar, N., *Spectrochemical Investigation of Aluminum Master Alloys.* Pakistan Journal of Analytical and Environmental Chemistry, 2010. **11**: p. 51-55.

175. Li, H.-K., et al., *Quantitative Analysis of Impurities in Aluminium Alloys by Laser-Induced Breakdown Spectroscopy Without Internal Calibration.* Transactions of Nonferrous Metals Society of China, 2008. **18**: p. 1-5.

176. Sabsabi, M. and P. Cielo, *Quantitative Analysis of Aluminium Alloys by Laser-Induced Breakdown Spectroscopy and Plasma Characterization.* Applied Spectroscopy, 1995. **49**: p. 499-507.

177. Hinrichs, J. and M. Hamester, *High Purity Aluminium Analysis by Glow Discharge Mass Spectrometry.* 2011, Thermo Fisher Scientific: Bremen, Germany.

178. *MassLynx Inorganic, Build 4,0,0,792.* 2003, GV Instruments.

179. Jardine, D., *Total Organic Carbon in Ammonium Nitrate.* 2009, Flinders Analytical Laboratory: Adelaide.

180. Llorent-Martínez, E.J., et al., *Investigation by ICP-MS of Trace Element Levels in Vegetable Edible Oils Produced in Spain.* Food Chemistry, 2011. **127**: p. 1257-1262.

181. *Hair Mineral Analysis*, in *Biolab Medical Unit - Nutritional and Environmental Medicine.* 2012: London.

182. LeBlanc, A., P. Dumas, and L. Lefebvre, *Trace element content of commercial shampoos: impact on trace element levels in hair.* Science of The Total Environment, 1999. **229**(1–2): p. 121-124.

183. Chauhan, A.S., et al., *Determiniation of Lead and Cadmium in Cosmetic Products.* Journal of Chemical and Pharamceutical Science, 2010. **2**(6): p. 92-97.

184. Price, R., *The Determination of Selenium in Shampoo by Flame Atomic Absorption Spectrometry.* Thermo Fisher Scientific - Application Note: 43050, 2010.

185. NATA, *Technical Note 17- October 2013 - Guidelines for the validation and verification of quantitative and qualitative test methods.* 2013, National Association of Testing Authorities, Australia (NATA).

186. Creed, J.T., C.A. Brockhoff, and T.D. Martin, *Method 200.8. Determination Of Trace Elements In Waters and Wastes By Inductively Coupled Plasma-Mass Spectrometry, Revision 5.4.* 1994, Environmental Monitoring Systems Laboratory, U.S. Environmental Protection Agency: Cincinatti, Ohio, USA.

187. Uhrovčík, J., *Strategy for determination of LOD and LOQ values – Some basic aspects.* Talanta, 2014. **119**(0): p. 178-180.

188. Currie, L.A., *Nomenclature in evaluation of analytical methods including detection and quantification capabilities: (IUPAC Recommendations 1995).* Analytica Chimica Acta, 1999. **391**(2): p. 105-126.

189. Currie, L.A., *Detection and quantification limits: origins and historical overview.* Analytica Chimica Acta, 1999. **391**(2): p. 127-134.

190. Thomas, R., *Practical Guide to ICP-MS: A Tutorial for Beginners.* 2nd ed. 2008, Boca Raton, Florida, USA: CRC Press.

191. AB SCIEX, *Defining Lower Limits of Quantification: A Discussion of Signal/Noise, Reproducibilty and Detector Technology in Quantitative LC/MS/MS Experiments.* 2010, AB SCIEX: Foster City, California, USA.

192. APVMA, *Guidelines for the validation of analytical methods for active constituent, agricultural and veterinary chemical products*. 2004, Australian Pesticides and Veterinary Medicines Authority: ACT, AUSTRALIA.

193. Cable, M., *Calibration Principles*, in *Calibration: A Technician's Guide*. 2005, ISA: Research Triangle Park, North Carolina, USA. p. 1-14.

194. NATA, *Guidelines for Estimating and Reporting Measurement Uncertainty of Chemical Test Results*. 2013, National Association of Testing Authorities (NATA): Rhodes, New South Wales, Australia.

195. Ellison, S., *Using reproducibility information in measurement uncertainty estimation.* VAM Bulletin, 2006(34): p. 9-11.

196. Ramanathan, P.S., *Measurement uncertainty in chemical analysis.* VAM Bulletin, 2006(34): p. 4-8.

197. *Tracability in Chemical Measurement: A guide to achieving comparable results in chemical measurement*. EURACHEM/CITAC (ECTRACE:2003) - Available to download from https://www.eurachem.org/index.php/publications/guides/trc.

198. Thompson, M. and R. Wood, *Harmonized guidelines for internal quality control in analytical chemistry laboratories (Technical Report)*, in *Pure and Applied Chemistry*. 1995. p. 649.

199. van Reeuwijk, L.P. and V.J.G. Houba, *Guidelines for Quality Management in Soil and Plant Laboratories*. 1998, International Soil Reference and Information Centre, Food and Agriculture Organization of the United Nations: Rome, Italy.

200. Brown, A. and P. Quincey, *Gravimetry of ambient air monitoring filters - Development of an optimised weighing protocol and selection of filter materials.* VAM Bulletin, 2006(35): p. 23-26.

201. Greef, J., *Coefficient of Variation of Wool Fibre Diameter in Merino Breeding Programs*. 2006, Department of Agriculture and Food, Government of Western Australia: Perth, Western Australia.

202. Weber, C.I., *Methods for Measuring the Acute Toxicity of Effluents and Recieving Waters to Freshwater and Marine Organisms*. Environmental Monitoring Systems Laboratory - Office of Research and Development - United States Environmental Protection Agency: Washington.

203. Filliben, J.J. and A. Heckert, *Star Plot*, in *NIST/SEMATECH e-Handbook of Statistical Methods*, C. Croarkin and P. Tobias, Editors. 2003.

204. O'Connor, B., et al., *DRAFT - Forensic Characterisation of Ammonium Nitrate Prills at Ambient Temperature by Combining Elemental and Synchnotron Radiation Diffraction Analysis*. 2011, Curtin University of Technology/ANSTO.

205. *Cal-Am Fact Sheet*, in *Incitec Pivot Limited*. 2006.

206. Fatima-Fertilizers. *Sarsabz Calcium Ammonium Nitrate (CAN) Fertilizer*. 30/09/2013]; Available from: http://fatima-group.com/fatimafertilizer/can.php.

207. Carter, J.F., et al., *The role of isotope ratio mass spectrometry as a tool for the comparison of physical evidence.* Science & Justice, 2014. **54**(5): p. 327-334.

208. Chacón, J.E. and T. Duong, *Multivariate plug-in bandwidth selection with unconstrained pilot bandwidth matrices*. TEST, 2010. **19**(2): p. 375-398.

209. Kiiski, H., *Properties of Ammonium Nitrate based fertilisers*, in *Department of Chemistry*. 2009, University of Helsinki: Heksinki.

210. Oxley, J.C., S.M. Kaushik, and N.S. Gilson, *Thermal decomposition of ammonium nitrate-based composites.* Thermochimica Acta, 1989. **153**(0): p. 269-286.

211. Sinditskii, V.P., et al., *Ammonium Nitrate: Combustion Mechanism and the Role of Additives.* Propellants, Explosives, Pyrotechnics, 2005. **30**(4): p. 269-280.

212. Kirk-Othmer, *Explosives and Propellants*, in *Kirk-Othmer Encyclopedia of Chemical Technology.* 2004, Wiley: New York.

213. Kendall, C. and E.A. Caldwell, *Fundamentals of Isotope Geochemistry*, in *Isotope Tracers in Catchment Hydrology*, C. Kendall and J.J. McDonnell, Editors. 1998.

214. Li, L., P. Cartigny, and M. Ader, *Kinetic nitrogen isotope fractionation associated with thermal decomposition of NH_3: Experimental results and potential applications to trace the origin of N_2 in natural gas and hydrothermal systems.* Geochimica et Cosmochimica Acta, 2009. **73**(20): p. 6282-6297.

215. Jones, C., et al., *Factors Affecting Nitrogen Fertilizer Volatilization.* 2013, Montana State University Extension.

216. Yerokun, O.A., *Ammonia volatilization from ammonium nitrate, urea and urea phosphate fertilizers applied to alkaline soils.* South African Journal of Plant and Soil, 1997. **14**(2): p. 67-70.

217. Butler, M., et al., *Quantifying Ammonia Volatilization from Surface-Applied Fertilizers in Kentucky Bluegrass Grown for Seed.* 2011, Central Oregon Agricultural Research Center. p. 1-7.

218. JIEDDO, *Victim Operated Improvised Explosive Device (VOIED) Recognition Guide - Afghanistan*, JIEDDO, Editor. 2011.

219. Saba, D.S., et al., *Geothermal Energy in Afghanistan: Prospects and Potential.* 2004, Centre on International Cooperation and Afghanistan Centre for Policy and Development Studies.

220. Benham, A., *Minerals in Afghanistan.* 2007, British Geological Survey.

221. Mitchell, C. and A. Benham, *Afghanistan: Revival and redevelopment.* 2008, British Geological Survey.

222. King, T.V.V., et al., *Surface Materials Map of Afghanistan: Iron-Bearing Minerals and Other Materials: U.S. Geological Survey Scientific Investigations Map 3152-B*, USGS, Editor. 2011.

223. Kokaly, R.F., et al., *Surface Materials Map of Afghanistan: Carbonates, Phyllosilicates, Sulfates, Altered Minerals, and Other Materials: U.S. Geological Survey Scientific Investigations Map 3152-A*, USGS, Editor. 2011.

224. Vitòria, L., et al., *Multi-Isotopic Approach (^{15}N, ^{13}C, ^{34}S, ^{18}O and D) for Tracing Agriculture Contamination in Groundwater*, in *Environmental Chemistry*, E. Lichtfouse, J. Schwarzbauer, and D. Robert, Editors. 2005, Springer Berlin Heidelberg. p. 43-56.

225. Silva, S.R., et al., *Forensic Applications of Nitrogen and Oxygen Isotopes in Tracing Nitrate Sources in Urban Environments.* Environmental Forensics, 2002. **3**(2): p. 125-130.

226. Heaton, T.H.E., *Isotopic studies of nitrogen pollution in the hydrosphere and atmosphere: A review.* Chemical Geology: Isotope Geoscience section, 1986. **59**(0): p. 87-102.

227. Motzer, W.E., *Nitrate Forensics.* HydroVisions Newsletter, 2006.

228. Rogers, K.M., E. Nicolini, and V. Gauthier, *Identifying source and formation altitudes of nitrates in drinking water from Réunion Island, France, using a multi-isotopic approach.* Journal of Contaminant Hydrology, 2012. **138–139**(0): p. 93-103.

229. Minet, E., et al., *Evaluating the utility of ^{15}N and ^{18}O isotope abundance analyses to identify nitrate sources: A soil zone study.* Water Research, 2012. **46**(12): p. 3723-3736.

230. Silva, S.R., et al., *A new method for collection of nitrate from fresh water and the analysis of nitrogen and oxygen isotope ratios.* Journal of Hydrology, 2000. **228**(1–2): p. 22-36.

231. Cosofret, S.C., C. Guillou, and F. Reniero, *Method for nitrate collection and determination of N and/or O isotope ratio*, E.P. Office, Editor. 2008. p. 15.

232. Freyer, H.D. and A.I.M. Aly, *Nitrogen-15 Variations in Fertilizer Nitrogen.* J. Environ. Qual., 1974. **3**(4): p. 405-406.

233. Johnson, F.J., *Recent Advances in Fertilizer Analytical Methods*, in *CENTO Seminar on Fertilizer Analytical Methods, Sampling, and Quality Control*. 1974: Pakistan.

234. Gehrke, C.W., et al., *A Comprehensive Nitrogen Method.* J. Ass. Office. Agr. Chem., 1697. **50**: p. 965-975.

235. Ross, P.J. and A.E. Martin, *A rapid procedure for preparing gas samples for nitrogen-15 determination.* Analyst, 1970. **95**(1134): p. 817-822.

236. Bremner, J.M. and D.R. Keeney, *Steam distillation methods for determination of ammonium, nitrate and nitrite.* Analytica Chimica Acta, 1965. **32**(0): p. 485-495.

237. Böhlke, J.K., S.J. Mroczkowski, and T.B. Coplen, *Oxygen isotopes in nitrate: new reference materials for $^{18}O:^{17}O:^{16}O$ measurements and observations on nitrate-water equilibration.* Rapid Communications in Mass Spectrometry, 2003. **17**(16): p. 1835-1846.

238. Alchin, D., *Ion Exchange Resins*. New Zealand Institute of Chemistry (NZIC).

239. SUPELCO, *Guide to Solid Phase Extraction*, Sigma-Aldrich, Editor. 1998.

240. *Flow Injection Analysis – Nutrients*. Marine Science Institute - University of California; Available from: https://www.msi.ucsb.edu/services/analytical-lab/instruments/flow-injection-analyzer.

241. Instruments, L. *QuikChem 8500 Series 2 FIA System - Frequently Asked Questions*. Available from: http://www.lachatinstruments.com/products/quik-chem-flow-injection-analysis/faq.asp.

242. Liao, N., *QuikChem Method 31-107-06-1B Determination of Ammonia in Brackish or Seawater by Flow Injection Analysis*. 2008, Lachat Instruments.

243. *Rioflex GX 10000 QY - Material Safety Data Sheet*, in *Maxam Australia*.

244. *Rioflex Matrix - Material Safety Data Sheet*, in *Maxam Australia*.

245. *Rioflex GX 7000 QY - Material Safety Data Sheet*, in *Maxam Australia*.

246. *Rioflex GX 5000 QY - Material Safety Data Sheet*, in *Maxam Australia*.

247. Martinkova, Z., et al., *Determination of Hexamine in the Dithane DG Fungicide Using Capillary Isotachophoresis*. Sensing in Electroanalysis, 2011. **6**: p. 369-378.

248. Pospichal, J., P. Gebauer, and P. Bocek, *Measurement of mobilities and dissociation constants by capillary isotachophoresis.* Chemical Reviews, 1989. **89**(2): p. 419-430.

249. *The Langmuir Isotherm*. [cited 2013 20/12/2013]; Available from: http://www.chem.qmul.ac.uk/surfaces/scc/scat3.htm.

250. *The Langmuir Adsorption Isotherm*. [cited 2013 20/12/2013]; Available from: http://infohost.nmt.edu/~jaltig/Langmuir.pdf.

251. Campbell, J.A., *Studies in saturation of the tissues with gaseous nitrogen: the gaseous nitrogen content of certain fats, fatty acids, etc., saturated with air, as estimated by a new apparatus.* Experimental Physiology, 1933. **23**(1): p. 211-218.

252. Watts, H., *A Dictionary of Chemistry and the Allied Branches of Other Sciences*. Vol. 5. 1868: Longmans, Green and Co.

253. Mukhtar, S., et al., *Assesment of Ammonia Adsorption onto Teflon and LDPE Tubing used in Pollutant Stream Conveyance.* Agricultural Engineering International; the CIGR Journal of Scientific Research and Development, 2003.

254. Siddons, E., *Initial Study of Metallised Polyethylene Terephthalate Recovered from Home Made Explosives Mixtures (DSTL/DOC57945).* 2011.

255. Phillips, S.A., et al., *Physical and Chemical Evidence Remaining After the Explosion of Large Improvised Bombs. Part 1: Firings of Ammonium Nitrate/Sugar and Urea Nitrate.* Journal of Forensic Sciences, 2000. **45**(2): p. 324-332.

256. Johnson, R. and S. Ellis-Steinborner, *Survey of Improvised Explosive Devices (IED) Detection Methods (U). DSTO-TR-1859, [RESTRICTED].* 2006, Defence Science Technology Organisation.

257. http://www-unix.oit.umass.edu/~mcclemen/581Carbohydrates.html. *Analysis of Carbohydrates.* 7/08/2012].

258. Paulus, J.K., D. Schlieper, and G. Groth, *Greater efficiency of photosynthetic carbon fixation due to single amino-acid substitution.* Nat Commun, 2013. **4**: p. 1518.

259. Edwards, G. and D.A. Walker, *C_3, C_4: Mechanisms, and Cellular and Environmental Regulation, of Photosynthesis.* 1983, Berkley: University of California Press.

260. Lara, M.V. and C.S. Andreo, *Chapter 18 - C_4 Plants Adaptation to High Levels of CO_2 and to Drought Environments*, in *Abiotic Stress in Plants - Mechanisms and Adaptations*, A. Shanker and B. Venkateswarlu, Editors. 2011.

261. Cheesman, O.D., *Environmental Impacts of Sugar Production: The Cultivation and Processing of Sugar Cane and Sugar Beet.* 2005, Oxford, UK: CABI.

262. Ellis-Steinborner, S. and R. Johnson. *Explosive Device Detection Issues (U) [CONFERENCE PRESENTATION].* in *5th Singapore International Symposium on Protection Against Toxic Substances.* 2006.

263. *The Journey of Sugar (Canadian Sugar Institute).* 11/10/2012]; Available from: http://www.sugar.ca/english/educators/thejourneyofsugar.cfm.

264. O'Leary, M.H., *Carbon isotope fractionation in plants.* Phytochemistry, 1981. **20**(4): p. 553-567.

265. O'Leary, M.H., S. Madhavan, and P. Paneth, *Physical and chemical basis of carbon isotope fractionation in plants.* Plant, Cell & Environment, 1992. **15**(9): p. 1099-1104.

266. Wieser, M.E. and W.A. Brand, *Isotope Ratio Studies Using Mass Spectrometry*, in *Encyclopedia of Spectroscopy and Spectrometry*, C.L. John, Editor. 1999, Elsevier: Oxford. p. 1072-1086.

267. Le Bot, B., et al., *Using and interpreting isotope data for source identification.* TrAC Trends in Analytical Chemistry, 2011. **30**(2): p. 302-312.

268. Ding, C. and X. He, *K-means clustering via principal component analysis*, in *Proceedings of the twenty-first international conference on Machine learning.* 2004, ACM: Banff, Alberta, Canada. p. 29.

269. Hatcher, L., *A step-by-step approach to using SAS system for factor analysis and structure equation modeling.* 1994, SAS Institute.

270. Nowicki, J. and S. Pauling, *Identification of Sugars in Explosive Residues by Gas Chromatography-Mass Spectrometry.* Journal of Forensic Sciences, 1988. **33**(5): p. 1254-1261.

271. Goodpaster, J.V. and R.O. Keto, *Identification of Ascorbic Acid and Its Degradation Products in Black Powder Substitutes.* Journal of Forensic Sciences, 2004. **49**(3).

272. Sellers, K. and R. Morehead, *Restek Application Note - Identify and Quantify Adulterants in Seized Cocaine Using GC/MS (RTX-440 Column) and HPLC/RI (Pinnacle II Amino Column)*. 2005, Restek.

273. Agilent, *Agilent 1200 Series Refractive Index Detector - Service Manual* 2006, Agilent Technologies: Germany.

274. Agilent, *LC and LC/MS - Your Essential Resource for Columns and Supplies*. 2012, Agilent Technologies: Canada.

275. Waters, *Waters 2414 Refractive Index Detector Operators Guide*. 2008, Waters Corporation: USA.

276. Jens-Michael, H., H. Franz-Josef, and L. Gerd, *Authentication of Vanilla Products*, in *Vanilla*. 2010, CRC Press. p. 237-249.

277. Kiely, T.F., *Forensic Evidence: Science and the Criminal Law*. 2nd ed. 2006, Boca Raton, FL, USA: Taylor & Francis.

278. Davies, P.J., B. Hall, and D. Armitt, *Quick Exploitation Report (2010-05-07-16) [SECRET]*. 2010.

279. Davies, P.J., et al., *Quick Exploitation Report (2011-03-15-24) [SECRET]*. 2011.

280. Davies, P.J., et al., *Quick Exploitation Report (2011-03-15-25) [SECRET]*. 2011.

281. Blackledge, R.D. *Glitter as Forensic Evidence*. in *Trace Evidence Symposium*. 2007. Clearwater Beach, Florida.

282. Blackledge, R.D. and J. Edwin L. Jones, *All that Glitters is Gold*, in *Forensic Analysis on the Cutting Edge: New Methods for Trace Evidence Analysis*, R.D. Blackedge, Editor. 2007, John Wiley & Sons, Inc.

283. Alibaba.com. *Glitter Waste*. 2013 [29/07/2013]; Available from: http://www.alibaba.com/trade/search?fsb=y&IndexArea=product_en&CatId=&SearchText=glitter+waste.

284. Nikon, *NIS-Elements AR, V3.1 (Build 578)*. 2009.

285. Nikon, *Motorized Multi-Purpose Zoom Microscope AZ100M*. 2007: Japan.

286. Vernoud, L., et al., *Characterization of multilayered glitter particles using synchrotron FT-IR microscopy.* Forensic Science International, 2011. **210**(1–3): p. 47-51.

287. *Trace Analysis of Glitter Particles - Application Brief AB-060*. 2005 [06/2012]; Available from: http://www.smithsdetection.com.

288. Hummel, D., *Hummel Polymer and Additives FTIR Library*. 2007, Thermo Scientific.

289. Hall, B., P. Davies, and T. Hensel, *Isotope Ratio Mass Spectrometry: Analysis of Homemade RDX. DSTO-TN-1045 [RESTRICTED]*. 2011.

290. Hall, B., P. Davies, and P. McCurry, *Isotope Ratio Mass Spectrometry: Analysis of Ammonium Nitrate and Ammonium Nitrate/Aluminium Explosives. DSTO-TN-0951 [RESTRICTED]*. 2010.

291. CAMO. *The Unscrambler X*. 2013 June 2013]; Version 10.1:[Available from: http://www.camo.com/rt/Products/Unscrambler/unscrambler.html.